External controls on sedimentary sequences: a field and analogue modelling-based study

Jochem Frederik Bijkerk

Submitted in accordance with the requirements for the degree of
Doctor in Philosophy

The University of Leeds
School of Earth and Environment

July, 2014

The candidate confirms that the work submitted is his own and that appropriate credit has been given where reference has been made to the work of others.

This copy has been supplied on the understanding that it is copyright material and that no quotation from the thesis may be published without proper acknowledgement.

© 2014 The University of Leeds and Jochem Frederik Bijkerk

The right of Jochem Frederik Bijkerk to be identified as Author of this work has been asserted by him in accordance with the Copyright, Designs and Patents Act 1988.

Acknowledgements

This work was co-funded by the British Geological Survey University Funding Initiative (BUFI award number: S194), the University of Leeds, and the Turbidites Research Group. CGG Data Management Ltd (UK) is kindly acknowledged for providing additional well data.

I would like to thank my supervisors, Paul Wignall, Colin Waters, Bill McCaffrey, Joris Eggenhuisen and Ian Kane, who guided me while I meandered along a large variety of topics. Paul is thanked for his relaxed supervision style and overview, helping me to condense four years' work into a coherent thesis. The in-depth knowledge of Colin on the Carboniferous, and his critical but encouraging stance on this thesis is greatly appreciated. I am grateful to Bill for his enthusiasm, support, and the numerous discussions on external control concepts. Joris' insights helped tremendously in designing experiments, and I enjoyed the many discussions that were vital in understanding the results. Ian is thanked for initiating this project and selecting a great set of additional supervisors in his stead.

This project was set up in conjunction with the mapping of the Pateley Bridge (Sheet 61) area by the British Geological Survey, enabling me to gain from experience of working alongside BGS staff while both projects could benefit from an integration of the results. Colin Waters, David Lawrence, David Millward, Gareth Jenkins, Oliver Wakefield, Richard Haslam, and Tim Kearsley are all thanked for this opportunity, and for sharing some good, after-fieldwork diners and ales. Dario Ventra and Matthieu Cartigny are thanked for their company, interest, and for joining me with Sanem Açikalin for a short field trip that helped place the Carboniferous of northern England in a wider perspective.

The analogue modelling data was collected with the help of Dineke Wiersma, Louisa Tlili and Niels Meijer. Additionally, Thony van Gon Netcher and Henk van der Meer provided invaluable technical support during these experiments. I could not have performed these experiments without their help, and all are kindly thanked for their efforts and company.

In Leeds, the highs and lows of the past years, as well as plenty of coffees and drinks were shared with many. Jen, Kat, Luca, Marco, Mattia, Menno, Riccardo, Rob, Roman, Sarah, thanks for sharing in the last couple of years. I also spend a large amount of my time in Utrecht, and I am glad to have shared this period with Age, Bob, George, Jan, João, Nate, Nathalie, Poppe and Renske. Thanks!

Erik Sens, Ferry Boekhorst, Jan de Vries, Jasper Hofenk, Ruben Goedegebuure, and Tom Overmeer are kindly thanked for taking my mind of work once in a while. My parents and brother are also thanked for their support and interest. It's done, and time to become less of a hermit again.

I am greatly indebted to Inez Enderink. Many thanks for your encouragement, patience and continued love throughout this project.

Abstract

The Carboniferous Central Pennine Basin provides an ideal testing ground to examine the effects of tectonic activity, climate variation, sea-level changes and evolving bathymetric conditions upon continental to marine strata. During deposition of the glacio-eustatically controlled Millstone Grit Group the bathymetry of the area changed, tectonic activity has been invoked to explain basin-margin unconformities and high frequency climate variations have been interpreted as a driver of small-scale cyclicity.

Tectonic activity does not appear to have affected the stratigraphic character of the Millstone Grit Group significantly. The inference of a major tectonic unconformity on the northern margin of the Central Pennine Basin is re-interpreted through recognition of an incised valley. The influence of active tectonics is minor but tectonic lineaments provide loci for syn-depositional structural activity.

Facies analysis of Gilbert-type deltas within incised valley fills indicates a highly variable flow regime. Contrastingly, Gilbert-type deltas during sea-level fall are formed under constant, low flow conditions. This difference is tentatively linked to variable monsoonal discharge.

Bathymetric differences combined with sea-level variations strongly influence stratigraphic development. Shelf height is inferred as a control on valley incision based on analogue modelling, detailed field investigation of the oldest part, and literature review of the entire Millstone Grit Group. The deepest incised valleys occur where fluvial systems incised into the highest shelf margins. Analogue modelling indicates that deep incised valleys are associated with increased sediment supply to the slope relative to incised valleys formed on lower shelf margins during the same magnitude sea-level falls (in agreement with field data). Additionally, lateral variations in shelf-margin height appear to have steered the positions of fluvial systems, increasing the likelihood of valley incision in specific locations. Integrating basin depth and basin-margin morphology in sequence stratigraphic models as a controlling factor on the behaviour and position of fluvial systems might thus improve insight into the position and size of incised valley systems and associated turbidite lowstand fans.

Table of Contents

List of Tables

List of Figures

1 Thesis Rationale

1.1 Introduction

Sequence-stratigraphic methods are commonly used to study shifts in the facies belts of fluvio-deltaic systems (e.g. Catuneanu et al., 2009; Helland-Hansen and Hampson, 2009), and generally relate such shifts to changes in accommodation space induced by sea-level fluctuations (e.g. Posamentier et al., 1988). One of the most important aspects of sequence-stratigraphic models is the recognition that periods of rapid sea-level fall are associated with the formation of incised valleys (Posamentier and Vail, 1988; Blum et al., 2013). These entrenched fluvial channel belt complexes provide a mechanism for fluvio-deltaic systems to traverse a shelf and to deliver sand-grade sediment directly to the slope, supplying sediment to turbidite fans. During subsequent sea-level rise, these incised valleys are typically infilled by a sand-rich succession (e.g. Shanley and McCabe, 1994). Both incised valleys and the correlative turbidite fan systems form important targets for hydrocarbon exploration. There is scope to improve the understanding of incised valley formation as sea-level fluctuations form only one of three external controls on the patterns of sediment accumulation and preservation. Tectonic influences can enhance the complexity of successions by steering the position of channels (e.g. Kane et al., 2010a) or providing regional differences in subsidence, whereas climatic changes can result in water and sediment supply variations that modify the sequence-stratigraphic patterns (e.g. Rittenour et al., 2007; Bijkerk et al., 2013).

The Upper Carboniferous deposits in the Central Pennine Basin provide an ideal testing ground to examine the relative influence of these three controls. This period is characterised by high frequency and amplitude eustatic sea-level variations related to the waxing and waning of ice sheets during major southern hemisphere glaciations (e.g. Ross and Ross, 1985; Maynard and Leeder, 1992; Rygel et al., 2008). Meanwhile, the Central Pennine Basin represents an area in which the basin configuration altered drastically throughout deposition of its infill from deep segmented sub-basins to an overfilled basin (e.g. Collinson, 1988; Waters and Davies, 2006), providing an opportunity to examine the effect of sea-level fluctuations on a single fluvio-deltaic system in various basin settings. Additionally,

the Central Pennine Basin is located in an equatorial setting in which climate variations might play a role, as has been inferred for both older (Falcon-Lang, 1999a; Wright and Vanstone, 2001) and younger Carboniferous strata in this basin (Broadhurst et al., 1980). The Pendleton Formation forms the initial influx of the Millstone Grit Group fluvial system in the northernmost area of the Central Pennine Basin during the Pendleian regional sub-stage of the Carboniferous (e.g. Waters et al., 2009), and is here studied in detail. No sequence-stratigraphic framework has been presented since recognition of an additional transgressive surface in this succession (Brandon et al., 1995), while recent sedimentological studies have provided details on the turbidite succession and indicated the occurrence of syn-sedimentary activity of major faults (Kane et al., 2009, 2010a; Kane, 2010). Thus, both eustatic and tectonic activity is manifest in this succession.

One major challenge in the study of external controls on a regional scale is that the effect of individual controls on a sedimentary succession is difficult to establish and quantify. Therefore, their effects are also studied in the controlled environment of analogue models. These flume experiments provide simple three-dimensional models in which the effect of external controls on the stratigraphic character can be studied in isolation and together through time, and with a known set of input parameters such as the magnitude of sea-level fluctuations or the amplitude of tectonic or discharge variations. Combined field studies and analogue models can improve the understanding of long term evolution of fluvio-deltaic systems.

1.2 Thesis objectives

This thesis aims to elucidate and quantify the effect of external controls upon the fluvio-deltaic systems of the Millstone Grit Group in the Central Pennine Basin. This aim has been accomplished through consideration of the following specific research objectives:

i) The effect of basin depth, and lateral variations in basin depth on fluvio-deltaic systems. The Central Pennine Basin is characterised by pronounced changes in bathymetry with deep depocentres developed adjacent to shallower basinal areas. Analogue models are used to examine:

a) If a recognisable link occurs between basin depth and the behaviour of the fluvial systems in the analogue models.

b) If the behaviour of fluvial systems in the analogue models is affected by lateral variations in basin depth;

c) How basin depth and sea-level fluctuations combined influence fluvio-deltaic systems;

d) How to define and quantify the effect of such basin-margin morphology control on fluvio-deltaic systems;

e) Whether such changes can be perceived in the published literature.

ii) Detailed examination of the Pendleton Formation in the northern part of the Central Pennine Basin and the adjoining shelf area. For this succession a regional-scale framework was developed based on:

a) Stratigraphic correlation between the Craven Basin and Askrigg Block based on field investigation and literature study;

b) Interpretation of depositional environments based on sedimentological facies analysis;

c) Development of a sequence-stratigraphic framework, allowing for a rigorous review of inferred controls on the succession from literature;

d) Testing of results obtained from analogue modelling.

iii) Sedimentological facies analysis has highlighted the occurrence of significant variations in the character of Gilbert-type delta foresets in the Pendleton Formation. The investigation focussed on:

a) Which variations occur within these delta foresets;

b) Which flow processes can generate these structures;

c) What external control triggers can be responsible for such conditions.

iv) Application of developed concepts to the entire Millstone Grit Group

1.3 Thesis structure

Chapter 2 describes the results from analogue models in which the influence of basin depth, and lateral variations in basin depth on fluvio-deltaic systems are examined. The response of the fluvial system to variations in basin depth is quantified through the efficiency of sediment transport to the basin margin and measurements of the gradient and curvature of the fluvial longitudinal profile. Additionally, the combined effect of sea-level variations and basin depth is examined. Subsequently, two literature case studies of shelf margins are described to illustrate applicability of the results to real world data.

Chapter 3 presents a sedimentological and sequence-stratigraphic analysis of the Pendleton Formation from the Carboniferous Craven Basin. In this chapter, stratigraphic sections through the Pendleton Formation are described for various parts of the Craven Basin and adjoining northern shelf. These are used to construct a palaeo-environmental model, based on lithofacies and a detailed sequence-stratigraphic interpretation. The model is compared and contrasted with previous examples and the results from the analogue modelling in Chapter 2.

Chapter 4 focuses on the detailed sedimentological character of Gilbert-type deltas that occur in the incised valley fill of the Bearing Grit that described in Chapter 3. These contain variations that can be related to flow conditions that provide additional insight into the character of the Millstone Grit fluvial system. A new depositional model is presented, which indicates a probable climate control on the sedimentary succession.

Chapter 5 provides an overview of the development of the Millstone Grit Group of which the Pendleton Formation of Chapters 3 and 4 forms the basal succession. The character of incised valleys throughout this group is analysed based on published data, and related to the findings in previous chapters.

2 Basin Depth as an Allogenic Control on Fluvio-Marine Sediment Partitioning

2.1 Abstract

Fluvio-deltaic systems tend toward an equilibrium state at which the longitudinal profile does not change shape and all sediment is bypassed. In progradational systems the longitudinal profile remains in disequilibrium because progradation requires constant aggradation along the length of the fluvio-deltaic profile. Here, four analogue models of sedimentary systems are examined to better understand the effect of downstream allogenic controls (basin depth, subsidence and sea-level variations) upon longitudinal patterns of sediment distribution that eventually determine large-scale stratigraphic architecture. Basin depth affects the curvature and gradient of the longitudinal profile: fluvio-deltaic systems prograding into deep basins are characterized by slower progradation than those draining into shallow basins. This lower progradation rate generates less concave and steeper longitudinal profiles and results in enhanced sediment bypass volumes to the shoreline and decreased downstream fining. Glacio-eustatic sea-level variations modulate the effects of basin depth on the longitudinal profile, which is closest to equilibrium during falling sea level and early lowstand, resulting in efficient sediment transport towards the shoreline at those times. Additionally, the strength of the response to sea-level fall differs dependent on basin depth. In deep basins, sea-level fall causes higher sediment bypass rates than in shallow basins and generates significantly stronger erosion. This results in an increasing probability of incised valley formation and can significantly alter shelf clinoform style. Basin depth thus forms a first order control on sediment partitioning along the longitudinal profile of sedimentary systems and the shelf clinoform style. It also forms a control on the availability of sand-grade sediment at the shoreline that can potentially be remobilized and redistributed into deeper marine environments. Key findings are subsequently applied to literature of selected field areas.

2.2 Introduction

Understanding source-to-sink sediment transport and sediment partitioning between the fluvial, deltaic and marine environments on geological timescales presents a major challenge in sedimentology and sequence stratigraphy (e.g. Bourget et al., 2013; Covault et al., 2011; Martinsen et al., 2010; Sømme et al., 2009). Sediment transport and its consequent distribution through the fluvio-deltaic system is largely governed by the concept of 'equilibrium' or 'grade' (e.g. Muto and Swenson, 2005). Equilibrium implies that all sediment is conveyed through the system without net erosion or deposition. All fluvio-deltaic systems evolve towards this state; (parts of) systems at too shallow gradients for sediment transport aggrade until they become capable of full sediment bypass, while (parts of) systems at a too steep gradient cut down until they are only energetic enough to bypass their sediment load. This concept is used in sequence-stratigraphic models to define whether a system is in a net erosional or depositional state (e.g. Catuneanu et al., 2009; Posamentier and Vail 1988; Shanley and McCabe 1994).

Sea-level fall can cause the lower reach of the longitudinal profile to become above grade resulting in net erosion and efficient sediment transport to the river mouth. During sea-level rise the fluvial system is below grade and becomes aggradational, resulting in reduced sediment transport to the shoreline. Upstream, away from direct influence of sea-level variations, the grade of systems is determined by changes in discharge, sediment supply, and tectonic regime (e.g. Bijkerk et al., 2013; Catuneanu et al., 2009; Hampson et al., 2013; Holbrook and Bhattacharya, 2012). Fluvio-deltaic systems thus respond to the combined effect of upstream and downstream allogenic forcing mechanisms and tend towards a graded state through continuous adjustments of the longitudinal profile. These adjustments shift sediment partitioning between the fluvial, deltaic and marine environments of a sedimentary system and therefore determine the large-scale stratigraphic architecture.

Variations in the grade of entire fluvio-deltaic systems can occur on geological timescales (Paola et al., 1992). System-scale static equilibrium is here defined as a state in which sediment input and output in a sedimentary system are equal, implying that the shape of the longitudinal profile does not change over such a period (Fig. 2.1a). This type of equilibrium differs from morphological definitions

of equilibrium (e.g. Mackin, 1948) that do not necessarily represent equilibrium conditions on geological timescales but focus on short term periods and small segments of a fluvio-deltaic system (Schumm and Lichty, 1965). Analogue and numerical modelling shows that systems approach system-scale static equilibrium conditions asymptotically through time (Postma et al., 2008). Systems that are far removed from equilibrium approach this state rapidly using a large percentage of the sediment load for aggradation of the fluvial system (Postma et al., 2008). Systems that are close to equilibrium conditions grade towards this state more slowly using a small percentage of the available sediment load: most sediment bypasses to the downstream endpoint of the longitudinal profile (Postma et al., 2008).

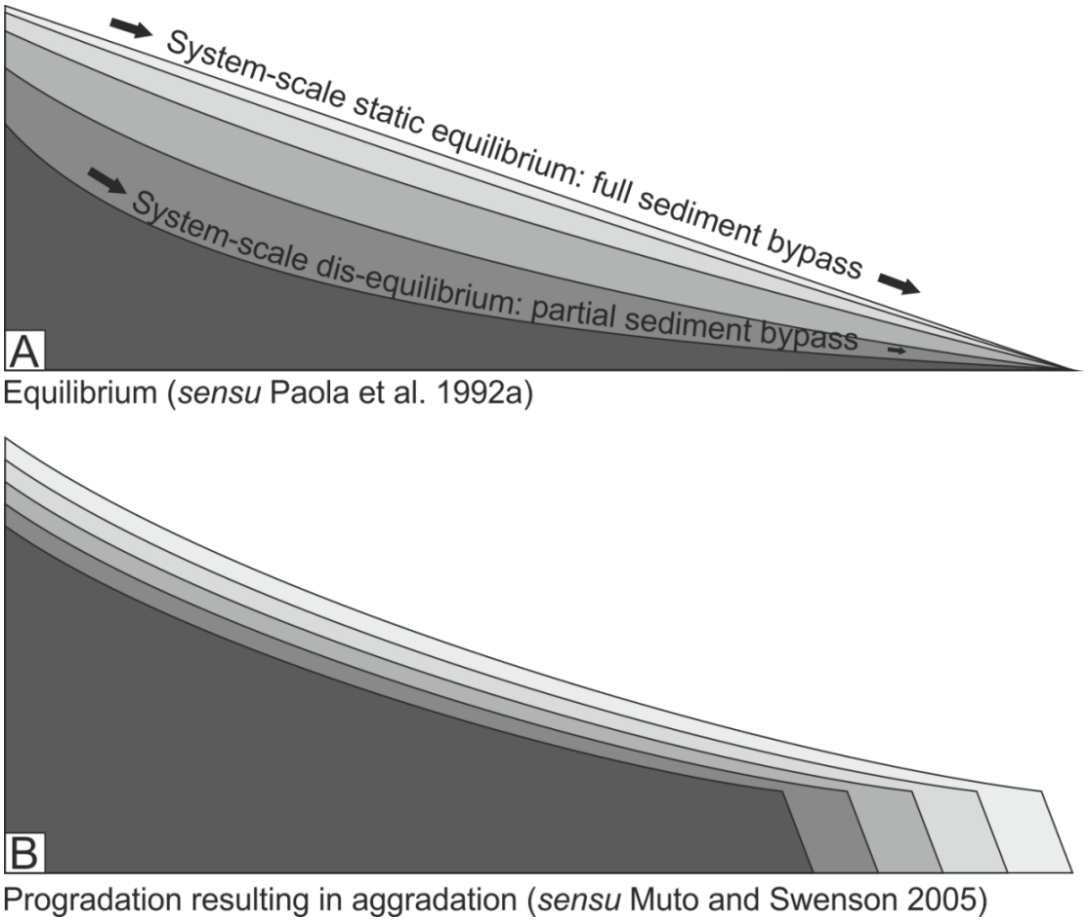

Figure 2.1 (a) System-scale static equilibrium (sensu Paola et al., 1992a) is only obtained over geological timescales. The linear equilibrium profile drawn here is idealized (cf. Postma et al., 2008) and will not form in natural systems for multiple reasons but illustrates that all fluvial accommodation space is infilled. (b) Development of fluvio-deltaic systems on geological timescales. Progradation results in aggradation of the topset and prevents these systems from achieving system-scale static equilibrium.

In many natural systems, sediment bypass through the fluvial system leads to progradation of a delta- or shelf-clinoform, resulting in a continuous lengthening of the longitudinal profile (Fig. 2.1b). This lengthening implies that system-scale static equilibrium can be reached only when sea level falls at the correct rate to extend the fluvial profile such that neither aggradation nor degradation of the fluvial profile occurs and the coastal trajectory is exactly an extension of the equilibrium profile (Helland-Hansen and Hampson, 2009; Muto and Swenson, 2005). Such conditions are not met in systems with a constant relative sea level, or a sea level that rises gently over geologic time due to subsidence. In such occurrences, a part of the fluvial sediment load is required for aggradation of the fluvial domain. This represents a departure from the system-scale static equilibrium profile (Voller and Paola, 2010) that is linked to the progradation rate and relative sea-level variations of that system. The magnitude of the departure is set in a feedback loop in which departure from system-scale static equilibrium determines fluvio-marine sediment partitioning, thereby setting the progradation rate, which has a feedback in determining the departure from system-scale static equilibrium (Fig. 2.1b).

As yet, it is unknown how basin depth, basin subsidence, and eustatic sea-level fluctuations govern the behaviour of this feedback mechanism and so produce the common stratigraphic patterns described by sequence stratigraphy. Three-dimensional analogue models are used to examine this concept in a controlled environment. Additional two-dimensional models are generated to study its effect of downstream fining. Subsequently, literature case studies of ancient natural systems are used to validate these findings.

2.3 Methods

2.3.1 Experimental facility

The results of four analogue models are described. The experimental setup consisted of a dual-basin configuration and allowed generation of two scenarios simultaneously: Model 1 (M1) and Model 2 (M2) (Fig. 2.2). Both models had a 1.6 m wide rectangular duct serving as a fluvial zone that was connected to a subsiding basin that deepened away from the shoreline with discrete shallow, intermediate and deep zones (Fig. 2.2). Sediment and water entered the experiment

diffusely through a pebble basket along the width of the fluvial duct. Before an experiment, each model was set to a downstream gradient of 0.01. The models had different subsidence scenarios, but reached the same basin shape and depth at the end of the experiments (Fig. 2.2; 2.3). Subsidence is generated with vertical adjustment of hexagonal blocks underneath the experimental set-up. Rows of these blocks are connected by overlying boards to generate smooth, rather than serrated, subsidence zone boundaries (Fig. 2.2). An adjustable overflow controls base level during these experiments. All models are executed with quartz sand of a narrow grain-size distribution (D_{10} = 146 µm, D_{50} = 217 µm, and D_{90} = 310 µm).

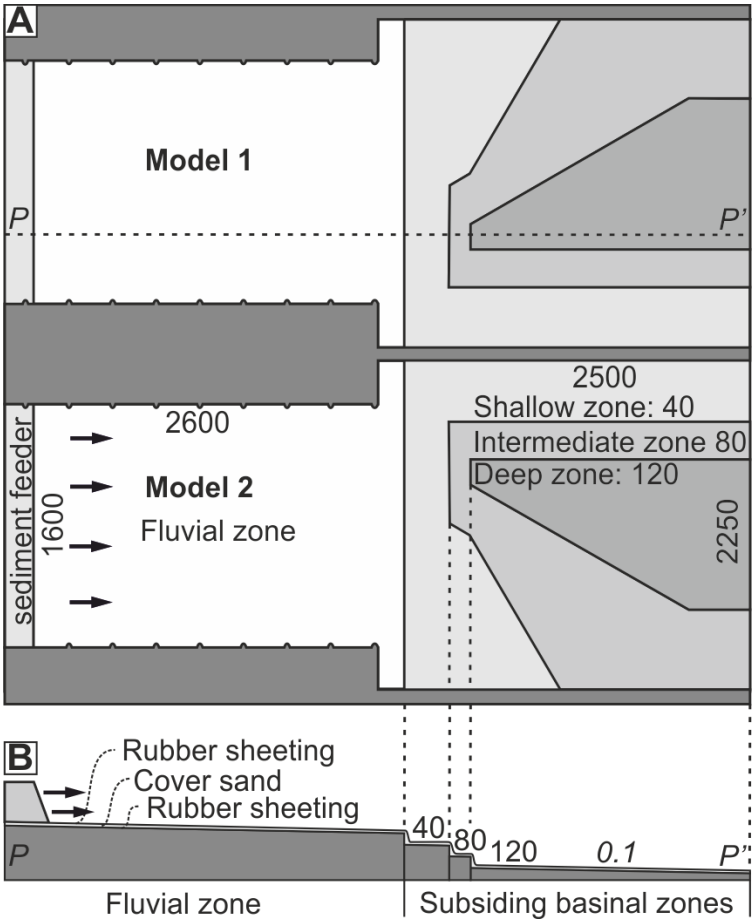

Figure 2.2 (a) Top view of the experiment setup, consisting of two mirror-image models. Sediment and water are added at the sediment feeder. In the fluvial zone no tectonic movement occurs. In the basin, 3 zones of distinct depth are formed. Dimensions (mm) are indicated in regular font, gradients in italic font. (b) Side view of the experiment, along transect P-P' in (a).

In Experiment 1 - Model 1 (E1_M1), the effects of basin depth is tested (Fig. 2.3a). In Experiment 1 - Model 2 (E1_M2) the joint effects of subsidence and basin depth are tested (Fig. 2.3b). In Experiment 2, sea-level variations are also included with different subsidence and discharge regimes for Model 1 (E2_M1) and Model 2 (E2_M2) (Fig. 2.3c, d; Table 2.1). In E1_M1, E1_M2, and E2_M2 water discharge and sediment input were constant at 1 m^3h^{-1} and 0.004 m^3h^{-1}, respectively. In E2_M1, these rates were 1.5 m^3h^{-1} and 0.004 m^3h^{-1} (Table 2.1).

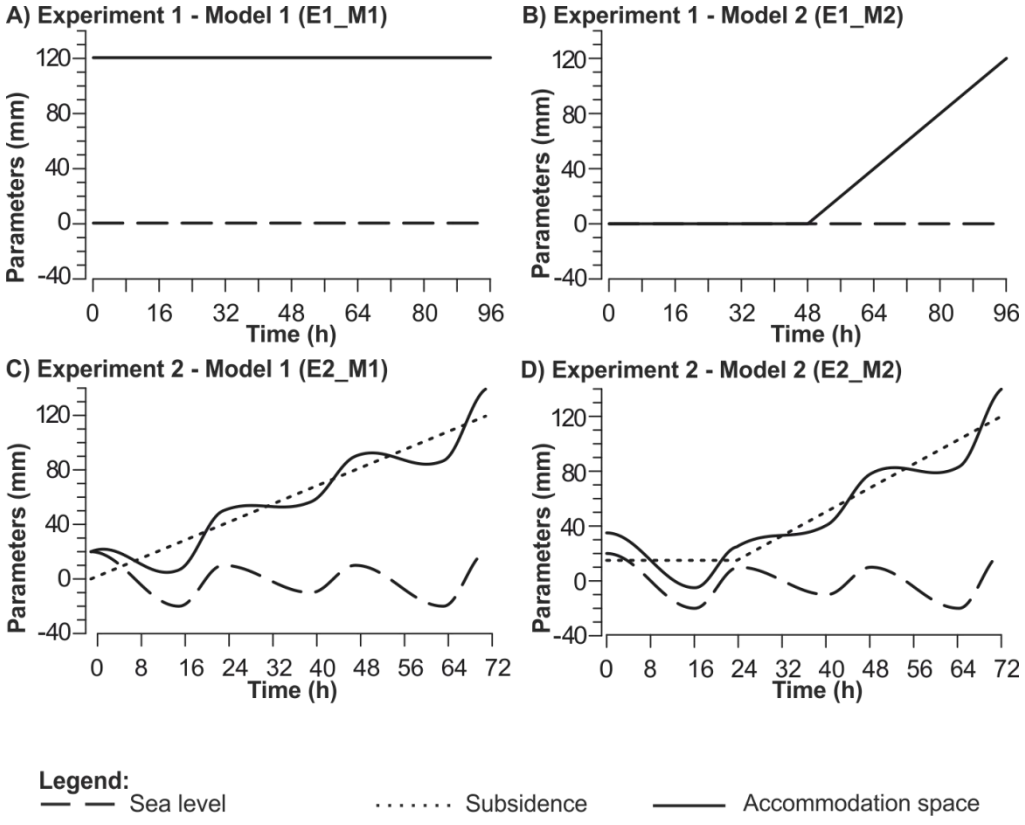

Figure 2.3 Input parameters. The accommodation space is given for the deep zone of the basin, the intermediate and shallow zones of the basin have an accommodation space of 2/3 and 1/3 of this value. Note that in (a) E1_M1, and (b) E1_M2, the subsidence and accommodation space curves overlay because base level is constant, (c) E2_M1, (d) E2_M2

Before Experiment 1 started, the basin of E1_M1 was subsided to its final configuration. Therefore, this system experiences only a spatial increase in basin depth as it progressively enters the shallow, intermediate and deep zones of the basin (Fig. 2.2; 2.3a). In E1_M2, the fluvio-deltaic system progrades in shallow water

during the first half of the experiment, whilst the basinal area subsides at a rate of 2.5 mm h^{-1} during the second half. This results in subsidence-controlled accommodation space on the delta plain, and both temporally and spatially increasing water depths (Fig. 2.2; 2.3b).

The subsidence rate in E2_M1 is continuous throughout the experiment, resulting in the creation of accommodation space on the delta plain and progradation into increasingly deeper water (Fig. 2.3c). In E2_M2, the entire basinal area is lowered 15 mm to accommodate sea-level lowstand 1 (at 16 h) before the experiment starts (Fig. 2.3d). Subsidence at different rates for the shallow, intermediate and deep zones starts after 24 h (Fig. 2.3d). Additionally, three asymmetric sea-level cycles of 24 h period and variable amplitude are modelled during Experiment 2: cycle 1 starts with a 40 mm fall, followed by a 30 mm rise; cycle 2 has a 20 mm fall and rise; cycle 3 has a 30 mm fall, followed by a 40 mm rise, returning sea level to the initial level (Fig. 2.3c, d).

	Q_w (m^3h^{-1})	Q_s (m^3h^{-1})	T (h)	ΔT(h)	Boundary conditions varied
E1_M1	1	0.004	96	8	Basin depth
E1_M2	1	0.004	96	8	Basin depth and subsidence
E2_M1	1.5	0.004	72	8	Basin depth, subsidence and sea-level variation
E2_M2	1	0.004	72	8	Basin depth, subsidence and sea-level variation
Scenario 1	5.5	0.007	8	0.5	Basin with constraining weir, no progradation
Scenario 2	5.5	0.007	8	0.5	Shallow water progradation (3 cm)

Table 2.1 Input parameters and boundary conditions of the experiments. Parameters Q_w and Q_s denote water and sediment discharge, respectively. Parameters T and ΔT denote the duration of the experiment and the interval between measurements.

2.3.2 Experimental procedure

The fluvio-deltaic systems were allowed to prograde to the basin margin during a start-up period prior to the actual experiment, so that experiments commenced with a self-adjusted fluvial profile that reached the basin margin at 0 h (Fig. 2.2). Sea level during this period was 0 mm. Time-lapse photographs were taken at 3 minute intervals to record the morphology of the fluvio-deltaic system.

The 96 h duration of E1_M1 and E1_M2 was subdivided into 12 intervals of 8 h (Table 2.1). Subsidence was applied to E1_M2 between these 12 intervals while

the experiment was paused. Digital Elevation Models (DEMs) were measured with a laser scanner before and after subsidence to accurately constrain sediment budgets. The 72 h duration of E2_M1 and E2_M2 was similarly subdivided in 8 h intervals. Sea level was adjusted at 20 min intervals (Table 2.1)

2.3.3 Scaling

The response of natural systems to external forcing and the resultant stratigraphic character depends on the ratio between timescales of forcing (T_{for}) and reactive timescales inherent to the system. For stratigraphic architecture, this reactive timescale has been termed the equilibrium time (T_{eq}) (Paola et al., 1992a). The ratio of T_{for}/T_{eq} has proven to be effective for the simulation of stratigraphic response to glacio-eustatic sea-level variations over geological timescales (Bijkerk et al., 2013; Paola et al., 2009; van Heijst and Postma, 2001).

Modern natural systems have equilibrium times in the order of $10^5 – 10^6$ yr and are dominated by 100 kyr glacio-eustatic sea-level variation (cf. Castelltort and Van Den Driessche, 2003). E1_M1, E1_M2 and E2_M2 have an estimated equilibrium time of ~100 h, based on the length of the longitudinal profiles at the start of the experiments, the width of the fluvial system and the water discharge. For E2_M1, the higher water discharge results in a shorter equilibrium time of ~72 h. The 24 h sea-level cycles thus approximate a quarter or third of the estimated equilibrium time: ratios representative of natural systems with glacio-eustatic sea-level variations. The sea-level cyclicity in Experiment 2 therefore represents high frequency, high amplitude glacio-eustatic sea-level variation and is expected to force the system away from equilibrium during sea-level rise, whereas low frequency sea-level variation might allow a sedimentary system to remain near equilibrium (Paola et al., 1992a).

Because glacio-eustatic sea level is mimicked, an asymmetric curve is generated in which the duration of sea-level fall is twice as long as sea-level rise. This is similar to the ratio observed in Pleistocene sea-level records (e.g. Lisiecki and Raymo, 2005); the slow accumulation of ice caps results in a slow eustatic sea-level fall, whereas rapid ablation of these ice caps at the glacial-interglacial transition causes fast eustatic sea-level rise (Oerlemans, 1991).

2.3.4 Dataset

Analyses are based on DEMs and supported by time-lapse images. DEM analyses are focused on the curvature of the longitudinal profile, the grade of the longitudinal profile, and the percentage of sediment input that is transported past the shoreline.

The curvature of the longitudinal profile is determined by the ratio between the volume below the sediment surface, and the volume below the achieved gradient. The latter is here defined as a straight line between the most proximal point of the DEMs and the rollover point (Fig. 2.4a). The grade of the longitudinal profile is calculated in a similar fashion but uses an approximation of the system-scale static equilibrium gradient instead of the achieved gradient (Fig. 2.4a). This gradient is characterized by full sediment bypass and based on the longitudinal profile of E2_M1 at 16 h, when the system achieved a near-linear, steep slope, and 100% sediment bypass over a 8 h period, implying system-scale static equilibrium.

The gradient at which a longitudinal profile achieves full sediment bypass is dependent on the ratio between water discharge and sediment discharge (e.g. Postma et al., 2008). High water to sediment discharge ratios results in low gradient longitudinal profiles, and vice versa. In E2_M1 this ratio is higher than in the other models. Therefore an adjustment is made based on the comparison of the longitudinal profiles of E2_M1 and E2_M2 at 0 h. These profiles indicated that the gradient of E2_M1 was 1.2 times steeper than that of E2_M2 while discharge in E2_M1 is 1.5 times higher, suggesting that the slope in these experiments has an inverse square root dependence on discharge (cf. Postma et al., 2008). In E1_M1, E1_M2, and E2_M2 full sediment bypass is thus considered to occur at a 1.2 times lower gradient than in E2_M1. The bypass gradient in these models represents a theoretical datum that is used to determine how closely a system approaches equilibrium conditions. Relative differences in longitudinal grade between E1_M1 and E1_M2 and E2_M2 can be compared since their upstream input parameters are equal (Table 2.1), but care should be taken when comparing the grade of E2_M1 and E2_M2 because the comparison depends on the validity of the above assumption.

Additionally, DEMs are used to calculate the ratio between sediment volume used for progradation and the total sediment volume, quantifying the efficiency of sediment transport to the shoreline (Fig. 2.4b).

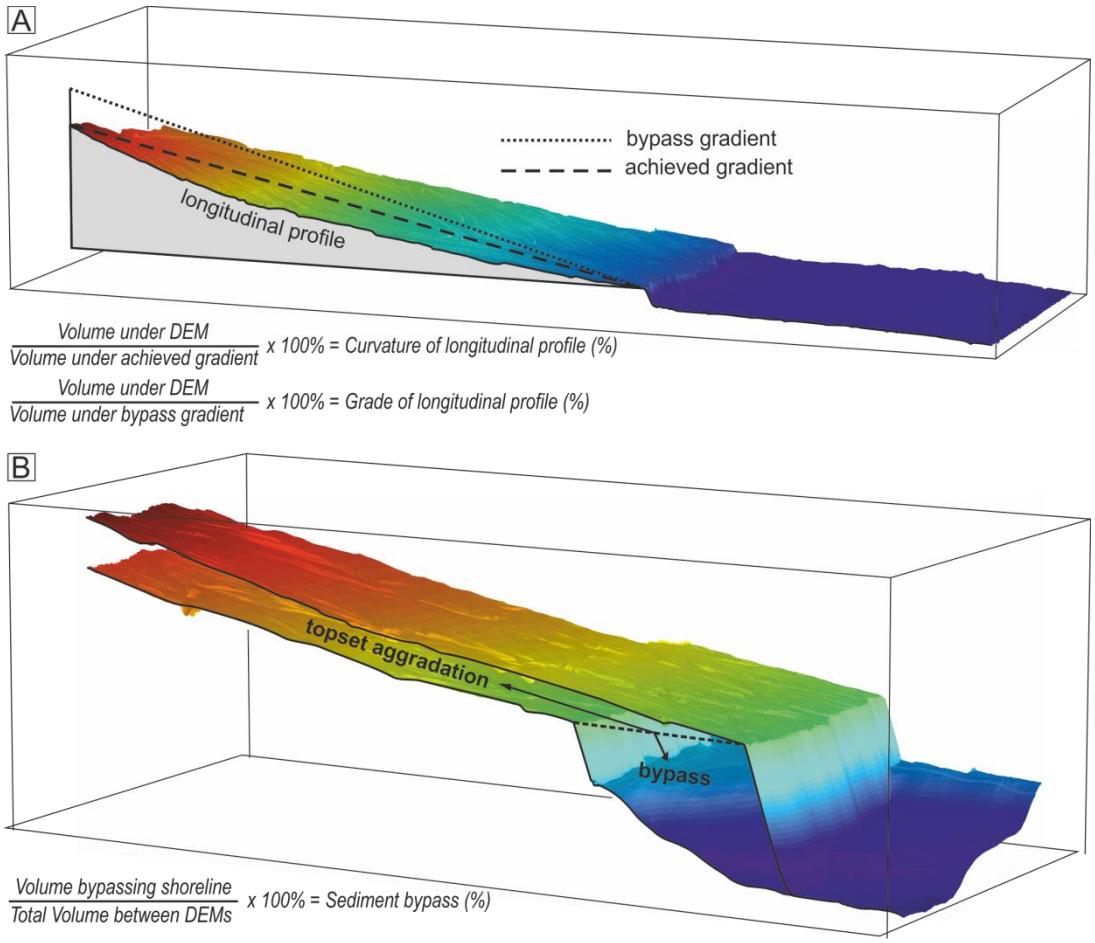

Figure 2.4 Representation of methods. (a) Curvature of the longitudinal profile (%) is calculated as the volume percentage of a triangle connecting the upstream and downstream ends of the longitudinal profile (the achieved gradient). High curvature percentages thus imply that the system becomes less concave. Grade of the longitudinal profile (%) is calculated with reference to an estimated bypass gradient. See text for discussion of the bypass gradient. (b) Sediment bypass is calculated as a percentage between the sediment volume transported past the shoreline of the initial height model, and the total sediment volume between two successive height models. Note the overall increase in basin depth and basin geometry in model E1_M1.

2.3.5 Grain-size experiments

Two distorted-scale models (Peakall et al., 1996), Scenario 1 and Scenario 2, were run in a 0.48 m wide, 12 m long rectangular flume to examine the effects of longitudinal grade on downstream sediment fining (Fig. 2.5). In Scenario 1, progradation is limited by a weir that allows aggradation up to the system-scale equilibrium gradient. Scenario 2 resembles shallow water progradation in 3 cm

water depth. Both models start as a 4 m long horizontal plain and run for 8 h with sediment and water input at 0.007 m^3h^{-1} and 5.5 m^3h^{-1}, respectively (Table 2.1; Fig. 2.5). The approximate equilibrium time at the start of these models is ~14 h. At half hour intervals, five point-measurements along the width of the flume were made at 0.25 m intervals to obtain a width-averaged longitudinal profile (Fig. 2.5b). In both experiments, grain-size samples of the final longitudinal profile were taken at 0.5 m intervals after the experiment finished. Additional grain-size samples were taken behind the downstream weir of Scenario 1. Settings were chosen such that average water depth on the fluvial topset was sufficient to prevent preferential transport of coarse grains (cf. Vollmer and Kleinhans, 2007). This resulted in the formation of current ripples but enabled assessment of the relation between downstream fining and topset curvature. Quartz sand with a bimodal grain-size distribution was used with peaks at 216 µm and 420 µm (D_{50} = 285 µm). The coarse tail with a diameter of >1 mm (7% by weight) was used to assess downstream fining.

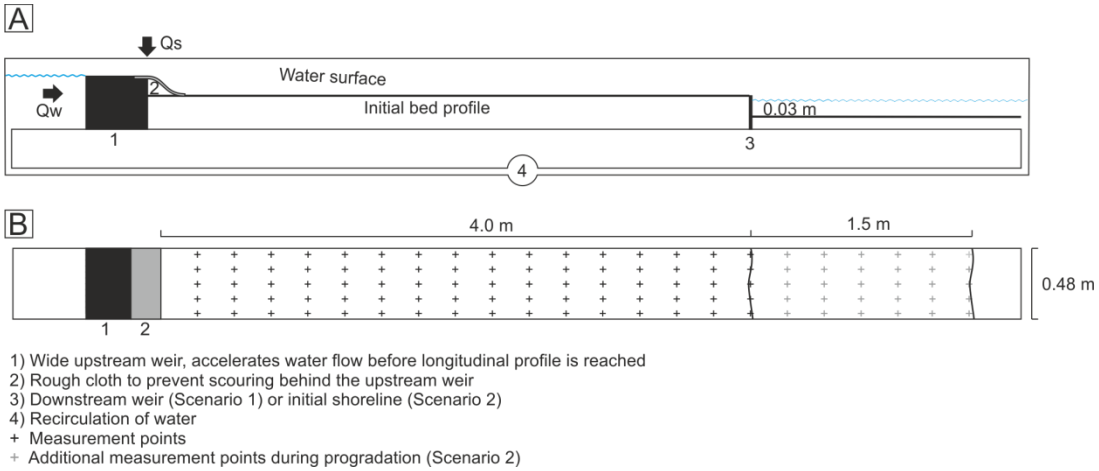

Figure 2.5 Experiment setup for Scenario 1 and 2. (a) Side view of experiment setup. (b) Top view of experiment setup.

2.4 Results

2.4.1 Experiment 1 - Basin 1 (E1_M1)

E1_M1 developed in a pre-formed basin with constant sea level and results in progradation of a delta-shelf system into increasing water depths (Fig. 2.6a - c; 2.8a, b). The curvature of the longitudinal profile increases from 91% to ~96% from 1 – 56 h and subsequently decreases to 94% (Fig. 2.4a; 2.6g). The grade of the longitudinal profile starts at 76% and increases to 92% from 1 – 56 h, after which it

remains constant (Fig. 2.4a; 2.6h). These trends correlate well with the sediment bypass pattern, which starts at ~24% of the sediment input volume and increases towards a maximum of 50% from 56 – 64 h. Subsequently, it decreases to ~43% (Fig. 2.4b; 2.6f).

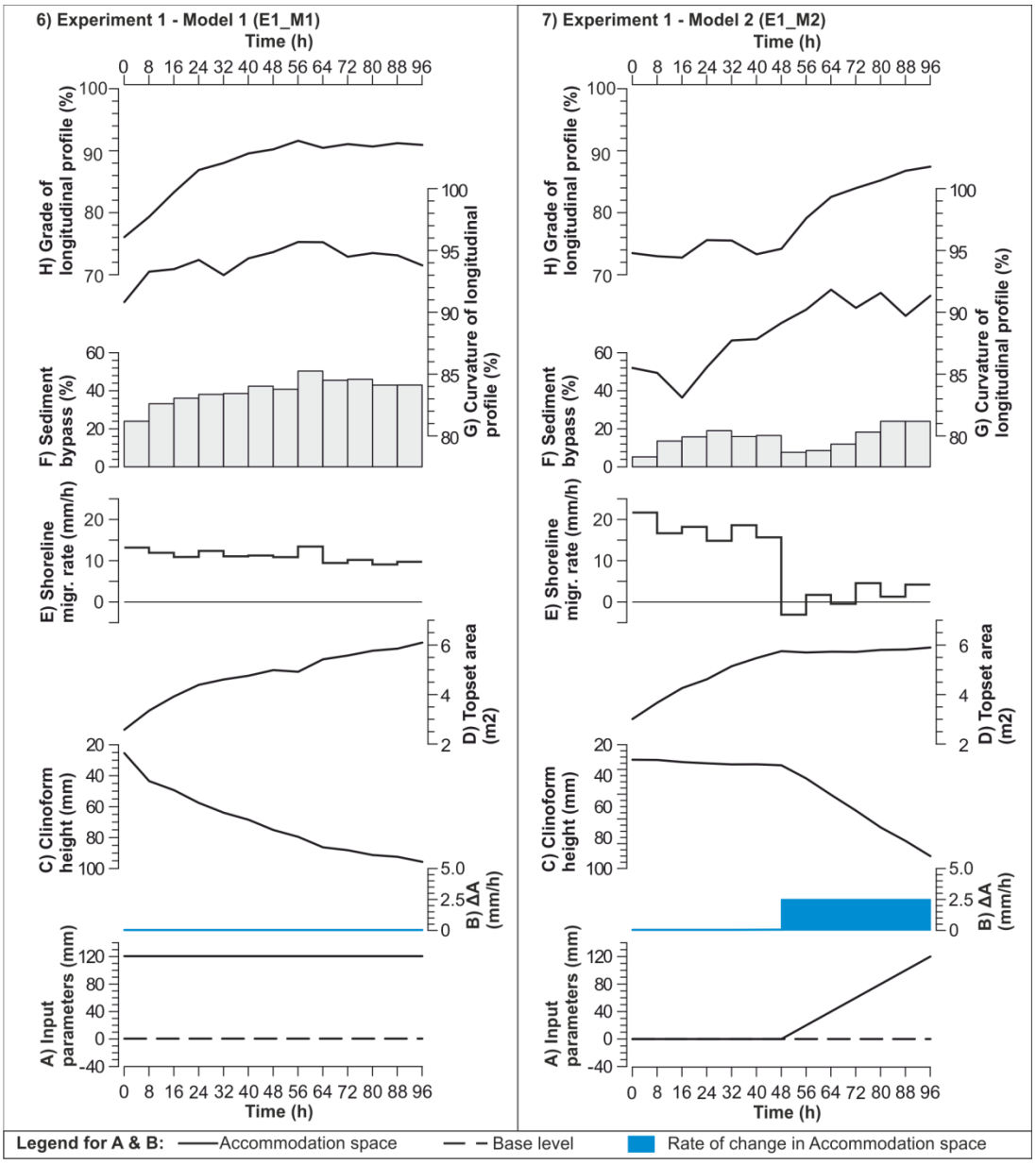

Figure 2.6 & 2.7 (a) Input parameters for E1_M1 and E1_M2. Accommodation space shown for the deep part of the basin, accommodation space in the intermediate and shallow parts is 2/3 and 1/3 of this value. (b) Rate of change in accommodation space, (c) Basin depth (mm) calculated along the strike of the clinoform, (d) Topset area, (e) Progradation rate, calculated between the shoreline of successive height models, (f) Sediment bypass, see Fig. 2.4b, (g) Curvature of the longitudinal profile, see Fig. 2.4a. (h) Grade of the longitudinal profile, see Fig. 2.4a.

Average clinoform height, measured along the strike of the clinoform, gradually increases from 25 – 96 mm during the experiment and correlates with the sediment bypass percentage and the longitudinal curvature and grade as well (Fig. 2.6c, f - h). The progradation rate decreases from 14 – 9 mm h^{-1} (Fig. 2.6e) and results in a gradual increase in the topset area from 2.6 – 6.1 m^2 (Fig. 2.6d).

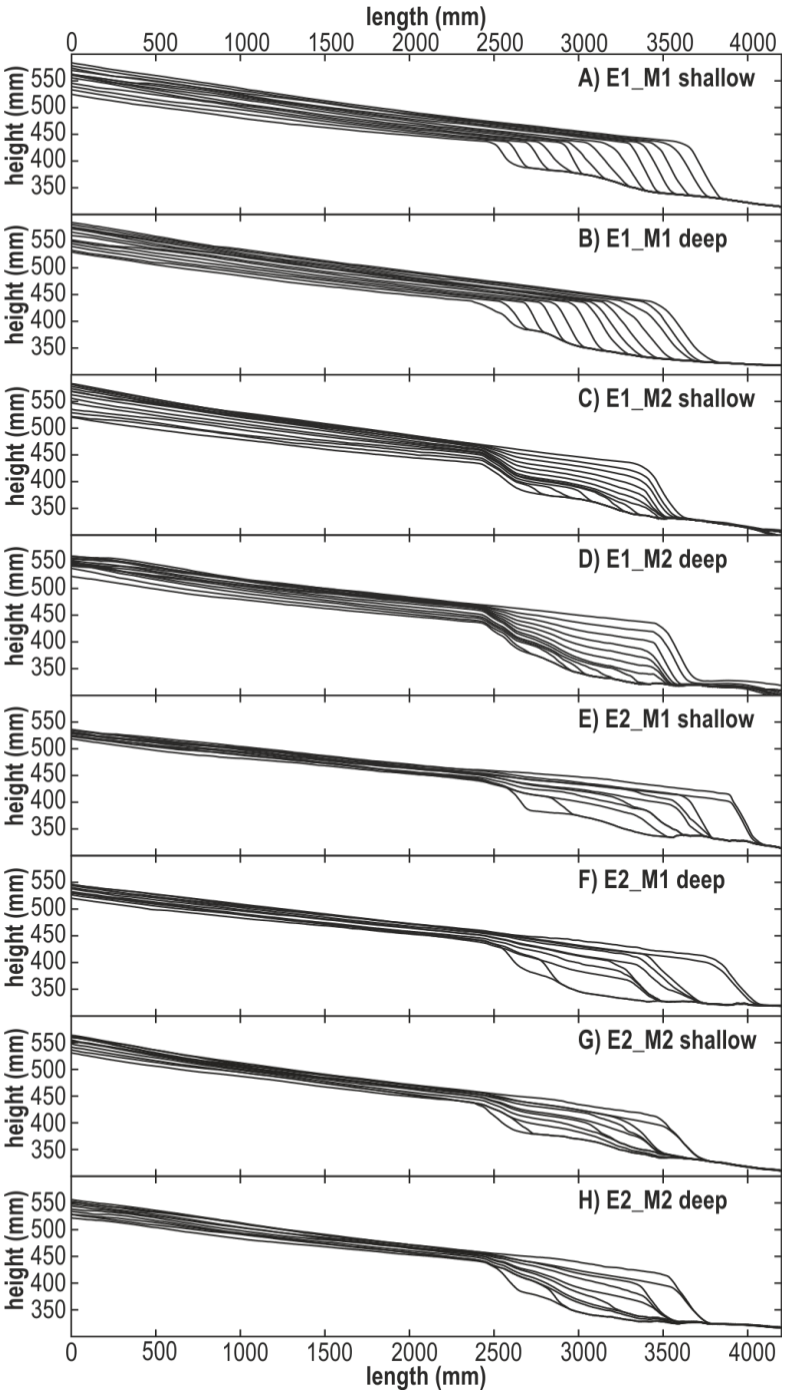

Figure 2.8 Width-averaged transects through the shallow and deep parts of each experiment. Transects mainly differ in the proximal part of the basin (see Fig. 2.2a). Each line represents an increment of 8 h (see Fig. 2.6a).

2.4.2 Experiment 1 - Basin 2 (E1_M2)

E1_M2 forms in a shallow ramp setting with constant sea level that subsides from 48 h onwards at a rate of 2.5 mm h^{-1} (Fig. 2.7a, b). Shallow water conditions allow for rapid progradation during the first half of the experiment. During the second half, tectonic subsidence results in accommodation on the topset and deepening of the basin, which reduces the progradation rate (Fig. 2.7c - e; 2.8c, d). At the start of the experiment, sediment bypass is 5% of the sediment input and increases to ~16% at 40 – 48 h (Fig. 2.7f). The initiation of subsidence reduces sediment bypass to 8% (Fig. 2.7f, 48 – 56 hour) after which it steadily increases to 24% at the end of the experiment (Fig. 2.7f, 88 – 96 hour). The curvature of the longitudinal profile starts at 86% and increases rapidly towards 92% at 64 h (i.e. becomes less concave) at which point it becomes approximately constant (Fig. 2.7g). The grade of E1_M2 initially remains low at 74% and gradually increases after the initiation of subsidence (Fig. 2.7e, h).

Sediment bypass is low in the rapidly prograding system and coincides with a strongly concave, low-gradient longitudinal profile (Fig. 2.7e - h, 0 – 48 hour). After 48 h, the basin subsides rapidly and a significant sediment volume is captured for topset aggradation, decreasing the sediment bypass rate (Fig. 2.7e - h, 48 – 72 hour; 2.8c, d). However, towards the end of the experiment this rate increases to its highest levels (Fig. 2.7c, e, f, 72 – 96 hour). This coincides with slow deep-water progradation and corresponds to an increased grade and decreased concavity of the longitudinal profile (Fig. 2.7e - h).

2.4.3 Experiment 2 - Basin 1 (E2_M1)

Throughout this experiment, subsidence is continuous and sea level mimics three glacio-eustatic cycles of constant frequency and variable amplitude (Fig. 2.9a). This results in three regression – transgression cycles (Fig. 2.8e, f) that are reflected in the cyclicity of the measured parameters (Fig. 2.9c - h).

The style of deposition and erosion changes significantly during a sea-level cycle and varies between cycles as well (Fig. 2.11; 2.12). During normal regression, the entire delta top is frequently active (Fig. 2.11a). During forced regression, two modes occur: small parts of the delta topset become inactive, generating short-lived

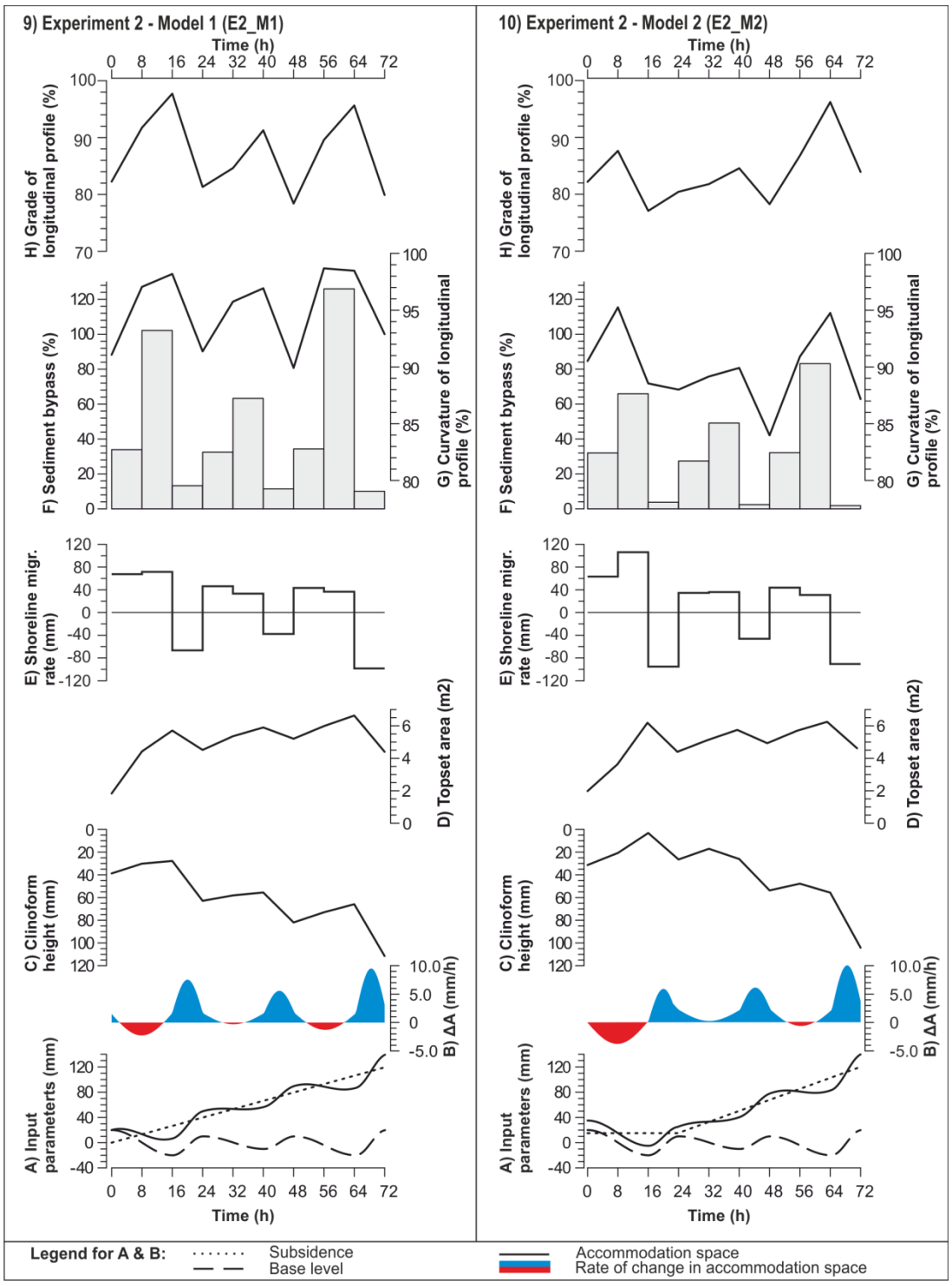

Figures 2.9 & 2.10 (a) Input parameters for E2_M1, and E2_M2. Accommodation space shown for the deep part of the basin, accommodation space in the intermediate and shallow parts is 2/3 and 1/3 of this value. (b) Rate of change in accommodation space, (c) Basin depth (mm) calculated along the strike of the clinoform (d) Topset area, (e) Progradation rate, calculated between the shoreline of successive height models, (f) Sediment bypass, see Fig. 2.4b, (g) Curvature of the longitudinal profile, see Fig. 2.4a. (h) Grade of the longitudinal profile, see Fig. 2.4a.

interfluves in cycle 1, 2 and the start of 3 (Fig. 2.11b). During sea-level fall 3, an incised valley forms that focuses much of the water and sediment discharge along a narrow section of the delta topset, generating long-lived interfluves (Fig. 2.11c). Focused discharge through the incised valley results in significant progradation focused at the deep basin, after which the valley mouth shifts towards the shallow basin at a later stage (Fig. 2.11d). During transgression, small lobes step back onto the lowstand shelf while in upstream locations discharge is still focused in the incised valley (Fig. 2.11e).

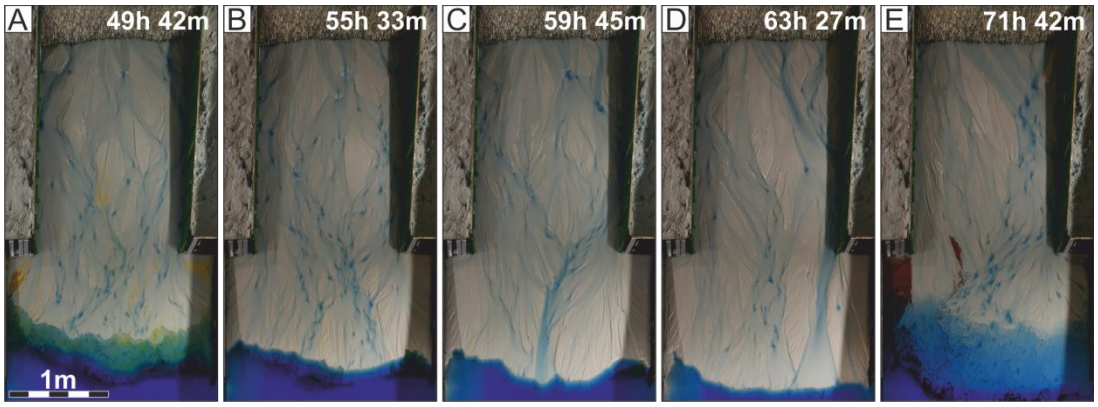

Figure 2.11 Topset morphology of E2_M1 during sea-level cycle 3. (a) Highstand Normal Regression, the entire surface area of the topset is frequently wetted. (b) Early Forced Regression, small interfluves emerge that are regularly eroded, (c) Incised valley formation during late Forced Regression initiates at the shoreline of the deep basin, (d) Valley widening due to lateral migration of the incised valley mouth during progradation (e) Transgression of the distal topset, continued upstream erosion from previous sea-level fall results in diachroneity of the sequence boundary.

The curvature and grade of the longitudinal profile, and sediment bypass show close correspondence to relative sea-level variations. The highest bypass rates are observed during late sea-level fall and lowstand and coincide with increasing curvature and longitudinal grade percentages (i.e. longitudinal profiles become less concave and steeper; Fig. 2.9f - h, 8 – 16, 32 – 40, 56 – 64 hour). Low sediment bypass occurs during the sea-level rise and coincides with a decreasing curvature percentage and decreasing longitudinal grade (Fig. 2.9f - h, 16 – 24, 40 – 48, 64 – 72 hour). Intermediate rates for sediment bypass, curvature and grade of the longitudinal profile occur during sea-level highstand and early sea-level fall (Fig. 2.9f – h, 0 – 8, 24 – 32, 48 – 56 hour).

During late sea-level fall in cycles 1, 2, and 3 the sediment bypass rate is 102, 63 and 126% of the sediment input, respectively (Fig. 2.9f). Sea-level fall 3 is smaller than sea-level fall 1 (30 vs. 40 mm) but results in incised valley formation and significantly higher sediment bypass (Fig. 2.9f). Valley incision coincides with an increased basin depth and a decreased concavity of the longitudinal profile (cf. Fig, 2.9c, f, 8 – 16 hour & 56 – 64 hour). Interestingly, it also coincides with a reduced longitudinal gradient in comparison with the first sea-level fall (cf. Fig. 2.9h, 16 hour & 64 hour), indicating that erosion within the incised valley occurs at a lower gradient than the estimated bypass gradient for unconfined flow along the entire width of the fluvial system.

Erosion-deposition maps also show that during sea-level fall 3 significantly more erosion occurs on the delta topset than during sea-level fall 1 (Fig. 2.12a, c). In the case of sea-level fall 3, erosion migrates upstream and results in significant erosion that persists until the end of the subsequent sea-level rise (Fig. 2.12d).

2.4.4 Experiment 2 - Basin 2 (E2_M2)

The input parameters of E2_M2 differ from E2_M1 in two ways. Firstly, water discharge is 1 m^3h^{-1} instead of 1.5 m^3h^{-1} (Table 2.1). Secondly, the system progrades on a shallow, non-subsiding ramp during sea-level fall 1, resulting in the very shallow water conditions at lowstand 1 (Fig. 2.10a, b, 8 – 16 hour).

Sediment bypass shows a similar response to sea-level variation as in E2_M1 but less sediment is bypassed overall, and the longitudinal profiles are more concave (cf. Fig. 2.9g & 2.10g). Another difference is that the curvature and grade of the longitudinal profile decrease during sea-level fall to lowstand at 16 h, whereas in E2_M1, these values increase (cf. Fig. 2.10g, h & 2.9g, h, 16 hour). This is related to the very high progradation rates that result from the shallow water depth of < 5mm (Fig. 2.10c, e, 8 – 16 hour).

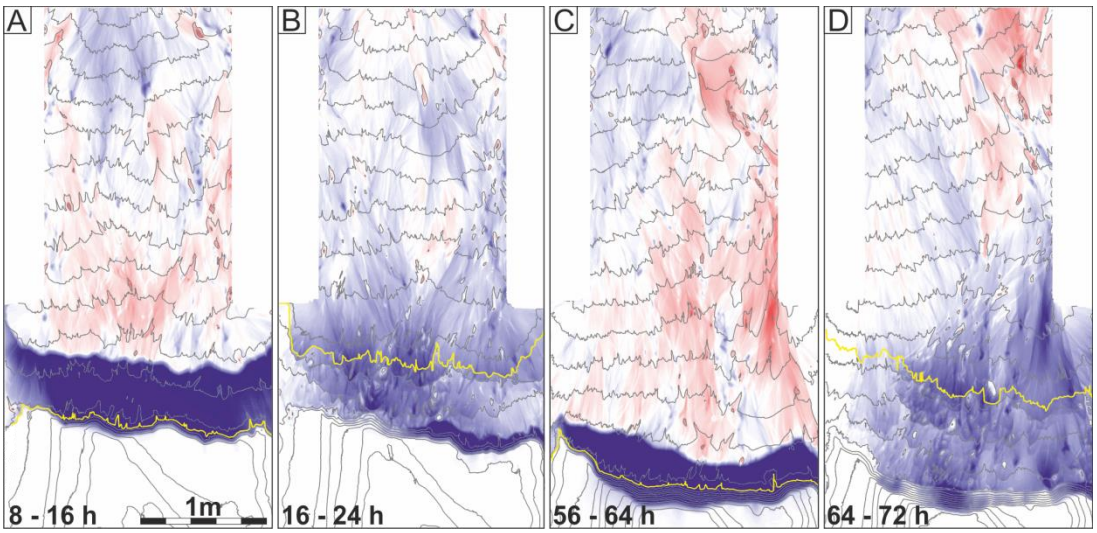

Figure 2.12 Erosion-deposition maps for E2_M1. Blue and red indicates respectively deposition and erosion; the intensity of the colours represents its magnitude. Grey contour lines are spaced at 10 mm vertical intervals and indicate topography at the end of the mapped interval. Yellow contour line represents the shoreline. (a) Lowstand 1 (8 – 16 h), relatively minor erosion and rapid progradation into the shallow basin. (b) Transgression 1 (16 – 24 h), deposition occurs along the entire longitudinal profile. (c) Lowstand 3 (56 – 64 h), erosion is more severe and has migrated far upstream. Less progradation occurs than in lowstand 1 due to the significantly deeper basin. (d) Transgression 3 (64 – 72 h), erosion related to the previous sea-level fall continues updip during the entire sea-level rise while the coastline is characterized by back-stepping lobes on the lowstand shelf.

2.4.5 Grain-size experiments

The distorted-scale models indicate that the curvature and grade of the longitudinal profile are both dependent on the rate of progradation. A weir obstructed progradation in Scenario 1 and resulted in a steep and nearly linear longitudinal profile that did not aggrade significantly after 5.5 h (Fig. 2.13a). In Scenario 2, the length of the fluvio-deltaic system increased from 4 to 5.5 m and resulted in a significantly more concave longitudinal profile (Fig. 2.13d). Additionally, the achieved gradient in the experiment with fixed length is significantly steeper than in the experiment with progradation ([1:107] vs. [1:180]), although sediment and water discharge were the same in both experiments (cf. Fig. 2.13a & 2.13d; Table 2.1).

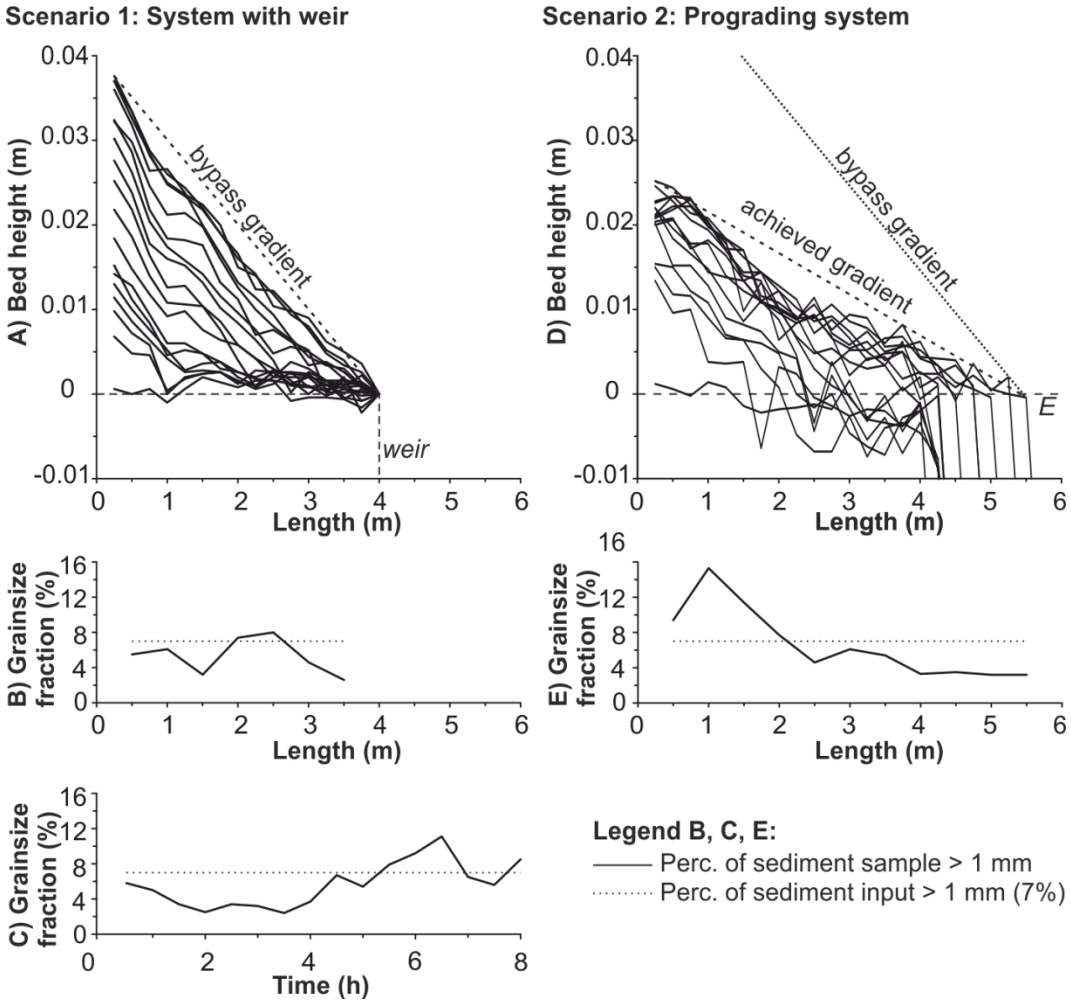

Figure 2.13 Longitudinal gradients and downstream fining trends. (a) Longitudinal profiles for Scenario 1 through time. The final profiles overlay each other, implying full sediment bypass along a bypass gradient. The dashed line represents initial bed height and position of weir. (b) Sediment samples collected along the final longitudinal profile indicate that the coarse-grained fraction (> 1 mm) is present along the entire profile without a clear downstream fining trend. (c) Grain-size samples collected below the downstream weir from 0 – 4 h are depleted of coarse-grained sand (> 1 mm), indicating downstream fining. From 4.5 h onwards, input and output of coarse-grained sand (> 1 mm) are roughly equal indicating that no downstream fining occurs. The peak in coarse-grained sand (6.5 h) might indicate progradation of a gravel front that accumulated upstream during the earlier stages of the experiment. (d) Longitudinal profiles for Scenario 2. Dashed line indicated by E indicates sea level and initial bed height. Bypass gradient is equal to Scenario 1. (e) Grain-size samples collected along the final longitudinal profile indicate that the coarse-grained fraction (> 1 mm) is mainly retained in the steep, proximal part of the system (0 – 2 m).

Grain-size data collected below the downstream weir (Fig. 2.5) indicate that after 4.5 h significant volumes of coarse-grained sand bypassed the weir, while samples along the final longitudinal profile do not indicate a downstream fining trend (Fig. 2.13b). In Scenario 2, coarse-grained sand is preferentially retained in the relatively steep, upper reach of the longitudinal profile (Fig. 2.13e).

2.5 Controls on Fluvial Profile Shape and Fluvio-Marine Sediment Partitioning

2.5.1 Basin depth

With constant sea level, prograding systems cannot achieve system-scale static equilibrium (Fig. 2.6f, h; 2.14a - d; Muto and Swenson, 2005). In shallow water conditions, such as occur at the start of E1_M1 and E1_M2, fluvio-deltaic systems require limited sediment volumes to prograde rapidly. This results in strongly concave profiles at significantly lower gradients than the bypass gradient (Fig. 2.7f, h, 0 – 48 hour; 2.14b). Such systems transport sediment inefficiently and deposit the bulk of their sediment load in the fluvial domain (e.g. Fig. 2.7f, 0 – 48 hour). The progradation rates in deep basins are significantly lower and allow the longitudinal profile to aggrade to a steeper gradient (i.e. approach the bypass gradient; e.g. Fig. 2.6e, h, 48 – 96 hour). Such systems transport sediment more efficiently and partition a significantly larger percentage of their sediment load to the shoreline (Fig. 2.6f, 48 – 96 hour; 2.14c).

Progradation will gradually slow in fluvio-deltaic systems that build into a spatially deepening water body (e.g. Fig. 2.6c, e) and allow the longitudinal profile to become steeper and less concave (Fig. 2.6g, h; 2.14d). This increases the efficiency of sediment transport and enhances sediment transport to the shoreline (Fig. 2.6f; 2.14d). Therefore, a shift in the longitudinal sediment partitioning can be expected in spatially deepening basins, over time depositing a smaller percentage of the sediment load in the fluvial and delta top systems and more in the progradational delta front and slope clinoform sequences (Fig. 2.6f; 2.14d). This process provides a potential mitigation mechanism for autoretreat (Muto, 2001; Muto and Steel, 2002a) that is further discussed in the autostratigraphy paragraph.

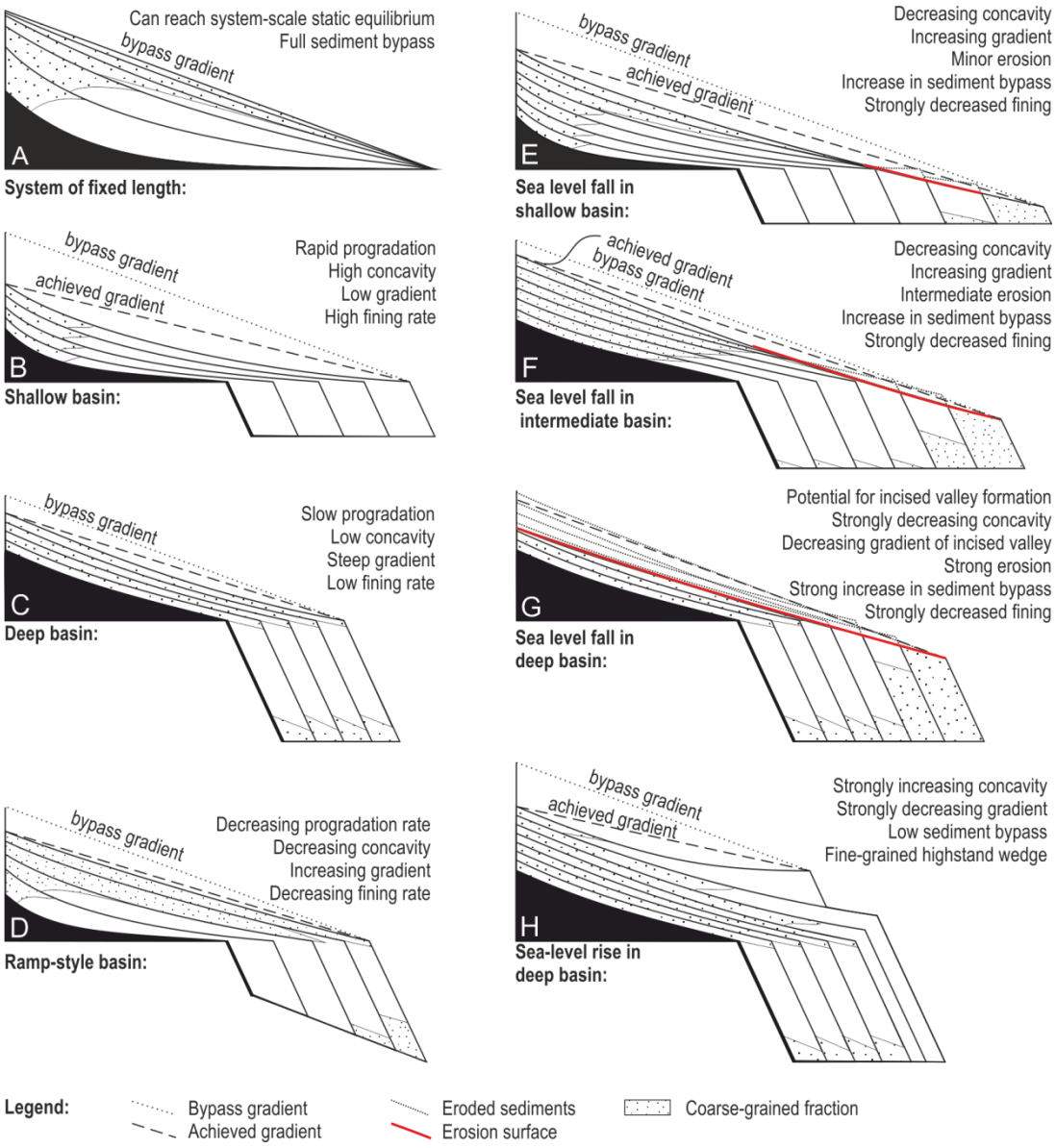

Downstream sediment fining occurs in both gravel- and sand-bed rivers and is mainly dependent on selective transport, although abrasion processes are also important in gravel-bed rivers (Frings, 2008; Paola et al., 1992b). Selective transport is ineffective in static equilibrated longitudinal profiles: fine-grained sand is more quickly transported than coarse-grained sand but the latter will arrive as well, removing the downstream fining trend (Fig. 2.14a). However, if a profile is below system-scale static equilibrium, selective transport as a result of downstream decreases in bed shear stress (Knighton, 1999; Rice and Church, 2001) or a downstream decrease in capacity to transport the coarse grains by suspension transport (Frings, 2008) can result in stable downstream fining trends in the rock

Figure 2.14 (previous page) Influence of basin depth on the longitudinal grade of sedimentary systems. Gradients and curvature are exaggerated. (a) In a system of fixed length equilibrium profiles can develop in which the sediment input is equal to the sediment output. (b) In sedimentary systems prograding into shallow basins, high progradation rates lead to strongly concave longitudinal profiles in which coarse sediment is largely retained upstream. (c) In deep basins the longitudinal profile can grade closely towards equilibrium because of low progradation rates, resulting in high sediment transport rates to the coastline and limited downstream fining. (d) Ramp basins will show a progressive grading towards equilibrium conditions and a decrease in downstream fining. (e) Sea-level fall in shallow basins or on a shelf. Rapid progradation will impede erosion but sea-level fall will still lead to an increase in grade, sediment bypass and reduced downstream fining. In exceptionally shallow settings, grade and concavity can be reduced. (f) Sea-level fall in basins of moderate depth leads to significant erosion and high sediment supply rates during late falling stage and lowstand. (g) Sea-level fall in deep basins will have the highest likelihood of generating incised valleys during sea-level fall, leading to high sediment bypass rates, and within the incised valley lowering the bypass gradient. (h) Sea-level rise increases concavity of the longitudinal profile and strong downstream fining, resulting in fine-grained highstand systems aggrading on the lowstand shelf deposits.

record (Fig. 2.14b, c). In Scenario 1, a nearly linear longitudinal profile develops after ~5.5 h. Longitudinal profiles at successive time steps overlap this profile, implying that the system has aggraded to an approximate bypass gradient (Fig. 2.13a; 2.14a). This approximately coincides with the arrival of coarse-grained sediment at the downstream weir in similar quantities as in sediment input (Fig. 2.13c). Downstream grain size sorting has thus become ineffective, which is further confirmed by the grain size distribution along the final longitudinal profile (Fig. 2.13b; 2.14a).

In Scenario 2, a progradational system developed with a low gradient, concave profile (Fig. 2.13d; 2.14b). Here, coarse-grained sand is retained in the steep upper reach of the fluvial profile, indicating that the transport capacity at lower gradients is insufficient to transport the coarse-grained sand fraction. The difference between both experiments suggests that the downstream fining rate correlates with the concavity and grade of the longitudinal profile (e.g. Wright and Parker, 2005a, 2005b) that in turn depend on basin depth. Changes in basin depth thus influence the

depositional character in the fluvial to marine domain and form a downstream allogenic control on the volume and grain size of available sediment that can potentially be remobilized and distributed into deeper marine environments (Fig. 2.14b - d).

2.5.2 Subsidence

E1_M2 examines the effects of basin depth and subsidence. Shallow water progradation during the first half of the experiment allows for high progradation rates in comparison to E1_M1 (cf. Fig. 2.7c, e & 2.6c, e). This results in a concave, low gradient longitudinal profile (Fig. 2.7g, h) and results in low sediment bypass volumes (Fig. 2.7f; 2.14b). From 48 h onwards, rapid subsidence results in much slower progradation and low sediment bypass rates (Fig. 2.7e, f). It also initiates a continuous increase in the grade and decrease in the concavity of the longitudinal profile (Fig. 2.7g). From 80 h onwards, sediment bypass into the subsiding basin increases to higher levels than bypass into the shallow basin before subsidence was initiated, even though the high subsidence rate is maintained (Fig. 2.7b, f). Subsidence therefore has two counteracting effects: subsidence upstream of the shoreline requires additional sedimentation and potentially increases the concavity of the longitudinal profile (Sinha and Parker, 1996). However, it also reduces the progradation rate by increased deposition on the topset and by an increase in clinoform height, allowing the fluvio-deltaic system to grade towards equilibrium. In this experiment, progradation across a rapidly subsiding basin (from 48 h onwards) was more efficient in bypassing sediment to the shoreline than the static shallow-water system (from 0 – 48 h) due to this increase in basin depth (Fig. 2.7f; 2.8c, d; 2.14d).

2.5.3 Sea level

In E2_M1, glacio-eustatic sea-level variations influence sedimentation in a basin that subsides at a constant rate (Fig. 2.9a, b). High-frequency sea-level variations form a strong additional control on the grade of the longitudinal profile (e.g. Blum and Hattier-Womack, 2009). As a first order approximation, a sequence-stratigraphic interpretation based on sea-level variations alone provides a good

explanation for the stratigraphic stacking pattern (Fig. 2.8e, f). During sea-level rise, the downstream reaches of the fluvio-deltaic system are aggradational and step back on the lowstand shelf (Fig. 2.11e). Sea-level rise predominantly raises the lower reach of the longitudinal profile, resulting in strongly concave profile, shifted away from the bypass gradient (Fig. 2.9g, h; 2.14h). During falling sea level, the lower reaches of the longitudinal profile are eroded while deposition continues upstream of sea-level influences (e.g. Fig. 2.12a). This generates a nearly linear profile that is close to the bypass gradient (Fig. 2.9g, h) and results in efficient sediment transport to the coastline (Fig. 2.9f; 2.14e, f). However, a sequence-stratigraphic solution based solely on sea-level fluctuations cannot explain why an incised valley only formed during the moderate sea-level fall 3 (30 mm, Fig. 2.12c, 48 – 64 h), and not in the larger sea-level fall 1 (40 mm, Fig. 2.12a, 0 – 16 h).

Coastal incised-valley initiation requires deep local erosion, and is typically triggered by relative sea-level fall (Strong and Paola, 2008). This occurs when a system locally becomes significantly above grade. These experiments indicate that the significant basin depth results in a low shoreline progradation rate (Fig. 2.6c, e) and a longitudinal profile that is close to equilibrium (e.g. Fig. 2.6h; 2.14c). This leads to a steep descending shoreline trajectory (Helland-Hansen and Hampson, 2009) during sea-level fall, which may cause the longitudinal gradient to become above the bypass gradient, triggering incised valley formation (Fig. 2.11; 2.12; 2.14g). After incised valley inception, discharge is funnelled through a narrow section of the fluvial system. This results in a lowering of the bypass gradient (cf. Fig. 2.9h, 16 & 64 h), causing increased and prolonged erosion (Fig. 2.9f; 2.14g). In the sea-level fall 3, erosion migrates upstream and persists till the following sea-level highstand (Fig. 2.12d). Erosion has thus decoupled from sea-level fall and is maintained by the lowering of the fluvial gradient within the incised valley, allowing for an increased diachroneity of the sequence boundary (cf. Fig. 2.12b & 2.12d; Strong and Paola, 2008). Conversely, in shallow basins, the gradient of rapidly prograding systems is further removed from the bypass gradient. Additionally, a similar sea-level fall will result in a more gradual descending shoreline trajectory due to the higher progradation rates. Therefore, the rate of sea-level fall needs to be much more dramatic to steepen the longitudinal profile sufficiently to cause it to become above grade and trigger incision. Basin depth thus strongly modulates the

sensitivity of the sedimentary system to the formation of incised valleys during sea-level fall.

Furthermore, the incised valley of E2_M1 initiated in the deep zone of the experimental basin (Fig. 2.2; 2.11c) and it is speculated that this is the most likely position, rather than lateral positions in the shallow to intermediate depth zones (Fig. 2.2). In basins with lateral depth differences, the deep segments will require relatively longer time spans of fluvial activity to infill. Additionally, the avulsion frequency might be reduced in such segments because it appears to be partially controlled by the lengthening of the distributary channels (Edmonds et al., 2009). Therefore, it is likely that channels are present at positions feeding into the deepest part of basins for prolonged periods, enhancing the probability of incision at such locations. Such control on the lateral position of incised valleys within basins is thought to be relevant mainly in systems with large lateral variation in basin depth along short distances such as rift basins.

In E2_M2, the longitudinal curvature and grade are more strongly affected by the rapid progradation rate than by the relative sea-level fall from 8 - 16 h (Fig. 2.10e). This causes the fluvio-deltaic system to move away from equilibrium, whereas in other occurrences equilibrium is approached during sea-level fall (Fig. 2.10g, h). The former scenario might occur in shallow basins or on wide shelves where sea-level either does not fall below shelf-edge or before it falls below shelf edge. In such cases, the reduction of the longitudinal gradient might result in aggradation rather than incision of the fluvio-deltaic succession even during sea-level fall (Ethridge et al., 1998; Petter and Muto, 2008; Prince and Burgess, 2013; Swenson and Muto, 2007; Wallinga et al., 2004).

2.5.4 Water-sediment discharge ratio

The ratio between water and sediment discharge forms an additional control on sediment transport and valley incision (Bijkerk et al., 2013) that is highlighted by the differences between E2_M1 and E2_M2 (Fig. 2.8; 2.9; 2.10). An increased water to sediment ratio results in more efficient sediment transport at lower gradients (e.g. Simpson and Castelltort, 2012). In E2_M1, the water to sediment ratio is 1.5 times higher than in E2_M2. This results in a ~1.2 times lower longitudinal gradient and between 1 to 1.5 times higher sediment bypass rates during sea-level fall, implying

significantly more deposition in the delta front (Fig. 2.8). Additionally, higher water discharge results in shorter equilibrium timescales (e.g. Paola et al., 1992a), which implies that a system can adapt more quickly to changing conditions such as sea-level fall. In E2_M1, the high water to sediment ratio resulted in low concavity and approximate equilibrium conditions during sea-level fall 1 (Fig. 2.9g, h). During sea-level fall 3 more favourable basinal conditions eventually triggered valley incision. In E2_M2, the longitudinal profile remained significantly more concave, resulting in lower sediment transport rates to the coastline indicating deposition on the topset (Fig. 2.10f, g). Therefore, the sedimentary system has not approached equilibrium closely, making it less prone to significant erosion and valley incision. Note however that relative sea-level fall is more modest as well which further limits the probability of incised valley formation (cf. Fig. 2.9b & 2.10b).

2.5.5 Autostratigraphy

Autostratigraphic principles (Muto et al., 2007) state that sedimentary systems influenced by constant discharge and a constant rate of relative sea-level rise may transition from initial normal regression, where sediment supply is still in excess of the accommodation creation, into transgression or "autoretreat". This is due to the increasing budget required to aggrade both slope and topset of the sedimentary system (Muto, 2001). At the autoretreat break, the increasing size of the system reaches a tipping point at which sediment supply cannot support further progradation, and 100% of the sediment load is partitioned to the topset. A subsequent increase in the topset area due to landward onlap can cause the system to autoretreat (Muto and Steel, 2002a).

The present results reveal an autoretreat mitigation mechanism. Relative sea-level rise implies progradation into increasing water depths, resulting in a slowing of the progradation rate. This leads to an adjustment of the grade and curvature of the longitudinal system and an increasing efficiency of sediment transport to the shoreline, thereby increasing the part of the sediment that is used to aggrade the slope, and decreasing the part of the sediment that is used to aggrade the topset. This mechanism of increasing fluvial transport efficiency during progradation into a deepening basin is well-illustrated in E1_M1. Here, the partitioning of sediment to the basin doubles during progradation into a basin of increasing depth (Fig. 2.6c, f),

despite a twofold increase in topset area (Fig. 2.6d) (note that relative sea level is static and the basin depth increase refers to a spatial increase). In E1_M2, a constant subsidence rate from 48 h onwards initially slows the progradation rate, which leads to an increased grade and decreased concavity. This results in increasing fluvial efficiency and increasing sediment bypass towards the end of the experiment (Fig. 2.7). Whilst not excluding the possibility of autoretreat, these results indicate that enhanced fluvial efficiency as a consequence of increasing basin depth may counter or delay its occurrence.

From 56 h onwards, both the curvature and grade of the longitudinal profile remain constant in E1_M1 (Fig. 2.6g, h). This suggests that the fluvial system does not increase its efficiency of routing sediment to the shoreline anymore. The increasing topset area (Fig. 2.6d) requires increasing amounts of sediment, as is reflected in the slow decrease in the sediment-bypass percentage (Fig. 2.6f) implying that autostratigraphic principles apply in a straightforward manner.

2.6 Application

2.6.1 Case study 1: Maastrichtian Fox Hill - Lewis shelf margin, Southern Wyoming

The Maastrichtian Fox Hill - Lewis shelf margin of Southern Wyoming is a well-studied shelf-margin succession that can be used to test the concepts from analogue modelling in a setting that is not influenced by high-amplitude, high-frequency glacio-eustatic variation, analogous to Experiment 1 in this study.

Over a period of 1.8 Myr, rapid shelf-margin accretion resulted in the formation of 15 clinothems (Fig. 2.15a; Carvajal, 2007; Carvajal and Steel, 2009; Carvajal and Steel, 2006) that can be subdivided into two stages. The first stage is deposited in a rapidly subsiding basin and is represented by clinothems C0-C9 (Fig. 2.15a). Based on the gradually rising shoreline trajectory, an overall deepening from ~250 to 600 m is recorded. Subsidence is directly linked to tectonic activity in the source area; Stage 2, represented by clinothems C10-15, initiates when thrusting and uplift in the source area ceases (Fig. 2.15a). These clinothems form a progradational

succession in a basin of constant depth, as reflected by the horizontal shoreline trajectory (Fig. 2.15a; Carvajal and Steel, 2006).

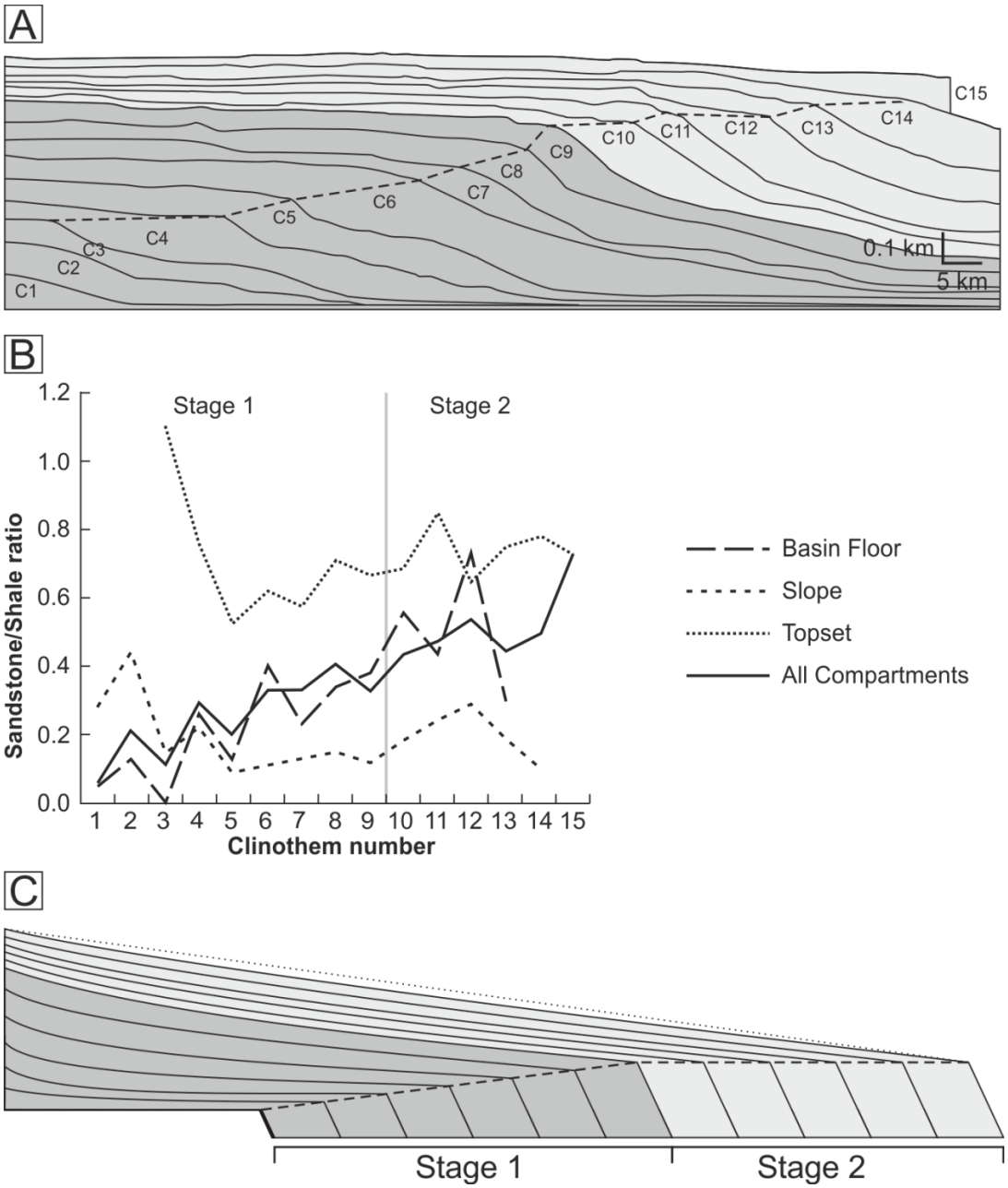

Figure 2.15 (a) Clinothem succession of the Maastrichtian Fox Hill – Lewis Shelf Margin, Southern Wyoming. Note that the aggradational succession in Stage 1 (C1-C9) represents a relative sea-level rise, and Stage 2 (C10-C15) a progradational succession during relative sea-level still stand. Simplified from Carvajal and Steel (2006). (b) Sand/shale ratios for individual clinothems. Modified from Carvajal (2007). (c) Alternative interpretation of sediment volume and grain size trends, with strongly exaggerated gradients in which the differences in sediment supply and grain size are attributed to the response of the longitudinal profiles to changes in basin depth and basin development.

The average sediment supply rate calculated for Stage 1 is ~747*109 m^3 / 100 kyr; the progradational succession of Stage 2 has a slightly higher sediment supply rate of 845*109 m^3 / 100 kyr during a period of tectonic inactivity (Carvajal, 2007). Carvajal (2007) considers the increase in sediment supply counter-intuitive since the cessation of thrusting in the source area is expected to correspond to a decrease in the sediment yield. The increase in sediment yield is therefore linked by Carvajal (2007) to modest uplift due to isostatic rebound of the source area. Additionally, the basin floor and overall sand/shale ratio increase over time, which has been ascribed to erosion of increasingly sandy source rock (Fig. 2.15b; Carvajal, 2007).

As an alternative hypothesis, it is suggested that both the increase in sediment volume and the increase in sand/shale ratio can be explained by the progressive increase in basin depth during Stage 1 and the cessation of relative sea-level rise at the transition from Stage 1 to Stage 2. The sea-level stillstand allows the longitudinal profile to grade closer towards equilibrium (Fig. 2.15c). This enhances the sediment bypass rate and allows transport of coarser-grained sediment into the basin, which increases the sand/shale ratio in both the basin floor, and overall (Fig. 2.15b).

2.6.2 Case study 2: Eocene Central Basin, Spitsbergen

The Eocene Central Basin of Spitsbergen provides several outcrops of well-preserved shelf-margin clinothem complexes. Sea-level cyclicity is estimated at ~300 kyr duration (Crabaugh and Steel, 2004). Two contrasting shelf-margin types, Type I and II, developed simultaneously within the region (Plink-Björklund and Steel, 2005) and demonstrate the influence of basin depth and progradation rate on incised valley formation.

Type I shelf margins are characterized by severe erosion in the falling stage shelf-edge deltas, accompanied by the formation of significant basin floor fans that are fed from across a disrupted slope (Plink-Björklund and Steel, 2005). Shelf margin accretion occurs mainly during the late lowstand and in water depths of 300 – 350 m (Plink-Björklund and Steel, 2005; Steel et al., 2007). Type II shelf margins are characterized by the absence of a basin floor fan and accrete with an amalgamated succession of falling stage, early and late lowstand deltas. Falling stage deltas are notably highly progradational. Of Type II margins, only the

Reindalen clinothems (numbers 26-27) show complete exposures including the clinothem top. In these clinothems, water depth is estimated at ~200 m (Plink-Björklund and Steel, 2002; Plink-Björklund and Steel, 2005; Plink-Björklund and Steel, 2007).

Both clinothem types are coeval, and sea level is interpreted to fall below the shelf edge in both shelf-margin styles (Plink-Björklund and Steel, 2005). Therefore, the different character is dependent on other inherent characteristics of these shelf types. Plink-Björklund and Steel (2005), suggest that higher rates of sediment fallout at the shelf-edge and upper slope during the falling stage in Type II shelf margins dampens incision and prevents deep channeling at the shelf edge. Alternatively, the shallow water depth of Type II clinothems facilitates high progradation rates, impeding incision due to the resultant low gradient of the descending shoreline trajectory (cf. Fig. 2.7e, f, 0 – 16 hour; 2.14e; Holbrook et al., 2006). Deeper basins in which Type I clinothems form are characterized by slower progradation rates, resulting in a steeper shoreline trajectory with the same rate of sea-level fall. This causes the longitudinal profile to become above grade and allows for sufficient shelf incision to generate incised feeder channels (cf. Fig. 2.7e, f, 48 – 64 hour; 2.14g; Strong and Paola, 2008). Consequently, the likelihood of shelf incision during sea-level fall increases with basin depth, resulting in the different development of Type I and Type II deltas. Dependent on the depth of the receiving basin, both the timing of shelf margin progradation differs and the gross architecture of basin infill is altered.

2.7 Conclusions

Analogue modelling is used to examine the impact of basin depth, subsidence, and relative sea-level variations on the temporal development of sedimentary architecture, focusing on the relationship between the grade of the longitudinal profile and the sediment partitioning between the fluvio-deltaic system and the basin. Fluvio-deltaic systems grade towards a longitudinal equilibrium gradient, at which the full sediment load is bypassed through the system thereby maintaining a static longitudinal profile. Progradational systems cannot achieve this state because lengthening of the longitudinal profile lowers the longitudinal gradient unless the fluvio-deltaic system aggrades. Therefore, this generates a departure from system-

scale static equilibrium that is governed by the progradation rate. Basin depth, subsidence, and sea-level variations act as allogenic controls on the migration of the shoreline. This affects the development of the longitudinal profile and therefore controls fluvial to marine sediment partitioning.

Shallow basin depth results in rapid lengthening of the sedimentary system. Therefore, the longitudinal profile has a low gradient, which results in significant deposition in the fluvial domain and strong downstream fining of the sediment load. In deep basins, progradation rates are significantly lower, allowing the longitudinal profile of sedimentary systems to steepen and approach equilibrium more closely. This results in high sediment supply to the shoreline with limited downstream fining. Increasing basin depth leads to a shift in the partitioning of sediment between the fluvial and marine domains. Basin depth thus influences the sediment partitioning of sedimentary systems and forms a first order control on the availability of sand-rich sediments that can potentially be remobilized and redistributed into deeper marine environments.

Subsidence has a dual effect: it can increase the concavity of the longitudinal profile and increases deposition on the topset, thus limiting sediment transport to the coastline. Counterintuitively, the resultant slow progradation rates allow the fluvio-deltaic system to grade towards equilibrium, eventually increasing sediment transport rates.

Sea-level variations rapidly alter the fluvio-deltaic longitudinal gradient. In deep basins, low progradation rates result in steep descending shoreline trajectories during sea-level fall, generating significantly greater erosion than in shallow basins. Deep basins therefore result in higher sediment yields at the shoreline and an increased probability of incised valley formation. The latter can alter the timing of shelf margin progradation and its gross morphology and therefore affect the transfer of sediment to deep marine sinks. The experimental results indicate that, during glacio-eustatic sea-level cyclicity, the longitudinal profile is closest to equilibrium during falling sea-level and early lowstand. This results in efficient sediment transport towards the shoreline, explaining delivery of increased sediment volumes of increasing grain size to lowstand systems tracts as a sea level and basin-depth-controlled parameter.

3 Allogenic Controls on Stratigraphic Architecture of the Carboniferous Craven Basin

3.1 Abstract

Sequence-stratigraphic analysis is applied to two sea-level cycles of the fluvio-deltaic succession on the Carboniferous Askrigg Block and in the adjacent Craven Basin. This provides field validation for a concept derived from analogue modelling: that sea level and basin-margin morphology influence the sediment volume and grain size of deltaic deposits through variations of the gradient and curvature of the fluvial longitudinal profile. Field and literature study has revealed the presence of a slowly prograding deep water shelf margin, incised by a major valley and associated with a large turbidite deposit during the initial sea-level cycle. This succession is differentiated from an overlying regressive shallow water succession during the successive sea-level cycle. Isopach-map-derived volumetric estimates and grain-size trends for these stratigraphic units indicate a four times larger sediment volume in the deep water cycle as well as substantially coarser grain size, indicating a consistency with the analogue modelling results. Lateral variation in basin depth during deposition of the turbidite system is thought to have steered the position of the incised valley laterally towards the deepest sub-basin. Additionally, the current sequence-stratigraphic interpretation challenges the concept of tectonic uplift of the southern Askrigg Block at this time.

3.2 Introduction

Sequence stratigraphy describes longitudinal shifts in facies-belt stacking-patterns of delta or shelf clinoforms as a function of sediment supply and accommodation space (Van Wagoner et al., 1988). Eustatic sea level, tectonics and sediment supply are generally considered as the major controls on such facies-belts shifts (Schlager, 1993). During periods of glacio-eustatic sea-level variations, accommodation-space changes are a rapid, large, and generally dominant control on the sequence-stratigraphic signature. During sea-level rise and highstand, fluvio-

deltaic systems tend to deposit relatively fine-grained sediments over wide areas. During falling stage and lowstand, the specific response of the fluvio-deltaic system is strongly dependent on the relative longitudinal gradients of the fluvial system and of the exposed shelf and slope: extension and aggradation of the fluvial profile is likely if the shelf and slope gradient is shallower than the fluvial gradient, whereas erosion and incision occur when the shelf and slope gradient is steeper than the fluvial gradient (e.g. Posamentier et al., 1992; Shanley and McCabe, 1993, 1994; Posamentier and Allen, 1999). This difference in response can also be related to the larger sediment storage capacity of steep shelf margins close to the delta front, which results in relatively slow progradation rates and thus a more steeply descending fluvial profile or shelf-edge trajectory (Helland-Hansen and Hampson, 2009). As a result, ramp-style basins are more likely to record a rapidly prograding shallow marine wedge (e.g. Plint, 1988; Hunt and Tucker, 1992), whereas fluvial systems at margins of a deep basin are prone to valley incision (e.g. Ritchie et al., 2004).

Analogue modelling indicates that deep basin margins allow a fluvial system to grade closer towards equilibrium conditions (Paola et al., 1992a), therefore becoming more efficient at transporting sediment while becoming more sensitive to erosion and subsequent valley incision (Chapter 2). Incised valleys efficiently transport sand-grade sediment to narrow sections of the shelf edge (Chapter 2, Blum and Tornqvist, 2000; Blum et al., 2013) where it can be further distributed in the marine domain in correlative lowstand fans (e.g. Posamentier and Vail, 1988; Posamentier et al., 1988). Therefore, understanding the controls on (loci of) valley incision can thus help predict the gross stratigraphic architecture of fluvio-marine sedimentary systems (Chapter 2).

In the absence of other forcing mechanisms acting on the river positions, the results in Chapter 2 suggest that valley incision aligns to the deepest basin margin areas when basinal bathymetry varies significantly. In tectonically active settings, such as rift basins, bathymetric contrasts regularly occur over short distances but fault systems and tectonic lineaments might also steer the position and direction of both fluvial (Leeder and Alexander, 1987; Hickson et al., 2005; Kim et al., 2010, Blum et al., 2013) and deep marine channels (Kane et al., 2010a). In the fluvial case, this can eventually also steer the position of valley incision (Wroblenski, 2006; Plint and Wadsworth, 2006; Deibert and Camilleri, 2006; Holbrook and Bhattacharya,

2012). Post-rift basins might preserve these bathymetric contrasts while active tectonics are subdued, thus providing an ideal tectonic setting to test the results from analogue modelling presented in Chapter 2.

This chapter provides a sequence-stratigraphic reassessment of fluvio-deltaic successions on the equatorial Carboniferous Askrigg Block and Craven Basin (Fig. 3.1) for the stratigraphic interval between the Cravenoceras malhamense ($E_{1c}1$) and Cravenoceras cowlingense ($E_{2a}1$) Marine Band. The outcrop belts for this interval span from a trunk channel belt at the northern margin of the Askrigg Block to basin floor deposits in the Bowland sub-basin (Fig. 3.1; 3.2). The area provides an opportunity to study both the lateral and longitudinal facies changes of a shelf margin, adjoining a basin that reaches a depth of several hundreds of metres and to examine the relative effect of different forcing mechanisms, such as sea-level variation and basin-margin morphology on the sedimentary succession.

3.2.1 Geological setting

The Craven Basin (Fig. 3.2) forms the northern sub-basin of the Central Pennine Basin that was infilled during the Namurian, and is part of the larger Pennine Basin that also includes the Askrigg Block, Stainmore Trough, Alston Block and Northumberland Trough in a northward direction (Fig. 3.1; Waters and Davies, 2006). The entire basin province probably formed in response to late Devonian and early Carboniferous north-south extension (Fig. 3.3a; Leeder, 1982; Leeder and McMahon, 1988; Gawthorpe, 1987; Fraser and Gawthorpe, 1990, 2003; Kirby et al., 2000) resulting in a series of grabens and half-grabens that are separated by intrabasinal highs (Fig. 3.1). Many of the block and basin margins are thought to reflect reactivation of pre-existing basement lineaments from a previous Caledonian orogenic phase (Moseley, 1972; Fraser and Gawthorpe, 1990; Soper et al., 1987; Gawthorpe et al., 1989). Alternative tectonic models additionally invoke strike-slip or escape-tectonics related to the Variscan Orogeny in the south (Dewey, 1982;

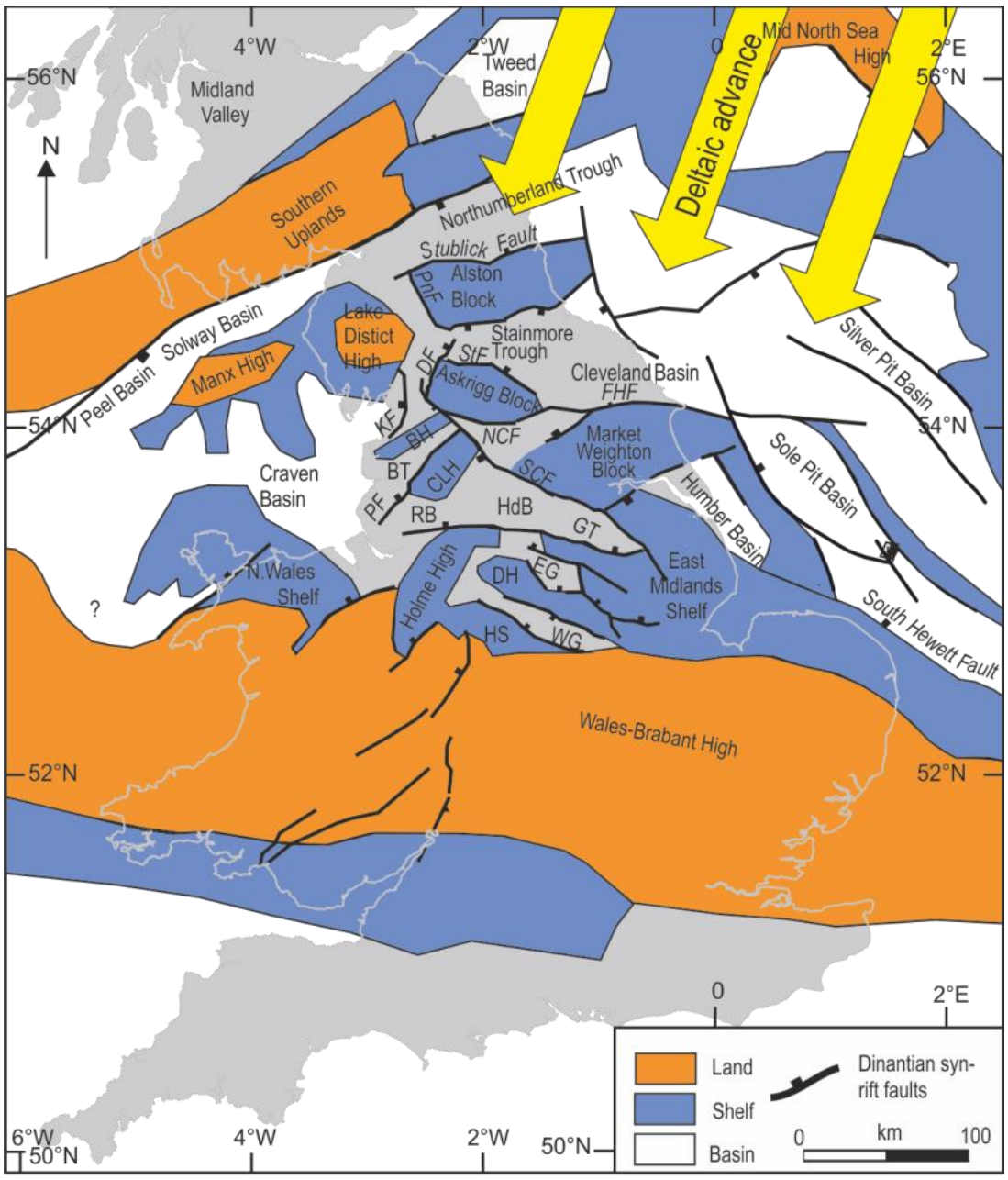

BH - Bowland High, BT - Bowland Through, CLH - Central Lancashire High, DH - Derbyshire High, EG - Edale Gulf, GT - Goyd Trough, HdB - Huddersfield Basin, HS - Hattern Shelf, RB - Rossendale Basin, WG - Widmerpool Gulf

DF - Dent Fault, FHF - Flamborough Head Fault, KF - Kendall Fault, NCF - North Craven Fault, PF - Pendle Fault, PnF - Pennine Fault, SCF - South Craven Fault, StF - Stockdale Fault

Figure 3.1 Outline of main land, shelf and basinal areas at the end of the Visean. Yellow arrows indicate the approximate direction from which the Millstone Grit Group arrived at the Central Pennine Basin during the Pendleian. Note that the northern Northumberland Trough and Stainmore Trough-Cleveland Basins were largely infilled with syn-rift deposits before the start of the Pendleian (Redrawn from Waters et al., 2009).

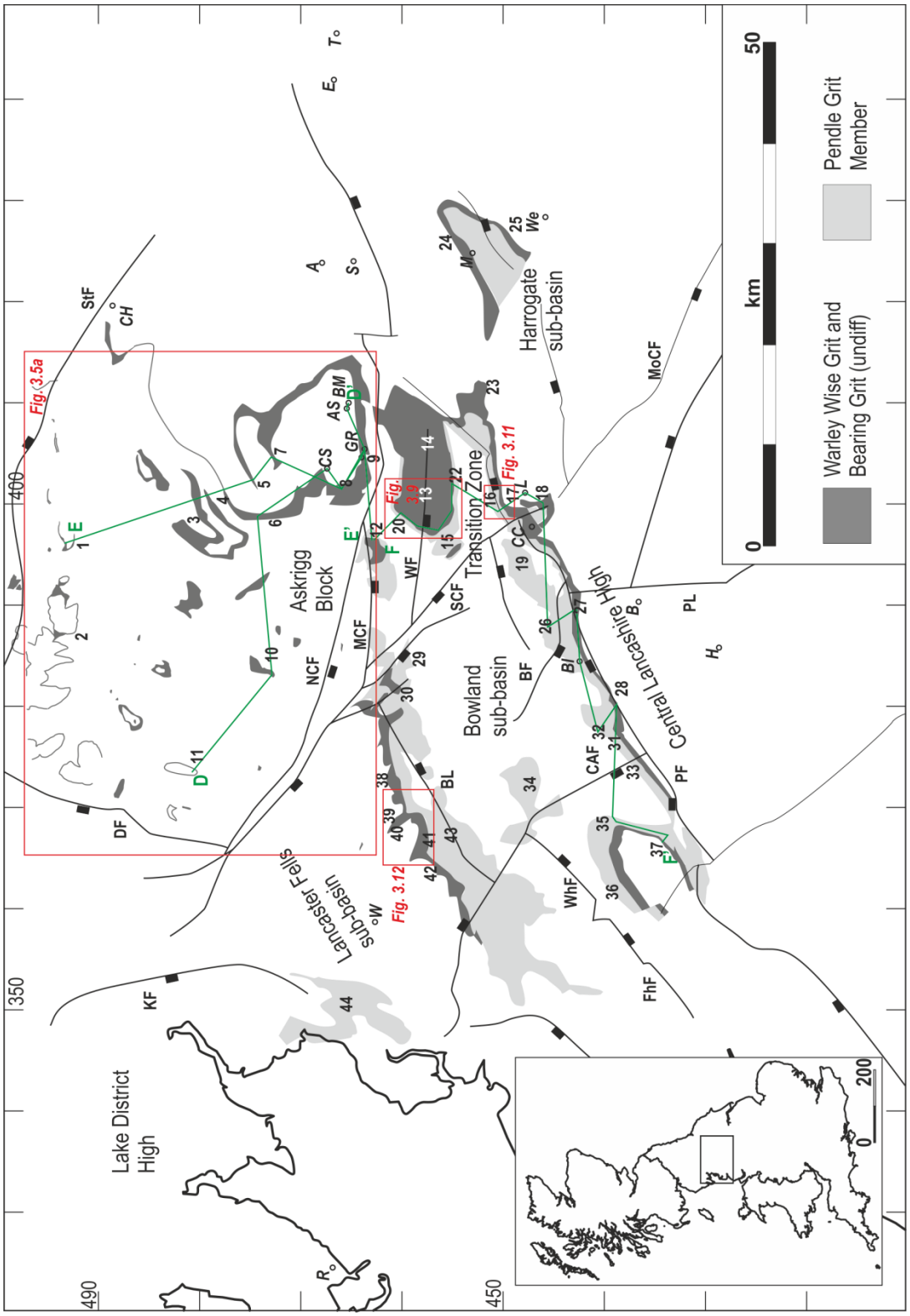
Fig. 3.5a
Fig. 3.9
Fig. 3.11
Fig. 3.12
Askrigg Block
Bowland sub-basin
Harrogate sub-basin
Transition Zone
Central Lancashire High
Lancaster Fells sub-basin
Lake District High
Warley Wise Grit and Bearing Grit (undiff)
Pendle Grit Member
km
0
50
200
StF
DF
KF
NCF
MCF
WF
SCF
BF
BL
CAF
PF
WhF
FhF
MoCF
PL
E
E'
F
D
D'
BM
AS
GR
CS
CC
BI
CH
T
E
A
S
M
We
B
H
R
W
1
2
3
4
5
6
7
8
9
10
11
12
13
14
15
16
17
18
19
20
21
22
23
24
25
26
27
28
29
30
31
32
33
34
35
36
37
38
39
40
41
42
43
44
400
350
490
450

Borehole locations
A = Aldfield 1 [42405 46810]
AS = Ashfold Side Beck No. 1 [41160 46615]
B = Boulsworth No.1 [39268 43479]
Bl = Blacko, Craven Water Board [38495 44183]
BM = Bewerley Mines No. 1B [41070 46623]
CC = Croft House, Cononley [39871 44701]
CH = Croft House, BGS [41982 48883]
CS = Coal Grove Head Shaft [40318 46703]
E = Ellenthorpe No.1 [44227 46705]
GR = Grimwith Reservoir 15 [40576 46424]
GR = Grimwith Reservoir LP18 [40612 46384]
H = Holme Chapel 1 [38608 42878]
L = Low Bradley 1 [40195 44786]
M = Moor Park Farm [42540 45330]
R = Roosecote 1, Barrow-in-Furness [32304 46866]
S = Sawley 1 [42451 46502]
T = Tholthorpe 1 [44682 46689]
W = Whitmoor 1 [46315 35874]
We = Weeton 1 [42980 44638]

Fault names
BL = Bowland Line
BF = Barnoldswick Fault
CAF = Clitheroe-Abbeystead Fault System
DF = Dent Fault
KF = Kendall Fault
MCF= Middle Craven Fault
MoCF = Morley-Campsall Fault
NCF = North Craven Fault
PF = Pendle Fault
PL = Pennine Line
StF = Stockdale Fault
SCF = South Craven Fault
ThF = Thornley Fault
WhF = Whitewell Fault
WF = Winterburn Fault

Outcrop locations:
Askrigg Block
1) Summer Lodge Beck, Swaledale [39715 49537]
2) Fossdale Gill, Swaledale [3879 4949]
3) Waldendale [40023 48098]
4) Coverdale [40123 47949]
5) Angram [40242 47603]
6) Kettlewell, Wharfedale [39972 47312]
7) How Stean Beck [4055 4728]
8) Coalgrove Beck, Yarnbury [4025 4663]
9) Hole Bottom, Hebden Beck [4025 4644]
10) Pen-Y-Ghent [3836 4730]
11) Whernside [3737 4813]

Transition zone
12) Threshfield Moor [3968 4622]
13) Barden Moor [3985 4588]
14) Barden Fell [4074 4582]
15) Flasby Fell [3957 4550]
16) Skipton Moor [4012 4504]
17) Bradley Moor [3999 4492]
18) Farnhill Moor [4009 4468]
19) Cononley Moor [3981 4475]
20) Threapland Gill [3996 4594]
22) Eastby [4029 4547]

Harrogate sub-basin
23) Beamsley Moor [4099 4524]
24) Harlow Carr Park [4276 4543]
25) Almscliff Crag [42680 44901]

Bowland sub-basin
26) Salterforth [3882 4448]
27) Noyna Rocks Quarries [38965 44264]
28) Faughs Delph Quarry [3819 4392]
29) Rathmell [3804 4599]
30) Whelp Stone Crag [37649 45949]
31) Nick O'Pendle Quarries [3772 4386]
32) Little Mearley Clough [37874 44116]
33) Wiswell Quarries [3753 4370]
34) Waddington Fells Quarries [3716 4478]
35) Leeming Quarry, Longridge Fell [36827 44057]
36) Tootle Height Quarry, Longridge [3616 4381]
37) Salesbury Hall, Longridge [3677 4359]

Lancaster Fells sub-basin
38) Bowland Knotts [3731 4609]
39) White Greet [3698 4599]
40) Far Costy Clough [36948 45952]
41) Croasdale [3673 4573]
42) Whitendale [3653 4569]
43) Baxton Fell Quarry [36815 45642]
44) Quernmore area [3490 4612]

Insert maps (red boxes)
Fig 3.5a: Askrigg Block
Fig 3.9a: Barden Moor
Fig 3.11: Skipton Moor
Fig 3.12: Bowland Knotts to Croasdale

Correlations (green lines)
D - D': Correlation Fig. 3.6a
E - E': Correlation Fig. 3.6b
F - F': Correlation Fig. 3.8

Figure 3.2 Map of the outcrop belts for the Pendleian Millstone Grit succession in the Craven Basin, based on 1:50.000 geological maps of the British Geological Survey. Borehole locations are indicated by italic letters at the map, key outcrop locations are indicated by numbers. Numbers in legend (e.g. [3879 4949]) refer to the Ordnance Survey coordinates. Tectonic lineaments are redrawn from Kirby et al. (2000).

Figure 3.3 (next page) (a) Chronostratigraphy for the Carboniferous. Dating of Namurian sub-stages based on Waters and Condon (2012), other ages are from Davydov et al. (2010). Major episodes of tectonic activity in the Craven Basin are from Kirby et al. (2000). Magnitude of Carboniferous eustatic sea-level fluctuations are based on Rygel et al. (2008), dark blue boxes indicate individual periods of major sea-level variation as recorded in the Central Pennine Basin (Waters and Condon, 2012). (b) Lithostratigraphic column for the Pendleian sub-stage, modified from (Kane et al., 2010a). 'E' refers to Genus Zone Eumorphoceras. Distinctive thick-shelled ammonoid horizons denoted in italics 'C' Cravenoceras, 'T' Tumulites.

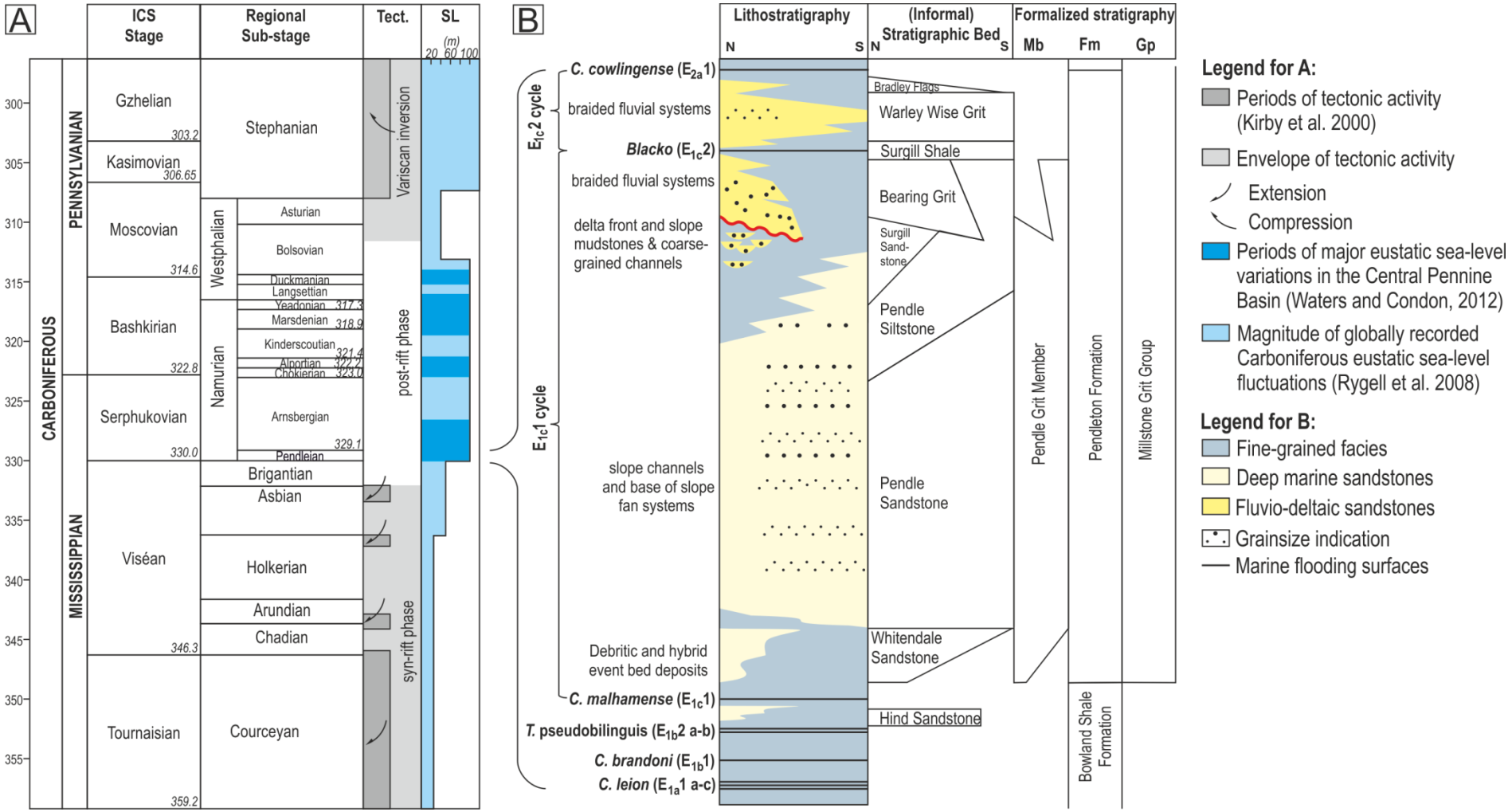
A
ICS Stage
Regional Sub-stage
Tect.
SL
(m)
20 60 100
CARBONIFEROUS
PENNSYLVANIAN
MISSISSIPPIAN
Gzhelian
303.2
Kasimovian
306.65
Moscovian
314.6
Bashkirian
322.8
Serphukovian
330.0
Viséan
346.3
Tournaisian
359.2
Stephanian
Westphalian
Asturian
Bolsovian
Duckmanian
Langsettian
Yeadonian 317.3
Marsdenian 318.9
Kinderscoutian 321.4
Alportian 322.2
Chokierian 323.0
Namurian
Arnsbergian
329.1
Pendleian
Brigantian
Asbian
Holkerian
Arundian
Chadian
Courceyan
Variscan inversion
post-rift phase
syn-rift phase
B
Lithostratigraphy
N S
(Informal) Stratigraphic Bed
N S
Formalized stratigraphy
Mb Fm Gp
C. cowlingense (E2a1)
E1c2 cycle
braided fluvial systems
Blacko (E1c2)
braided fluvial systems
delta front and slope mudstones & coarse-grained channels
E1c1 cycle
slope channels and base of slope fan systems
Debritic and hybrid event bed deposits
C. malhamense (E1c1)
T. pseudobilinguis (E1b2 a-b)
C. brandoni (E1b1)
C. leion (E1a1 a-c)
Bradley Flags
Warley Wise Grit
Surgill Shale
Bearing Grit
Surgill Sand-stone
Pendle Siltstone
Pendle Sandstone
Whitendale Sandstone
Hind Sandstone
Pendle Grit Member
Pendleton Formation
Bowland Shale Formation
Millstone Grit Group
Legend for A:
Periods of tectonic activity (Kirby et al. 2000)
Envelope of tectonic activity
Extension
Compression
Periods of major eustatic sea-level variations in the Central Pennine Basin (Waters and Condon, 2012)
Magnitude of globally recorded Carboniferous eustatic sea-level fluctuations (Rygell et al. 2008)
Legend for B:
Fine-grained facies
Deep marine sandstones
Fluvio-deltaic sandstones
Grainsize indication
Marine flooding surfaces

Coward, 1993; Maynard et al., 1997), or E-W extension related to rifting of the North Atlantic (Haszeldine, 1984, 1989), although this rift phase is commonly inferred to take place during the Cenozoic. During the late Brigantian, the Craven Basin transitioned from a syn- to post-rift tectonic phase (e.g. Gawthorpe, 1987; Kirby et al., 2000; Fraser and Gawthorpe, 2003) and thermal relaxation subsidence became the dominant structural control on basin evolution (Fig. 3.3a; e.g. Leeder, 1982).

During the Namurian, the Central Pennine Basin was diachronously infilled by the Millstone Grit Group, commencing with the Craven Basin (Ramsbottom, 1966). The Millstone Grit Group was deposited by a continental-scale coarse-grained fluvio-deltaic system (Gilligan, 1919) that was sourced from Laurentia-Baltica in the north-east (Hallsworth et al., 2000), draining an area including present-day East Greenland (Morton and Whitham, 2002). Thick clastic deposition in the Craven Basin occurred during the Pendleian and Arnsbergian regional sub-stages (Fig. 3.3) and coincides broadly with Glaciation C1 (Fielding et al., 2008; Waters and Condon, 2012). The onset of the Millstone Grit river system has been related to a major rerouting of the East Greenland fluvial system (Morton and Whitham, 2002), with a marked increase in water discharge (Cliff et al., 1991) and with a transition from a greenhouse to icehouse setting (Fig. 3.3a; Waters and Condon, 2012).

Eustatic sea-level fluctuations resulted in the highly cyclic character of the Millstone Grit Group (e.g. Ramsbottom, 1977a, 1979; Ramsbottom et al., 1978; Holdsworth & Collinson, 1988, Martinsen et al., 1995). Major sea-level rises with approximately 100 and 400 kyr periodicity (Waters and Condon, 2012) resulted in the deposition of marine mudstones, with pelagic faunas dominated by thick-shelled ammonoids (e.g. Holdsworth and Collinson, 1988). These fossils have been used to identify individual sea-level cycles, thus providing an excellent control for stratigraphic correlation. The exact timing of these maximum marine conditions has both been correlated to maximum transgression, as maximum flooding surfaces (Waters and Davies, 2006) or to peak highstand corresponding to the best connection to the open oceans (Martinsen et al., 1995). At low eustatic sea level, the Central Pennine Basin was an interior sea with tortuous connections to the open oceans, resulting in brackish or fresh water conditions (Eagar et al., 1985;

Holdsworth and Collinson, 1988) and limited development of waves and tides (e.g. Aitkenhead and Riley 1996; Brettle et al., 2002, Wells et al., 2005).

Radiometric dating and marine band occurrences indicate that the period of eustatic cyclicity during the Pendleian and Arnsbergian interval is approximately 100 kyr (Fig. 3.3; Waters and Condon, 2012). Here, two of these cycles are examined: the lower cycle initiates at the Cravenoceras malhamense Marine Band ($E_{1c}1$), the second cycle initiates with the Blacko Marine Band ($E_{1c}2$). At the top of the succession the Cravenoceras cowlingense Marine Band ($E_{2a}1$) indicates the top of the examined interval and the start of the Arnsbergian sub-stage.

3.2.2 Structural framework

The northern margin of the Craven Basin is flanked by the Askrigg Block, a large, north-tilting rift block (Fig. 3.2) that is underlain by the Wensleydale Granite batholith (Bott, 1961, Dunham, 1974). The Askrigg Block remained a shelfal area during the Visean and Serphukovian and underwent only minor tectonic deformation. It is separated from the Craven Basin by the Craven Fault system (Fig. 3.2). Near the Lancaster Fells and Bowland sub-basins, the Middle Craven Fault trends NW-SE and accommodates most displacement (Fig. 3.2; Kirby et al., 2000). From the western margin of the Bowland sub-basin eastwards, the Craven Fault system splays and starts to interact with intra-basinal faults (Fig. 3.2). The North Craven Fault trends E-W and merges with the Middle Craven Fault near Grassington (Arthurton et al., 1988). The South Craven Fault continues along a NW-SE trend and forms the NE-boundary for the Central Lancashire High, which forms a SE-tilted intra-basinal tiltblock-high (Fig. 3.2). The Central Lancashire High was emergent and tectonically active up to the Visean but was drowned during the Pendleian (Kirby et al., 2000). The triangular area between the North and South Craven Faults, and the northward extension of the Pendle Fault is referred to as the Transition Zone (Fig. 3.2; Kirby et al., 2000). This area contains numerous southward-throwing normal faults creating a stepped morphology (Arthurton, 1984). The Pendle Fault forms the bounding fault for the NW-side of the Central Lancashire High (Fig. 3.2). Parallel to this trend, the Bowland Line defines the crest of the Bowland High, a NE-tilted intra-basinal high that separates the Lancaster Fells and Bowland sub-basins (Fig. 3.2; Arthurton et al., 1988; Kirby et al., 2000).

The eastern area of the Craven Basin is referred to as the Harrogate sub-basin (Fig. 3.2; e.g. Kirby et al., 2000). During the Visean, it probably formed a northward-dipping halfgraben, bounded by the North Craven Fault, separating it from the Askrigg Block in the west and the Cleveland Basin in the east (e.g. Fraser and Gawthorpe, 2003). Internally, the Harrogate sub-basin is dissected by numerous WSW-ENE-trending faults that form en-echelon with the northeastward continuation of the Pendle Fault. The southern margin of the Harrogate sub-basin is poorly resolved due to limited seismic and borehole data (Cooper and Burgess, 1993; Kirby et al., 2000) but is flanked by the Market Weighton Block (Fig. 3.1; Fraser and Gawthorpe, 2003).

During the Namurian, active extension had largely ceased and the arrival of sediments of the Millstone Grit Group infilled the inherited rift-formed bathymetry (Fig. 3.3a; Kirby et al., 2000). However, active uplift of the southern margin of the Askrigg Block has been invoked to explain the intra-$E_{1c}1$ unconformity surface at the base of the Pendleian Millstone Grit Group on the Askrigg Block (Chubb & Hudson, 1925; Rowell and Scanlon, 1957a; Dunham and Wilson, 1985; Gawthorpe et al., 1989; Brandon et al., 1995), an interpretation that will be challenged later in this study. In the Craven Basin, a simultaneous period of tectonic activity is also inferred (e.g. Arthurton, 1984; Kane, 2010; Kane et al., 2010a).

3.2.3 Stratigraphic Framework

3.2.3.1 Transgressive surfaces in the Craven Basin

In the Craven Basin, transgressions and highstands during the Pendleian are associated with goniatite-bearing marine intervals in an otherwise unfossiliferous succession (Fig. 3.3b; 3.4a; Bisat, 1923; Ramsbottom et al., 1962, 1978; Ramsbottom, 1974; Brand, 2011; Waters and Condon, 2012). The base of the Pendleian occurs in the Bowland Shale Formation and is defined at the level of the Cravenoceras leion Marine Band ($E_{1a}1$), which consists of three closely-spaced (metre-scale) intervals containing goniatites ($E_{1a}1$a-c) separated by barren mudstones (Fig. 3.4; Waters and Condon, 2012). The Cravenoceras brandoni Marine Band ($E_{1b}1$) forms the next marine surface and is followed by two transgressions indicated by *Tumulites pseudobilinguis* ($E_{1b}2$ a-b) bearing shales (Fig. 3.4; Waters and Condon, 2012).

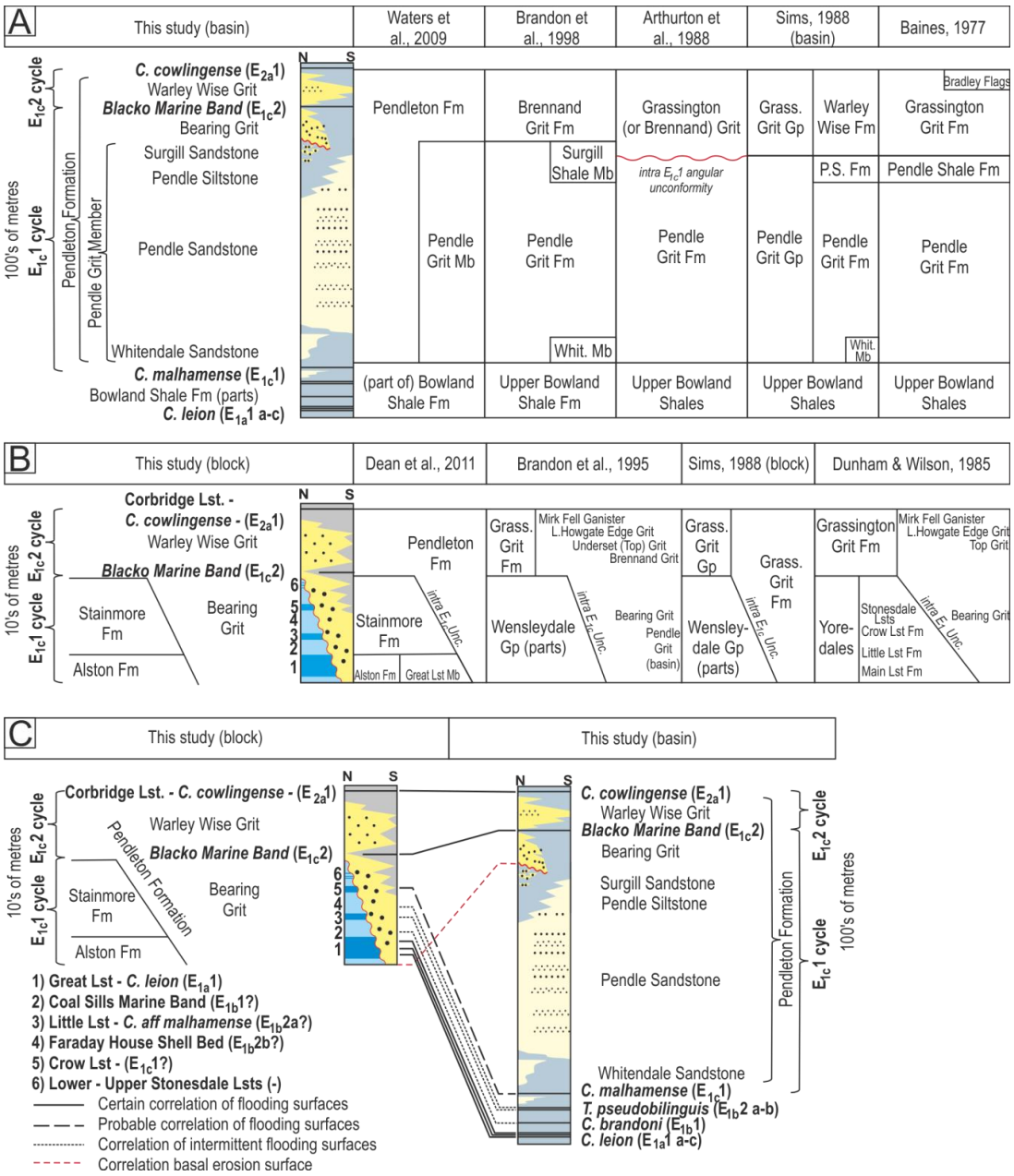

Figure 3.4 (a) Stratigraphic nomenclature compared to key references for the Craven Basin, and (b) theAskrigg Block . See references within these publications for older and local names. (c) Preferred correlation of flooding surfaces between the Askrigg Block and Craven Basin (see section 3.2.3). Note that if the Cravenoceras malhamense Marine Band in the Craven Basin is correlated to the Little Limestone on the Askrigg Block, higher limestones in the Stainmore Formation cannot correspond to eustatic variations recorded in the Craven Basin. Additionally, such correlation would place the Crow Limestone in the same sea-level cycle as the Bearing and Pendle Grits, which is considered improbable.

The Cravenoceras malhamense Marine Band ($E_{1c}1$) forms the base of the studied interval. Above this marine band, coarse-grained clastics of the Millstone Grit Group enter the Craven Basin (Fig. 3.4). The next transgression is recorded by the Blacko Marine Band ($E_{1c}2$) (Fig. 3.4), which lacks a goniatite fauna but contains the bivalve *Sanguinolites* and the brachiopod *Lingula* sp. (Brandon et al., 1995).The base of the Arnsbergian is defined by the Cravenoceras cowlingense Marine Band ($E_{2a}1$) (Fig. 3.4; Stephens et al., 1941; Dunham and Stubblefield, 1945). The Cravenoceras leion ($E_{1a}1$), malhamense ($E_{1c}1$) and cowlingense ($E_{2a}1$) Marine Bands have been proposed as higher amplitude flooding phases reflecting a long-period eccentricity forcing (~400 kyr) based on the areal extent of the goniatite fauna in these marine bands (Waters and Condon, 2012).

3.2.3.2 Transgressive surfaces on the Askrigg Block

On the Askrigg Block and in the Stainmore Trough further north, *C. leion* is recovered from the Great Limestone (Alston Formation) and *C. cowlingense* from the Corbridge Limestone (Stainmore Formation), enabling a correlation between these limestones and corresponding transgressive surfaces in the Craven Basin (Fig. 3.4c; Wilson and Thompson, 1959; Johnson et al., 1962). In between these two limestones a complex succession occurs, containing both limestones and clastic sediments with brackish fauna that resulted from sea-level fluctuations, local delta lobe development and tectonic influences (e.g. Elliot, 1975; Leeder and Strudwick, 1987). The absence of biostratigraphically-useful fossils has hindered correlation between both areas.

The Great Limestone forms a succession of tens of metres of limestones and cherts that show a cyclic $\delta^{18}O$ patterns with three peaks (Tucker et al., 2009; Gallagher, 2011). This is followed by a deltaic succession (Dunham and Wilson, 1985; Tucker et al., 2009) with brackish fossils (Fig. 3.4c; Brand, 2011). Overlying, the Little Limestone forms another major limestone that occurs throughout the northern part of the Pennine Basin (Dean et al., 2011). On the Askrigg Block, the Little Limestone is generally thin (~1.2 m) but directly overlain by the thick Richmond Chert of up to ~30 m thickness (Dunham and Wilson, 1985). Above the Little Limestone, the Faraday House Shell Bed indicates a marine interval within the overlying clastic succession (Fig. 3.4c; Scanlon and Rowel, 1957b; Dunham and

Wilson, 1985; Dunham, 1990). This succession is followed on by the Crow Limestone and Chert, which form a widespread calcareous succession up to ~23.5 m thick (Dean et al., 2011). On the northern Askrigg Block, the Crow Limestone is overlain by the laterally discontinuous Lower Stonesdale Limestone (Brand, 2011) consisting of three cm- to dm-scale limestones over a total thickness of 0.6 m (Fig. 3.4c; Dunham and Wilson, 1985). This succession is overlain by the Upper Stonesdale Limestone that records two similar limestone beds of total thickness 0.3 m. Locally, the Hunder Beck Limestone is recorded at an intermediate level in an expanded succession (Brand, 2011; Dunham and Wilson, 1985). The Upper Stonesdale Limestone has been correlated to the Belsay Dene Limestone northward (Brand, 2011) and the Blacko Marine Band southward (Brandon et al., 1995).

On the southern Askrigg Block, the Blacko Marine Band occurs at an intermediate level between the Bearing and Warley Wise Grits, two Pendleian-age Millstone Grit Group channel-belt-complex deposits (Fig. 3.4b). This succession is overlain by a marine interval containing *C. cowlingense* including the Mirk Fell Ironstone that overlies the Mirk Fell Ganister palaeosol in the Stainmore Bain (Rowel and Scanlon, 1957b), and the Cockhill Marine Band on the southern Askrigg Block (Dunham and Stubblefield, 1944). Both marine intervals are correlated with the Corbridge Limestone, a major limestone throughout the northern part of the Pennine Basin (Dean et al., 2011; Brand, 2011).

3.2.3.3 Craven Basin to Askrigg Block correlation of transgressive surfaces

It is here considered that particularly the higher amplitude sea-level highstands in the Craven Basin (i.e. the Cravenoceras leion, malhamense, and cowlingense Marine Bands; Waters and Condon, 2012) resulted in a significant flooding on the Askrigg Block shelf that produced extensive limestones. Similarly, minor eustatic flooding (at 100 kyr periods) produced relatively extensive deposition that contrasts with locally developed units produced by autocyclic processes like delta lobe switching

The three $\delta^{18}O$ cycles in the Great Limestone (Tucker et al., 2009; Gallagher, 2011) can be interpreted as glacial-interglacial variation in ice-volume (e.g. Miller et al., 1991), which would support the interpretation that the Great Limestone

resembles the three successive transgressions recorded by the Cravenoceras leion Marine Band (E_{1a}1a-c).

The overlying major limestone (i.e. the Little Limestone) has previously been correlated with the Cravenoceras malhamense Marine Band (E_{1c}1) (e.g. Arthurton et al., 1988; Brand, 2011) based on an occurrence of *C.* aff *malhamense* in shales above this limestone (Johnson et al., 1962). These goniatite specimens resemble *C. malhamense* in most characteristic traits but include characteristics of *C. cowlingense* as well. Such correlation would imply that the E_{1b}1 and E_{1b}2a-b transgressions in the Craven Basin are represented by the indistinct marine horizons between the Great and Little Limestone (cf. Fig. 3.4c). Meanwhile, the regionally extensive Crow Limestone, the Faraday House Shell Bed, the Lower Stonesdale Limestone and the Hunder Beck Limestone would not be represented by a basinal marine band, implying that they do not correspond to a sea-level rise or that this sea-level rise is not recognised in the Central Pennine Basin (cf. Fig. 3.4c). This entire interval would have formed between the transgression recorded in the Little Limestone and deposition of the Bearing and Pendle Grit sandstones during the following sea-level fall. The subsequent minor Upper Stonesdale Limestone has previously been correlated to in the Blacko Marine Band and thus would have a basinal equivalent, as well as the overlying Corbridge Limestone (Cravenoceras cowlingense Marine Band; cf. Fig. 3.4c)). Such alternating pattern in which transgressions are either clearly recorded on the Askrigg Block or the Craven Basin is considered an indication that this correlation is incorrect.

Here, a correlation between the Cravenoceras malhamense Marine Band (E_{1c}1) and Crow Limestone is preferred. This correlation implies that each high-amplitude flooding surface in the Craven Basin is correlated to a major limestone on the Askrigg Block (the Cravenoceras leion Marine Band (E_{1a}1) with the Great Limestone, Cravenoceras malhamense Marine Band (E_{1c}1) with the Crow Limestone and the Cravenoceras cowlingense Marine Band (E_{2a}1) with the Corbridge Limestone (Fig. 3.4c). The Cravenoceras brandoni Marine Band (E_{1b}1) would then correlate with the marine indicators in the succession between the Great and Little Limestone (Fig. 3.4c) while the two transgressions indicated by *Tumulites pseudobilinguis* (E_{1b}2 a-b) correlate with the Little Limestone and the overlying Faraday House Shell Bed (Fig. 3.4c). A correlation between the Cravenoceras malhamense Marine Band (E_{1c}1) and Crow Limestone implies that transgressions

result in a relatively consistent pattern on both the Askrigg Block and the Craven Basin. In neither correlation scheme, the dm-scale Lower Stonesdale Limestones and Hunder Beck Limestone have an equivalent flooding surface in the Central Pennine Basin and these might have resulted from different mechanisms than marine transgression, such as high frequency climate variation. For the similar Upper Stonesdale Limestone, no marine flooding surface is inferred in the preferred, second scheme. Based on mapping presented in this chapter, the correlation of the Blacko Marine Band with the Upper Stonesdale Limestones (Brandon et al., 1995) is challenged later in this chapter (Fig. 3.4c). A further implication of the preferred scheme is that *C.* aff *malhamense* above the Little Limestone is an earlier form than *C. malhamense*.

3.2.3.4 Lithostratigraphy

A recent lithostratigraphic classification has formalised and replaced a large number of local stratigraphic names, and places the entire Pendleian part of the Millstone Grit Group in the Pendleton Formation (Fig. 3.3; Fig. 3.4a, b; Waters et al., 2009). The Pendleton Formation thus includes the Pendle Grit, Bearing Grit and Warley Wise Grit referred to in this thesis. Within the Pendleton Formation only the Pendle Grit is formally assigned a Member status (Fig. 3.3; Waters et al., 2009). However, because the current study requires a higher resolution framework, an informal lithostratigraphic scheme is proposed below the order of Member (Fig. 3.3; 3.4) that follows protocols commonly used by the British Geological Survey (BGS) and includes e.g. the Bearing Grit and Warley Wise Grit. In Figure 3.4a and 3.4b the current terminology for the Craven Basin and the Askrigg Block is compared with previous schemes.

On the Askrigg Block, the Blacko Marine Band ($E_{1c}2$) occurs between two channel-belt-complex deposits, previously referred to as the Grassington Grit (Fig. 3.4; Dakyns, 1892; Martinsen, 1990, Brandon et al., 1995). This succession represents the full Pendleton Formation on the Askrigg Block. The lower channel-belt complex, the Bearing Grit (Philips, 1836) is erosionally based, and cuts out progressively older strata towards the south (Fig. 3.4; Dunham and Wilson, 1985). The upper channel-belt complex, here referred to as Warley Wise Grit, is closely overlain by the Cravenoceras cowlingense Marine Band ($E_{2a}1$) or equivalents (Fig.

3.4). Formerly, the Bearing Grit (Philips, 1936) has only been used on the Askrigg Block. The name was derived from the numerous ore-bearing veins that are present in this coarse-grained sandstone or grit. The Warley Wise Grit was formerly only used in the Craven Basin and its type section is at Warley Wise, Colne [3942 4438]. In this study both names are used on the Askrigg Block and in the Craven Basin (Fig. 3.4).

In the Craven Basin, the base of the studied interval is formed by the Cravenoceras malhamense Marine Band ($E_{1c}1$). This marine band is located in the Bowland Shale Formation, which is overlain by the Pendle Grit Member of the Pendleton Formation (Fig. 3.3; 3.4; Dakyns et al., 1879; Waters et al., 2009). The Pendle Grit Member is subdivided in several informal units: the Whitendale Sandstone occurs locally at the base of the Pendle Grit Member and is characterised by debritic and turbiditic beds (Sims, 1988; Brandon et al., 1998). The Pendle Sandstone forms a sand-rich succession characterized by predominantly channelized turbidite sandstones (e.g. Sims, 1988; Kane et al., 2009; 2010a), resulting in a ~500 m succession of mainly coarse-grained sandstones in its Pendle Hill type area (Fig. 3.2; Earp et al., 1961). Other areas, such as Skipton Moor (Fig. 3.2) show alternations of small channelized sandstones and shales (Baines, 1977; this work). The Pendle Siltstone is a siltstone-dominated slope succession that occurs towards the top of the Pendle Grit Member (Fig. 3.3; 3.4). The Surgill Sandstone occurs at the top of the Pendle Grit Member, and is interpreted as feeder system to the turbidite succession (Fig. 3.3; Baines, 1977; Sims, 1988, Brandon et al., 1998; Kane, et al., 2010). The formerly used Surgill Shale is here retained solely for the shale interval (Earp et al., 1961) that includes the Blacko Marine Band ($E_{1c}2$), and does not include the Pendle Siltstone, or Surgill Sandstone (Fig. 3.3; cf. Brandon et al., 1998; Kane et al., 2010a).

In sections near the margin of the Craven Basin, the Pendle Grit Member is overlain by the Bearing Grit, the Blacko Marine Band and finally the Warley Wise Grit. In more distal locations, the Bearing Grit is absent. Locally, the Bradley Flags, a fine-grained delta top facies is developed stratigraphically above the Warley Wise Grit (Baines, 1977; Waters, 2000) prior to transgression and deposition of the Cravenoceras cowlingense Marine Band ($E_{2a}1$) (Fig. 3.3; 3.4).

Initially, the entire Pendleton Formation was interpreted as a single progradational turbidite-fronted delta fed by the Pendleton Formation on the Askrigg Block (Baines, 1977). A subsequent model suggested that the fluvial feeder for the Pendle Grit Member turbidite system came from the northwest, after which it avulsed onto the Askrigg Block resulting in a progradational succession on the Askrigg Block and in the Craven Basin including both the Bearing and Warley Wise Grit as defined here (Sims, 1988; Martinsen, 1990, 1993). Recognition of the Blacko Marine Band ($E_{1c}2$) resulted in a correlation between the Bearing Grit on the Askrigg Block with the Pendle Grit Member in the Craven Basin below the Blacko Marine Band (Brandon et al., 1995). Above this horizon, the Underset Grit (here referred to as Warley Wise Grit; Fig. 3.4) on the Askrigg Block was correlated with the Brennand Grit in the Craven Basin (the Bearing and Warley Wise Grits of this study; Fig. 3.4a) (Brandon et al., 1995). The latter correlation is based on the occurrence of the Blacko Marine Band overlying turbiditic strata belonging to the Pendle Grit Member in the Blacko Borehole (Fig. 3.2).

In this study, the Blacko Marine Band ($E_{1c}2$) is considered to occur between the Pendle Grit Member and Warley Wise Grit at distal locations in the Craven Basin (sensu Brandon et al., 1995). However, in the proximal Craven Basin, the Blacko Marine Band ($E_{1c}2$) is thought to occur between the Bearing Grit and the Warley Wise Grit (Fig. 3.4a).

3.3 Methods

Results are based on extensive stratigraphic and sedimentological fieldwork in combination with literature study. During fieldwork, stratigraphic sections were logged and correlated based on e.g. marine band occurrences, landscape features, thickness patterns and coal seam occurrences providing a lithostratigraphic framework constrained by marine band occurrences that represents quasi-chronostratigraphic surfaces. Additionally, logged sections were subdivided into facies and facies associations and combined with more detailed sedimentological studies on sand-grade outcrops in which also palaeocurrents were recorded, enabling reconstructions of palaeogeographic environment. Borehole records have been studied in areas where outcrops are of poor quality or absent. A total of 11 facies,

and 5 facies associations are recognised and described in Section 3.4.6 and 3.4.7 (see Table 3.1). Data sources for the boreholes are provided in Appendix 1. Additionally, thickness variations of the Pendle Grit Member, Bearing Grit and Warley Wise Grit based on literature and fieldwork have been collated. These values are used to construct isopach maps and estimate the sediment budgets during deposition of these units, allowing for a comparison between deposition in the Craven Basin and the analogue modelling results in Chapter 2.

3.4 Results

The Sections 3.4.2 to 3.4.5 are organised by structural domains indicated in Figure 3.2. The domains contain several sections for which the entire stratigraphic interval is described. Sections are numbered on Figure 3.2 or more detailed maps. Section 3.4.6 describes and interprets commonly observed facies throughout the field area and Section 3.4.7 provides an environment interpretation based on these facies. Section 3.4.8 describes the thickness trends of the stratigraphic units, the limitations to this dataset, and the resultant sediment volumes.

3.4.1 Location descriptions on Askrigg Block

3.4.1.1 Swaledale

Description

In Swaledale on the northern side of the Askrigg Block (Fig. 3.2; 3.5a, b), coarse-grained to pebbly cross-bedded sandstones referred to as the Lower Howgate Edge Grit occur in a N-S trending, erosionally-based channel belt complex. This complex is ~12.5 km wide and up to 50 m thick between Fossdale Gill [3879 4949] and Summer Lodge Beck [39715 49537] (Fig. 3.2; 3.6; e.g. Dunham and Wilson, 1985; Sims, 1988, Brandon et al., 1995). At Fossdale Gill, the channel belt complex contains two sandstone intervals, separated by a shale interval. The lower sandstone interval is incised into the Crow Limestone. At the top of the succession an Arnsbergian-age coal is observed (Dunham and Wilson, 1985). Laterally, this channel belt complex is replaced by the Mirk Fell Ganister, a palaeosol, overlain by the Cravenoceras cowlingense Marine Band ($E_{2a}1$) (Rowell and Scanlon, 1957b).

Northward in the Stainmore Trough the Lower Howgate Edge occurs as a 26 m thick cross-bedded sandstone interval above the Upper Stonesdale Limestone at Wetshaw Fourth Whim [3980 5024].

Interpretation

This fluvial channel belt complex is overlain by the Cravenoceras cowlingense Marine Band and is thus of Pendleian age. Incision into the Crow Limestone suggests an E_{1c} age (Fig. 3.c) but the succession cannot be related to either or both the Bearing or Warley Wise Grit because marine fossils are not reported.

3.4.1.2 Coverdale

Description

Wilson (1957; 1960) describes a SW-NE oriented cross section along Coverdale in which cross-bedded sandstones are focussed along two stratigraphic levels (Fig. 3.5d). The sandstones that are present near Providence Mine, Great Whernside in the lower level of the Pendleton Formation pinch out abruptly west of Lords Gill, north of Little Whernside [4019 4784] (Fig. 3.5, Section C-C'; Fig. 3.6). In Lords Gill, and in Hindlethwaite Gill 4.5 km NNE [4056 4807], this succession is replaced by a ~15 m succession containing predominantly fine-grained and argillaceous sediments, including multiple laterally discontinuous coals overlying palaeosols (Fig. 3.5; Wilson, 1957). This succession is overlain by a shale succession that contains *Lingula* sp. (Wilson, 1960; Brandon et al., 1995). Cross-bedded sandstones of the upper stratigraphic interval overlie this marine interval.

Interpretation

The succession that pinches out near Lords Gill is assigned to fluvio-deltaic channels in the Bearing Grit. The laterally occurring heterolithic strata probably represent as an overbank setting deposited during the $E_{1c}1$ sea-level cycle. This succession is overlain by the *Lingula sp.* containing Blacko Marine Band ($E_{1c}2$), implying that the overlying, laterally continuous fluvio-deltaic sandstones belong to the Warley Wise Grit.

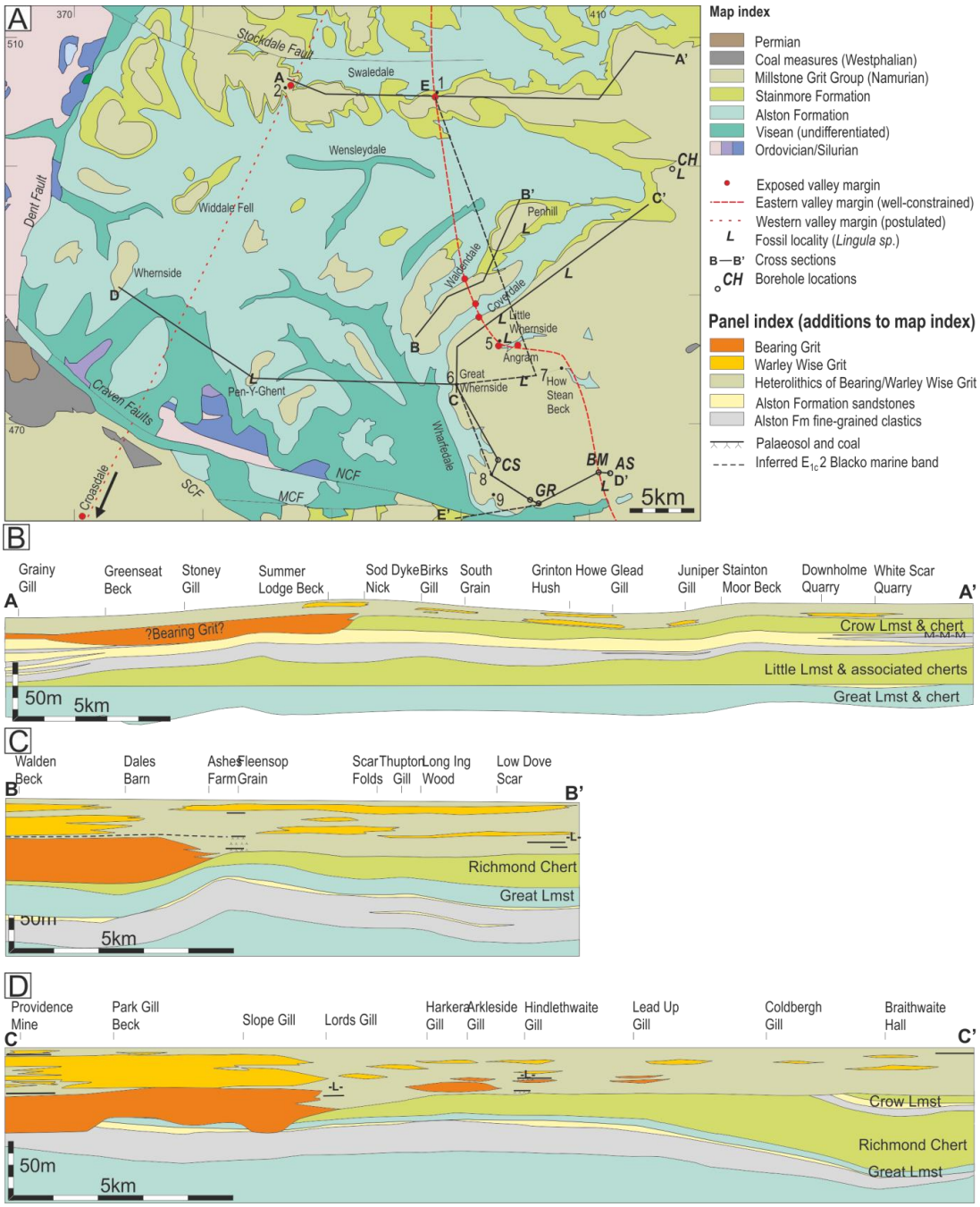

3.4.1.3 Waldendale and Penhill

Description

Waldendale exposes a similar succession as Coverdale (Fig. 3.5, Section B-B'). The lower cross-bedded sandstone level has a 25 m maximum thickness, thins rapidly towards the northeast and disappears on the west side of Fleensop Moor [4008 4812] (Fig. 3.2; 3.5; Wilson, 1957). On the north side of Fleensop Moor, several coal seams occur in the lower part of the succession (e.g. Coal Gill and Back Dyke, Wilson, 1957). At Melmerby Moor (Penhill) [4055 4859], the lower part of

Figure 3.5 (previous page) (a) Locations and relevant features in the Bearing and Warley Wise Grit on the Askrigg Block. Cross sections D-D' and E-E' are presented in Fig. 3.6. Red dots indicate positions where the rapid pinch out of the Bearing Grit channel belt complex is observed. Fossil localities of the Blacko Marine Band are indicated with symbol (L). Background is a 1:625.000 geological map of the British Geological Survey. The Bearing and Warley Wise Grit are not indicated on the map but form the basal part of the Millstone Grit Group. Note the unconformable relationship between the Millstone Grit Group and the Stainmore and Alston Formations as indicated by the progressive absence of the Stainmore Formation southward. (b) Section at the northern margin of the Askrigg Block where the position of the Blacko Marine Band is unknown. The erosionally-based channel belt observed west of Summer Lodge Beck is tentatively correlated in the Bearing Grit (Modified from Dunham and Wilson, 1985). Panel levelled at the top of the Great Limestone cyclothem. (c, d) Sections along Waldendale and Coverdale, indicating the eastern valley margin and lateral occurrences of a heterolithic succession including coals and palaeosols overlain by the Blacko Marine Band (Modified from Wilson, 1960). Panels levelled at approximate position of the Cravenoceras cowlingense Marine Band.

---

the succession contains *Lingula* sp. interpreted as the Blacko Marine Band within a shale at Rowantree Holes [4048 4849] (Wilson, 1960; Brandon et al., 1995). The top of the succession is dominated by cross-bedded sandstones.

Interpretation

The lower sandstone-dominated succession is interpreted as a fluvio-deltaic setting in the Bearing Grit, and pinches out towards the northeast. The adjacent fine-grained succession containing several coal seams at Fleensop Moor represents an overbank setting deposited before the transgression that resulted in deposition of the Blacko Marine Band, implying deposition during the $E_{1c}1$ sea-level cycle. The sandstones overlying the *Lingula* sp. containing shale interval are interpreted as the fluvio-deltaic Warley Wise Grit.

3.4.1.4 Angram

Description

Crook Dyke [4026 4760] is located on the NW-side of the Angram Reservoir (Fig. 3.2). At the base of the section, the Underset Limestone is exposed. This level is overlain by a shale- and siltstone-dominated succession containing several palaeosols and coals (Fig. 3.6; Brandon et al., 1995) up to the Blacko Marine Band. Between this *Lingula sp.*-containing interval and the higher Cravenoceras cowlingense Marine Band, several sandstones are observed belonging to the Warley Wise Grit level. Nearby, the Angram Dam section [4033 4763] formed an N-S oriented trench that records a rapid northward thinning of the lowest Millstone Grit sandstones (Tonks, 1925).

Interpretation

The sections in Crook Dyke and at the Angram Dam are closely-spaced and differ significantly. The Angram Dam section indicates a rapid pinch out of the lowest sandstones of the Millstone Grit Group. These are probably part of the Bearing Grit, based on its outcrop pattern updip in Coverdale and Waldendale (Sections 3.4.1.2 and 3.4.1.3), and downdip in How Stean Beck (Sections 3.4.1.5).

Because of this close-by pinch-out of the Bearing Grit, it is probable that the shale- and siltstone-dominated interval in the Crook Dyke section above the Underset Grit and below the Blacko Marine Band represents a overbank succession that is broadly time-equivalent to the main Bearing Grit succession (e.g. Brandon et al., 1995).

3.4.1.5 How Stean Beck

Description

How Stean Beck (Fig. 3.2; 3.5) is a tributary to the River Nidd on the SE-side of the Askrigg Block near Stean and Middlesmoor that lies ~3 km south from Angram and provides exposures from the base of the Bearing Grit to the top of the Warley Wise Grit [4082 4744] to [4053 4725]. The base of the succession is exposed in a waterfall where the Three Yard Limestone of the Alston Formation is overlain by cross-bedded sandstones [4081 4743]. Exposures indicate a lower cross-bedded sandstone level of ~15 m, overlain by a ~3.5 m argillaceous interval with abundant

carbonaceous material and another ~6 m thick cross-bedded sandstone (Fig. 3.6). Sets have a thickness of 0.45 – 1.3 m and contain medium-grained to granular sandstone, where granules are located at the base of beds. Cross bedding is developed as planar tangential cross beds mainly, with trough cross bedding occurring towards the top of the succession. A pebble lag at 7.4 m with 2 cm pebbles suggests that the lower sandstone level contains at least two channel storeys. Flow directions in this succession are ~E (Fig. 3.6). Along How Stean Beck, regular exposures of the top of the second sandstone level, and patchy exposures in argillaceous sediments overlying this succession occur. At the confluence of Strait Stean Beck and Great Blowing Gill [4055 4728] the top of the second sandstone level is overlain by a well-exposed heterolithic interval. This interval contains carbonaceous silty shales containing cm-scale plant fragments at its base and coarsens up to fine-grained sandstones, intercalated with thin shales and siltstones over 4.5 m. The siltstones and fine-grained sandstones are strongly bioturbated. Sands towards the top of the coarsening-up succession show current ripples. The overlying succession is formed by predominately micaceous shale and is poorly exposed, but has yielded *Lingula sp.*. A 13 m thick channelized sandstone succession sharply overlies this shale succession in exposures surrounding Strait Stean Beck [4054 4727]. Beds are 0.4 – 1 m, contain medium- to very coarse-grained sand, and show planar cross bedding indicating E – SE flow directions (Fig. 3.6). This channelized sandstone contains at least two storeys and is overlain be a thin coal seam. Poor outcrops continue upstream of a rain gauge at [4053 4726]. In Backstean Gill, a nearby tributary of How Stean Beck, the heterolithic succession above the upper channelised sandstone has been interpreted as a deltaic environment and overlying shales yielded *C. cowlingense* (Martinsen, 1990).

Previous descriptions by Dunham and Wilson (1985) and Martinsen (1990) indicate a well-developed coal above the basal channelised sandstone, and a thin coal seam above the second sandstone interval. Neither is observed but might well correlate with the carbonaceous shales that are observed at both positions (Fig. 3.6). Additionally, Martinsen (1990) also describes the occurrence of *Lingula sp.*, as well as palaeosol development on top of each sandstone level.

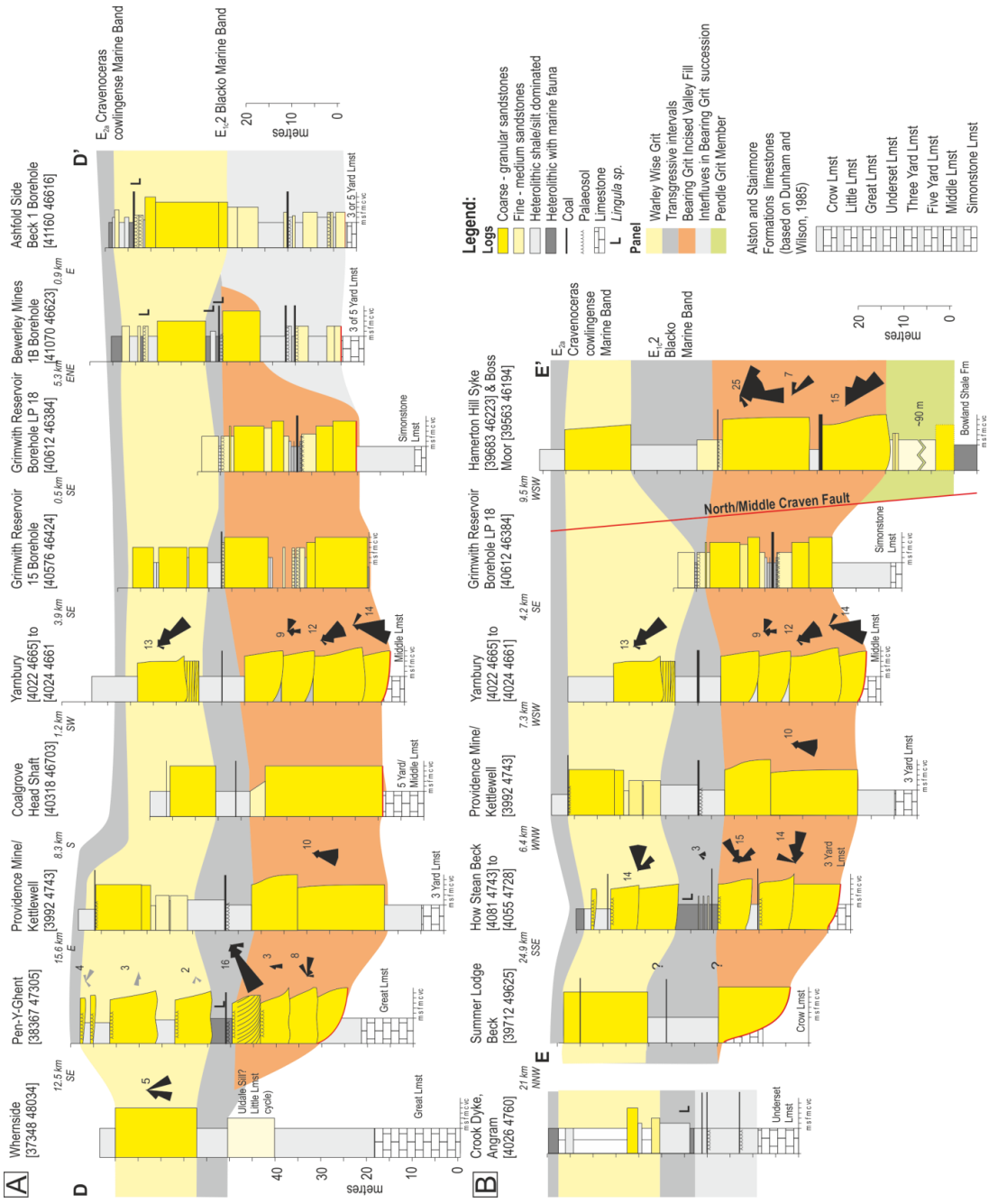

Figure 3.6 (a) Cross section D – D' (see Fig. 3.5a) is approximately perpendicular to palaeoflow on the southern margin of the Askrigg Block. (b) Cross section E –E' is approximately parallel to palaeoflow along the eastern outcrop belt. Individual sections are described in Results (Section 3.4.1). Panels levelled at approximate positions of the Blacko Marine Band. The Warley Wise Grit interval of Pen-y-ghent is based on Martinsen (1990). Coalgrove Head Shaft is based on Dunham and Wilson (1985). Bewerley Mines No. 1B Borehole is based on Brandon et al. (1995). Crook Dike section based on Wilson (1957) and Brandon et al. (1995). Summer Lodge Beck section based on Dunham and Wilson (1985). Other sections based on fieldwork and borehole drilling records (Appendix 1).

Interpretation

The occurrence of *Lingula sp.* indicates the level of the Blacko Marine Band ($E_{1c}2$) within the heterolithic unit. This places the succession below this level in the Bearing Grit, and the overlying succession up to the Cravenoceras cowlingense Marine Band ($E_{2a}1$) in the Warley Wise Grit (Fig. 3.6). Both the Bearing and Warley Wise Grit consist mainly of fluvio-deltaic channel deposits. Deposits overlying both sandstone-dominated intervals are deltaic and probably reflect sea-level rise prior to deposition of the marine bands.

3.4.1.6 Providence Mine & Great Whernside

Description

Approximately 5.5 km east from the section at How Stean Beck, exposures occur along the flanks of Great Whernside [3993 4744] (Fig. 3.2; 3.5a). Only sandstones are exposed, but the succession can be related to a continuous section in the Providence Mine (Dakyns, 1892; Dunham and Wilson, 1985).

Near Caseker Crag [39921 47432] ~15 m of coarse-grained planar cross-bedded sandstones are exposed overlying the Three Yard Limestone, indicating flow directions to the south (Fig. 3.6). At the SE-side of the outcrop, this succession is overlain by ~8 m of trough cross-bedded sandstone that is occasionally very coarse-grained to pebbly, also indicating southward flow directions. These sandstones are overlain by a ~20 m unexposed interval containing a coal seam, which is inferred from pits along this level in the Hag Dyke area (Fig. 3.6). On top of this unexposed interval, a poorly outcropping 10 m thick cross-bedded sandstone is exposed south of Caseker Crag [39918 47387], and near Hag Dyke [39960 47291] (Fig. 3.2). The section in the Providence Mine has been reported by Dakyns (1892) and is reproduced in Dunham and Wilson (1985). It exposes 28.6 m of sandstone at the base, overlain by a ~7 m shale succession. On top, a 0.6 m coal seam is overlain by a 17 m heterolithic unit. The upper sandstone interval contains 9 m sandstone overlain by a thin coal and shale interval in which Dunham and Wilson (1985) infer the Cravenoceras cowlingense ($E_{2a}1$) Marine Band (Fig. 3.6).

Interpretation

The sections at How Stean Beck and at Great Whernside are very similar in that both record a lower cross-bedded sandstone interval of similar thickness overlain by a coal seam and shale, followed by an upper sandstone level (Fig. 3.6). The heterolithic interval at Great Whernside is slightly thicker than at How Stean Beck, whereas the upper channelized sandstone is thinner. Outcrops on the flanks of Great Whernside are too limited to assess the depositional environment in the fine-grained interval or the upper sandstone. However, based on the overall similarity in sandstone patterns, it is considered likely that the shale interval corresponds to the Surgill Shales, and that the upper sandstone level belongs to the Warley Wise Grit.

3.4.1.7 Yarnbury area

Description

Yarnbury is located ~7 km SSE from Great Whernside and provides another section through the Bearing and Warley Wise Grit (Fig. 3.2). A basal cross-bedded sandstone level, overlying the Middle Limestone is well-exposed along Hebden Beck between [4022 4665] to [4024 4661]. The thickness of this sandstone succession is approximately 30 metres although its top is only intermittently exposed. Cross sets range from 0.2 and 1.5 metres, recording flow directions to the SE and S. The succession contains coarse- to very coarse-grained, planar tangential cross-bedded sandstones at its base, and transitions to predominantly trough cross-bedded sandstones, coinciding with an overall coarsening of the succession. Sandstones are coarse-grained to granular and contain abundant quartzitic or limestone pebbles of up 5 cm. The upper part of this sandstone contains planar tangential cross sets in medium-coarse to granular sand, and contains only small pebbles (Fig. 3.6).

At Green Hill, north of Yarnbury [4008 4676], the unconformable relation between this sandstone level and the underlying limestones can be observed (cf. Baines, 1977). Green Hill exposes the Middle Limestone (Alston Formation) while within 30 m SE, sandstones are exposed at a lower topographic level. The slight tectonic dip (~5 degree to the SE) cannot explain their relative positions, and

indicates that this sandstone is deposited in an incisional channel at this location, which might also explain the downdip occurrence of limestone pebbles.

A ~10 m unexposed interval occurs above the previously described sandstone level, on top of which another ~10 m sandstone interval is developed. This sandstone is best exposed at a disused quarry along Coalgrove Beck [4025 4663], but can be traced southward to Hole Bottom (Fig. 3.2). The base of the quarry exposes a 3 m thick succession of medium-grained tabular beds of 0.2 – 0.5 m thickness that show horizontal or low angle lamination. Individual beds are sharp-based and amalgamate laterally with other beds. The top of this interval is incised by medium-coarse planar cross-bedded sandstones. The top of the quarry exposes coarse-grained trough cross-bedded sandstones, containing pebbles up to 0.6 cm. Flow directions are SE to S in the cross-bedded strata. The Cravenoceras cowlingense Marine Band ($E_{2a}1$) has been reported from a nearby trial pit at Bolton Gill [4031 4654] (Dunham and Stubblefield, 1944), indicating that the full Pendleton Formation is present.

A section from Coalgrove Head Shaft [40318 46703] described by Dunham and Wilson (1985), describes a similar succession to that observed at Yarnbury, with a thick lower sandstone and a thin upper sandstone, separated by a fine-grained interval containing a coal seam (Fig. 3.6).

Interpretation

The thickness of the lower sandstone interval at Yarnbury is similar to How Stean Beck and Great Whernside, as well as the occurrence of a coal seam within the argillaceous interval between the lower and upper sandstones. Presumably, the shale interval again corresponds with the Surgill Shales, implying that the lower sandstone is the Bearing Grit, whereas the upper sandstone belongs to the Warley Wise Grit. The Bearing Grit is erosionally-based and cross-bedded, suggesting deposition in fluvio-deltaic channels. The upper part of the Bearing Grit interval is poorly exposed and gradually becomes finer-grained. The base of the Warley Wise Grit differs from the previously described exposures; the plane bed deposits at the base are interpreted as a mouthbar deposit overlain by deltaic channelized sandstones, although the exposure is too limited for a full understanding of the depositional setting.

3.4.1.8 Hole Bottom

Description

Hole Bottom (Fig. 3.2) is located 2 km south from the outcrops at Yarnbury along Hebden Beck and provides a rare exposure close to the North Craven Fault that can be correlated to the Yarnbury area. The lower sandstone level is cross-bedded and has a total thickness of approximately 30 metres. Cliff exposures are inaccessible but indicate that this succession consists of at least 3, probably 4 channel storeys. Overlying this succession is an unexposed interval of approximately 15 metres, containing a significant coal seam, based on the occurrence of a line of coal pits. An upper sandstone level can be traced towards the Warley Wise Grit level in the Yarnbury area although at Hole Bottom only loose boulders of cross-bedded sandstone are preserved.

Interpretation

Based on the correlation with the Yarnbury area, the lower sandstone in interpreted as a multi-storey fluvio-deltaic channel succession in the Bearing Grit. The upper sandstone is correlated to a channel exposure in the Warley Wise Grit. The unexposed interval probably contains the Blacko Marine Band.

3.4.1.9 Grimwith to Greenhow

Description

Along the margin of the Askrigg Block, exposures of the Bearing and Warley Wise Grit are limited. Several boreholes however provide a W-E cross section through the succession from the Grimwith Reservoir to Greenhow (Fig. 3.5a; 3.6). Grimwith Reservoir 15 Borehole [40576 46424] was drilled near the top of the Pendleton Formation (Fig. 3.6). It forms a crude record through nearly the entire formation, containing two pebbly sandstone successions at the base of the succession overlain by a shale interval containing a coal seam (Fig. 3.6). On top of this succession, medium-grained sandstones form the upper part of the sequence. Grimwith Reservoir Borehole LP 18 [40612 46384] provides a more detailed section through the lower two pebbly sandstones, and indicates the presence of a coal seam between the two pebbly sandstones (Fig. 3.6).

Bewerley Mines No. 1B Borehole, Greenhow [41070 46623] has been described by Brandon et al. (1995) and contains the Blacko Marine Band at approximately the same stratigraphic level of the shale interval in the Grimwith Boreholes, near Hole Bottom and at Yarnbury (Fig. 3.6; Section 3.4.1.7; 3.4.18). Additionally, another marine horizon is observed slightly below the Cravenoceras cowlingense Marine Band that is interpreted as an initial flooding surface (Fig. 3.6; Brandon et al., 1995). The basal part of the Bearing Grit succession is poorly developed and consists of a heterolithic succession of fine-grained sandstones, palaeosols, coals, silt- and mudstones.

Ashfold Side Beck 1 Borehole [41160 46616], shows a similar succession east of Bewerley Mines 1B Borehole. The Cravenoceras cowlingense Marine Band is recognised, with a marginal marine band slightly lower in the succession. The basal part of the Bearing Grit is a heterolithic succession containing thin coal seams, palaeosols, and thin sandstones. The Blacko Marine Band is not exposed, but at its approximate stratigraphic position based on the Bewerley Mines No. 1B Borehole, a medium- to coarse-grained sandstone is observed. This sandstone probably forms an amalgamation of the Bearing Grit and Warley Wise Grit, or a thick development of the Warley Wise Grit sandstones (Fig. 3.6).

Interpretation

The Grimwith Boreholes provide a similar succession to that observed at Yarnbury, which based on thickness suggests that the Blacko Marine Band occurs in the shales on top of the lower two pebbly sandstones. A correlation of the Grimwith Boreholes with the Bewerley Mines No. 1B Borehole by Brandon et al. (1985), also suggests the occurrence of the Blacko Marine Band at this level, providing a consistent horizon for the Blacko Marine Band within the succession. Additionally, a correlation of the Grimwith Boreholes with the Bewerley Mines No. 1B and Ashfold Side Beck 1 Boreholes, suggests that the pebbly sandstones in the Bearing Grit are replaced by a heterolithic succession eastward, similar to the eastward pinch out observed in Waldendale and Coverdale (Section 3.4.1.1; Fig. 3.5).

3.4.1.10 Pen-y-ghent

Description

Extensive outcrops occur of the Pendleian succession occur on the western flank of Pen-y-ghent [3838 4734] (Fig. 3.7), located in the south west of the Askrigg Bloc. Access to part of the outcrops was limited due to adverse weather conditions during visits.

On the SW flank [3836 4732], a multi-storey channel belt is recognised (Fig. 3.5; 3.7a). The basal storey is embedded in underlying shales and reaches ~10 m high but has a limited width of ~100 metres. The overlying storey is ~ 6 m thick, contains abundant pebble lags and cross beds record eastward flow. The third storey is ~8 m at the SW flank of Pen-y-ghent and records flow directions to the WSW. It pinches out within 500 m in a northward direction and is here replaced by predominantly fine-grained sediments. The upper storey also pinches out rapidly in a northward direction and is best exposed on the south flank (Fig. 3.7b). Sandstones are medium- to coarse-grained and pebbles are absent. At the base of the highest storey, ~5 m high Gilbert-type foresets are observed that are overlain by trough-cross-bedded sandstones, indicating WSW flow directions [38367 47305]. Outcrops in the overlying succession have not been observed. Martinsen (1990) however, describes a 15 cm shaley coal in the 5 m thick overlying shale interval, followed by two coarse-grained ~ 8 m thick trough cross-bedded channelized sandstones with palaeosol development at their tops, indicating westward flow directions. This succession is overlain by a heterolithic succession containing thin channelized sandstones interpreted as crevasse channels (Martinsen, 1990). Dunham and Wilson (1985) also record deposition in a deltaic complex, with marine incursions indicated by *Lingula sp.* fauna, although a precise stratigraphic position of these fossils is not given. Additionally, Dunham and Wilson (1985) infer the Cravenoceras cowlingense Marine Band ($E_{2a}1$) at the top of the here described succession (Fig. 3.5).

Interpretation

The lower succession of cross-bedded sandstones is interpreted as a multi-storey fluvio-deltaic channel deposit. This interval is assigned to the Bearing Grit because *Lingula sp.* has been recorded in the overlying succession, indicating the

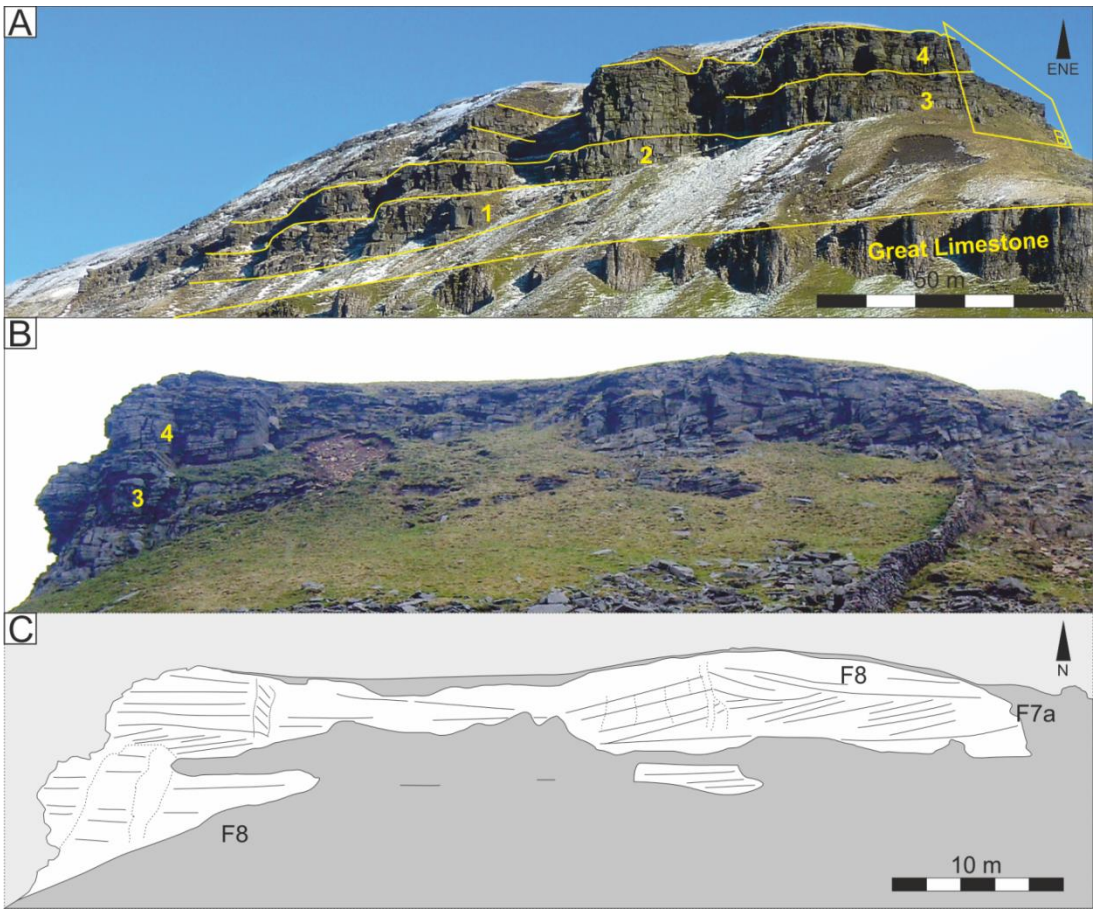

Figure 3.7 (a) Photo-interpretation from the Bearing Grit succession on the SW flank of Pen-y-ghent. Channel storeys containing cross-bedded sandstones (F8) indicated by yellow numbers. (b, c) Occurrence of large-scale foresets (F7a) at the base of channel storey 4 at Pen-y-ghent. Photo in (a) from http://jameshandlon.com/2010/11/18/ascent-of-pen-y-ghent/ (cropped) and photo in (b) from http://irlsey.wordpress.com/2013/05/18/pen-y-ghent-north-yorkshire/ (cropped) because weather conditions did not allow photos from sufficient distance

position of the Blacko Marine Band. The occurrence of a Gilbert-type delta at the top of this multi-storey fluvial succession records a coastline position on top of previous fluvial deposits, indicating an overall transgression that can also explain the overlying coal seam. The exact stratigraphic position of the *Lingula sp.* is unclear though and could occur either within the argillaceous succession above the Gilbert-type delta Grit as suggested in Figure 3.6, or slightly higher. The occurrence of *Lingula sp.* suggests the presence of the Blacko Marine Band ($E_{1c}2$) at an intermediate level within the succession and thus places the higher cross-bedded sandstone level(s) in the Warley Wise Grit.

3.4.1.11 Whernside

Description

Whernside [37348 48034] is located on the southwest Askrigg Block at ~13 km NW from Pen-y-ghent (Fig. 3.2; 3.5a). Here, no marine fauna has been observed in the Millstone Grit succession, which makes stratigraphic correlations debatable. At this location, a Lower and Upper Howgate Edge Grit have been mapped previously, where only the Lower Howgate Edge Grit is correlated to the Pendleton Formation; the Upper Howgate Edge Grit is of probably Arnsbergian age based on BGS mapping (Hicks, 1957; Dunham and Wilson, 1985; Martinsen, 1990). The Lower Howgate Edge Grit is a coarse-grained, trough cross-bedded sandstone containing pebbles of up to 2 cm (Fig. 3.6). The entire succession is approximately 18 m thick and records S to SW flow directions.

Interpretation

The Lower Howgate Edge Grit is a fluvio-deltaic channel succession belonging to either the Bearing or Warley Wise Grit. Based on a correlation of incised valley fill margins in the Bearing Grit both up and downstream of Whernside, it is considered likely that the Lower Howgate Edge Grit of Whernside correlates with the Warley Wise Grit (see discussion).

3.4.2 Location descriptions Transition Zone

The Transition Zone forms a small part of the Craven Basin adjacent to the Askrigg Block. Its boundaries within the Craven Basin are defined by the SE-trending South Craven Fault and the SW-trending continuation of the Pendle Fault (Fig. 3.2).

3.4.2.1 Hamerton Hill Syke, Threshfield Moor

Description

Hamerton Hill Syke is a small stream along a NW-SE dextral fault, located on the downthrown side of the North Craven Fault, ~ 7.5 km SE of Yarnbury (Fig. 3.2, 3.5). The Bowland Shale Formation is intermittently exposed from [39726 46154] to [39693 46179]. At 15 m below the base of a cross-bedded sandstone level, laminated fine- to medium-grained, carbonaceous sandstones are observed in 2 -5

cm beds. The overlying cross-bedded sandstones occur at two levels of respectively ~15 m and ~20 m, separated by a thin fine-grained interval containing a 0.9 m coal seam (Fig. 3.6; 3.8; Arthurton et al., 1988). In the lower level, coarse- to very coarse-grained sandstones containing abundant <5 cm pebbles form metre-scale trough cross beds, indicating flow directions to the southeast. The upper channel level contains medium- to very coarse-grained sandstones with pebbles of up to 3.5 cm, and is also exposed in quarries on Boss Moor [39563 46194]. Here, beds are both planar and trough cross-bedded in sets of up to 1.3 m, indicating flow towards the south mainly. This succession is overlain by a ~20 m unexposed interval. Arthurton et al. (1988) recorded a thin coal, coaly mudstone and planty siltstone at the base of this interval. At Dolmire Hill, this coal seam has also been reported (Baines, 1977). The overlying sandstone is poorly exposed and only fine- and medium-grained sandstones have been observed in a small quarry [39659 46222]. Arthurton et al. (1988) suggests a ~20 m thickness of this sandstone based on feature mapping, and observes coarse-grained or pebbly sandstones at this stratigraphic level at other locations. The succession is presumably overlain by a shale succession (Arthurton et al., 1988).

Interpretation

No marine bands are observed in the area, which makes a correlation of the fluvial strata to either Bearing or Warley Wise Grit tentative. It is considered likely that the two coarse-grained channelized sandstones represent a continuation of the major Bearing channelized sandstones on the southern margin of the Askrigg Block. These occasionally also develop two pebbly sandstone levels separated by a coal seam (Fig. 3.6). The higher coal seam, overlain by ~20 m shale succession likely corresponds to the Surgill Shales, in which case the upper level with fine- to medium-grained sandstone corresponds to the Warley Wise Grit (Fig. 3.6).

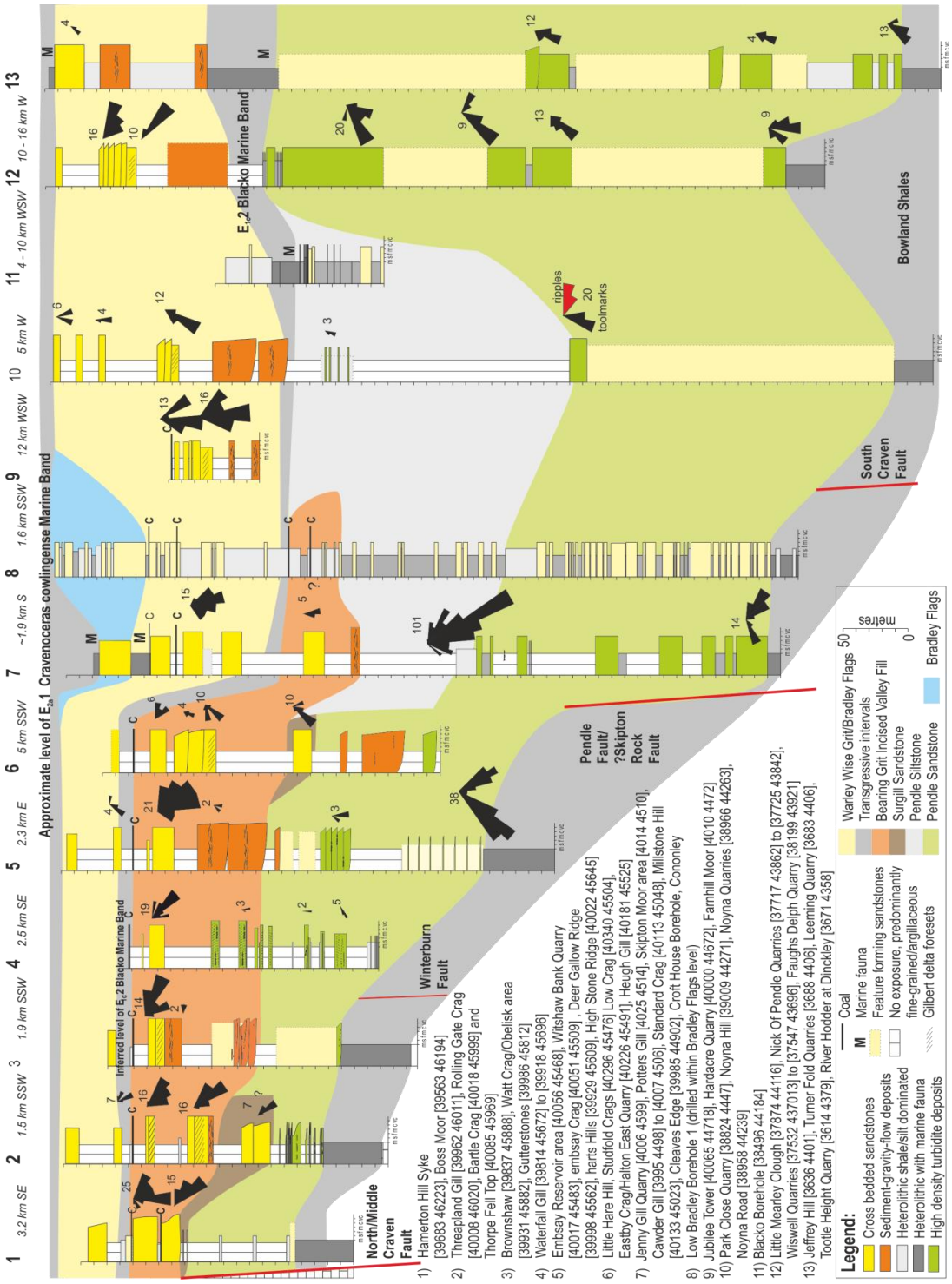

Figure 3.8 Cross section F – F' (see Fig. 3.2 for location) indicating longitudinal differences in stratigraphy in the Craven Basin. Sections 1 – 6 are levelled from a coal seam at the top of the Bearing Grit. Sections 7 - 9 are correlated based on the occurrence of two coal seams near the top of the Warley Wise Grit. Overall, the panel is levelled from the inferred position of the Cravenoceras cowlingense Marine Band. See Fig 3.2 for locations

3.4.2.2 Raven Nest Crags, Threapland Gill to Thorpe Fell: Barden Moor

Description

Raven Nest Crags [40085 46086] is a location on the northern side of Barden Moor (Fig. 3.2; 3.9). The base of the section starts at the contact of a poorly exposed shale succession of ~50 m that onlap Cracoean reef mounds (Fig. 3.9b; Black, 1958; Rigby and Mundy, 2000). At the top of the shale succession Raven Nest Crag forms a quarry exposure revealing ~10 m of medium- to very coarse-grained sandstones, with rare 1 cm pebbles. Beds range from 0.2 up to 2 metres. Cross bedding is observed in some of the beds, indicating eastward flow. Most beds appear massive, although this might be related to outcrop quality. The successive interval of 30 m is unexposed and overlain by ex-situ boulders of Millstone Grit sediment that are positioned at the stratigraphic level of Rolling Gate Crag [40008 46020] (Fig. 3.9).

Threapland Gill [39962 46011] forms a stream section along the NW-side of Barden Moor that can be correlated with Raven Nest Crags (Fig. 3.8; 3.9). The stream exploits a small fault resulting in a rare, but disturbed exposure of the Pendle Grit Member at close proximity to the North Craven Fault. At the base of the succession, turbiditic limestones are overlain by an unexposed succession on poorly-drained terrain that probably contains the Bowland Shale Formation. Mapping indicates rare shales outcrops laterally that agree with such interpretation (e.g. Fig. 3.9). The contact between the Bowland Shale Formation and overlying sandstones is marked by a prominent change in the topographic gradient. Turbiditic sandstones are intermittently exposed from this level upward along a stratigraphic thickness of ~30 m (Fig. 3.8; 3.9). Individual turbidite deposits are generally less than 1 m thick but reach up to ~4 m in one example. Beds generally show fining upward sequences from (very) coarse-grained sandstones containing abundant granules and <3 cm pebbles at their base, to medium- or fine-grained sandstones at their top. Pebbles at the base of beds are generally horizontally aligned, suggestive of traction carpet deposition. Quartz pebbles are common but lithic and granite pebbles are observed as well. Above the turbidite succession an interval of ~15 m is unexposed, on top of which a ~26 m thick sandstone succession is observed. The lower part is poorly exposed and appears partially rotated due to landslip on the SW-side of Threapland Gill [39972 45999]. Cross-bedding is observed in the upper 10 m of this succession,

indicating S – SE flow directions in coarse-grained to granular sandstones with ~2 cm pebbles.

The successive ~20 m are unexposed, overlain by a major sandstone level that is exposed on either side of Threapland Gill. Northward, Rolling Gate Crag exposes a ~20 m sandstone succession (Fig. 3.8). The top is formed by 4 m of trough cross-bedded sandstones, overlying Gilbert-type foresets that reach a maximum height of 16 m, showing E - SE flow directions. Grain size in this succession is medium to granular, containing abundant pebbles of up to 4 cm. At the base of these deltaic foresets, metre-scale structureless and faintly-laminated deposits are observed, interbedded with medium- to coarse-grained toe-set sandstones of the Gilbert-type delta. On the southern side of Threapland Gill, The Crags [39967 45964] expose a similar succession (Fig. 3.9). A feature representing this stratigraphic level can be traced in the landscape providing a reliable correlation to more southern outcrops at Barden Moor (Fig. 3.9). The successive 25 m forms an unexposed succession and is presumably fine-grained. It is overlain by a sandstone succession exposed at Bartle Crag [40018 45999] and Peter's Crag [39986 49559], which are similar in grain size as the stratigraphically lower Rolling Gate Crag (Fig. 3.9). At Bartle Crag only a thin succession is exposed containing trough cross-bedded sandstones. This interval also forms a landscape feature that can be traced southward towards the Obelisk. Maps from the Coal Authority indicate the presence of a coal seam approximately 10 metres higher in the succession (Coal Authority, 2012). On top a coarse-grained sandstone is poorly exposed (Fig. 3.9).

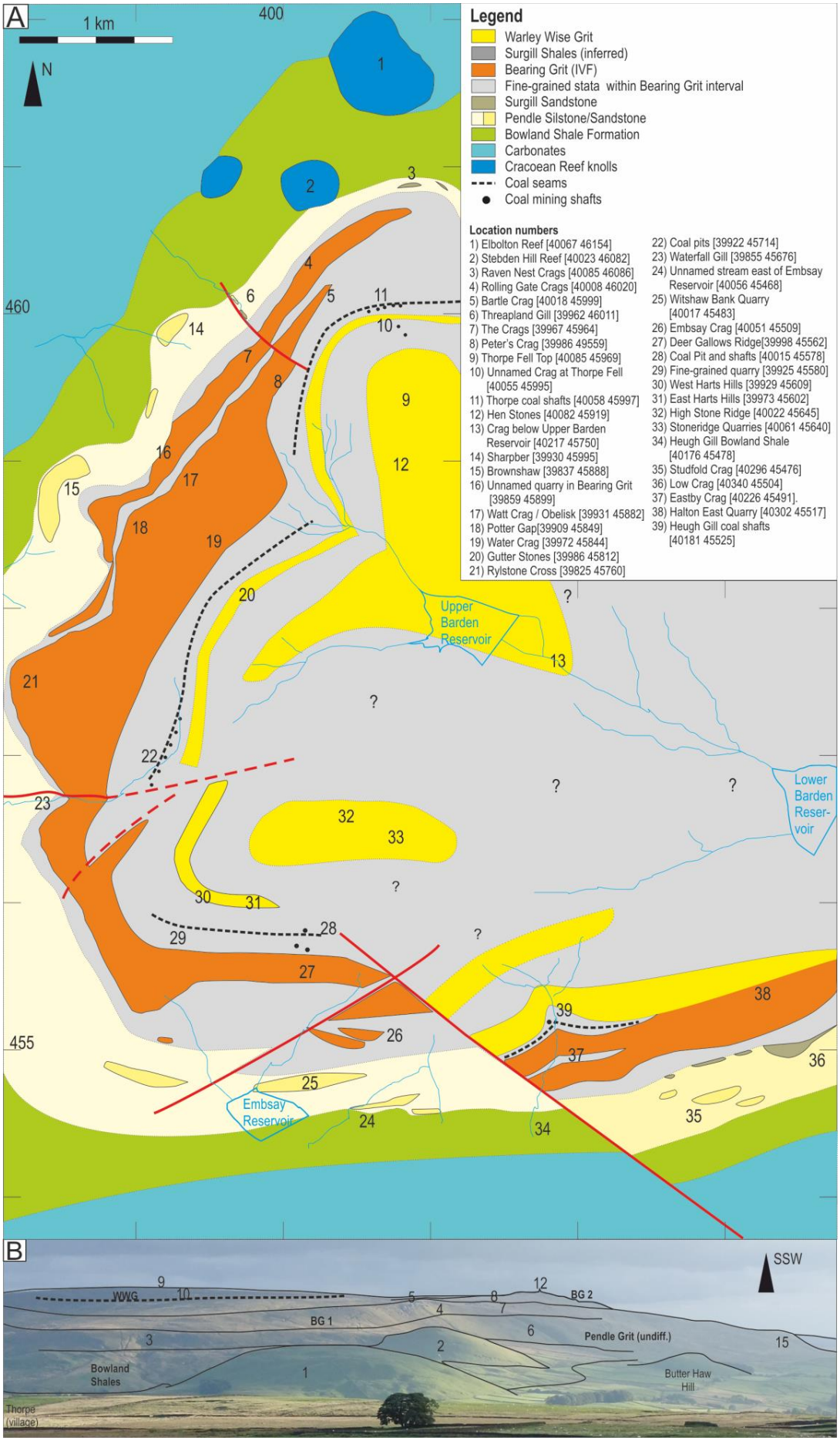
A
1 km
N
400
460
455
Legend
Warley Wise Grit
Surgill Shales (inferred)
Bearing Grit (IVF)
Fine-grained stata within Bearing Grit interval
Surgill Sandstone
Pendle Silstone/Sandstone
Bowland Shale Formation
Carbonates
Cracoean Reef knolls
Coal seams
Coal mining shafts
Location numbers
1) Elbolton Reef [40067 46154]
2) Stebden Hill Reef [40023 46082]
3) Raven Nest Crags [40085 46086]
4) Rolling Gate Crags [40008 46020]
5) Bartle Crag [40018 45999]
6) Threapland Gill [39962 46011]
7) The Crags [39967 45964]
8) Peter's Crag [39986 49559]
9) Thorpe Fell Top [40085 45969]
10) Unnamed Crag at Thorpe Fell [40055 45995]
11) Thorpe coal shafts [40058 45997]
12) Hen Stones [40082 45919]
13) Crag below Upper Barden Reservoir [40217 45750]
14) Sharpber [39930 45995]
15) Brownshaw [39837 45888]
16) Unnamed quarry in Bearing Grit [39859 45899]
17) Watt Crag / Obelisk [39931 45882]
18) Potter Gap[39909 45849]
19) Water Crag [39972 45844]
20) Gutter Stones [39986 45812]
21) Rylstone Cross [39825 45760]
22) Coal pits [39922 45714]
23) Waterfall Gill [39855 45676]
24) Unnamed stream east of Embsay Reservoir [40056 45468]
25) Witshaw Bank Quarry [40017 45483]
26) Embsay Crag [40051 45509]
27) Deer Gallows Ridge[39998 45562]
28) Coal Pit and shafts [40015 45578]
29) Fine-grained quarry [39925 45580]
30) West Harts Hills [39929 45609]
31) East Harts Hills [39973 45602]
32) High Stone Ridge [40022 45645]
33) Stoneridge Quarries [40061 45640]
34) Heugh Gill Bowland Shale [40176 45478]
35) Studfold Crag [40296 45476]
36) Low Crag [40340 45504]
37) Eastby Crag [40226 45491].
38) Halton East Quarry [40302 45517]
39) Heugh Gill coal shafts [40181 45525]
Upper Barden Reservoir
Lower Barden Reser-voir
Embsay Reservoir
B
SSW
WWG
BG 1
BG 2
Pendle Grit (undiff.)
Bowland Shales
Butter Haw Hill
Thorpe (village)

Figure 3.9 (previous page) (a) Interpretation of west and south side of Barden Moor (see Fig. 3.2 for location). Note the two stratigraphic levels within the Bearing Grit at which Gilbert-type deltas occur. The position of the coal seam above the inferred level of the Bearing Grit (see section 3.4.2.8) is used as a correlation surface in for sections 2 – 5 in Figure 4.11. (b) Photo interpretation of the north-west side of Barden Moor. Note the relative stratigraphic positions of the Bowland Shales, Cracoean reefs, and overlying fluvio-deltaic sediments of the Surgill Sandstone. The top of the Cracoean reefs occurs near the base of the Surgill Sandstone, indicating shallow water conditions near the northern flank of Barden Moor, rapidly deepening southward as indicated by the thickening of the Pendle Grit turbidites.

Interpretation

Marine bands are not observed in the area, which makes correlations tentative. The cross-bedded sandstones at Raven Nest Crag overlie the Bowland Shale Formation and are considered part of the Surgill Sandstone of the Pendle Grit Member. This interval can be correlated to the cross-bedded sandstones in Threapland Gill, where this interval forms the top of a turbidite-fronted delta system in water depths of several tens of metres. The turbiditic facies are assigned to the Pendle Sandstone (Fig. 3.3; 3.9).

The succession from the Rolling Gate Crag level up to the coal seam is tentatively correlated to the Bearing Grit and this correlation will be discussed in Section 3.4.2.8. This stratigraphic interval consists of two stratigraphic levels at which Gilbert-type delta foresets occur, suggesting a delta front environment, in which the structureless metre-scale deposits in the delta represent sediment-gravity-flow deposits. The overlying coarse-grained cross-bedded sandstone probably corresponds to a fluvio-deltaic channel setting in the Warley Wise Grit.

3.4.2.3 Brownshaw to Obelisk section: Barden Moor

Description

This section is located on the western side of Barden Moor (Fig. 3.8; 3.9). Brownshaw [39837 45888] forms a large landscape feature at the base of the succession that suggests the presence of sandstones in the lower 60 m of the Pendle Grit Member, based on a correlation to Threapland Gill (Section 3.4.2.2). Only

blocks of massive sandstones with shale clasts are exposed along the base of the landscape feature, suggesting a turbiditic origin.

The basal Bearing Grit level, correlating to Rolling Gate Crag (see above) is exposed in an unnamed quarry [39859 45899] and forms a feature on the crest of Brownshaw. The unnamed quarry exposes three metre-scale, structureless, normally graded, pebbly deposits. Pebbles of up to 3.5 cm in diameter occur at the base, while the maximum grain size at the top of beds is granular. Mud clasts are concentrated towards the top of the bed. The second level of the Bearing Grit, correlating to Bartle Crag (Fig. 3.9) is well-exposed from the Obelisk southward and is ~35 m thick. At several outcrops, such as at Potter Gap [39909 45849] large-scale foresets are observed, closely associated with erosionally-based metre-scale structureless deposits becoming faintly laminated towards the bed top (Fig. 3.10). The succession is overlain by trough cross-bedded sandstones [39935 458772] (Fig. 3.10). Generally, sandstones are coarse- to very coarse-grained, with occasional granular beds. Pebbles range up to ~4 cm in size. Both the large-scale foresets, as well as the overlying trough cross beds indicate flow directions towards the E and SE.

Figure 3.10 (next page) Outcrop character of the Bearing Grit at the west side of Barden Moor indicates a close association of sediment-gravity-flow deposits and deltaic Gilbert-type foresets. F6 indicates sediment-gravity-flow deposits, F7B-D indicate various types of Gilbert-type foresets discussed in Chapter 5, F8 indicates cross-bedded sandstones. (a, b) Northward directed overview of the upper level of the Bearing Grit taken from Potter Gap towards the Obelisk (see Fig. 3.9). Tectonic dip is sub-horizontal and can be observed at outcrop 6 at the right hand side of the figure. Steeper dips represent depositional dip of large-scale foresets. At outcrop 1 (see c, d) Gilbert-type delta foresets are erosionally overlain by sediment-gravity-flow deposits. These sediment-gravity-flow deposits are overlain by Gilbert-type deltas in outcrop 2 and 3, followed on by sediment-gravity-flow deposits (see outcrop 3) and Gilbert-type deltas (outcrop 4 and 5, see e, f). Outcrop 6 shows trough cross-bedded sandstones, overlying the entire succession.

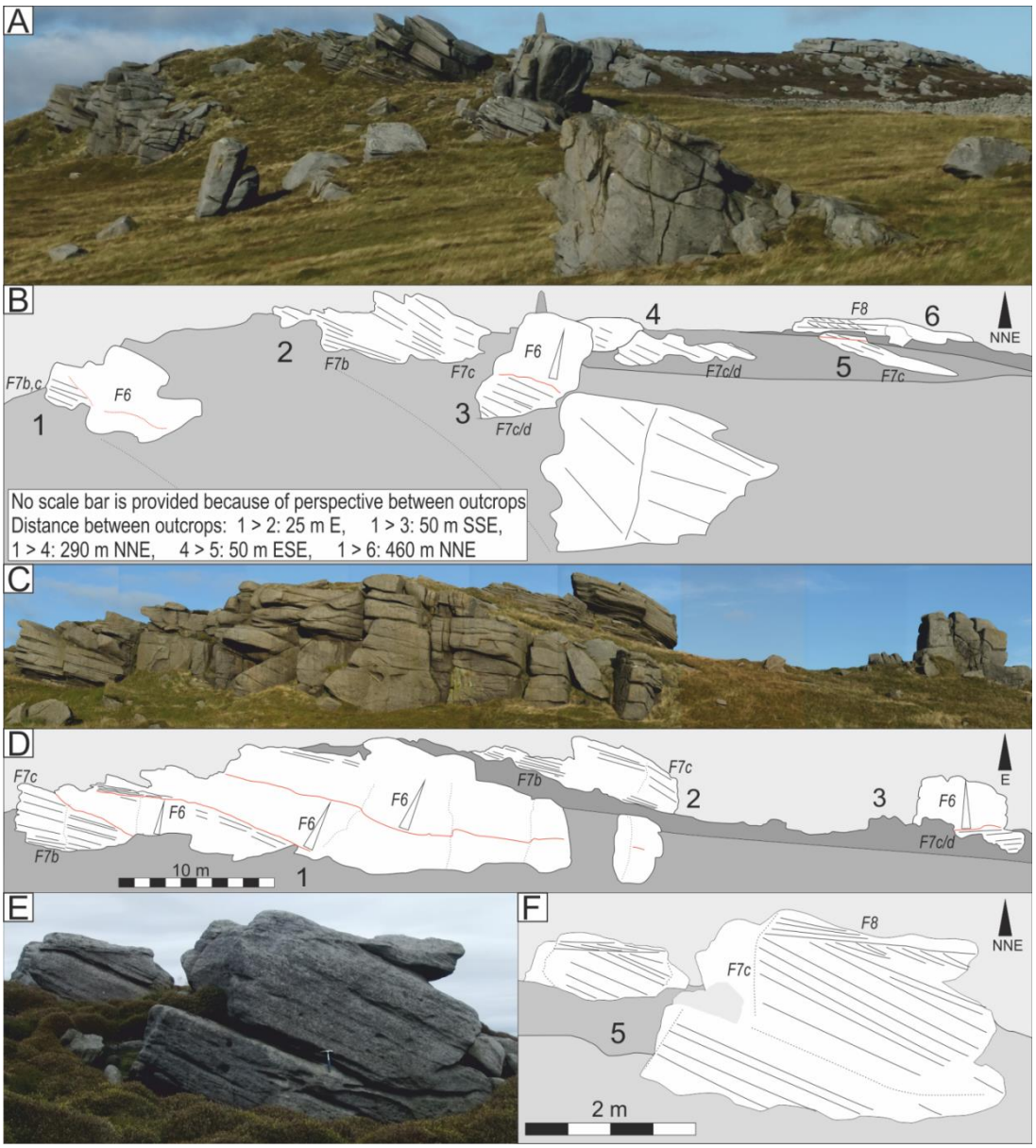

Interpretation

The Pendle Grit succession is very poorly exposed but forms a major landscape feature. Therefore, it is considered likely that locally a sand-rich succession is present. The overlying basal part of the Bearing Grit consists entirely of sediment-gravity-flow deposits, suggesting a more distal delta toe position with respect to the correlative Gilbert-type delta foresets and sediment-gravity-flow deposits at Rolling Gate Crag (see Section 3.4.2.2; Fig. 3.9). The upper Bearing Grit level features Gilbert-type delta foresets alternated with sediment-gravity-flow deposits.

3.4.2.4 Barden Moor: south side

Description

The south side of Barden Moor forms the northern flank of the Skipton Anticline. The succession is highly faulted, making lateral correlations and thickness estimates difficult (Fig. 3.9). The Bowland Shale Formation is best exposed at Heugh Gill from [40167 4545] up to [40176 45478] (Fig. 3.8; 3.9). Above this location, cm- to dm- scale, fine-grained turbidite beds are observed in a heterolithic succession. Toolmarks on sharp-based, thin turbiditic sandstones indicate SE – SW flow directions. This succession is faulted against a ~ 15 m thick medium- to very coarse-grained sandstone containing pebbles up to 1.5 cm that correlates to Eastby Crag, a cross-bedded channelized sandstone (Fig. 3.9; cf. Hudson and Mitchell, 1937).

The base of the Pendle Grit Member is best exposed at an unnamed stream to the east of Embsay Reservoir [40056 45468] (Fig. 3.9). It exposes a succession of thin turbiditic sandstones, interbedded with shales and siltstones indicating SE – W flow directions. Higher in the Pendle Grit Member, NNW and ENE-oriented quarry faces in Witshaw Bank Quarry [40017 45483] expose a turbidite channel (Fig. 3.8; 3.9). Laterally persistent beds occur in the ENE face and strongly lenticular beds in the NNW face, suggesting SSE flow directions. Approximately 25 m is exposed in metre-scale, erosionally-based coarse-grained to granular turbiditic sandstones with 1 cm pebbles. Most beds are structureless and show no grading or slight normal grading. Some beds show S2 type banding, alternating cm-scale coarse- and medium-grained layers (Lowe, 1982). Lines of mud clasts are frequently observed as well as pods of disintegrating shale rafts that result in metre-scale debritic intervals.

Above this turbidite channel, a ~35 m thick succession is unexposed on top of which a ~3 m thick coarse-grained, massive sandstone is exposed, containing some shale clasts. Embsay Crag [40051 45509] exposes two crudely-bedded channelized sandstone bodies that are closely overlain by a cross-bedded sandstone succession, representing a succession similar to the western side of Barden Moor (Fig. 3.9). Embsay Crag is characterised by lenticular, coarse-grained to granular sandstone beds that contain abundant <4 cm pebbles. These beds contain crude cross beds or vague laminations. Notably, shale clasts or intermittent shale or siltstones

are not observed. Directly above this level, cross-bedded sandstones are observed at [40085 45533] that correlate to the cross-bedded sandstone levels at Deer Gallows Ridge [39998 45562] towards the west, and Eastby Crag towards the east [40226 45491] (Fig. 3.9).

Above Deer Gallows Ridge, coal shafts and a coal pit occur in a generally unexposed succession [40015 45578]. Laterally, fine-grained sandstones flagstones and massive sandstones are exposed in a small quarry [39925 45580]. This succession is overlain by small outcrops at West and East Harts Hills [39929 45609] [39973 45602], which expose a 2 m succession medium- to very coarse-grained trough cross-bedded sandstones, containing pebbles of up to 1 cm. At a slightly higher level, High Stone Ridge, and Stoneridge Quarries [4004 4564] expose a 5 m thick succession of medium- to coarse-grained cross-bedded sandstones without pebbles. Tectonic dips are erratic, which makes it difficult to estimate the thickness of the intermittent succession.

Eastby Crag to Halton East Quarry forms a nearly continuous outcrop in cross-bedded sandstones (Fig. 3.9). At Halton East Quarry Crag, the base of the succession is formed by sub-horizontally deposited 0.1 - 0.3 metre thick massive beds. The contact between successive massive beds is marked by <4 cm laminated sandstone intervals showing bed-parallel or ripple cross lamination. This succession is overlain by large-scale planar cross beds of up to 7 m height, indicating flow directions to the east. Above, metre- and decimetre-scale trough cross bedding is observed over a ~8 m interval that transitions to planar cross bedding upwards. Pebbles are mainly located at the base of this succession and range up to 3 cm. Flow directions are towards the SE to SW. A coal seam is probably present above Eastby Crag at the head of Heugh Gill [4018 4553], based on maps of the Coal Authority (Coal Authority, 2012).

Approximately 60 m below the level of Halton East Quarry, several sandstones are exposed (Fig. 3.9). The highest sandstones form a relatively continuous feature for ~2.5 km, from [4026 4549] to [4049 4553] that thickens to ~15 m at Low Crag [4034 4550]. This level exposes metre-scale cross bedding at the top of outcrops indicating SE- SW flow directions, whereas lower beds are predominantly massive (Fig. 3.8; 3.9). Grain size is medium to very coarse sand, and

pebbles range up to 3 cm. This level is assigned to the Surgill Sandstone, similar to exposures in Threapland Gill and Raven Nest Crags (see section 3.4.2.2).

Stratigraphically lower exposures (between 35 – 80 m lower) occur near Studfold [40259 45473] to [40312 45479]. At Studfold, blocks that are probably in-situ show massive, coarse-grained to granular, generally pebbly sandstone beds with floating pebbles of up to 5 cm. Shale clasts as well as decimetre-scale log imprints are occasionally observed. The outcrop has a height of ~30 m, and a probable width ~500 m. An additional outcrop at this level occurs at Little Hare Head [40527 45529]. Here a small quarry exposes 5 metre of 0.5 -1 m beds in medium- to coarse-grained sandstone with occasional <1.5 cm floating pebbles. Some beds show wavy laminations at the base that transition into massive sandstones upwards.

Interpretation

The south side of Barden Moor provides a faulted but complete stratigraphic succession of the Pendleian succession. The Pendle Sandstone consists of thick turbidite channel and heterolithic deposits exposed at Witshaw Bank Quarry and nearby locations. Eastward, Low Crag indicates the top of the Surgill Sandstone as a cross-bedded interval, suggesting progradation of the coastline up to at least this position during the deposition of the Pendle Grit Member. The channelized sandstones that occur at slightly lower stratigraphic level do not feature cross-beds and might represent very proximal gravity-flow deposits in the Pendle Grit.

The metre-scale sediment-gravity-flow deposits at Embsay Crag occur at a higher stratigraphic level than the Surgill Sandstones and are similar to the sediment-gravity-flow deposits at the base of the Bearing Grit on the west-flank of Barden Moor. The overlying succession that is exposed directly above Embsay Crag, at Deer Gallows Ridge, Eastby Crag and Halton East Quarry forms a thick, laterally continuous, cross-bedded succession containing Gilbert-type delta foresets in the latter location, consistent with a correlation to the Bearing Grit.

The subdivision between the Bearing and Warley Wise Grit is based on mapping because of the absence of marine band control, and is taken in the persistent unexposed interval containing a coal seam, similar to the west-side of Barden Moor.

3.4.2.5 Flasby Fell

Description

At Flasby Fell (Fig. 3.2), the Cravenoceras malhamense Marine Band is observed within the Bowland Shale Formation (Arthurton et al., 1988), placing the overlying succession in the Pendleian. The overlying Pendle Grit Member is poorly exposed. However, several channelized sandstones can be inferred based on the occurrence on landscape features. At an unnamed stream, [3968 4539], thin bedded turbidites are formed, occasionally containing debritic caps containing numerous mud clasts. The overlying succession is well-exposed along a ridge line at Crag Wood [3962 4544] to [3955 4552]. It consists of lenticular sand bodies containing crudely-bedded and massive, coarse-grained to granular sandstones, with shale clasts of up to 10 cm width and abundant pebbles of up to 2.5 cm. In some beds, pebbles are aligned along backsets dipping towards the northwest, indicating SE flow directions.

These outcrops occur in the hanging wall of a NW-SE-oriented fault zone and dip up to 32° NE. At Sharp Haw, on the footwall of this fault, the base of this succession occurs at a 40 - 60 m higher topographic level and is dipping 12° NE. This suggests that the extensive outcrop of Crag Wood might be deposited in a growth fault (cf. Mundy and Arthurton, 1980) although an absence of continuous overlying strata at either side of the fault makes this inference inconclusive.

At Rough Haw [3963 4559], similar structureless and crudely-laminated deposits are observed. Here, trough cross-bedded sandstones are observed several metres higher.

Interpretation

The Blacko and Cravenoceras cowlingense Marine Bands are not recognised at Flasby Fell, making stratigraphic correlations unreliable. The Pendle Grit Member is poorly exposed but several small channels are inferred based on landscape features.

The structureless and crudely-laminated sandstones of Sharp Haw and Rough Haw probably represent sediment-gravity-flow deposits that are closely overlain by cross-bedded sandstones. This suggests a delta front environment similar to that observed on the western side of Barden Moor. This similarity and the

occurrence directly above strata assigned to the Pendle Grit Member (Arthurton et al., 1988) suggests that these strata belong to the Bearing Grit. The steep dip of deposits at Sharp Haw is probably related to growth-faulting in the delta front.

3.4.2.6 Skipton Moor, Croft House borehole and Low Bradley 1 Borehole

Description

At Skipton Moor (Fig. 3.2; 3.11), the boundary between the Bowland Shale Formation and Pendle Grit Member is well exposed. Deposition of the Pendle Sandstone turbidites occurs over a stratigraphic interval of ~220 m. The basal sandstones coalesce into relatively continuous sheet sandstone, whereas stratigraphically higher channelized deposits of several hundred metres width are embedded within fine-grained deposits (Fig. 3.11). Basal surfaces of individual channels are sharp and generally erosional. Channels sandstones have a gross thickness of approximately 5 – 15 m and individual beds are generally up to 1.5 m. Grain sizes are poorly sorted (medium – granular) but rarely contain pebbles. Outcrops are generally small and strongly weathered, which impedes a detailed analysis of sedimentary structures, or changes between the base and top of the succession. Sandstones frequently show a surface texture where horizontal lenses form, up to 5 cm high and ~1 metre wide, resembling ropy lava flows, and referred to as 'ropy weathering' (Baines, 1977), which has been interpreted as a primary structure (e.g. Sims, 1988). On adjacent, typically less exposed rock faces, weathering patterns are typically massive or blocky. At the top of the quarries, sandstones are typically fractured in similar patterns as the ropy texture described above, regardless of facies or tectonic dip. It is considered likely that this structure is secondary and related to the significant weathering of these natural exposures. In a small quarry exposure occurs near Snaygill [39954 44995], the same pattern is preserved in the fracture pattern but no differences in grain size is observed that could explain the 'ropy weathering' as a primary structure (Fig. 3.11).

Except for Jenny Gill Quarry [4006 4599] and Potters Gill [4025 4514] at the base of the Pendle Sandstone, and outcrops along Cawder Gill at the transition from the Pendle Sandstone to the Pendle Siltstone [39970 44989] to [40064 45052], good outcrops are absent (Fig. 3.11). Within the exposed channelized bodies, sandstones

are predominantly structureless, high density turbidite facies, rarely exposing internal

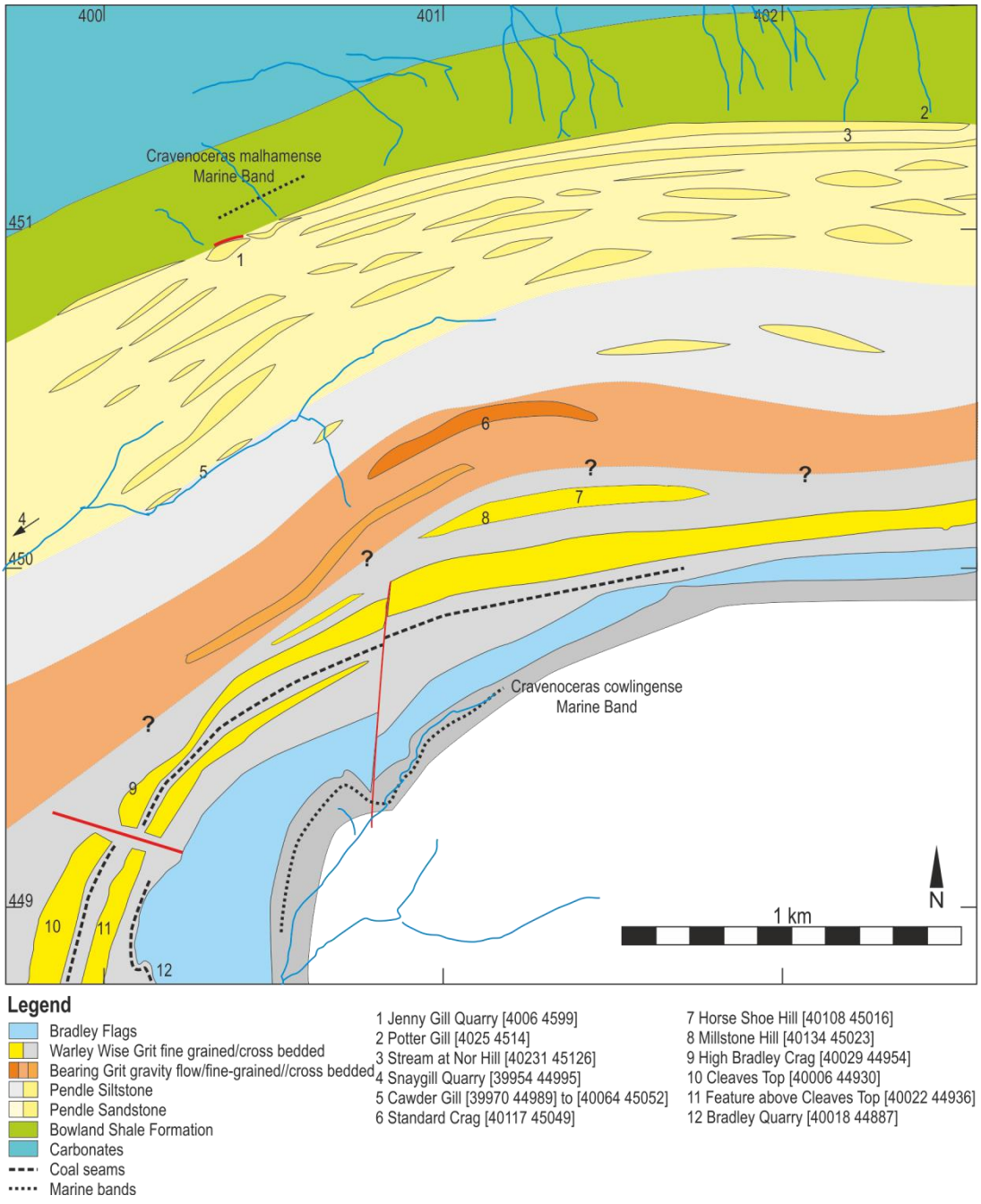

Figure 3.11 Outcrop map at Skipton and Bradley Moor. See Fig. 3.2 for location within Craven Basin. Thick turbiditic sandstones in the Pendle Sandstones coalesce into a continuous sheet near the base, higher up they are deposited in shale-encased small channels. The position of the Bearing Grit is inferred from correlation with the Low Bradley Borehole (see Sections 3.4.2.6 and 3.4.2.8).

structures. Thin fine-grained turbiditic beds are occasionally observed in metre-scale successions towards the top of channels. At Jenny Gill Quarry, the basal flows were erosive, based on the occurrence of a metre-scale shale raft that is still partially attached to the underlying shale facies. Additionally, a SE-dipping growth fault has been suggested by Sims (1988). Tectonic dips of turbiditic strata in Jenny Gill Quarry are approximately 20° S while both overlying and underlying strata dip at approximately 30 -35° S, suggesting the presence of an unexposed growth fault.

The top of the turbidite succession at Skipton Moor is characterised by the Pendle Siltstone that forms a slope deposit dominated by siltstones with rare turbiditic sandstones and shales.

The Pendle Siltstone is overlain by structureless sandstones at Standard Crag [40117 45049] of which ~3 m is exposed. These deposits are typically very coarse-grained, occasionally conglomeratic with abundant 1 cm pebbles. Standard Crag is overlain by a ~20 m unexposed interval, on top of which cross-bedded sandstones are deposited. Discontinuous cross-bedded sandstone bodies occur at several levels in the overlying succession, where for example Millstone Hill [40134 45023] forms an intermediate level (Fig. 3.11).

Cleaves Top and its lateral equivalents [40044 44970] to [39973 44844] form a prominent escarpment near High Bradley of which ~5 m is exposed. At the base of the exposure, 1 m thick cross sets are observed, overlain by sets of several decimetres. Sandstones are coarse- to very coarse-grained, with frequent granules. Lags frequently contain 2 cm pebbles, and occasionally reach 3 cm. Common planar cross bedding, and rare trough cross bedding indicates flow directions towards the S - SW. The 0.6 m thick Bradley Coal overlies this escarpment succession and has been mined extensively, providing a marker horizon at Skipton and Farnhill Moor. The Bradley Coal is overlain by another 10 – 15 m thick, cross-bedded sandstone (Fig. 3.11; Baines, 1977; Addison, 1997). This succession is followed by a 21 m silty mudstone containing a thin coal at its base and marine fauna near its top in the Croft House Borehole (Addison, 1997; Waters, 2000). On top, the Bradley Flags form a fine-grained delta abandonment facies, best exposed at the Bradley Quarry [40019 44886], which is overlain by the Cravenoceras cowlingense ($E_{2a}1$) Marine Band (cf. Baines, 1977; Waters, 2000).

The Croft House borehole [46540 44701] at Cononley Moor indicates a marine horizon within the proximal Craven Basin (Fig. 3.2; cf. Riley, 1996; Addison, 1997). Outcrop maps indicate that the top of the borehole is located slightly below the Cravenoceras cowlingense Marine Band ($E_{2a}1$) (Addison, 1997; Waters, 2000). The borehole provides a record through a 13.7 m succession of fine-grained sandstones that correlate to the Bradley Flags. The underlying shale and siltstone succession contains a coal seam at its base and a marine *Sanguinolites* facies towards its top, similar to the facies described for the Blacko Marine Band (Riley, 1996). However, a correlation of this marine horizon with the Blacko Marine Band would suggest an absence of the entire Warley Wise Grit. Additionally, nearby borehole occurrences of the Blacko Marine Band at Elsack Moor [3937 4484] 4 km to the west (Brandon et al., 1995) exclude the possibility of the Blacko Marine Band above a significant succession of cross-bedded sandstones. Alternatively, Riley (1996) proposes that this marine horizon is an initial flooding surface of the Cravenoceras cowlingense Marine Band that is locally separated from the maximum flooding by the Bradley Flags.

The Low Bradley 1 Borehole, on Bradley Moor is drilled within the Bradley Flags at [40195 44786] and provides a continuous succession down to the Bowland Shales (Fig. 3.2; 3.8). Above the Bowland Shales, a sand-rich succession with subordinate shales is present that gradually transitions in a silty shale-dominated succession with subordinate thin sandstones. Overlying this succession are two coal seams, approximately 15 m apart in a silt-dominated succession. Approximately, 90 m higher the succession becomes sand-dominated and contains two additional coals seams, approximately 22 m apart. This succession is overlain by a sandstone-dominated succession near the top of the borehole equating to the Bradley Flags.

Interpretation

The base of the succession in the Skipton Moor and Low Bradley 1 Borehole is similar in both thickness and character, and interpreted as a slope succession with numerous minor turbidite channels, within a heterolithic succession containing shales, siltstones and thin turbiditic sandstones. This succession is interpreted as the Pendle Sandstone and is overlain by a sand-poor succession interpreted as the Pendle Siltstone in both occurrences.

The top of the succession in the Low Bradley 1 Borehole can be correlated to the outcrop section at Skipton Moor via two coal seams at the approximate levels of the Bradley Coal and the coal below the Bradley Flags (Fig. 3.8). The two coal seams that occur ~90 m lower in the Low Bradley 1 Borehole correspond broadly to the stratigraphic level of Standard Crag and the overlying cross-bedded sandstone in the Skipton Moor succession (Fig. 3.8; 3.11). These coals indicate peat-accumulation and thus a sub-aerial delta top environments near the base of the fluvio-deltaic succession. It is considered therefore considered likely that this occurred during the $E_{1c}1$ cycle and is associated with the Bearing Grit.

The marine fauna exposed in the Croft House Borehole probably represent an initial flooding surface of the Cravenoceras cowlingense Marine Band, based on occurrences of the Blacko Marine Band in nearby boreholes (cf. Brandon et al., 1995; Riley, 1996). This suggests that the Warley Wise Grit occurs below this level, which on Skipton Moor equates to the Millstone Hill and Cleaves Edge levels. Additionally, it suggests that the fine-grained Bradley Flags formed during transgression.

3.4.2.7 Farnhill Moor

Description

Farnhill Moor [4008 4470] is located south of Skipton and Bradley Moor and can be correlated to these locations via the Bradley Coal and the Cravenoceras cowlingense Marine Band (Fig. 3.8). The basal sandstones in the Warley Wise Grit are exposed near Jubilee Tower [4006 4471] and are structureless, coarse- to very coarse-grained metre-scale beds with some granules. A gap of ~15 m separates this succession from the overlying cross-bedded facies that is best exposed at Hardacre Quarry [40090 44679]. Here, large-scale foresets of 7 – 8 m height are overlain by cross-bedded sandstones, indicating SE-flow directions (Fig. 3.15b) . About 2 m of the overlying cross-bedded succession is exposed at the top of the quarry but additional exposures indicate that this succession reaches an approximate thickness of 18 m, and records SE-SW flow directions. This succession is overlain by the Bradley Coal.

Interpretation

The correlation of the Bradley Coal between Skipton Moor and Bradley Moor suggests that the large-scale foresets exposed at Hardacre Quarry are part of the Warley Wise Grit. This implies that both the Bearing and the Warley Wise Grit contain large foresets that are interpreted as Gilbert-type delta deposits.

3.4.2.8 Correlation of Transition Zone area

At Threshfield Moor, Barden Moor and Flasby Fell marine flooding surfaces have not been observed, while this area records large differences in the sedimentological character at the block to basin transition (cf. Fig. 3.6; 3.8). Here a tentative correlation is made between these areas, and with areas with marine band control.

On the Askrigg Block, the Bearing Grit is frequently split into two sandstone levels, separated by a coal seam. An additional coal seam occurs at the top of the Bearing Grit in a shale interval of 10 -20 m thickness that also contains the Blacko Marine Band. Above the Warley Wise Grit, another coal seam is occasionally observed (Fig. 4.6). Additionally, although both the Bearing Grit and Warley Wise Grit are frequently granular or pebbly, maximum pebble size in the Bearing Grit is consistently larger, ranging up to 5 cm in diameter, whereas the Warley Wise Grit typically contains pebbles of up to 2 cm and rarely reaches up to 3 cm.

Threshfield Moor lies close to the North Craven Fault and exposes a thick coal seam (Skirethorn Coal) deposited between two levels of very coarse-grained, pebbly cross-bedded sandstones. A thinner coal seam is observed at the base of the overlying ~20 m shale interval (Section 3.4.2.1). It is considered likely that the lower coal seam corresponds to the coal seam within the Bearing Grit on the Askrigg block, while the upper coal seam at the base of a 20 m shale interval is considered to correspond to the top of the Bearing Grit (Fig. 3.6). The maximum pebble sizes for the Bearing Grit on the Askrigg Block and at Threshfield Moor are similar in this correlation, supporting this correlation.

At Barden Moor, only one coal seam is known. It is worked extensively near Waterfall Gill and Thorpe Fell (Fig. 3.8; 3.9) and overlies two stratigraphic levels at which Gilbert-type deltas and sediment-gravity-flow deposits with pebbles of up to

4 – 5 cm occur. This coal seam is tentatively correlated with the thin upper coal seam on Threshfield Moor. Flow directions at Threshfield Moor indicate that channels flowed towards Barden Moor implying that deposits are likely deposited by the same fluvio-deltaic systems (cf. Fig. 3.2; 3.8). In this correlation, the two very coarse-grained, pebbly channelized sandstones at Threshfield Moor correspond to the two levels at which pebbly Gilbert-type deltas occur on Barden Moor. The Warley Wise Grit at Threshfield Moor is variably fine-grained to pebbly and might fit well with the sandstone level above the coal seam on Barden Moor that is occasionally pebbly as well but relatively finer-grained than the two levels at which Gilbert-type deltas occur (e.g. at Hart Hills and Thorpe Fell; Fig. 3.9).

At Skipton Moor, the entire Pendleian succession has significantly expanded in thickness, indicating a significant step in the basin morphology (Fig. 3.8). Here, the Bradley Coal forms an abundantly worked coal seam at an intermediate level within the Warley Wise Grit. Another thin coal seam occurs between the top of the Warley Wise Grit and Bradley Flags. The Low Bradley 1 Borehole indicates two additional coal seams near the base of the fluvio-deltaic succession (Fig. 3.8) that correlate with the approximate level of the Standard Crag and are here associated with sub-aerial conditions at the stratigraphic level of the Bearing Grit (Fig. 3.8). In this case, the sediment-gravity-flow deposits at Standard Crag resemble the same stratigraphic interval as Embsay Crag on Barden Moor, although the precise boundary between the Bearing Grit and Warley Wise Grit is unclear in the absence of the Blacko Marine Band.

3.4.3 Location descriptions of Harrogate sub-basin

3.4.3.1 Beamsley Moor

Description

Beamsley Moor is positioned at the boundary between the Transition Zone and the Harrogate sub-basin and presents a broadly similar succession as Skipton Moor (Fig. 3.2). The basal contact between the Bowland Shales and the Pendle Grit Member is not known precisely but the lowest channelized sandstones within the Pendle Sandstone are observed in Kex Beck [40807 45261]. The transition from the Pendle Sandstone to the Pendle Siltstone occurs at the confluence of Kex Beck and

Howgill Sike [40921 4539], above which only minor sandstones occur. In comparison to Skipton Moor, the thickness of the siltstone- and/or shale-dominated Pendle Siltstone increases significantly from ~90 to ~280 m. Overlying this succession are massive bedded, coarse-grained to granular sandstones with rare 1 - 2 cm floating pebbles that form the prominent Beamsley Beacon escarpment [4097 4524]. This escarpment is similar in character to Standard Crag at Skipton Moor. Based on the scale of the landscape feature, at least 30 m of predominantly sandstones are present although only the top ~7 m are exposed. Beds are strongly weathered and frequently show a 'ropy weathering' style.

Cross-bedded sandstones, exposed in small quarry exposures near the triangulation point at [40997 45241] and near Little Crag [4101 4529] to [4102 4534] are observed at ~20 m above this level and indicate southward flow directions. This interval is ~10 - 15 m thick and is overlain by an unexposed interval of ~40 m, presumably containing mainly siltstone and argillaceous sediments. This is followed on by another cross-bedded sandstone succession of which up to 5 m is exposed at Trundle Stones [40984 45188], and High Combs [4111 4538]. These outcrops contain both planar and trough cross-bedded sandstones in beds of ~0.5 m, indicating S – SE flow directions. Grain size is medium- to very coarse sand, with pebbles up to 2 cm. A 5 – 10 m unexposed interval separates Trundle Stones from micaceous flagstones that are very poorly exposed in old workings east of Beacon Hill House [40985 45176].

Interpretation

The successions at Beamsley and Skipton Moor have very similar sedimentological and stratigraphic patterns. Therefore, the Beamsley Beacon escarpment, and directly overlying cross-bedded succession is included in the Bearing Grit. The Trundle Stones and High Combs succession overlying the ~40 m unexposed interval is assigned to the Warley Wise Grit.

3.4.3.2 Harlow Carr Park section

Description

The Harlow Carr Park section lies on the northern limb of the Harrogate Anticline and provides a relatively continuous, near-vertical section along a tributary of Oak Beck from the Harlow Carr Gardens northward (Fig. 3.2). The section exposes the contact of the Bowland Shale Formation and the Pendle Siltstone at the first occurrence of siltstones and sandstones at [42777 45219]. Up to [42763 45434] approximately 160 - 170 m of alternating dark siltstones and sandstones are exposed. Sandstones occur in packages of less than 8 m thick. Individual sandstones are 0.2 - 0.5 m thick and typically fine- to medium-grained. Sandstone packages are separated by siltstone-dominated successions of up to 50 m that occasionally contain cm-scale turbidites.

From [42763 45434] up to [42757 45437] a ~70 m interval is dominated by interbedded carbonaceous and micaceous siltstones and fine-grained sandstones that are interpreted as a delta slope and delta mouthbar environment (e.g. Cooper and Burgess, 1993). At the top of this section, parallel-laminated, medium-grained sandstones are observed that represent a mouth bar type setting. Laterally, cross-bedded sandstones are observed at this stratigraphic level at [4272 45447], indicating SE flow directions in a heavily overgrown, ~4 m high outcrop. Sandstones are medium to coarse grained, and contain rare pebbles of up to 2 cm in diameter. A ~20 m unexposed interval separates this succession from a laterally continuous sandstone interval starting at [42755 45443]. These cross-bedded sandstones are typically coarse-grained and contain pebble lags with 1 cm pebbles. The thickness of the succession is difficult to reconstruct due to limited exposures and decreasing tectonic dip but is estimated at ~ 70 m. The Cravenoceras cowlingense Marine Band is observed just above the succession (Ramsbottom, 1974).

The nearby Moor Park Farm Borehole at [425749 453199] is located at the base of the Warley Wise Grit (Fig. 3.2). To a depth of ~43 m, the borehole contains a cover succession of sand and soft brown clay. From 43 m to 61 m the borehole contains shales, with coal and fireclay bands (a type of fine-grained palaeosol).

Interpretation

The Blacko Marine Band is not observed in the Harrogate sub-basin. This makes correlations debatable but it is considered likely that the lower cross-bedded level represents the Surgill Sandstone, while the upper cross-bedded sandstone level represent the Warley Wise Grit. The inference of the Surgill Sandstones is supported by the occurrence of palaeosols below the base of the Warley Wise Grit in the Moor Park Farm Borehole and implies coastline progradation into the Harrogate sub-basin during deposition of the Pendle Grit Member.

A correlation of the overlying sandstones with the Bearing Grit is unlikely, considering the eastward pinch out of the Bearing Grit on the Askrigg Block (Fig. 3.2; 3.5). The current interpretation also fits with the finer grain size of this succession in comparison with the Bearing Grit on the Askrigg Block and the Barden Moor areas.

3.4.3.3 Almscliff Crag and Weeton 1 Borehole

Description

Weeton Borehole 1 [429808 446384] and Almscliff Crag [4268 4490] occur on the southern limb of the Harrogate Anticline (Fig. 3.2). Almscliff Crag forms a prominent exposure, resulting from a local thickening of the succession due to growth faulting (e.g. Chisholm, 1981; Sims, 1988). About 40 m are exposed in the growth-faulted succession. The overlying succession is ~65 m thick but largely unexposed. The regional tectonic dip is approximately 20° S, whereas tectonic dips within the growth-faulted succession are 20° to 30° E. Within the growth-faulted succession, strata are disturbed with occurrences of minor syn- and antithetic faults. Sandstones in the growth-faulted succession are generally coarse- to very coarse-grained with rare granules and ~1 cm pebbles. At multiple levels metre-scale log-prints are observed, typically associated with shale clasts at the same horizons. Most of the lower part of the succession consists of parallel-laminated sandstones, occasionally alternated by low angle cross laminations or sigmoidal cross sets. Towards the top of the growth-faulted succession, trough cross-bedding becomes dominant, indicating flow directions towards the SW.

In Weeton 1 Borehole (Appendix 1), a marine horizon is observed at 50 m depth that probably corresponds to the Eumorphoceras bisulcatum Marine Band ($E_{2a}2$) and is underlain by the Arnsbergian Oatlands Sandstone. The top of the Pendleian sandstones probably occurs at 245 m. Very carbonaceous shales with marine fauna belonging to the Bowland Shale Formation are observed at 350 m and indicate the likely occurrence of the Cravenoceras malhamense Marine Band. This suggests that the Pendle Grit succession is 105 m thick. Sandstone intervals reach up to 8 m maximum and are alternated by micaceous siltstones and shales. The Bearing and Warley Wise Grit are not observed.

Interpretation

Based on similar reasoning as for Harlow Carr Park exposure (Section 3.4.3.2) it is considered likely that the Bearing Grit is absent. This implies that the growth-faulted succession at Almscliff Crag corresponds to the Warley Wise Grit, which is consistent with the observed grain sizes.

The Weeton 1 Borehole suggests a thin development of the Pendle Grit and an absence of the Warley Wise Grit. The latter implies that the Warley Wise Grit has pinched out between Almscliff Crag and the Weeton 1 Borehole, suggesting that growth faulting at Almscliff Crag probably occurred in a delta front setting.

3.4.4 Location descriptions of Bowland High and Lancaster Fells sub-basin

3.4.4.1 Bowland Knotts and White Greet

Description

Bowland Knotts [3727 4605] and White Greet [3698 4599] lie near the crest of the Bowland High tilt block that separates the Bowland and Lancaster Fells sub-basin (Fig. 3.2; 3.12). In this area, the Pendle Grit Member has an approximate thickness of 450 m and consists of mainly fine-grained and argillaceous deposits, alternated with occasional sandstones. On Hasgill Fell [3718 4598] and Crutchenber Fell [3732 4599], the succession is largely covered in peat and till but stream sections indicate the presence of minor sandstone bodies (Fig. 3.12). Along the River Hodder, sandstone packages of up to 3 m thickness are seen from [37083 45895] to [37023 45899]. Individual beds are mostly dm-scale, but range up to 1.1

m. Grain size ranges from fine- to coarse-grained sand, and some beds contain rare granules. Shale clasts occur frequently. Rare toolmarks indicate flow directions towards the SW.

The top of the Pendle Grit Sandstone on Crutchenber Fell occurs at Cat Knot Well [37227 45983] (Fig. 3.12). Here, sandstones are coarse- to very coarse-grained, contain rare granules, 1 cm diameter pebbles and abundant shale clasts. These outcrops appear to correlate to Green Knots [37309 46038] located 1.3 km ENE through a faint landscape feature. Green Knots occurs stratigraphically ~40 m below the scarp-forming sandstones at Bowland Knotts. It contains very coarse-grained to granular sandstones that occasionally form conglomeratic beds with <3 cm pebbles. These sandstones are structureless, planar laminated or crudely cross-bedded.

The crestline of Bowland Knotts is formed by a ~50 m thick succession of massive and crudely-bedded sandstones. Individual beds reach up to 6 m thickness, are typically normally graded and contain pebbles of up to 4 cm. At some levels, <15 cm shale clasts are observed. At the triangulation point [37222 46030] (Fig. 3.15c, d) and an unnamed outcrop at [37290 46065] the lenticular nature of these beds is seen. At both locations winged scours incise into underlying sandstones; scour fills show crude laminations towards the base of the scour and become massive upwards while pebble size decreases both upwards and towards the scour wings. Flow directions, derived from the scour orientation suggest SW and SE flow directions. At the triangulation point, backsets are observed in the medium-grained to granular sandstone bed overlying the scour fill, indicating flow directions towards the south east (Fig. 3.15d). Facies strongly resemble the sediment-gravity-flow deposits observed at the base of the large-scale foresets at Barden Moor and Flasby Fell.

The succession is overlain by ~80 m unexposed interval, on top of which a ~9 m thick trough cross-bedded sandstone is exposed at Foster's Crag [37250 46080] and Cold Stone [37109 46075]. Grain size is coarse to very coarse sand, with rare pebbles reaching up to 2 cm. At the base, foresets are metre-scale, decreasing in height upward. Flow directions are southward.

Both the level at which sediment-gravity-flow deposits are observed and the cross-bedded facies can be traced southward to White Greet (Fig. 3.12). At White

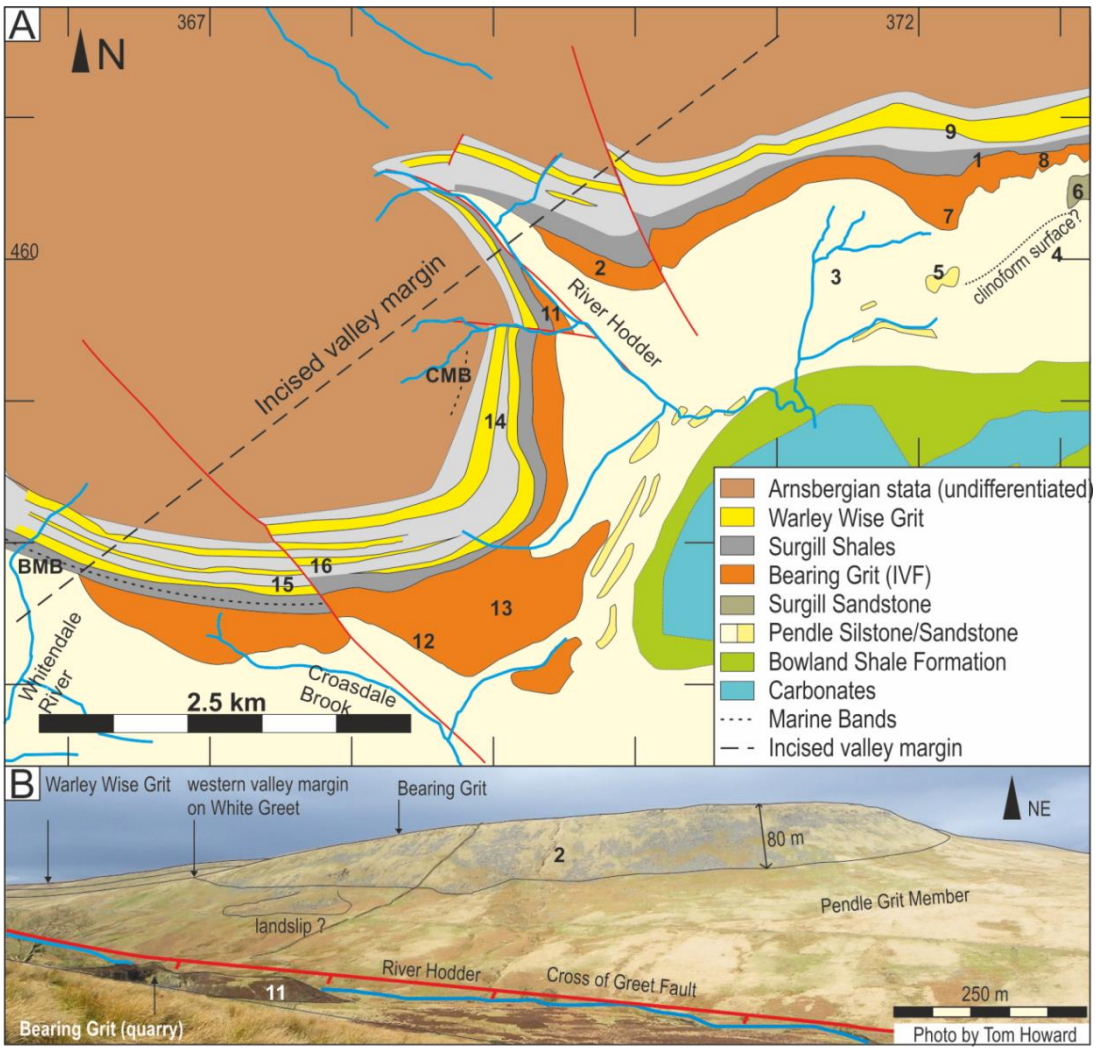

Locations

1) Bowland Knotts [3727 4605]
2) White Greet [3698 4599]
3) Hasgill Fell [3718 4598]
4) Crutchenber Fell [3732 4599]
5) Cat Knot Well [37227 45983]
6) Green Knots [37309 46038]
7) Triangulation point [37222 46030]
8) Unnamed outcrop [37290 46065]
9) Foster's Crag [37250 46080]
10) Cold Stone [37109 46075]
11) Far Costy Clough Quarry [36948 45952]
12) Reeves Edge [3685 4575]
13) Saddle Hill [3694 4575]
14) Bloe Greet [3694 4586]
15) Great Bulls Stones [36747 45765]
16) Little Bulls Stones [36785 45776]

BMB) Blacko Marine Band [36553 45811]
CMB) Cravenoceras cowlingense Marine Band [36878 45923]

Figure 3.12 (a) Outcrop map for Bowland Knotts to Croasdale (see Fig. 3.2 for location within the Craven Basin). The Bearing Grit succession is well-exposed at Bowland Knotts and can be traced to White Greet (2), where it rapidly pinches out westward. A similar westward pinch out is observed at Croasdale, where this succession is overlain by the Blacko Marine Band. (b) Westward pinch out of the Bearing Grit at White Greet. Note that overlying units are continuous on top of the Bearing Grit but not visible due to perspective.

Greet, the lower level forms a ~80 m thick deposit that rapidly pinches out towards the northwest over a distance of 800 m along the river Hodder (Fig. 3.12b). The upper level forms a landscape feature than continues westward. On the other side of the River Hodder, this interval is partially exposed along Far Costy Clough where a quarry [36948 45952] exposes 12 m of very coarse-grained to pebbly, metre-scale, wedge-shaped massive sandstone beds, with abundant shale clasts. This is overlain by a ~50 m unexposed interval. On top, a~40 m thick planar and trough cross-bedded succession from [36928 45947] to [36917 45951] indicates S to SSW flow directions. This succession comprises coarse- to very coarse-grained sandstones, occasionally containing pebbles of up to 2 cm in diameter. At the base of the succession foresets of up to 3.5 m height occur, overlain by smaller sets.

Interpretation

The Pendle Sandstone in this area consists of relatively small sandstone channel features, similar to the succession at Skipton Moor. The correlation of Green Knots in the Surgill Sandstone with Cat Knot Well at the top of the Pendle Sandstone through a landscape feature suggests the progradation of a shelf clinoform (Fig. 3.12). A sand body with a similar clinoform structure has been mapped one kilometre further east at Halstead Fell [37398 45998] (Arthurton et al., 1988).

The succession that forms the crestline at Bowland Knotts is assigned to the Bearing Grit and probably represents a delta toe setting, based on the similarity of the crudely-laminated sandstones with those observed in the delta toe at Barden Moor and Flasby Fell. This correlation to the Bearing Grit is further supported by the recognition of the Blacko Marine Band in Croasdale, and a correlation to this area (see Section 3.4.4.2). The overlying cross-bedded succession at Foster's Crag probably corresponds to the Warley Wise Grit.

3.4.4.2 Whitendale and Croasdale

Description

Along the Whitendale River the basal ~50 m of the Pendle Grit is exposed from [36536 45590] to [36560 45680] and is included in the Whitendale Sandstone (sensu Sims, 1988; Fig. 3.2). Features in the Pendle Sandstone occur over the

successive ~150 m and are generally laterally discontinuous. Outcrops are poor and typically limited to stream sections. They consist of thick turbidite beds in packages up to ~30 metres thick. A good exposure occurs at Baxton Fell Quarry [36815 45639]. Here, the lowest 5 m contains predominantly 0.1 - 0.3 m thin, coarse-grained to granular sandstone beds with abundant pebble lags containing pebbles of up to 2 cm. This succession probably represents a phase of sediment bypass and is overlain by a 21 m succession of medium-grained to granular, normal graded sandstone beds with rare shale clasts. Beds reach up to 2 m thickness but are lenticular and pinch out laterally. Most beds are massive but on some occasions cm-scale banding is observed towards the top of beds. Rare tool and scour marks at the base of beds indicate SW flow directions.

In the headwaters of Whitendale River, Brandon et al. (1995; 1998) infers the presence of the Blacko Marine Band based on the occurrence of *Sanguinolites* in a 6 m thick, burrowed siltstone succession at [36553 45811] that forms part of a 75 m thick fine-grained succession (Fig. 3.2; 3.12). Eastward, a large but poorly-exposed sandstone level of over 100 m thickness has been mapped below the Blacko Marine Band that correlates to the sandstones at Reeves Edge [3685 4575], Saddle Hill [3694 4575], and Bloe Greet [3694 4586] (Fig. 3.12; Hughes, 1987; Brandon et al., 1998). This sandstone level is generally pebbly and structureless and has previously been assigned to the Surgill Shale Member of Brandon et al. (1995; 1998) or the Brennand Grit of Arthurton et al. (1988). Southward, along Whitendale, this level is recognised at the Whitendale Hanging Stones [36437 45645] and Brennand Hanging Stones [36399 45586] (Fig. 3.2). Here, these deposits are very coarse-grained to conglomeratic, metre-scale, structureless and faintly-laminated sandstones with pebbles up to 4 cm. These sandstones are deposited in crude troughs of over 10 metres wide, similar to deposits observed at the Bowland Knotts crestline (see Section 3.4.4.1).

Sapling Crag [36487 45693] in the Whitendale valley exposes coarse-grained to granular sandstones over a ~15 m interval at a slightly lower stratigraphic level. This outcrop contains plane bed lamination with 1 - 3 cm pebbles at its base and clear trough cross bedding towards the tops, indicating S to SW flow directions.

In Croasdale, the Blacko Marine Band is overlain by the Warley Wise Grit that reaches a cumulative thickness of ~145 m. It contains three channelized

sandstone levels, of which the lowest is well-exposed and thickens at the outcrop of Great and Little Bulls Stones [36747 45765], indicating the presence of a larger channel fill (Fig. 3.12). The outcrop reaches a total height of ~ 18 m, including a ~2 m unexposed interval that presumably contains a mudstone. The outcrop is trough cross-bedded at the base, and planar cross sets with tangential toe sets are observed towards the top. Sandstones are medium-coarse-grained to granular, with <2 cm pebbles occurring at several levels. At the base of the outcrop, cross sets of up to 3 m are observed, decreasing in height upwards. Flow directions range from SE to W and are primarily directed towards the SW. The Cravenoceras cowlingense Marine Band is not observed with certainty in this area, but at a tributary of Far Costy Clough [36878 45923], Crossdale Beck [36847 463461, and Middle Gill [36671 461371], *Sanguinolites sp.* and other marine indicators occur within metres of the top of the Warley Wise Grit. These suggest a marine transgression above the Warley Wise Grit corresponding to the Cravenoceras cowlingense Marine Band (Brandon et al., 1998).

Interpretation

It is here considered that the major sandstone level below the Blacko Marine Band at Croasdale correlates to the structureless sandstones at White Greet and Bowland Knotts northward, and with the succession at Brennand and Whitendale Hanging Stones southward (Fig. 3.12). Because of its occurrence directly below the Blacko Marine Band, the succession belongs to either the Surgill Sandstone or Bearing Grit. Due to the scale of this sandstone body, and the sedimentological character that is similar to the sediment-gravity-flow deposits at Flasby Fell and Barden Moor, it is considered likely that this interval represents a Bearing Grit incised valley fill. Placement of this stratigraphic level to the Bearing Grit also complies with the observation that this stratigraphic level occurs below the Blacko Marine Band ($E_{1c}2$) (Brandon et al., 1998), while reflecting the character of the Brennand Grit of Arthurton et al. (1988) in the Settle District to the east (Arthurton et al., 1988). The rapid westward pinch out of this sandstone level at White Greet [36920 46035] (see section 3.4.4.1) and Croasdale [36608 45779] is interpreted as the western margin of the incised valley. Previously, this succession was interpreted as a shelf edge or slope channel in the Surgill Sandstone during sea-level fall (Brandon et al., 1995). However, the multi-kilometre width (limited by eastward outcrop extend), the updip continuity of these deposits at the top of the Pendle Grit

Member (Fig. 3.12a), and its 80 – 100 m thickness (Fig. 3.12b) do not fit with such origin, especially since other Surgill Sandstone deposits are substantially thinner and smaller (e.g. Fig. 3.9).

The sandstones occurring at slightly lower stratigraphic level: i.e. at Sapling Crag in the Whitendale valley and Green Knott near Bowland Knotts (Fig. 3.12) are thought to represent the Surgill Sandstone and form the feeder system to the Pendle Grit turbidite system.

3.4.4.3 Rathmell and Whelp Stone Crag

Description

Rathmell is a village ~7 km east from Bowland Knotts (Fig. 3.2). Several stream sections in its vicinity expose parts of the Pendle Grit Member, which has a cumulative thickness of approximately 490 m. Sandstones are generally discontinuous and primarily present in the lower 150 m of the succession, for example along Long Gill [37831 45839], and several quarries in the Gisburn Forest at [37558 45761] and [37527 45784]. Sandstones are typically medium- to coarse-grained and massive. This interval is overlain by a 300 m thick siltstone-dominated succession. Towards the top of the succession, some small channelized sandstone deposits are exposed at Hesley Beck [37949 45994] to [37945 45995]. Here, the succession contains primarily dark grey siltstones with fine-grained dm-scale turbidite beds with E-W-oriented toolmarks. Rare flutes at adjacent locations suggest westward flow directions. A small, medium- to coarse-grained channelized sandstone exposure of 3 m height is also observed, and consists of beds of up to 0.5 m.

Whelpstone Crag [37612 45925] and Scoutber Crag [37756 46027] expose the overlying succession (Fig. 3.2). The base of this succession is exposed on western side of Whelpstone Crag near the triangulation point at [37601 45926] and at [37631 45953]. Approximately 8 m of massive and crudely planar laminated sandstones are observed; individual beds are lenticular and can reach up to ~4 m in thickness. Grain size ranges from coarse-grained to granular sandstones and pebbles reach up to 4 cm in diameter. In massive beds, floating pebbles occur throughout the

entire bed. In the structured beds, pebbles are organised along diffuse horizons. Shale clasts occur at specific horizons and reach up to ~ 10 cm.

The top of the preserved succession is exposed in a small quarry on the eastern side of Whelpstone Crag. It exposes large-scale foresets of ~5 - 6 m height of coarse-grained sandstone that contain <3 cm pebbles, overlain by decimetre-scale trough cross beds of similar grain size. Flow directions within the large foresets are SE-oriented whereas the overlying succession indicates flow to the SW to SE. The thickness of the entire succession is estimated at ~30 m, which suggests it forms part of the Bearing Grit, based on the thickness of the successions in Croasdale and at Bowland Knotts.

Interpretation

The succession in the Rathmell area strongly resembles the Bearing Grit succession at Bowland Knotts, except for the occurrence of a Gilbert-type delta. The occurrence of this delta fits well with the interpretation of a delta toe setting for the massive and crudely-laminated sandstones at Whelpstone Crag, and similar deposits at Bowland Knotts and Whitendale and Brennand Hanging Stones.

3.4.5 Location descriptions of Bowland sub-basin

3.4.5.1 Blacko Borehole

Description

The Blacko Borehole [38496 44184] as described by Brandon et al. (1995) provides a key section (Fig. 3.2; 3.8). It was drilled at the base of the Warley Wise Grit outcrop belt that is well-exposed at Noyna Rocks Quarry, Foulridge [38966 44263] to the east, and Faughs Delph Quarry, Newchurch in Pendle [38199 43921] to the west. From ~60 m depth, the borehole exposes flaggy sandstones under a thick cover of alluvium. From 72.70 m and 94.18 m, the Surgill Shale is exposed as a silty mudstone. Marine fossils, such as gastropods, *Sanguinolites sp.*, ostracods and fish debris are observed between 78.94 m and 94.18 m in dark grey, silty mudstone (Brandon et al., 1995). This succession is underlain by dm-scale ganisteroid sandstones at 96.49 and 97.84 m depth. Down to 147.52 m, the succession is dominated by dark silty mudstones, alternated with thin sandstone

beds. This succession is underlain by a medium- to coarse-grained sandstones interpreted as the Pendle Grit Member.

Blacko Hill is located 1 km east from the Blacko Borehole and poorly exposes sandstones at three levels. A basal lenticular sandstone is exposed in small quarries at [38602 44224] and [38557 44207] and consists of structureless pebbly deposits. This is overlain by an unexposed, depressed interval on top of which a cross-bedded sandstone is observed at [38595 44213]. The top of the succession consists of thinner sandstone bodies and occurs in small diggings at [38593 44194]. Based on the structural dip, and the depth at which the Blacko Marine Band occurs in the borehole record, it is probable that the entire Blacko Hill succession is deposited within the Warley Wise Grit.

Interpretation

The Blacko Borehole suggests that the Warley Wise Grit directly overlies the Pendle Grit Member, implying the absence of the Bearing Grit.

3.4.5.2 Salterforth & Noyna Rocks

Description

Between Barnoldswick and Foulridge, the Pendle Grit Member forms a broad outcrop belt that is rarely well-exposed (Fig. 3.2). Features indicate that the lower 250 m of the Pendle Grit Member consists predominantly of sandstones with impersistent thin interbedded, fine-grained or argillaceous sediments. Outcrops are rare and most information on this succession is obtained from old quarries that contain sandstones in faces of up to 30 m height. Remnants of ~25 m high quarry faces can be seen at Upper Hill Quarry [3883 4447] (currently Dalesview Holiday vacation park). Metre-scale, erosionally-based turbidite beds are observed with occasional shale clasts. Access to the quarry face was not allowed, precluding detailed observations. Park Close Quarry [38824 4447] exposes the top of the Pendle Sandstone (Fig. 3.8). The SW face exposes an ~8 m amalgamated channelized deposit that pinches out in a NE-direction on perpendicular quarry faces, suggesting S to SSE flow direction of the channel. The SSW corner of the quarry exposes the top of a lower channelized sandstone. Individual beds are

normally graded, medium- to very coarse-grained with frequent granules at the base of beds, and reach up to 2 m thickness.

On the SE quarry face, thin-bedded sandstones are exposed adjacent to the channelized sandstones. These 5 – 30 cm thick turbidite beds are typically fine- to medium-grained and separated by subordinate shale and siltstone layers. The thicker beds frequently contain large shale clasts that are not observed in the channel axis. Flow directions from toolmarks at the beds bases indicate southward flow directions, whereas ripples at the bed tops indicate eastward flow directions (Fig. 3.8). These deposits are interpreted as channel margin deposits, and related to channel overspill. The shift in flow directions from base to top of individual beds probably represents a channel overspill-effect where the toolmarks at the base of the bed records the early high velocity flow regime, parallel to the channel axis whereas the ripples at the top record the flow direction of a low concentration turbulent cloud that does not necessary correspond to the channel direction (e.g. Kane et al., 2010b).

The overlying, predominantly fine-grained succession between this location and Noyna Rocks is approximately 220 m thick, estimated via tectonic dips of the succession.

At Noyna Rocks, near Foulridge, coarse-grained sandstones that overlie the Pendle Siltstone are exposed at several levels, separated by unexposed, presumably fine-grained intervals (Fig. 3.2; 3.8). The lowest interval consists of coarse-grained to granular structureless sandstones and includes 2 - 3 cm diameter pebbles. Where these deposits are thickly present, the outcrop belt forms a prominent ridge, such as at Noyna Hill [39010 44274] to [38937 44269] where the landscape feature suggests a thickness of ~60 m for these sandstones. These deposits are separated by a ~25 m thick, well-developed topographic depression, suggesting deposition of shales. This succession is overlain by a second sandstone level that is exposed in Noyna Rocks Quarry. On the north quarry face [38965 44263], a single set of large foresets is observed that transition into a bioturbated, siltstone and fine-grained sandstone bottomset. Foresets are at least 7 m high, are concave up with depositional dips of ~14° at the base, and 20° degree at the top, and indicate WSW flow directions. The siltstone and fine-grained sandstone toeset dips at an approximate angle of 5° and shows bioturbation. On top of these large-scale foresets, erosionally-based channel deposits occur. This succession is overlain by a 40 m unexposed interval, on top of

which a successive ~40 m interval exposes at least three minor sandstone levels, indicating SE to SW flow directions, separated by unexposed intervals of presumably fine-grained sediments.

Interpretation

The Pendle Sandstone succession exposed between Salterforth and Noyna Rocks has not been logged in detail but appears significantly more sand-rich than sections closer to the Askrigg Block, which is similar to previous interpretations (e.g. Earp et al., 1961; Sims, 1988), and features larger channels or channel complexes than observed at locations closer to the Askrigg Block.

Considering the close similarity of the successions at Noyna and at Blacko Hill along the same outcrop belt, it is considered likely that the succession overlying the Pendle Siltstone belongs entirely to the Warley Wise Grit. The lower sandstone level consists of structureless sediment-gravity-flow deposits and is separated from a single set of large-scale foresets interpreted as Gilbert-type foresets by an unexposed, presumably fine-grained succession. The base of these foresets is transitional in a bioturbated, siltstone-dominated bottomset suggesting a low energy environment, unlike that for the Gilbert-type deltas in the Bearing Grit (see Chapter 4). The lowest cross-bedded sandstones overlie the deltaic foresets erosionally and are followed on by a heterolithic succession containing multiple single storey cross-bedded sandstones that probably correspond to a high-accommodation delta top environment.

3.4.5.3 Pendle Hill & Faughs Delph

Description

At Pendle Hill, the Pendle Grit Member is ~400 m thick (Fig. 3.2). The basal succession at Pendle Hill is characterized by hybrid-event beds and debritic deposits. Approximately 20 m is of this succession is exposed at Little Mearley Clough from [37874 44116] upwards. Below this point the Bowland Shale Formation is frequently exposed (Fig. 3.8). The basal two beds of the Pendle Grit Member are poorly-sorted sandy debrites of ~1 m thickness that contain limestone clasts and sandstone clasts. Several of the overlying beds also contain debritic intervals, indicated by abundant shale clasts and friable sandstones. Tool marks indicate S to

SW flow directions. Stratigraphically higher exposures in the Pendle Sandstone indicate the succession consists mostly of sandstones, although outcrop quality is very poor.

Approximately 65 m of the upper part of the Pendle Sandstone is well-exposed in Nick of Pendle Quarries from [37717 43862] to [37725 43842] in two successive channelized bodies, separated by a poorly exposed heterolithic interval. The channelized sandstone beds range up to 3 m thick at the base of the channel, but are typically ~1 m. Beds are normally graded, ranging in grain size from medium to very coarse sand, and appear internally structureless. Beds are amalgamated, resulting in very rare argillaceous or siltstone breaks in the succession. Shale clasts are also rare, but do occur in concentrated layers. Sandstones overlying such layers are frequently horizontally laminated and carbonaceous. Flow directions from rare toolmarks in the lower channel indicate WSW currents. In the intervening heterolithic interval, predominantly 0.2 – 0.5 m thick, fine- to coarse-grained sandstones are exposed, separated by siltstones and shales. The upper part of many beds is dominated by shale clasts, frequently coinciding with large scour surfaces (cf. Sims, 1988; Kane et al., 2009). *Arenicolites* burrows are observed on some surfaces. Scours, toolmarks and primary current lineation indicate S to SW flow directions (Fig. 3.8).

The upper part of the Pendle Sandstone is also exposed in Wiswell Quarry, ~2 km downdip from Nick of Pendle Quarries (Fig. 3.2). Here large exposures are present over a stratigraphic interval of ~90 m [37532 437013] to [37547 43696]. Beds are typically between 0.5 and 1 m and are tabular for the length of exposure (maximum of ~20 m). They are generally ungraded or normally graded. Grain sizes range from fine- to coarse-grained sandstone, and rarely become very coarse-grained or granular. Beds typically occur in 8 – 16 m thick packages that typically become more amalgamated upwards. The top of amalgamated intervals is typically strongly scoured with ‘megaflutes’ (cf. Kane et al., 2009). These scour surfaces are lined with mm – cm thick veneers of very well-sorted very coarse-grained to granular sandstone and generally incise into, and are overlain by shale-clast-bearing intervals. In the less amalgamated parts of the succession, sandstones are generally thinner and slightly finer while the interbedded fines increase in thickness. In the lower part of the succession [37535 43704] flow directions are typically SSW although eastward flow directions are observed on one bed, based mainly on large scour features and

rare toolmarks. In the upper part of the succession [377545 4398], toolmarks, flutes and ripples in heterolithic strata also indicate S to SW flow directions (Fig. 3.8).

In the Pendle Hill area, the Pendle Siltstone is very thin or absent as the Pendle Grit Member is separated from the Warley Wise Grit by a thin shale succession, presumably containing the Blacko Marine Band.

The Warley Wise Grit is exposed along the Clitheroe – Sabden road [37751 438805]. Here, two partially exposed channel storeys display very coarse-grained to granular trough cross-bedded sandstones over a 5 m stratigraphic interval, indicating E to SE flow directions. At Faughs Delph Quarry at Newchurch in Pendle, the Warley Wise Grit is well-exposed [38199 43922] (Fig. 3.2; 3.8). The western quarry face exposes concave up large-scale foresets of ~8 m, representing a Gilbert-type delta (Fig. 3.13). Foresets are formed in medium- to coarse-grained sandstones with rare 1 – 2 cm pebbles top and indicate flow towards the south. Contacts between individual foreset beds are micaceous, and occasionally show millimetre-thick shale intervals. Burrows are also observed at this level. The erosionally-based cross-bedded succession overlying these foresets is over ~14 m thick and consists of 5 storeys (Fig. 3.13e, f). The contact with the underlying large-scale foresets is exposed in the northern and western quarry face (Fig. 3.13c, d). The cross-bedded succession itself is best exposed in the eastern quarry face. These sandstones are generally coarse-grained to granular, with abundant pebbles throughout storey 3 and at the base of storey 4. Cross beds indicate eastward flow directions.

Interpretation

In the Pendle Hill area, the entire Pendle Grit Member is sand-rich with only subordinate heterolithic intervals. The transition in sedimentary character from Nick of Pendle Quarries to Wiswell Quarries represents a change in depositional environment from turbidite channels to a more proximal lobate setting, in which case the amalgamated packages represent lobe elements. The scour surfaces or megaflutes occur near the top of the amalgamated packages and might record the closest position of the channel mouth, before switching to a different position (Kane et al., 2009). Unlike the other areas discussed above, deposition of turbiditic sandstones continues up to the transgression by the Blacko Marine Band, suggesting a highly active, sand-rich feeder system to this area of the Craven Basin.

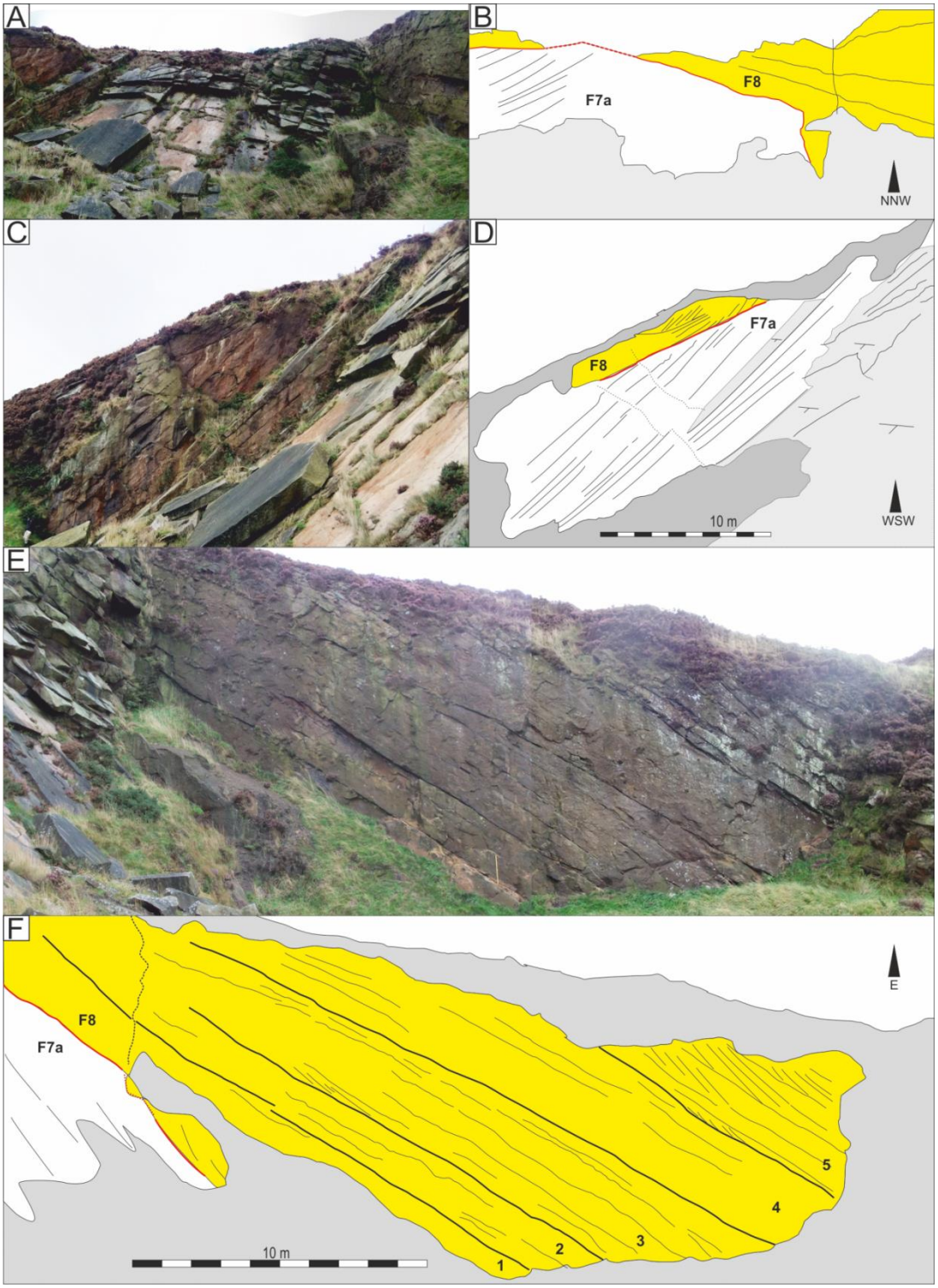

Figure 3.13 Exposure at Faughs Delph Quarry in the Warley Wise Grit [38199 43922]. (a, b) Overview of the quarry exposures, indicating the contact between large-scale foresets (F7a) in white, and overlying cross-bedded sandstones (F8) in yellow. (c, d) Western quarry face exposing Gilbert-type delta foresets with topset indicating steep tectonic dip. (e, f) Eastern quarry face exposing the overlying multi-storey sandstone. Numbers indicate channel storeys referred to in text (section 3.4.5.3).

The Warley Wise Grit consists of a similar succession as at Noyna Rocks, Foulridge (Section 3.4.5.3). A single set of Gilbert-type deltas is overlain by an erosionally-based, coarser-grained fluvial succession, suggesting that it represents a fluvio-deltaic channel that was deposited at a later stage than the deltaic foreset.

3.4.5.4 Waddington Fells

Description and interpretation

Waddington Fells Quarry [37183 44772] (Fig. 3.2) is an active quarry that is described in detail in Kane et al. (2010). It exposes a major multi-storey, multi-lateral turbidite channelized deposit in the Pendle Sandstone. Sandstones are medium to very coarse grained, and regularly contain pebbles up to ~2 cm in diameter, which has led to a misinterpretation as Warley Wise Grit (cf. Earp et al., 1961; Sims, 1988). The quarry exposes a ~40 m high, and 650 m wide succession of turbidite channelized sandstones perpendicular to flow. Within this succession, lateral accretion of channel deposits is controlled by growth faulting along a major tectonic structure (Kane et al., 2010a). A NE-SW trending syn-sedimentary normal fault is inferred on the NW margin of the quarry, resulting in thalweg flow pattern parallel to the fault trend. The growth-fault follows the trend of the Bowland Line, a major syn-rift tectonic lineament (Fig. 3.2).

3.4.5.5 Longridge Fell

Description

Both the Pendle Grit Member and Warley Wise Grit are exposed at Longridge Fell (Fig. 3.2; 3.8). The Pendle Grit Member is estimated to have a thickness of 475 m (Aitkenhead et al., 1992). The basal part of the succession consists of interbedded turbiditic sandstones and argillaceous deposits. The middle part is well-exposed in several quarries, notably Leeming Quarry (active) [36828 44058] and quarries near Turner Fold [36880 44061] and [36886 44051] (Fig. 3.2). In these locations, the succession is dominated by sandstones, resulting in up to 20 m high quarry faces. Sandstones are deposited in tabular 1 – 4 m thick packages, separated by laterally continuous shale breaks of up to ~ 1 dm. Within these packages, individual beds are highly amalgamated, and range in height from ~0.15

m to 0.60 m. Amalgamation surfaces are generally picked out by lines of shale clasts or slight changes in grain size. Beds are normal graded, and grain sizes range from very coarse to medium sand. In sliced blocks at Leeming Quarry additional amalgamation surfaces are recognised, as well as internal structures such as dunes or antidunes that are not apparent from conventional outcrops. Flutes and toolmarks indicate that palaeoflow was towards the S to SW at all locations (Fig. 3.8). These sandstones are probably also deposited in a lobe setting, where the amalgamated packages represent individual lobe elements, separated by thin argillaceous or siltstone interlobe elements (e.g. Prelat et al., 2009).

At Tootle Height Quarry [36196 43840] to [336142 43787] (Fig. 3.2), extensive exposures are present although poor accessibility and measures to stabilise the quarry face have limited the outcrop quality. The base of the succession consists of tabular packages similar to other quarry exposures on Longridge Fell. Towards the top of the exposed succession, more channelized deposits occur over a thickness of ~10 m. This channelized succession is underlain by a continuous shale clast conglomerate along the length of the exposure. The overlying sandstones are slightly coarser-grained and contain 1.5 cm pebbles at the base of some beds. Although unclear from the present exposure, old photographs of the quarry face show large-scale, unidirectional, erosional stepping within a laterally accreted sandstone body, which has been interpreted asa laterally migrating, single storey channel (Sims, 1988; Kane et al., 2010; Photographs by A. Sims and provided by I. Kane).

The Pendle Grit Member and Warley Wise Grit are separated by a ~60 m mudstone-dominated succession. A relatively continuous 190 m-thick section occurs in the River Ribble near Salesbury Hall from the top of the Pendle Grit Member [36790 36310] to the top of the Warley Wise Grit [36756 43586] (Bridge, 1988; Aitkenhead et al., 1992). At the base of this mudstone-dominated interval, *Sanguinolites* is observed (Brandon et al., 1995), indicating the likely position of the Blacko Marine Band. The Warley Wise Grit contains three sandstone-dominated intervals over a total thickness of ~120 m, separated by fine-grained deposits. Only the upper level contains clear cross bedding. The lower two intervals consist of structureless sandstones interpreted as sediment-gravity-flow deposits (Aitkenhead et al., 1992; Bridge, 1988).

Interpretation

The gradual transition from heterolithic, to lobate and eventually channelized deposits in the Pendle Grit Member on Longridge Fell is thought to represent the evolution from a basin floor to slope setting and thus an increasing proximity to the sediment source. Similar to the Pendle Hill area, the succession remains sand-rich to the top of the Pendle Grit Member, indicating an active feeder system. The Warley Wise Grit is thought to represent an overlying fluvio-deltaic system.

3.4.6 Facies

The rock types described in the above section range in grain size from mudstones to pebbly sandstones, and are deposited by a variety of processes. Eleven facies and five facies associations are recognised, and are used to interpret the depostional environment and develop a palaeogeographical reconstruction.

3.4.6.1 Facies 1: Shales

Description

Shales occur throughout the outcrop area, and are described in boreholes records and observed in some stream sections. Shales are dark grey to black, mm-scale laminated sediments that form a mixture of clay- and silt-sized particles (Fig. 3.14e, f, g). Generally, shales are barren of fauna except for certain thin beds in which marine fauna is observed; so-called ‘marine bands’ that indicate periods of fully-marine salinity.

Interpretation

Clay-size particles can only settle from suspension in low energy environments, which can occur in a several depositional settings. Shale successions that are continuous over stratigraphic intervals of tens of metres without the influx of coarser-grained sediments suggest a distal position relative to sediment sources. This occurs during the deposition of the Bowland Shale Formation and during deposition of ‘marine bands’. Shales also occur interbedded with siltstones and sandstones and carbonaceous fragments, in which case the depositional environmental interpretation is derived from these deposits (e.g. Fig. 3.14e, f, g).

These vary from a slope setting in combination with turbiditic sandstones, to an overbank setting on the delta top succession.

3.4.6.2 Facies 2: Siltstones

Description

Siltstones form light grey, laminated deposits that are exposed in stream sections, and occasionally adjacent to quarries. Parting planes within the siltstones frequently show mica flakes and carbonaceous material.

Interpretation

Silt-size particles can be transported by suspension but settle more rapidly than mud-size particles when entering low energy environments, frequently resulting in a gradual transition between these facies. Similar to shales, siltstones are observed throughout the entire field area in several environment settings where they are generally observed in close association with coarser sediments. In these cases, the occurrence and sedimentological character of these deposits provides the environmental interpretation, which can vary from a slope to delta top setting. Trace fossils occurrences from the Pendleian succession in the Craven Basin, frequently observed in siltstones, have been used as an additional indicator for depositional environment (Baines, 1977; Eagar, 1985).

Figure 3.14 (next page) (a) Turbidite channel exposure. Note the lenticular nature individual beds of Facies 4: Thick Turbidite Sandstones, and the debritic intervals (arrows) related to disintegration of shale clasts. Witshaw Bank Quarry [4002 4548]. (b) Close up of amalgamation surface in Facies 4. (c) Close up of debritic interval. (d) Internal laminations within a single bed of Facies 4. Note coarser-grained lens at base of bed and parallel cm-scale laminations towards top. Potter Gill, Skipton Moor [4025 4514]. (e) Erosional channel base of Thick Turbiditic Sandstones into Facies 1: Shales. (f) Small channel near the top of the Lower Slope association incising in shales. Cawder Gill, Skipton Moor [4002 4502]. (g) Facies 3: Thin Turbiditic Sandstones alternated with Facies 1 in Cawder Gill (h) Facies 3: Thin Turbiditic Sandstones adjacent to a major turbidite channel containing Facies 4. Salterforth Quarry [3882 4448]. (i) Palaeoflow indicator at base and (j) sinuous to linguoid ripples at the top (Tc) of a Thin Turbiditic Bed, Cawder Gill.

3.4.6.3 Facies 3: Thin Turbiditic Sandstones

Description

Thin Turbiditic Sandstones are generally sharp-based, cm- to dm-scale, fine- to medium-grained, fining upward sandstones that are interbedded in shale and/or

siltstone successions (Fig. 3.14g-j). They are occasionally observed in association with thick turbiditic sandstones towards the top of turbidite channel or lobe deposits. Thin Turbiditic Sandstones provide palaeoflow indications from rare flutes and frequent tool marks at their base, as well as linguoid ripples at their tops.

Interpretation

Thin turbiditic sandstones are interpreted as (partial) Bouma sequences that were deposited by low density turbidity currents (sensu Lowe, 1982), or turbidity currents (sensu Mulder and Alexander, 2001). These deposits form from flows in which sediment was fully supported by the fluid turbulence implying a low (<9%) sediment concentration during deposition (Bagnold, 1962). Where these thin turbiditic sandstones are deposited adjacent to turbidite channels, it is likely that they formed from the overspill of larger channelized flows.

3.4.6.4 Facies 4: Thick Turbiditic Sandstones

Description

Decimetre to metre-scale, medium- to very coarse-grained, non- or normally graded sandstones with <2 cm pebbles near their base are frequently observed in the Pendle Grit turbidite system (Fig. 3.14a). Beds rarely show internal structures at outcrop, although in rare clean surfaces such structures are frequently present. They include small coarse-grained lenses, (anti)dune-like structures and cm-scale grain size banding (Fig. 1b, d). Clean surfaces also indicate that sandstone-on-sandstone amalgamation surfaces of successive flows are more common than appreciated in most quarry or natural exposures. In the latter cases, amalgamation surfaces are recognised by sudden shifts in grain size, or lateral changes in a bed contact: e.g. when a siltstone or shale layer is cut out laterally, resulting in a sandstone-on-sandstone contact. Palaeoflow indicators are rare apart from the basal beds of sandstone-dominated intervals that incise into shales (e.g. Fig. 3.14a, f). Beds frequently contain cm- to dm-scale shale clasts, typically towards or at the top of individual beds. Additionally, metre-scale pods of shale clasts aggregates occur in which chaotically-structured sandstones are mixed with cm- to dm-scale shale clasts, locally resulting in intervals of debritic character (Fig. 3.14c).

Interpretation

These facies are interpreted as arising from deposition from high-density turbidity currents (sensu Lowe, 1982), also referred to as concentrated density flows (sensu Mulder and Alexander, 2001). Observed coarse-grained scour fills are similar to the S1 facies, grain size banding is similar to as S2-type banding, and structureless graded or non-graded beds represent S3 or Bouma Ta facies, all of which are characteristic for high-density turbidity currents (Lowe, 1982). Based on the abundant amalgamation surfaces and the frequent occurrence of shale clasts, the currents that deposit these sandstones are capable of erosion, which also fits this interpretation (Mulder and Alexander, 2001). High-density turbiditic currents are thought to have transported the bulk of sand-grade sediment transport during deposition of the Pendle Grit turbidite system.

3.4.6.5 Facies 5: Debritic Sandstones

Description

These sandstone beds range from dm- to m-scale, are poorly sorted and generally have a chaotic internal structure. These sandstones generally contain some silt, small shale fragments and shale clasts.

Interpretation

Debritic sandstones are mass-flow deposits originating from cohesive flows, capable of frictional freezing during which all grain sizes are deposited simultaneously resulting in a chaotic deposit (Mulder and Alexander, 2001; Haughton et al., 2003).

3.4.6.6 Facies 6: Structureless and crudely-laminated sandstones

Description

Erosionally-based, moderately sorted, coarse-grained to conglomeratic sandstones occur in beds up to 10 m thick and contain pebbles up to 5 cm in diameter (Fig. 3.15c, d, e). These beds typically show normal grading, with abundant large pebbles embedded in very coarse-grained to granular deposits located near the base of the bed, decreasing in both abundance and size upward. The

top of beds are typically coarse-grained and contain rare granules but no pebbles. Commonly, crude diffuse parallel or cross-cutting laminations occur towards the top of the beds. Local areas of distinct weathering, with circular depressions and unsorted sediment are thought to resemble dewatering structures. Structureless and crudely-laminated sandstones occur in several settings. They are observed on top of cross bedding strata and both under- and overlie large-scale foresets. At Stone Man Crag, Barden Moor [3982 4576], 4 m high backsets are recognised within these deposits. Smaller backsets are recognised at Crag Wood, Flasby Fell [3959 4548], and the Triangulation Point, Bowland Knotts [3722 4603] (Fig. 3.14d).

Interpretation

These sandstones are interpreted as sediment-gravity-flow deposits. Gradual normal grading on a metre-scale in mainly structureless beds suggests gradual deposition. This excludes slumps, slides or cohesive flows as a depositional mechanism. The occurrence of laminations towards the top of beds might reflect a decrease in the rate of deposition or a decrease in the sediment concentration, and reflect the waning phase of a high density turbidity current (Cartigny et al., 2013). Additionally, the occurrence of backsets provides indirect support for the interpretation of high density turbidity currents, because such flows are typically supercritical (Cartigny et al., 2013). Backsets form when a supercritical flow decelerates and becomes subcritical via a hydraulic jump. A hydraulic jump causes rapid deposition directly downstream of the event, resulting in updip migration of the hydraulic jump and backset formation (Massari, 1996; Nemec, 1990, Postma and Roep, 1985).

There are several differences between Facies 4 and 6. The latter are generally several metres thick, whereas metre-scale beds are relatively rare in the thick turbiditic sandstone beds (Facies 4) of the Pendle Grit Member. The pebble size in structureless and crudely-laminated sandstones is significantly larger (5 vs 2 cm), and shale clasts are much rarer. Additionally, internal laminations are much more clearly developed in Facies 6. More importantly, Facies 6 is observed on top of trough cross-bedded strata interpreted as fluvial channelized sandstones as well as at the toe of 10 m scale Gilbert-type foresets, suggesting it can occur in the delta top and front environment, whereas thick turbiditic sandstones occur in a marine setting.

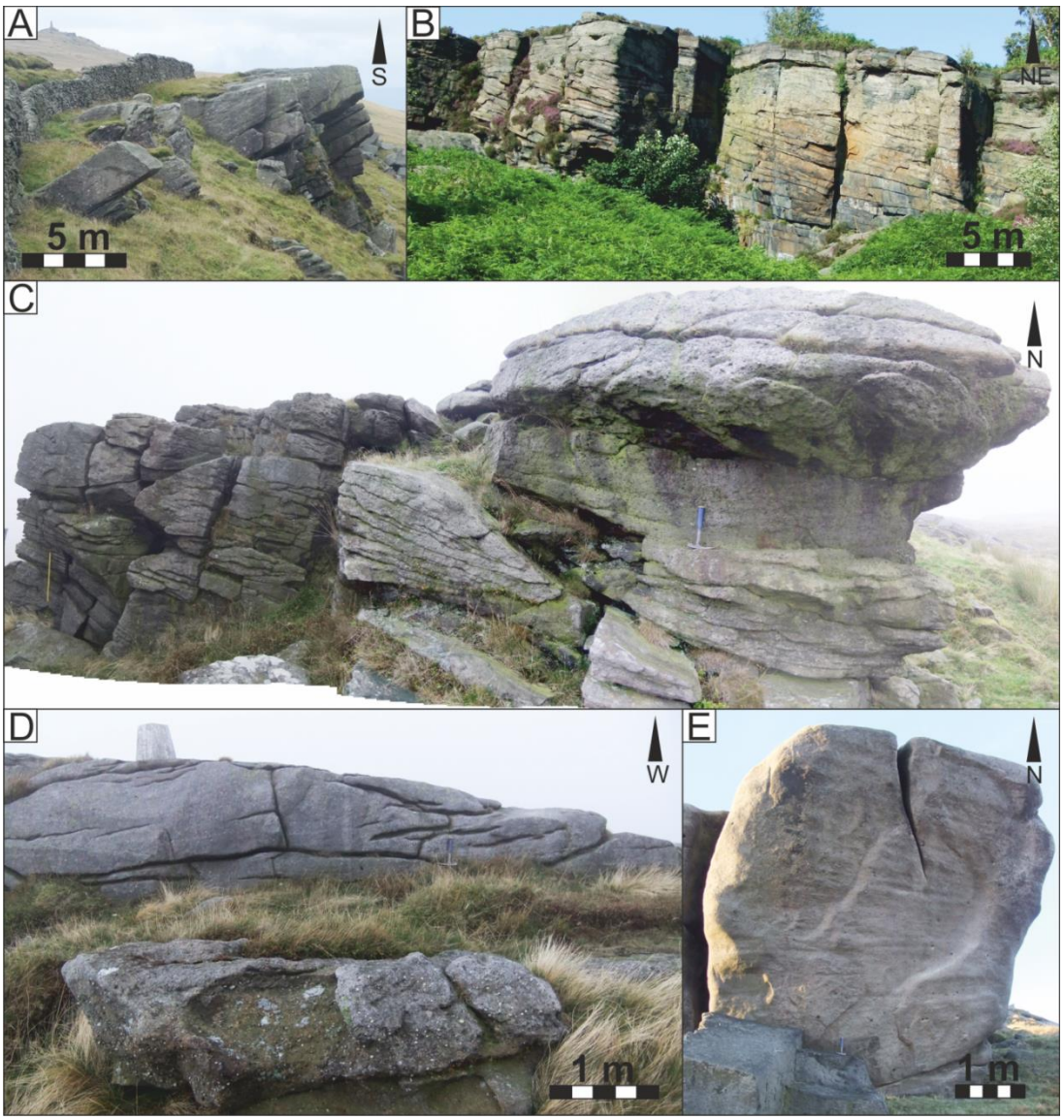

Figure 3.15 (a) Facies 7: Large-scale foresets overlain by Facies 8: Cross-bedded sandstones, Rolling Gate Crag, Barden Moor [4001 4602] (see Fig. 3.9). (b) Facies 7 and Facies 8 at Hardacre Quarry, Farnhill Moor [4000 4467]. (c) Facies 6: Sediment-gravity-flow deposits at the Triangulation Point, Bowland Knotts [3722 4603]. Note the lenticular nature of these deposits. Large scours indicate approximate southward flow direction. Beds are typically metre-scale based on normal fining trends but fracture patterns occasionally obscure details. Photo is optically distorted, hammer is 25 cm. Scale bar (left) is 1 m. (d) Deposits directly above outcrop (c), indicate northward-facing cross sets both in grain fabric and weathering pattern that are interpreted as back sets. (e) Fining up sediment-gravity-flow deposits with diffuse laminations at Potter Gap, Barden Moor [3991 4584] (Fig. 3.10: outcrop 3).

3.4.6.7 Facies 7: Large-scale foresets

Description

Large-scale foresets are here defined as foresets with minimal set height of 5 m (Fig. 3.15a, b). The maximum observed height of large-scale foresets is 16 m (Rolling Gate Crag, Barden Moor [4001 4603]). Several types of large-scale foresets are distinguished that differ in grain size, overall geometry, internal structures and facies association. Their deposition is discussed at length in Chapter 4. Large-scale foresets can occur in medium- to very coarse-grained sediment containing pebbles of up to 4 cm in diameter. Individual foresets can be concave up or straight and range from 8° - 29° in depositional dip.

Interpretation

Foresets of more than 5 m height are interpreted to record the steep bar front of Gilbert-type deltas through a variety of depositional mechanisms (Chapter 4). The height of 5 m is used as a cut-off value for regular bar and dune foresets observed in fluvio-deltaic outcrops, as such heights are rarely achieved in braided fluvial systems of similar scale (e.g. Bristow, 1988; 1993a).

3.4.6.8 Facies 8: Cross-bedded sandstones

Description

Both planar and trough cross-bedded sandstones are observed in the field area (Fig. 3.16a, b, c). Beds containing foresets are frequently up to ~2 m high and rarely reach 3 m. They occur in medium- to very coarse-grained sandstones containing granules and pebbles of up to 5 cm in diameter. Planar cross beds are bounded by tabular bounding surfaces resulting in the development of relatively continuous beds. Foresets are generally tangential but in rare occurrences non-tangential examples are observed. Pebbles occur at the toes of foresets.

Trough cross-bedded sets are bounded by either one or two curved bounding surfaces. The basal bounding surface is typically an elongated scour that is infilled with tangential foresets. Grain sizes are frequently slightly coarser than in planar cross-bedded examples while pebbles frequently occur through the entire bed. Water escape structures are occasionally observed and tree log impressions occur regularly in trough cross-bedded strata.

Interpretation

Cross-bedded sandstones are interpreted as dune deposits from unidirectional currents that transport sand under traction, saltation and suspension in braided river systems. Non-tangential, planar foresets form when most of the sediment avalanches along the lee side of a dune or bar, and form the deposits of straight-crested dunes. Tangential, planar foresets also form from straight-crested dunes when abundant suspended or saltated sediment is deposited at base of the lee-side of a dune. This causes foresets to approach the bottomset laminae asymptotically, resulting in tangential foresets (Boggs Jr, 2006). The occurrence of a separation eddy on the lee-side of a dune can also result in tangential foresets (e.g. Collinson, 1970). Trough cross bedding forms the deposit of sinuous or isolate dune bed forms. These infill scours that from in front of the prograding dune or bar due to the increased strength of the separation vortex.

The coarse grain size and general absence of non-tangential planar sets suggest that saltation and suspension transport of coarse grain sizes is common, implying relatively high flow rates. The slightly coarser grain sizes, occurrence of pebbles throughout trough cross beds and more frequent log imprints and dewatering structures suggest higher flow rates in comparison with tangential planar cross beds.

3.4.6.9 Facies 9: Parallel-laminated sandstones

Description

Laminated sandstones are characterised by cm-scale parallel laminations and occur in coarse- to very coarse-grained sandstones (Fig. 3.16b, d). Laminated sandstones with abundant pebbles are observed within a trough cross-bedded succession in beds of up to a metre in thickness. Additionally, isolated outcrops of parallel-laminated sandstones of up to 3 m thick are observed, in which pebbles and granules are absent (Fig. 3.16d).

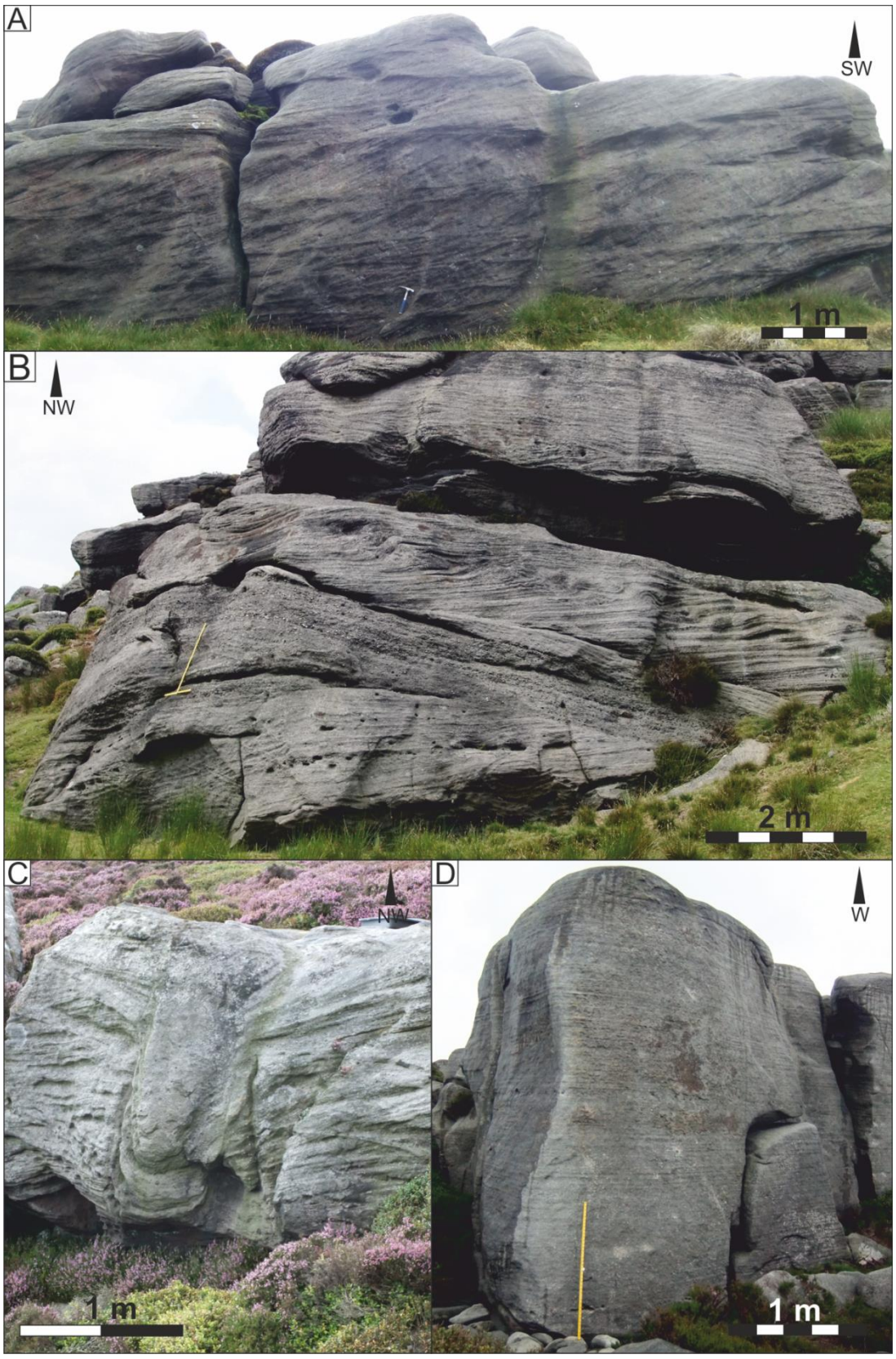
A
SW
1 m
B
NW
2 m
C
NW
1 m
D
W
1 m

Figure 3.16 (previous page) (a) Facies 8: Tangential planar cross beds, Obelisk Barden Moor [3993 4588]. (b) Non-tangential planar cross bed (facies 8), overlain by Facies 9: Parallel-laminated Sandstones and Facies 8 containing dewatering structures. Deer Gallows Ridge, Barden Moor [4000 45556] (c) Facies 8 containing dewatering structures, Deer Gallows Ridge, Barden Moor. (d) Facies 9: Parallel-laminated sandstones, Hen Stones, Barden Fell [4082 4596]

Interpretation

Bed parallel laminations can occur during lower and upper stage plane bed deposition. These deposits record bed aggradation via upper stage plane bed deposition, because coarse sand is not transported during lower stage plane bed deposition. Upper stage plane bed lamination develops at higher flow conditions than dune cross-stratification in similar grain sizes, thus suggesting an increase in flow velocity in comparison with cross-bedded sandstones.

3.4.6.10 Facies 10: Coal

Description

Coals are rare and their thickness ranges from a few centimetres to ~1 metre within the Pendleian Millstone Grit Group successions of the field area. The thicker coals appear relatively continuously and have been mined extensively. Their thickness and position are generally well-documented in old mining records, and their position in the field can be determined from the presence of old pits. In field exposures, coals are generally interbedded with carbonaceous shales.

Interpretation

Coal seams record the accumulation of organic material in peat mires and suggest prolonged waterlogged conditions within the fluvio-deltaic domain (e.g. Falcon-Lang and Dimichele, 2010; Jerrett et al., 2011). Coal seams are here considered relatively reliable correlation surfaces when marine band control is absent or landscape features cannot be traced.

3.4.6.11 Facies 11: Palaeosols

Description

Hard quartzitic, well-cemented sandstones or rooted horizons are observed at the top of cross-bedded sandstone intervals. Frequently, they are overlain by organic rich shales or coals.

Interpretation

Palaeosols record prolonged soil formation, indicating the abandonment of the channel on top of which the soil formation occurs. Rooted horizons indicate the presence of vegetation of a former channel location. Quartz enrichment of these horizons might result from faster weathering rates of the feldspar component of the Millstone Grit within soils, while the quartz cements in ganisters form from dissolved silica derived from plant opal and thus reflect the prolonged vegetation.

	Facies	Lithology	Facies interpretation	Relationship	Fig
1	Shales	Dark grey to black, mm-scale laminated mud- and siltstone, barren or containing marine fauna.	Low energy environments with mud-settling on a basin floor, slope or delta top setting. Marine fauna indicate marine incursions during high sea level.	Variable, dependent on depositional setting.	3.14e, f, g
2	Siltstones	Light grey laminar deposits at mm- to cm-scale. Parting planes frequently contain mica flakes and carbonaceous material.	Low energy environment allowing for the deposition of silt on the slope, delta front or delta top.	Variable, dependent on depositional setting.	-
3	Thin Turbiditic sandstones	Sharp-based cm- to dm-scale fining upward beds in fine- to medium-grained sandstone. Frequently contain flutes and scours at base and linguoid ripples at top of beds.	Deposits from low density turbidity currents on the upper and lower slope.	Interbedded with facies 1 and 2. Occasionally observed near top of turbidite channels filled with facies 4.	3.14g, h
4	Thick Turbiditic sandstones	Medium- to very coarse-grained, normal graded, dm – m scale, sandstones with < 2 cm pebbles. Mostly structureless, rare grain-size banding, coarser-grained lenses, or dune-like structures. Bed amalgamation common. Contains cm- to dm-scale shale clasts.	Deposits from high density turbidity currents on the upper and lower slope.	Interbedded with facies 1, 2, 3. Deposited in channels and turbidite lobes on the lower slope. Rarely observed on upper slope.	3.14a, b, d, e, f
5	Debritic sandstones	Decimetre to metre-scale beds with chaotic sedimentary fabric of poorly-sorted sediments, ranging from muds to granular sediment and containing shale clasts.	Debris flow deposits resulting from frictional freezing, depositing all grain sizes en-masse.	Occurs at base of turbidite succession. Also occurs when large shale rafts disintegrate.	3.14c
6	Structure-less and crudely-laminated sandstones	Erosionally-based, moderately sorted, normal graded, coarse-grained to conglomeratic sandstones in <10 m beds with <5 cm pebbles. Crude diffuse parallel or cross-cutting laminations typically occur in upper part of beds. Dm- to metre-scale backsets occur locally. Shale clasts are rare.	Sediment-gravity-flow deposits in the delta top and delta front environment.	Closely associated with facies 7B, 7C, 7D, 8, 9. Delta front and delta top setting.	3.15c, d, e, 4.6c, 4.7, 4.8, 4.9
7A	Large-scale foresets	Concave up >5 m foresets in fine- to coarse-grained sand, rare granules and pebbles. Foreset beds internally massive, 0.3 – 1 m thick. Rare, faint foreset-parallel laminations at top of foreset. Foresets transition into a bioturbated siltstone toeset. Foreset beds separated by micaceous siltstones.	Gilbert-type deltas formed by suspension settling under homopycnal conditions.	Delta front. Closely association with cross-bedded sandstones and siltstones.	3.15b, 3.13, 4.3
7B	Large-scale foresets	Foresets (>5 m), coarse-grained to granular sand with <4 cm pebbles. Individual foreset beds are internally massive and range from 3 - 20 cm with poor normal grading.	Gilbert-type deltas formed by oversteepening and subsequent collapse at the top of the foreset under homopycnal conditions.	Delta front. Closely associated with facies 6, 7C, 7D, 8, 9.	4.4

	Facies	Lithology	Facies interpretation	Relationship	Fig
7C	Large-scale foresets	Foresets (>5 m), in coarse-grained to granular sediment, with frequent <4 cm pebbles. Individual foreset beds are strongly laminated and reach thicknesses of <2m.	Gilbert-type deltas overridden by a hyperpycnal current resulting in traction structures on the foreset.	Delta front. Closely associated with facies 6, 7C, 7D, 8, 9.	3.15a, 4.5
7D	Large-scale foresets	Foresets (>5 m) in coarse-grained to granular sediment, with frequent <4 cm pebbles. Individual foreset beds show foreset-bed (sub-) parallel laminations and reach thicknesses of <2m. Within bed-parallel laminations small dm-scale dunes migrate (obliquely) down the foreset.	Gilbert-type deltas overridden by a strong (relative to 7C), and variable hyperpycnal current resulting in traction structures on the foreset.	Delta front. Closely associated with facies 6, 7C, 7D, 8, 9.	4.6
8	Cross-bedded sandstones	Coarse- to very coarse-grained, straight planar, tangential planar and trough cross-bedded sandstones, including granules and 5 cm pebbles.	Fluvio-deltaic channel deposits containing both straight- and sinuous-crested dune bed forms.	Observed in delta top. Rarely observed in at the top of the upper slope association where interpreted as sub-aerial shelf-edge channels.	3.16a, b, c, 4.7
9	Parallel-laminated sandstones	Cm-scale laminated coarse- to very coarse-grained sandstones with granules and <3 cm pebbles.	Upper stage plain bed deposits indicating a higher flow regime than facies 8.	Observed in the delta top environment.	3.15b, d 4.5a, d
10	Coals	Organic-rich deposits, frequently interbedded with shale, silt and fine-grained sandstones.	Coals record the accumulation of organic material in peat mires.	Observed in the delta top environment, typically above palaeosols.	-
11	Palaeosols	Hard quartzitic, well-cemented sandstones or rooted horizons typically at the top of cross-bedded sandstones and frequently overlain by organic-rich shales or coals.	Palaeosols develop during prolonged abandonment and frequently precedes minor coal seams.	Observed in the delta top environment, typically below coals.	-

	Facies Associations	Facies	Formations	Figures
1	Lower slope	1, 2, 3, 4, 5	Pendle Grit Sandstone	
2	Upper slope	1, 2, 3, 4	Pendle Siltstone	
3	Gilbert-type deltas with fine-grained toesets	2, 7A, 8	Bearing and Warley Wise Grit	3.7, 3.13
4	Gilbert-type delta with structureless sandstones in toeset	2, 6, 7B, 7C, 7D, 8, 9	Bearing Grit	3.10
5	Delta top	1, 2, 6, 8, 9, 10, 11,	Bearing and Warley Wise Grit	3.7

Table 3.1 Description of main lithofacies and facies associations present within the $E_{1c}1$ and $E_{1c}2$ cycles.

3.4.7 Facies Associations

3.4.7.1 Facies Association 1: Lower slope facies association

The lower slope facies association contains shale, siltstone, thin turbiditic sandstones, thick turbidite sandstones and debritic sandstones.

Before deposition of the Pendle Grit Member, deposition in the Craven Basin is characterised by the Bowland Shale Formation, suggesting a quiet but not necessarily a deep marine setting as this shale succession also onlap the Askrigg Block (e.g. Black, 1950). Towards the basin centre, the Bowland Shales probably represent a basin floor setting while a slope setting is more likely towards the basin margins. This is further supported by the occasional influxes of sand-grade sediment within this formation, such as the Hind Sandstone that is interpreted as a slope deposit (Fig. 3.3) and slope failures in the Bowland Shale Formation (Kane, 2010).

In the Whitendale and Pendle Hill areas (Fig. 3.2), the base of the Pendle Grit Member is characterised by debritic sandstones (Facies 5) that are assigned to the Whitendale Sandstone. These deposits have been related to the onset of turbidite deposition and grading or smoothing of the longitudinal slope profile (Kane et al., 2010a). These are followed by the Pendle Sandstone, a heterolithic succession in which shales (Facies 1), siltstones (Facies 2) and thin turbidite facies (Facies 3) are common, interbedded with packages of thick turbiditic sandstones (Facies 4). In locations close to the basin margin these sandstone packages of thick turbiditic sandstones (Facies 4) are frequently erosionally-based, strongly amalgamated and discontinuous perpendicular to flow (Fig. 3.14a-c, e, f). Laterally, these packages are replaced by heterolithic fine-grained facies in both directions (e.g. Fig. 3.11) suggesting deposition occurred predominantly in channels or channel complexes.

In locations further removed from the basin margin, thick turbiditic sandstones (Facies 4) occur in sand-rich packages as well (e.g. Wiswell Quarries and Longridge Fell; Fig. 3.2). Here, these packages are less amalgamated, and individual beds are more tabular, suggesting that the depositing currents are generally less erosional and less confined. Beds near the tops of such packages do record large scour surfaces or ‘megaflutes’ that are associated with break of slope (Kane et al., 2009), suggesting these deposits are formed on the proximal basin floor and near the base of the slope.

3.4.7.2 Facies Association 2: Upper Slope facies association

The upper slope facies association occurs stratigraphically above the Lower Slope Facies Association, and contains predominantly siltstones (Facies 1), with subordinate shale (Facies 1), thin turbiditic sandstones (Facies 3) and rare small channel deposits containing thick turbiditic sandstones (Facies 4). Shales occur mainly towards the base of the association that becomes siltier upwards. Similarly, thin turbiditic sandstones and small turbidite channelized sandstones become increasingly rare upward. Due to the fine-grained nature of the upper slope sediments, exposures are rare. The field expression of the Upper Slope Facies Association is generally a featureless vegetated slope, underlain by feature-forming turbidite channels of the Pendle Sandstone in the Lower Slope Facies Association. Baines (1977) reports abundant trace fossil fauna in this succession suggestive of a slope environment. The Upper Slope Facies Association coincides with the Pendle Siltstone.

In some locations, channelized sandstones occur at the top of the Upper Slope Facies Association (Sections 3.4.2.4; 3.4.3.2; 3.4.4.1; 3.4.4.2). They are predominantly massive, with cross bedding (Facies 8) occurring towards the top of the channel exposures. These sandstones are assigned to the Surgill Sandstones and are interpreted as the shelf edge feeder channels to the turbidite channels in the Pendle Sandstone.

3.4.7.3 Facies Association 3 and 4: Delta front facies association

The Delta Front Facies Association occurs in the Bearing Grit and Warley Wise Grit and contains large-scale foresets (Facies 7), structureless and crudely-laminated sandstones (Facies 6) and cross-bedded sandstones (Facies 8). Siltstones (Facies 2) occur in this depositional environment as well but are rarely exposed. The position of the delta front is defined by the occurrence of Gilbert-type delta foresets (Facies 7). In Chapter 4 a further distinction is made between different types of large-scale foresets and between two types of delta front facies associations: a regular Gilbert-type delta facies association and a sediment-gravity-flow-dominated Gilbert-type delta facies association.

3.4.7.4 Facies Association 5: Delta top facies association

The Delta Top Facies Association occurs in the Bearing Grit and Warley Wise Grit. In this facies association, shales (Facies 1), siltstones (Facies 2), cross-bedded sandstones (Facies 8), coals (Facies 10) and palaeosols (Facies 11) are observed. Additionally, in the Bearing Grit, parallel-laminated sandstones and sediment-gravity-flow deposits are observed. Within the delta top facies association, successions range from sandstone-dominated to heterolithic. Heterolithic successions generally contain fine- to medium-grained sandstones, interbedded with shales, siltstones, coals and palaeosols and are interpreted as an overbank environment that is rarely exposed at outcrop but are frequently recognised in boreholes.

The sandstone-dominated successions are generally formed by (very) coarse-grained cross-bedded sandstones (Facies 8) that are organised both in multi- and single-storey channels. Single-storey channels consists of multiple levels of cross beds, typically fining upward overall and decreasing in set height. Multi-storey channels consist of several stacked channel stories.

3.4.8 Sediment volumes of stratigraphic units

Isopach maps have been constructed based on the stratigraphic thickness patterns of the Pendle Grit Member, Bearing Grit and Warley Wise Grit, and flow directions measured in these successions. Sediment volumes have been estimated from these maps by multiplying the areal extent of each interval with stratigraphic thickness (Fig. 3.17; 3.18). Sediment volumes are not corrected for compaction or tectonic shortening and so represent an order of magnitude estimate.

Based on the known occurrence of the Pendle Grit Member, a volume of ~900 km^3 is estimated (Fig. 3.17), which is probably an underestimate because, at the southern outcrop limit in the Bowland sub-basin, the Pendle Grit is still ~400 m thick (Fig. 3.17). Additional sediment volumes might also be present at depth in the Rossendale and Huddersfield sub-basins that are located south of the Central Lancashire High (Fig. 3.1). On the (drowned) Central Lancashire High, the Pendle Grit succession is ~270 m thick in the Boulsworth 1 Borehole, and ~300 m in the Holme Chapel 1 Borehole, but the southward and eastward extent and thickness of

the formation are largely unknown (Evans and Kirby. 1999; Chadwick et al., 2005). At Heywood 1 Borehole, 20 km south of Holme Chapel 1, a ~60 m sandstone succession probably corresponds to the Pendle Grit Member.

A sand-rich turbidite succession is present in the north-western Lancaster Fells sub-basin (Quernmore area; Brandon et al., 1998) that might indicate an additional sediment pathway along the N-S trending Dent and Kendal Fault systems (Fig. 3.2; 3.17). The onshore area has been included in the volume calculation but a potential continuation in the Irish Sea has not. Pendleian strata are not reported for the Irish Sea Basins (Waters et al., 2011) making large sediment volumes from the Pendle Grit Member in this area unlikely.

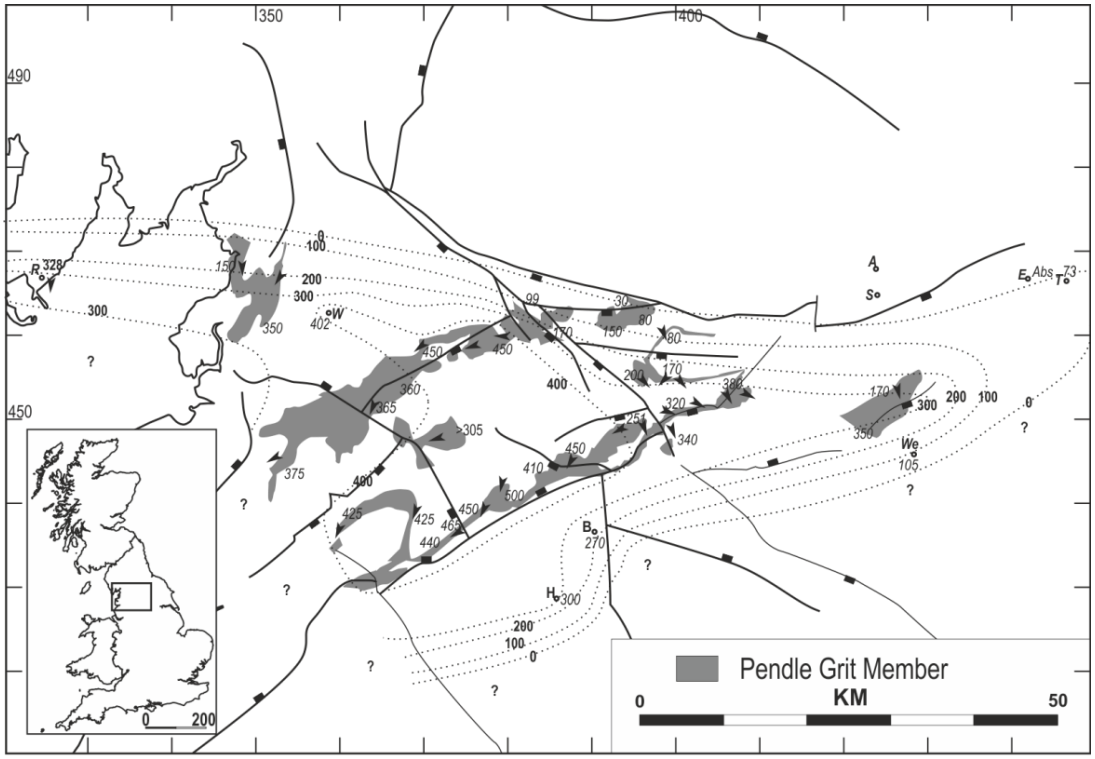

100 *Thickness estimates of the Pendle Grit Member in specific areas (metres)*
100 Isopachs of thickness estimates (metres)

Pendle Grit volume: 900 km3

Figure 3.17 Outcrop map for the Pendle Grit Member with thickness estimates, flow directions and isopachs. Thickness estimates and flow directions derived from both fieldwork and literature (Aitkenhead et al., 1992; Baines, 1977, Brandon et al., 1998; Cooper et al., 1993; Earp et al., 1961; Jones, 1943; Sims, 1988; Waters, 2000). For borehole abbreviations, see Fig. 3.2.

In the east of the Harrogate sub-basin, an additional depocentre is considered unlikely based on the position of the incised valley on the Askrigg Block, and the sand-poor character of the Pendle Grit Member in the northern and western part of the Harrogate sub-basin

The Bearing Grit occurs entirely within in the outcrop area and inaccuracies will be based on the paucity of data mainly. Its volume is estimated at 100 km^3 (Fig. 3.18).

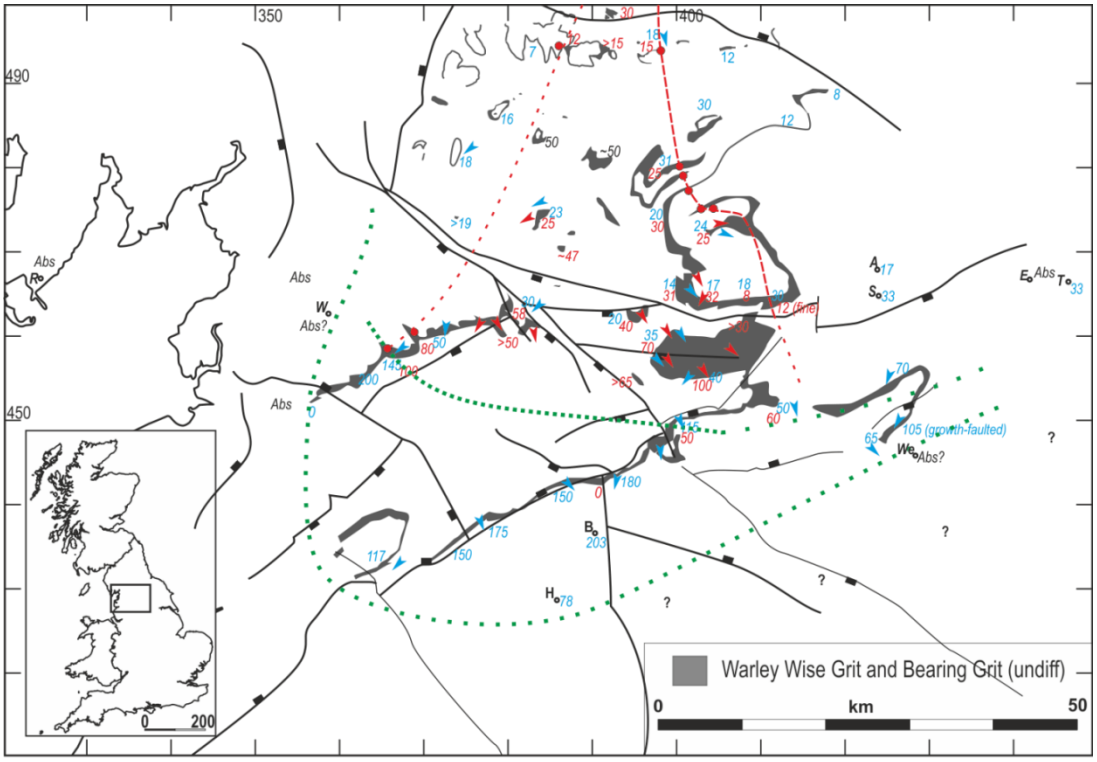

Figure 3.18 Outcrop map for the Bearing and Warley Wise Grit with thickness estimates, flow directions and isopachs. Thickness estimates and flow directions derived from both fieldwork and literature (Aitkenhead et al., 1992; Baines, 1977, Brandon et al., 1998; Cooper et al., 1993; Dakyns et al., 1890; Dunham and Wilson, 1985; Earp et al., 1961; Jones, 1943; Martinsen, 1990; Sims, 1988; Waters, 2000; Wilson, 1960). For borehole abbreviations, see Fig. 3.2.

The Warley Wise Grit is estimated at 250 km^3 in volume and is largely contained within the outcrop area (Fig. 3.18). The Warley Wise Grit thins rapidly in the Lancaster Fells sub-basin and is not present in the Whitmoor 1 or Roosecote Boreholes. In the Harrogate Basin, it occurs at Almscliff Crag (Fig. 3.2) but has probably pinched out or thinned substantially in the Weeton 1 Borehole to the southeast (Fig. 3.18). In Tholthorpe 1 Borehole a thickness of 33 m is suggested (Sims, 1988), suggesting a substantial eastward thinning (Fig. 3.18). In the Bowland sub-basin and on the Central Lancashire High, the formation thins from ~200 m in the Boulsworth borehole to ~80 m in the Holme Chapel 1 Borehole (Riley and McNestry, 1988); a trend that coincides with the southward thinning in the Bowland Basin (Fig. 3.18).

The above estimates indicate that during the $E_{1c}1$ sea-level cycle approximately 4 times more sediment was deposited than during the $E_{1c}2$ sea-level cycle.

3.5 Discussion

3.5.1 Depositional environments

3.5.1.1 Pendle Grit Member

The Pendle Grit Member is associated with the lower and upper slope facies associations. In proximal areas, close to the Askrigg Block margin (e.g. the Transition Zone and lateral equivalents; Fig. 3.2), the Pendle Grit is relatively sand-poor and characterised by small sand bodies in comparison to the more distal deposits in the Bowland Basin, suggesting a downdip transition in its depositional character.

At proximal locations, such as Skipton Moor (Section 3.4.2.6; Fig. 3.11), the lowest part of the Pendle Sandstone forms a laterally amalgamated succession of small channelized sandstones consisting of thick turbiditic sandstones (Facies 4) that probably resemble a turbidite-fan apron near the base of slope (Fig. 3.11). This is followed by a ~200 m thick succession that contains numerous small channels consisting of thick turbiditic sandstones (Facies 4), embedded within a heterolithic succession (Facies 1, 2, 3) interpreted as a lower slope setting. Small, coarse-grained

turbidite systems require relatively steep slopes, implying that the ~200 m thick slope succession coincides with a significant progradation of the shoreline (Fig. 3.8) to maintain a sufficient angle for sediment transport. This inference fits well with the observation of cross-bedded sandstones in the Surgill Sandstone on the south-side of Barden Moor directly updip of Skipton Moor (Fig. 3.2; 3.8; 3.9). The Surgill Sandstones form the feeder system to the Pendle Grit in locations close to the Askrigg Block margin and probably resemble entrenched distributary channels on a prograding shelf margin.

The Pendle Siltstone, which occurs stratigraphically above the Pendle Sandstone is interpreted as an upper slope environment in these proximal locations but is poorly exposed. However, recognition of clinoform structures at Bowland Knotts and Halstead Fell is consistent with this interpretation (Fig. 3.12). The sand-poor nature of this upper slope environment relative to the contemporaneous lower slope environment is probably related to the generation mechanism of turbidity currents: slope failures, and successive transformation into a high density turbidity current capable of depositing thick turbiditic sandstones (Facies 4) requires time and run out length and will thus not be present on the upper part of the slope. In this interpretation, the facies in the Pendle Grit succession in proximal locations form a prograding shelf clinoform.

In the Bowland Basin (Fig. 3.2), the Pendle Sandstone is relatively sand-rich and deposited in major channel complexes at Pendle Hill and Waddington Fells that correspond to a slope environment, consisting mainly of Facies 4 besides Facies 1, 2, and 3. It is noted that quarries mainly expose Facies 4 – the target of quarry men – and thus results in a bias towards the sand-rich environments. In more distal areas, such as Longridge Fell, the base of the succession records poorly exposed heterolithic strata, probably representing a base of slope or basin floor that infrequently received sand-grade sediment (Fig. 3.8). These deposits are succeeded by lobate sand bodies, interpreted as break of slope deposits, and are eventually overlain by channelized sandstones. These downdip transitions in depositional environment are thus thought to represent different longitudinal positions along the shelf clinoform. The stratigraphic transition from a basin floor to slope setting at Longridge Fell probably records an increasing proximity to source during deposition of the Pendle Grit Member.

3.5.1.2 Bearing Grit

The Bearing Grit is associated with both the delta top and delta front facies association, and is characterised by cross-bedded sandstones (Facies 8) and parallel-laminated sandstones interpreted as upper stage plane bed deposits (Facies 9) in the delta top (e.g. Fig. 3.7; 3.10). In the delta front, large-scale foresets are interpreted as Gilbert-type delta foresets (Facies 7) and structureless or crudely-laminated sandstones are interpreted as sediment-gravity-flow deposits (Facies 6). On the Askrigg Block, the Bearing Grit consists of a channel belt complex with a strongly erosional contact at its base, and a sharply-defined eastern margin. In the Craven Basin, a sharply-defined western margin is preserved at White Greet and at Croasdale. Laterally, overbank succession containing multiple palaeosols and minor coals are preserved within the same sea-level cycle.

The Bearing Grit is interpreted as an incised valley fill, based on the large preserved thickness (up to 80 m), which contains both stacked Gilbert-type deltas and multi-storey channels, the strongly erosional contact at the base of the Bearing Grit, and the clear lateral margins. Additionally, the multiple coals and palaeosols that occur adjacent to the Bearing Grit indicate a probable development of interfluves. A basinward shift of facies belts is observed on the Askrigg Block, where multi-storey channel deposits of the Bearing Grit overlie shelfal limestones, which can be interpreted as a Type 1 sequence boundary. In the Craven Basin, the precise position of the sequence boundary is more difficult to establish precisely. It is placed below in-valley Gilbert-type deltas as these probably formed during sea-level rise.

3.5.1.3 Warley Wise Grit

The Warley Wise Grit consists of a delta front and delta top facies association and is characterised by cross-bedded sandstones (Facies 8) and large-scale foreset interpreted as Gilbert-type deltas (Facies 7) (e.g. Fig. 3.13). Structureless sandstones (Facies 6) do occur at a distinct lower level but are separated from the Gilbert-type foresets by an thick unexposed interval, which makes it impossible to relate these deposits. The relative coarser grain size of these lower deposits suggests that they do not form part of a contemporaneous depositional system with the Gilbert-type deltas.

The Warley Wise Grit is deposited over a wide area, and is not associated with the occurrence of interfluves or a rapid pinch out of its channel deposits laterally. Fluvial channels are typically sharp-based but the Warley Wise Grit consistently overlies the Blacko Marine Band both on the Askrigg Block and in the Craven Basin. This suggests regular fluvial erosion and does not indicate significant incision associated with a Type 1 sequence boundary.

At Hardacre Quarry, Faughs Delph Quarry and Noyna Rocks Quarry, the deltaic foresets are significantly finer-grained than the overlying cross-bedded succession. This suggests that the overlying succession represents a later depositional period associated with an abrupt basinward shift in facies belts. This surface can be interpreted as a generally non-erosional Type 2 sequence boundary that is onlapped landwards by the overlying Bradley Flags. In such interpretation, the Warley Wise Grit is deposited during sea-level fall and represents a forced regressive succession.

3.5.2 Sequence-stratigraphic interpretation of stratigraphic architecture

Stratigraphic and sedimentological observations on the succession between the Cravenoceras malhamense ($E_{1c}1$) and Cravenoceras cowlingense Marine Bands ($E_{2a}1$) have led to an alternative depositional model to previously proposed models (cf. Baines, 1977; Sims, 1988; Martinsen, 1990; Brandon et al., 1995).

3.5.2.1 Early Pendle Grit – Early Falling Stage Systems Tract (Fig. 3.19c)

Deposition of the Pendle Grit Member commenced after the Cravenoceras malhamense Marine Band, during sea-level highstand or early sea-level fall (Fig. 3.3). Flow indicators in the Pendle Grit close to the Askrigg Block – Craven Basin boundary indicate that sediment was derived from a northerly direction across the Askrigg Block (Fig. 3.8; 3.17). Deposition of the Pendle Grit Member during this early stage occurred along a wide front, ranging from the Harrogate sub-basin in the east, to the Morecambe Bay area in the west, where it is proven in the Roosecote borehole (Fig. 3.17; Rose and Dunham, 1977; Colin Jones, personal communication). In proximal positions in the Craven Basin, the Pendle Sandstone is characterised by numerous small turbidite channels that record deposition of several

tens of flows at most, and are encased in argillaceous sediments (Fig. 3.9; 3.11; 3.19). The occurrence of numerous small turbidite channels along the entire width of the Lake District High and Askrigg Block suggest sediment delivery along a wide front, indicating that the fluvial system was not incised into a valley, which would narrow the area of active deposition.

In areas close to Askrigg Block - Craven Basin transition, the top of the early Pendle Grit Member is represented by the Surgill Sandstone. This interval contains cross-bedded channelized sandstones, which are interpreted as sub-aerial shelf-edge channels, suggesting progradation of the coastline from the Askrigg Block edge into the proximal Craven Basin during early sea-level fall (Fig. 3.8; 3.9; 3.12; 3.19c).

When upstream erosion from shelf edge channels connects directly into a deltaic channel, it starts to receive enhanced volumes of water and sediment discharge, allowing increasing erosion rates and development into an incised valley, while adjacent gullies will become sediment-starved (van Heijst et al., 2001).

3.5.2.2 Late Pendle Grit – Late Falling Stage and Lowstand Systems Tract (Fig. 3.19d)

During progressive sea-level fall (late falling stage systems tract?) the fluvio-deltaic system to Pendle Grit became incised. The eastern margin of an incised valley is well-exposed on the Askrigg Block (Fig. 3.5; 3.6; 3.19d) and the western margin is exposed in the Craven Basin at White Greet and Croasdale (Fig. 3.2; 3.12; 3.18). This incised valley routed significant sediment volumes towards the active shelf edge at the Bowland sub-basin and the submerged Central Lancashire High.

At the base of the turbidite succession in the Bowland sub-basin, large mudstone clasts are observed that have a terrigenous origin, suggesting an erosional character of the fluvial feeder system (Kane et al., 2010a). Turbidite channels in the Bowland sub-basin (e.g. at Pendle Hill and Waddington Fells Quarry, Fig. 3.2) are significantly larger than those that formed in locations close to the Askrigg Block during early sea-level fall (e.g. Skipton Moor; Fig. 3.2; 3.11; 3.19c, d). This probably reflects the character of the incised fluvial system, which will have been

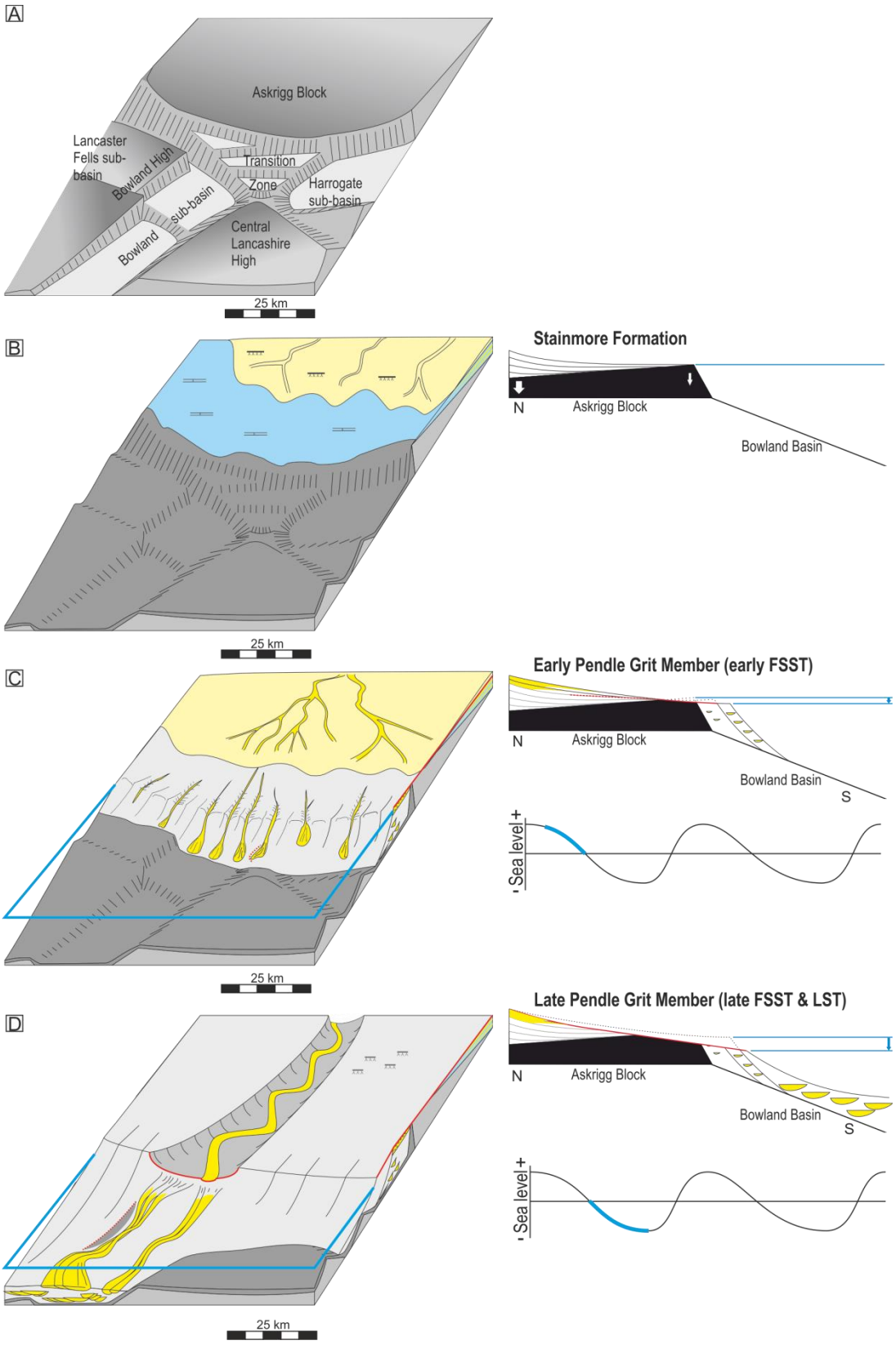
A
Askrigg Block
Lancaster Fells sub-basin
Bowland High
Transition Zone
Harrogate sub-basin
sub-basin
Bowland
Central Lancashire High
25 km
B
25 km
Stainmore Formation
N
Askrigg Block
Bowland Basin
C
25 km
Early Pendle Grit Member (early FSST)
N
Askrigg Block
Bowland Basin
S
Sea level +
-
D
25 km
Late Pendle Grit Member (late FSST & LST)
N
Askrigg Block
Bowland Basin
S
Sea level +
-

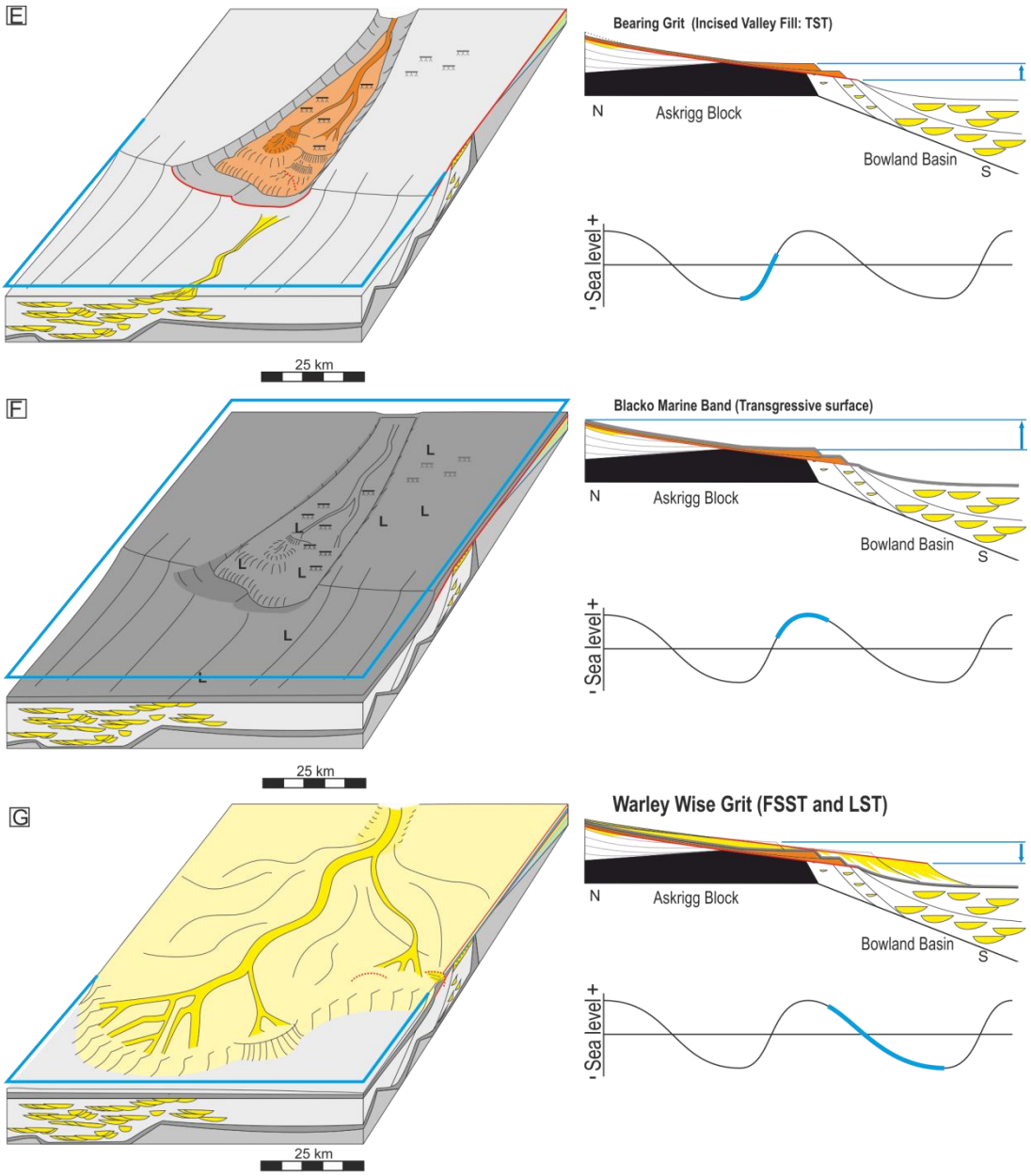
E
Bearing Grit (Incised Valley Fill: TST)
N
Askrigg Block
Bowland Basin
S
Sea level +
-
25 km
F
Blacko Marine Band (Transgressive surface)
N
Askrigg Block
Bowland Basin
S
Sea level +
-
L
25 km
G
Warley Wise Grit (FSST and LST)
N
Askrigg Block
Bowland Basin
S
Sea level +
-
25 km
Mixed limestone - siciliclastic strata (Yoredale cycles)
Coarse-grained sandstones (Pendle Grit - Warley Wise Grit)
Coarse-grained sandstones (Bearing Grit)
Heterolithic strata
Marine shales (Bowland Shales)
Major erosive contacts
Coal seams
L
Lingula occurences (indicative of the E 2 marine band)
Syn-sedimentary faults
Relative turbidite channel size

Figure 3.19 (previous pages) (a) Structural template for the Askrigg Craven area at the end of the Visean. (b) Deposition of the Stainmore Formation on the Askrigg Block, varying between fine-grained clastic and calcareous deposition on a shallow shelf, while in the Craven Basin, the rift-topography was draped by the Bowland Shales. (c) Deposition of the early Pendle Grit: the shelf margin was fed by distributary feeder channels (Surgill Sandstones), resulting in a progradational shelf clinoform with numerous small channels. Growth-faulting occurred at the base of the Pendle Grit at Jenny Gill Quarry, Skipton Moor above the Pendle Fault system. Progressive sea-level fall and slowing progradation in increasing water depths should lead to an increase in the efficiency of the fluvial system, resulting in larger sediment volumes and coarser-grained sediment deposited in the turbidite system. (d) Deposition of a lowstand fan in the Bowland Basin. The lowstand fan was fed by an incised river system of which the margins indicate that it drained towards the Bowland Basin. Rapid deposition of a thick sequence of turbidite deposits might have re-activated extensional faults along the Bowland Line and resulted in growth-faulting, locally steering the position and character of channels at Waddington Fells Quarry (Kane et al., 2010a). Valley incision during sea-level fall results in a highly efficient fluvial system, which corresponds with the very coarse-grained nature of the Pendle Grit in the Bowland Basin. (e) Deposition of Bearing Grit within the incised valley coincides with the shut off of the Pendle Grit turbidite system. The valley infill is characterised by a very coarse-grained succession of stacked sediment-gravity-current fronted Gilbert-type deltas. Growth-faulting is recognised in the succession at Flasby Fell above the South Craven Fault. During the initial infill of the incised valley, the updip fluvial system remains erosional and efficient resulting in a very coarse-grained succession. (f) Transgression initially resulting in deposition of in-valley coal seams, and eventually in deposition of the Blacko Marine Band, a regional shale succession containing *Lingula sp.* (g) The Warley Wise Grit was deposited as a shallow water delta during the subsequent sea-level fall, forming a forced-regressive succession. This fluvial system entered the Askrigg Block in the same area as the Bearing Grit, suggesting the Bearing Grit valley was underfilled. Growth-faulting occurred near tectonic lineaments in the Harrogate sub-basin. Rapid, shallow water progradation resulted in a lower efficiency fluvial system, resulting in smaller sediment volumes and finer grain size.

strongly erosional during valley incision and will have transported large amounts of sediment to the Bowland sub-basin, rather than distribute sediment along a wide front such as occurs during deposition of the early Pendle Grit (Fig. 3.2; 3.19c, d). At distal locations in the Bowland Basin, such as Longridge Fell, the lower part of the Pendle Grit Member is relatively argillaceous, followed by sand-rich lobate deposits. Only towards the top of the succession major channels reach the area, which probably indicates that channels might only have arrived here after substantial progradation on the shelf and slope.

3.5.2.3 Bearing Grit – Incised Valley Fill: Transgressive Systems Tract (Fig. 3.19e)

During early sea-level rise, sand supply to the turbidite system was halted and valley infill is recorded by the Bearing Grit in the proximal Craven Basin, and on the Askrigg Block (Fig. 3.19e). The Bearing Grit is characterised by the occurrence of stacked Gilbert-type deltas with sediment-gravity-flow deposits in the delta toe at Barden Moor and Barden Fell in the Transition Zone at the eastern side of the incised valley (Fig. 3.10; Section 3.4.2.3). This provides an indication of the position of the coastline during sea-level rise (Fig. 3.18). On the western side of the incised valley in the proximal Craven Basin, a Gilbert-type delta is observed only at Whelpstone Crag (Section 3.4.4.3). At other locations such as Far Costy Clough and Bowland Knotts, the Bearing Grit consist entirely of sediment-gravity-flow deposits, which are typical of the Bearing Grit delta front succession and suggests that the delta front was located slightly further upstream (see Chapter 4).

In Coverdale and Waldendale on the Askrigg Block, the eastern valley margin is clearly observed by the rapid pinch out of the Bearing Grit sandstone (Fig. 3.5; Wilson, 1957; 1960; Section 3.4.1.2). Adjacent, a relatively thin heterolithic succession containing multiple palaeosols and coals is observed that is overlain by the Blacko Marine Band, for example at Crook Dyke (Fig. 3.6; 3.19d; Wilson, 1957; 1960; Brandon et al., 1995). This succession probably corresponds to the Pendle Grit feeder system during early sea-level fall prior to valley incision. At How Stean Beck (Section 3.4.1.5), the Blacko Marine Band is observed overlying the Bearing Grit but a clear valley margin is not observed. Flow directions in the Bearing Grit at this location are due east, which suggests that the valley margin is located further

north and east (Fig. 3.6; 3.18). Near the North Craven Fault, several boreholes along a W-E oriented transect indicate the pinch out of the Bearing Grit eastward near Greenhow (Fig. 3.6; 3.18; Section 3.4.1.9). Laterally, channelized sandstones are replaced by a heterolithic succession containing several thin coals and palaeosols, representing interfluve deposits (Fig. 3.6). A southward continuation of the eastern valley margin suggests that the pebbly successions at Barden Moor and Barden Fell represent the Bearing Grit in the Craven Basin. Further east the presence of the Bearing Grit is unlikely (Fig. 3.18; 3.19a, e). A northward continuation of the eastern valley margin trend implies a correlation with the valley margin near Summer Lodge Beck in Swaledale on the northern margin of the Askrigg Block (Fig. 3.5; 3.6; 3.18; 3.19d). This inferred incised valley has important implications for the correlation between the Blacko Marine Band and the Upper Stonesdale Limestones and will be discussed in Section 3.5.3.

The western incised valley margin is poorly constrained as it is only exposed at White Greet and Croasdale in the Craven Basin, and near Fossdale Gill, Swaledale on the Askrigg Block (Fig. 3.5a). If these positions are connected, then the incised valley would include Pen-y-ghent whileWhernside is placed outside the incised valley. This would explain the observed differences in thickness and sedimentary character between these locations (Fig. 3.5a; Fig. 3.6a). At Whernside, a multi-storey channel is exposed in a relatively thin succession, which, if placed outside the incised valley, belongs to the Warley Wise Grit (Fig. 3.6). At Pen-y-ghent, a much thicker succession is present, internally subdivided by the Blacko Marine Band, suggesting that both the Bearing Grit and Warley Wise Grit are present (Fig. 3.5; 3.6). Additionally, a Gilbert-type delta is recorded at the top of a multi-storey channelized sandstone in the Bearing Grit at Pen-y-ghent. This indicates an overall retrogradation of the coastline from the Craven Basin onto the Askrigg Block during deposition of the Bearing Grit, which fits well with the inference of an incised valley fill (Fig. 3.19f).

3.5.2.4 Warley Wise Grit: Falling and Lowstand Systems Tract (Fig. 3.19g)

During the subsequent sea-level fall the Warley Wise Grit prograded into the Craven Basin. The Warley Wise Grit appears to have entered the Askrigg Block in the same position as the Bearing Grit fluvial system, suggesting that the Bearing Grit

incised valley might not have been infilled completely (Fig. 3.18; 3.19). In underfilled valleys, rivers tend to occupy the original valley, whereas in (over)filled valleys, the successive fluvial system avulses to a position on the floodplain (Strong and Paola, 2008, Martin et al., 2011). The Warley Wise Grit has been deposited from the eastern Harrogate sub-basin to the western Lancaster Fells sub-basin implying a wider distribution than the Bearing Grit (Fig. 3.18). In the Bowland Basin, progradation of the Warley Wise Grit occurred in relatively shallow water and was fronted by Gilbert-type deltas observed at Noyna Rocks Quarry and Faughs Delph Quarry (Fig. 3.8; 3.13). Foresets of these Gilbert-type deltas transition gradually into a siltstone bottomset. At lower levels in the Warley Wise Grit, sediment-gravity-flow deposits are observed, but evidence for the close association between Gilbert-type foresets and sediment-gravity-flow deposits similar to that seen in the Bearing Grit is not observed (e.g. Fig. 3.10). No evidence for valley incision is observed in the Warley Wise Grit. Therefore, these deltas are interpreted to have formed during forced regression and are erosionally overlain by fluvio-deltaic channels (Fig. 3.19). The multi-storey character of the overlying channel belt might reflect high progradation rates, resulting in some aggradation during sea-level fall and lowstand (Petter and Muto, 2008), and reflect aggradation of the fluvial system during lowstand. Subsequently, sea-level rise and maximum transgression are locally recorded by the Bradley Flags and the Cravenoceras cowlingense Marine Band ($E_{2a}1$).

3.5.3 Intra-$E_{1c}1$ unconformity

An important difference between the stratigraphic model proposed here and previous models is the recognition of a large incised valley on the Askrigg Block that is responsible for significant erosion at the base of the Bearing Grit. In previous models, this erosional contact is referred to as the intra-$E_{1c}1$ unconformity and has been related primarily to a period of tectonic activity (Hind, 1902; Chubb & Hudson, 1925; Rowell and Scanlon, 1957a; Dunham and Wilson, 1985; Gawthorpe et al., 1989; Brandon et al., 1995). In the current model sea-level induced valley incision is considered the primary cause for this unconformity.

The inference of a tectonic unconformity is mainly based on the relatively continuous outcrop belt ranging from Swaledale, along Waldendale and Coverdale

to Wharfedale and the southern Askrigg Block margin. However, this transect falls entirely within the incised valley and would therefore also record an increasing influence of sea-level incision (Fig. 3.5). Additionally, the Askrigg Block forms a large northward tilting area during the Visean, which results in a ~4.5 times thinner succession towards the crest of the Askrigg Block at its southern margin than at its northern margin at the Stockdale Fault (Fig. 3.2; 3.5; Collier, 1991, Dunham and Wilson, 1985; Fraser and Gawthorpe, 2003). This pronounced thinning has led to a condensed Alston and Stainmore Formation on the southern margin of the Askrigg Block, which can greatly enhance the appearance of a major angular unconformity with limited erosion since the erosional contact is characterised by the age of the underlying strata, rather than the (unknown) removed thickness.

The strength of erosion, based on the age of underlying strata, is reduced outside of the incised valley as defined in this chapter. At Whernside located westward of the incised valley fill, a deltaic sandstone belonging to the Little Limestone cyclothem (the Uldale Sill) is present below the Warley Wise Grit (Fig. 3.4; Dunham and Wilson, 1985). Within the incised valley, Bearing Grit sediments lie directly on top of the older Great Limestone (e.g. at Dodd Fell and Waldendale; Fig. 3.4; 3.5). In Coverdale and Waldendale erosion also appears to decrease outside the incised valley (Fig. 3.5) but because these sections trend NE, the decreasing amount of erosion could also relate to thickening of strata produced by the northward tilt (Fig. 3.5). At the southern margin of the Askrigg Block, erosion decreases slightly along an E-W trending transect from the Yarnbury section to Ashfold Side Beck 1 Borehole (Fig. 3.6). The pattern in which erosion decreases both in a westerly and easterly direction is difficult to explain by tectonic movement but it fits well with a valley incision hypothesis. However, the Three or Five Yard Limestones underlying the siliciclastic succession at Bewerley Mines 1B Borehole and Ashfold Side Beck 1 Borehole belong to the Alston Formation, suggesting a significant hiatus outside of the inferred incised valley as well (Fig. 3.6). This unconformity can be explained by tectonic uplift but could also relate to erosion at the base of the braid plain that fed the small turbidite channels in the early Pendle Grit Member (Fig. 3.19c), or non-deposition of the Stainmore Formation along the southern margin of the Askrigg Block.

Detailed tectonic-unconformity models struggle to explain the stratigraphic patterns documented here. Prior to deposition of the Crow Limestone Martinsen

(1990, p 19; 1993) infers that a period of northward tilt resulted in erosion on the southern margin while creating accommodation space for the Crow, Lower, and Upper Stonesdale Limestones on the northern margin (Fig. 3.4). During the subsequent period in which the Bearing and Warley Wise Grit are deposited, the Askrigg Block tilting is reversed to a SSE direction to explain the occurrence of a the Mirk Fell Ganister palaeosol as a condensed sequence while in a SSE of the Askrigg Block a ~60 m thick multi-storey channel succession is formed. This implies a highly active, variable and "wobbly" tectonic pattern of the Askrigg Block over very short durations, which is unlike previous tectonic periods during which the Askrigg Block behaved as a consistently northward-tilting half-graben. Additionally, the model fails to explain how the combined Bearing and Warley Wise Grit succession thins eastwards from Yarnbury towards Ashfold Side Beck 1 Borehole (Fig. 3.6).

Brandon et al. (1995) suggests that the $E_{1c}1$ unconformity formed after deposition of the Lower Stonesdale Limestones but before deposition of the Upper Stonesdale Limestone by uplift and erosion of the southern margin of the Askrigg Block (Fig. 3.4). The Blacko Marine Band is thought to onlap this unconformity from the south while the correlative Upper Stonesdale Limestones are thought to onlap the unconformity from the north. This would explain the absence of the Upper Stonesdale Limestone at the same locations as the Lower Stonesdale Limestone but occurring above, instead of below the unconformity. This implies that the previous zone of maximum uplift on the southern margin Askrigg Block is overlain by a ~30 m multi-storey sandstone and is transgressed during deposition of the Blacko Marine Band while the unconformity on the northern Askrigg Block remains sub-aerially exposed. Additionally, the Bearing Grit pinches out along the Bewerley Mines Borehole - Angram - BGS Croft House Borehole transect (Fig. 3.2; 3.5). This (northward) pinch out is thought to imply that the channel belt complex exposed at the northern margin of the Askrigg Block (Section 3.4.1.1) has to correlate with the Underset Grit (here referred to as Warley Wise Grit). In turn, this implies that the Blacko Marine Band occurs at a lower stratigraphic level, suggesting a correlation with the Upper Stonesdale Limestone.

The Brandon et al. (1995) model infers tectonic uplift of the southern margin of the Askrigg Block during deposition of the Bearing Grit (between the Lower and Upper Stonesdale Limestone), which is difficult to reconcile with the thickness

pattern of the Bearing Grit: it is considered unlikely that significant tectonic uplift occurs simultaneously with deposition of a ~30 m thick Bearing Grit succession along southern margin of the Askrigg Block. Additionally, it requires a highly active, variable tectonic arrangement so that the zone of most significant uplift (the southern margin of the Askrigg Block) is subsequently flooded during the Blacko-transgression while the zone of mild erosion near the northern margin remains sub-aerially exposed, and is onlapped by the Upper Stonesdale Limestone from the north. This contrasts with the previously interpreted behaviour of the Askrigg Block and is considered unlikely during the overall post-rift tectonic regime.

Rather than a northward pinch-out of the Bearing Grit as suggested by Brandon et al. (1995), the Bewerley Mines – Angram – BGS Croft House Borehole transect is here considered to record the pinch-out of the Bearing Grit at the eastern incised valley margin. The Swaledale 'Lower Howgate Edge Grit' channel is thought to represent the trunk channel of the Bearing Grit (Fig. 3.5; Fig. 3.19e). This implies that the correlative horizon for the Blacko Marine Band occurs at a higher stratigraphic level that the Lower Howgate Edge Grit (Bearing Grit) at Swaledale, and does not correlate to the Upper Stonesdale Limestone (see Section 3.2.3.3). In this model, the Upper Stonesdale Limestones would not have a correlative marine flooding surface in the Craven Basin, similarly to the Lower Stonesdale and Hunder Beck Limestones (Fig. 3.4c). Note that this does not exclude the correlation between the Blacko Marine Band and the Belsay Dene Limestone in the northern part of the Pennine Basin.

Sea-level-induced valley incision can more parsimoniously explain the thickness and erosion patterns in the Bearing and Warley Wise Grit than tectonic inferences. Additionally, a sea-level-induced incised valley can explain the continuation of the valley feature in the proximal Craven Basin as observed Croasdale and on White Greet (Fig. 3.2; 3.12), and stacked Gilbert-type deltas on Barden Moor that are considered to represent an incised valley fill near the eastern margin (Fig. 3.2; 3.9; 3.10). Similar stacked deltas have been observed in other incised valley fills in the Millstone Grit Group of the Central Pennine Basin (Hampson, 1997; Jones and Chisholm, 1997). Northward, the incised valley probably correlates with the N – S trending Rogerley Channel on the Alston Block. The Rogerley Channel can be interpreted as a compound incised valley succession of which the lower level incises into the Crow Limestone and of which the upper

level incises into the Corbridge Limestone (Dunham, 1990; Waters et al., 2014). Therefore, the lower level is probably time-equivalent to the Bearing/Warley Wise Grit succession and likely represents a continuation of the inferred Bearing Grit incised valley fill. The upper level of the Rogerley channel probably corresponds to the Marchup/Red Scar Grit incised valley (Waters et al., 2014).

3.5.4 Tectonic activity in the Craven Basin

Indications for tectonic activity have also been observed in the Bowland sub-basin and the Transition Zone during the late Pendleian. In the Bowland sub-basin, Arthurton (1984) suggests that the Catlow and the Sykes Anticlines of the Ribblesdale Foldbelt were active during the formation of the intra-$E_{1c}1$ unconformity. This is based on a thickening of the Pendle Grit on either limb of the Catlow Anticline, and a folded expression of the Pendle Grit, whereasthe Bearing Grit is relatively unaffected. A detailed depositional model (Kane, 2010) proposes that slope instability recognised by syn-sedimentary slumping, and injectite formation in the Hind Sandstone (Fig. 3.3) are related to growth of the NE-SW trending Sykes Anticline, a structure parallel to the Bowland Line (Fig. 3.2). Additionally, at Waddington Fells Quarry in the Bowland Basin a major syn-sedimentary normal fault is observed that trapped large turbidite channels along a similar structural trend as the Sykes Anticline (Kane et al., 2010a).

At Flasby Fell in the Transition Zone, an angular unconformity between the Pendle Grit Member and the Bearing Grit was suggested between the Pendle and Bearing Grit (Mundy and Arthurton, 1980; Arthurton et al., 1988). Firstly, this inference relies on the dip of landscape features in the Pendle Grit Member, which is considered insufficient to prove the presence of an angular unconformity (Martinsen, 1990). Additionally, growth faulting is observed in the Bearing Grit on Flasby Fell, which can result in an angular contact with the underlying Pendle Grit. Finally, sediment-gravity-flow deposits such as observed on Flasby Fell are observed at relatively steep depositional dips on Barden Moor (see Chapter 4). These observations undermine the notion of a tectonically-caused angular unconformity at this location.

The structural activity of the Catlow and the Sykes Anticlines in the Bowland Basin can support a minor active tectonic phase. However, indications of

structural activity are mainly observed during periods of rapid sedimentary loading over major pre-existing (syn-rift) faults. This implies that structural actively does not necessarily rely on tectonic activity. Differential loading and compaction might result in growth faulting and in an extreme case might result in reactivation of major fault structures. Such process could explain the broadly contemporaneous compressional regime at Sykes Anticline and extensional regime at Waddington Fells Quarry along the same tectonic trend (Kane, 2010; Kane et al., 2010a).

In the Transition Zone (Fig. 3.2; 3.19), growth faulting has also been observed at Jenny Gill Quarry on Skipton Moor in the Pendle Grit Member (Sims, 1988) along the trend of the Pendle Fault (Fig. 3.2; 3.11; 3.19c). At Sharp Haw, Flasby Fell growth faulting in the Bearing Grit (Mundy and Arthurton, 1980) occurs along the South Craven Fault trend (Fig. 3.2; 3.19e). In the Harrogate Basin, growth faulting at Almscliff Crag (Chisholm, 1981) occurs in the Warley Wise Grit along a nearby syn-rift normal fault (Fig. 3.2; 3.19g; Kirby et al., 2000). In each location, faulting is associated with a phase of rapid coarse-grained sedimentation overlying a fine-grained succession above a tectonic lineament. In the Ashover Grit growth-faulting is also observed in an area close to transition between the Derbyshire High - Widmerpool Trough, potentially indicating a correlation with underlying tectonic lineaments as well while an active tectonic control is not considered in this system (cf. Chisholm and Waters, 2012).

3.5.5 Application of analogue modelling

Analogue modelling (see Chapter 2) indicates that the efficiency of sediment transport to the coastline is strongly affected by basin depth and sea level. In deep basins (relative to shallower basins) progradation rates are slow, which allows the fluvial system to grade closer towards equilibrium. This strongly increases the sediment volume and grain size that is transported towards the shelf edge while sea-level fall further enhances this effect on fluvial efficiency (Chapter 2). Based on the sequence-stratigraphic interpretations, sediment volumes and grain sizes, a comparison is made with the experimental results from Chapter 2.

After the $E_{1c}1$ maximum transgression, the fluvial feeder to the Pendle Grit Member reaches the field area, which results in progradation of the coastline into the Craven Basin at least up to the south-side of Barden Moor (Eastby; Fig. 3.9), and

Bowland Knotts (Fig. 3.12; Arthurton et al., 1988). Subsequent incised valley fill deposits of the Bearing Grit are exposed at Barden Moor and pinch out near Skipton Moor (Fig. 3.2; 3.8; 3.11). The deposits at Barden Moor and Skipton Moor provide an estimate of 8 to 15 km progradation from the Askrigg Block margin during the $E_{1c}1$ cycle. Delta top deposits of the Bearing Grit near the western incised valley margin are most distally exposed at Whelpstone Crag, suggesting a similar progradation estimate of ~9.5 km (Fig. 3.2). During the $E_{1c}2$ sequence, the Warley Wise Grit prograded at least up to Longridge Fell (Fig. 3.2), after which the formation is lost in the subsurface. Based on the above estimated lowstand shoreline during the $E_{1c}1$ cycle, this suggests a further ~30 km progradation of the lowstand coastline during the $E_{1c}2$ sea-level cycle (Fig. 3.6).

Both sea-level cycles are thought to have a ~111 kyr duration (Waters and Condon, 2012), implying that the progradation rate and sediment volumes during these cycles differed significantly. During the $E_{1c}1$ cycle, the Pendle Grit Member (900 km^3), and the Bearing Grit (100 km^3) were deposited, while during the $E_{1c}2$ cycle, only the Warley Wise Grit Mb (250 km^3) formed, indicating that ~4 times more sediment arrived in the Craven Basin during the former cycle. This difference in sediment volume is here related to the substantially larger basin depth (up to 3 times deeper) and slower progradation rates during deposition of the Pendle Grit (~3 times slower; Fig. 3.17; 3.18; 3.19c, d).

Grain-size variations also correspond with the inference of changes in fluvial efficiency (Chapter 2). Maximum grain size increases progressively during deposition in the Pendle Grit Member, from granules in proximal small channels at Skipton Moor up to 2 cm pebbles in major channels in the Pendle Sandstone at Waddington Fells and Longridge (Fig. 3.2). This might be related to the gradual increase in basin depth from tens of metres near the Askrigg Block (e.g. Threapland Gill, Section 3.4.2.2) to ~400 m in the Bowland sub-basin over a distance of ~15 km (Fig. 3.8; 3.17) (based on the thickness of the Pendle Grit Member but not correcting for isostatic loading or compaction). This will have slowed progradation substantially and facilitated valley incision: both increase the efficiency of the fluvial system.

During the following sea-level rise, sediment supply to the Pendle Grit turbidite system was halted. In the analogue models (Chapter 2), upstream erosion in

the incised valley continued during sea-level rise suggesting that high efficiency of the fluvial system was temporarily maintained upstream of the transgressed area. Such a time-lag in the response of the fluvial gradient implies that the fluvial system will have remained close to equilibrium and efficient at routing sediment towards the coastline. This could explain the large volume and coarse-grained nature of the Bearing Grit incised valley fill that includes 4 – 5 cm pebbles (Fig. 3.19). An additional influence of discharge variability on this succession is described in Chapter 4.

The Blacko Marine Band ($E_{1c}2$) reflects maximum transgression and will have significantly reduced the gradient of the fluvial system and therefore its efficiency (Fig. 3.19). During highstand, siltstones and shales are deposited both on the Askrigg Block and Craven Basin. No coarse-grained sediment is transported into the shallow basinal environment of the study area; it is probably retained within the upstream fluvial system and might be vacated during subsequent periods of sea-level fall.

During the subsequent sea-level fall and lowstand, shallow water conditions on the shelfal area will have allowed rapid progradation of the Warley Wise Grit to the previous lowstand shoreline (Fig. 3.18; 3.19g). Due to deposition of the Pendle Grit Member, basin depth is much reduced, resulting in a rapidly prograding shallow water wedge fronted by Gilbert-type deltas. High progradation rates during sea-level fall will have inhibited fluvial incision and steepening of the fluvial gradient significantly. This is reflected by the substantially smaller volume of the Warley Wise Grit, and the reduction in grain size.

Previously, the evidence for active tectonics during the late Pendleian has been discussed and it is here considered unlikely that active tectonics have steered fluvial pathways on the Askrigg Block towards the Bowland Basin. Here, the position of the incised valley is considered to have been controlled (in part) by the relatively deep depocentre in the Bowland sub-basin. Fluvio-deltaic systems draining into deep basins prograde more slowly than those in shallower basins. This enhances the efficiency of shelfal incision, increasing the likelihood of valley incision at these positions in comparison to adjacent shallower segments. During valley incision, the fluvial system is probably graded to near-equilibrium conditions. This leads to the bypass of (nearly) the entire sediment load of rivers to the shelf

edge, and might explain the exceptionally large sediment volume in the Pendle Grit Member in the Bowland sub-basin (Fig. 3.17; 3.19) as well as its sand-rich and coarser nature in comparison with minor turbidite channels in the proximal Craven Basin.

It can also be argued that these differences in grain size, and sediment volume might be explained by differences in the magnitude of sea-level fall, or upstream tectonic events, while the position of incised valleys can be random. These hypotheses require comparison to additional areas and are considered in Chapter 5.

3.6 Conclusions

A reinterpretation of the stratigraphic succession following the Cravenoceras malhamense ($E_{1c}1$) and Blacko ($E_{1c}2$) Marine Bands of the Carboniferous Askrigg Block and Craven Basin area is proposed based on a combination of extensive fieldwork and literature study. In the current model a prograding deep water shelf margin, characterised by numerous minor turbidite channels, is recognised. This succession is incised by a large valley, forming the fluvial feeder system to a major turbidite fan system. The eastern valley margin is recognised on the Askrigg Block, and the western valley margin is observed in the Craven Basin. Near the incised valley mouth, stacked Gilbert-type deltas are observed in the valley fill, indicating deposition during sea-level rise. Valley incision can explain the intra-$E_{1c}1$ unconformity at the base of the fluvial $E_{1c}1$ succession on the Askrigg Block and challenges the importance of a previously suggested period of tectonic reactivation during the late Pendleian.

A comparison of the volumes and grain sizes of the turbidite and incised valley system during the $E_{1c}1$ cycle, and the successive shallow water delta during the $E_{1c}2$ cycle fits well with modelling results described in Chapter 2. During the $E_{1c}1$ cycle four times more sediment of significantly coarser grain size was deposited than during the $E_{1c}2$ cycle, which is here interpreted as a response of the fluvial system to the substantially deeper basin. Additionally, valley incision is focussed at the deepest area of the Craven Basin, which supports the modelling prediction that valley incision is most likely at the deepest areas in basins if significant lateral variation occurs in basin-margin morphology.

Chapter 4 Delta Front Character and Processes in the Carboniferous Craven Basin

4.1 Abstract

Sequence-stratigraphic analysis of the Pendleian succession in the Craven Basin suggests that large-scale foresets represent Gilbert-type deltas developed on a forced regressive delta front and as incised valley fill, in contrast to an earlier distributary channel bar model for these deposits. These large-scale foresets contain enigmatic structures that are poorly described in existing literature. Detailed facies description and process-based interpretation of these deposits resulted in identification of four different Gilbert-type foreset styles: (1) homopycnal suspension-dominated foresets, (2) homopycnal grain-flow-dominated foresets, (3) hyperpycnal internally-laminated foresets, (4) hyperpycnal foresets with superimposed bedforms or 'intrasets' that migrated down-foreset. Sediment-gravity-flow deposits, derived from within the fluvial system are closely associated with foresets types (2), (3) and (4), suggesting a river-flood-dominated system with incrementally higher fluvial flood stages resulting in progressive development of foresets deposited under homopycnal, then hyperpycnal conditions through to sediment-gravity-flow deposits. For foreset types (3) and (4), an observed reduction in foreset angle is related to enhanced shear stress on the foreset and used to estimate excess density of fluvial outflow. This suggests low excess densities during such flood events. The sediment-gravity-flow-dominated Gilbert-type delta type occurs only in the incised valley fill and is tentatively linked to heightened monsoonal river flood activity during deglaciations.

4.2 Introduction

Sedimentological structures result from both depositional and erosional processes and can be used to interpret palaeo-environmental settings. In the Carboniferous Central Pennine Basin (Fig. 3.1), process-based interpretation of sedimentological structures dates back to the 19th century (Sorby, 1859; Gilligan,

1919), with, for example, cross bedding ("false-" or "drift-bedding") in coarse-grained sandstones of the Millstone Grit Group being explained as the depositional product of uni-directional currents. This led to the early palaeo-environmental interpretation of a deltaic setting fed by a large northerly derived river (Gilligan, 1919; Walker, 1955). Subsequent research has significantly advanced the understanding of the Millstone Grit fluvio-deltaic system (e.g. Holdsworth and Collinson, 1988; Martinsen et al., 1995; Waters and Davies, 2006); the long history of research has also resulted in multiple reinterpretations of sedimentological features over time.

Large-scale foresets are one of the most enigmatic facies in the Central Pennine Basin and can reach up to several tens of metres in height. They are recognised in some of the larger fluvio-deltaic successions: the Lower Kinderscout Grit (e.g. Collinson, 1968; McCabe, 1977; Hampson, 1997), the Roaches-Ashover Grit (Jones, 1980; Jones and Chisholm, 1997), and the Bearing and Warley Wise Grits (Chapter 3; Baines, 1977; Sims, 1988). Initially, Collinson (1968) interpreted such large foresets in the Lower Kinderscout Grit as a Gilbert-type delta (*sensu* Gilbert, 1883; 1890; Bates, 1953). This model was subsequently challenged because the sedimentological complexity and facies association of these deposits was considered unlikely for deltaic deposits. An alternative model of deep distributary delta top channels was proposed in which these large-scale foresets were deposited as large-scale alternate fluvial bars (Fig. 4.1; McCabe, 1975; 1977). The same model was also adopted for the Bearing and Warley Wise Grit (Baines, 1977), the Roaches-Ashover Grit (Jones, 1980; Jones and McCabe, 1980) and is featured in some textbooks (e.g. Reading, 1996; Collinson et al., 2006). A sequence-stratigraphic reinterpretation of the Millstone Grit succession (Martinsen, 1990; 1993; Read, 1991; Maynard, 1992; Church, 1994; Church and Gawthorpe, 1994, 1997; Wignall and Maynard, 1996; Reid, 1996; Hampson et al., 1996, 1999; Davies et al., 1999) also resulted in a reinterpretation of such large-scale foresets as Gilbert-type deltas at the mouth of incised valley fills (Hampson, 1997; Jones and Chisholm, 1997). An in-valley occurrence of these large-scale foresets could explain the relatively narrow belts in which they occur, as well as the stacking of several sets of Gilbert-type deltas, due to increasing accommodation space during sea-level rise (Hampson, 1997; Jones and Chisholm, 1997).

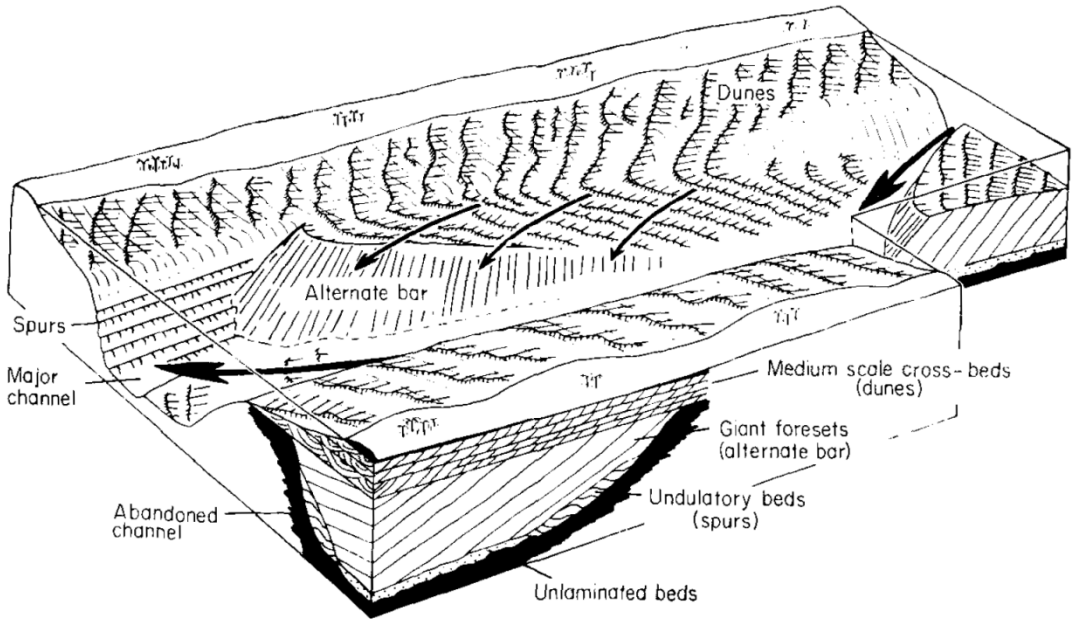

Figure 4.1 Alternate bar model explaining large-scale foresets within 1 – 2 km wide distributary channels (from McCabe, 1977; featured in Reading, 1996; Collinson et al., 2006).

In Chapter 3, studies of the initial infill of the Craven Basin by the Millstone Grit Group during the Pendleian are described. The wide outcrop belt in the Craven Basin (e.g. Fig. 3.2) and the high resolution chronostratigraphic framework in this area (e.g. Fig. 3.4) have allowed for the distinction between two sandstone successions containing contrasting styles of Gilbert-type deltas. In the Bearing Grit, stacked Gilbert-type deltas occur in the Transition Zone of the Craven Basin. These are interpreted as an incised valley fill deposited during sea-level rise (Fig. 3.19a, e). A single set of Gilbert-type deltas at the base of multi-storey channel deposits in the overlying Warley Wise Grit of the Bowland sub-basin is interpreted as the delta front of a progradational succession deposited during sea-level fall (Fig. 3.19a, g). The multi-storey channel deposits probably reflect the subsequent lowstand and early sea-level rise.

The Bearing Grit Gilbert-type deltas are closely associated with facies 6: structureless and crudely-laminated sandstones (e.g. Fig. 3.15; 3.10) and frequently contain small-scale cross beds migrating down-foreset, a phenomenon that is apparently not described in the modern sedimentological literature on deltas. Descriptions of similar structures in the Lower Kinderscout Grit (Collinson, 1968)

predate modern literature on Gilbert-type deltas (e.g. Nemec, 1990), or consider a fluvial origin for these large foresets which strongly influences the inferences regarding depositional processes (McCabe, 1975, 1977; Baines, 1977; Jones, 1980; Jones and McCabe, 1980). This chapter describes these large-scale foreset facies and facies associations in the Bearing and Warley Wise Grit and evaluates the flow processes that resulted in these deposits. Additionally, an attempt is made to link the different Gilbert delta types to climate and sea-level forcing.

4.3 Methods

On the basis of their outcrop characteristics, facies 7: large-scale foresets (Chapter 3) were subdivided into 4 subtypes (A-D). Additionally, facies transitions were recorded and depositional dip measurements were taken on three-dimensional outcrops and corrected for tectonic dip using the Stereonet8 program (Allmendinger et al., 2012; Cardozo and Allmendinger, 2013). Additional measurements were taken from photographs that were oriented dip-perpendicular. Because of the general absence of shale and siltstone-exposures, tectonic dips were mostly estimated from cross-bedded deposits.

A Markov chain analysis was attempted to test whether statistically-significant relationships are present between different Gilbert delta sub-types and associated facies. Differences in the depositional dips for different Gilbert delta sub-types were statistically examined using one-sample Kolmogorov-Smirnov tests (e.g. Chapman McGrew Jr. and Monroe, 1993). Differences in foreset angle of facies types 7C and 7D were used to estimate the critical Shields stress exerted on the foreset surface, and have subsequently been combined with Froude-scaling of experimental data (Kostic et al., 2002; Kostic and Parker, 2003a, 2003b) to relate these Shields stresses to fluvial conditions following the approach of Kostic et al. (2002).

4.4 Results

Four types of Facies 7: large-scale foresets are described in detail. Other facies mentioned in this chapter are described in Chapter 3 and are tabulated in Table 3.1.

4.4.1 Facies descriptions

4.4.1.1 Facies 7 Type A (7A): Concave up Gilbert-type delta foresets

These large-scale foresets have a minimal set height of 5 m (Fig. 4.2; 4.3), occur in fine- to coarse-grained sandstone and contain sparse granules and pebbles. Individual beds are between 0.3 and 1 m thick, with granules and pebbles occurring at the base while foreset beds are otherwise ungraded. Foreset beds are concave up and transition into bioturbated siltstones in the toeset (Fig. 4.3a, b). The angle at the top of foresets reaches up to 23°, while at the base of the foreset angles are approximately 15°. Bioturbated siltstones in the toe of the delta are observed at a depositional angle of 5° (Fig. 4.3c). Generally foreset beds are internally massive but faint laminations, (sub-)parallel to the bed surface have occasionally been observed towards the top of the foreset. Micaceous siltstones and shales are observed between individual foreset beds (Fig. 4.3d), resulting in sharply defined beds.

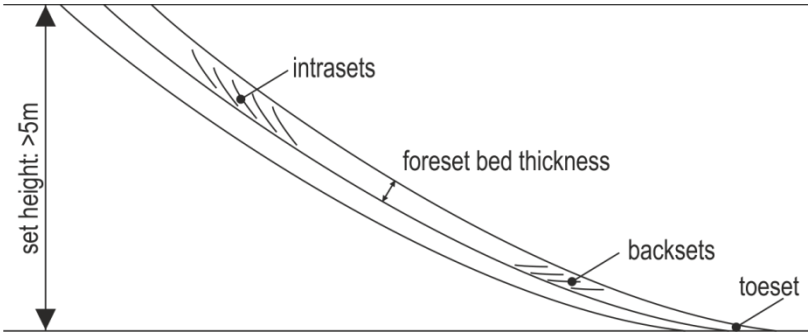

Figure 4.2 Definition sketch indicating terminology used throughout the chapter.

4.4.1.2 Facies 7 Type B (7B): Structureless Gilbert-type delta foresets

These large-scale foresets have a minimal set height of 5 m and typically form in coarse-grained to granular sandstone, with frequent <4 cm pebbles (Fig. 4.4b; c, d). Foresets appear straight in outcrop although fully exposed foresets have not been seen anywhere. Depositional dips range from 10° - 27° suggesting that beds might be concave up over longer distances. Individual foreset beds are internally massive and range from 3 – 20 cm, and generally show poor normal grading. Coarsest sandstones occur in the lower half of the foreset beds. Contacts

between individual foreset beds are made of medium- to coarse-grained sandstone. Where multiple 7B type foreset beds are observed in succession, individual beds are well-defined, resulting from more significant weathering of the finer-grained top of the bed (Fig. 4.4a, c, d). Decimetre-scale structureless intervals that are interbedded with foresets of facies 7C or 7D are also assigned to facies 7B. In these occurrences the fine-grained top of the foreset bed is absent.

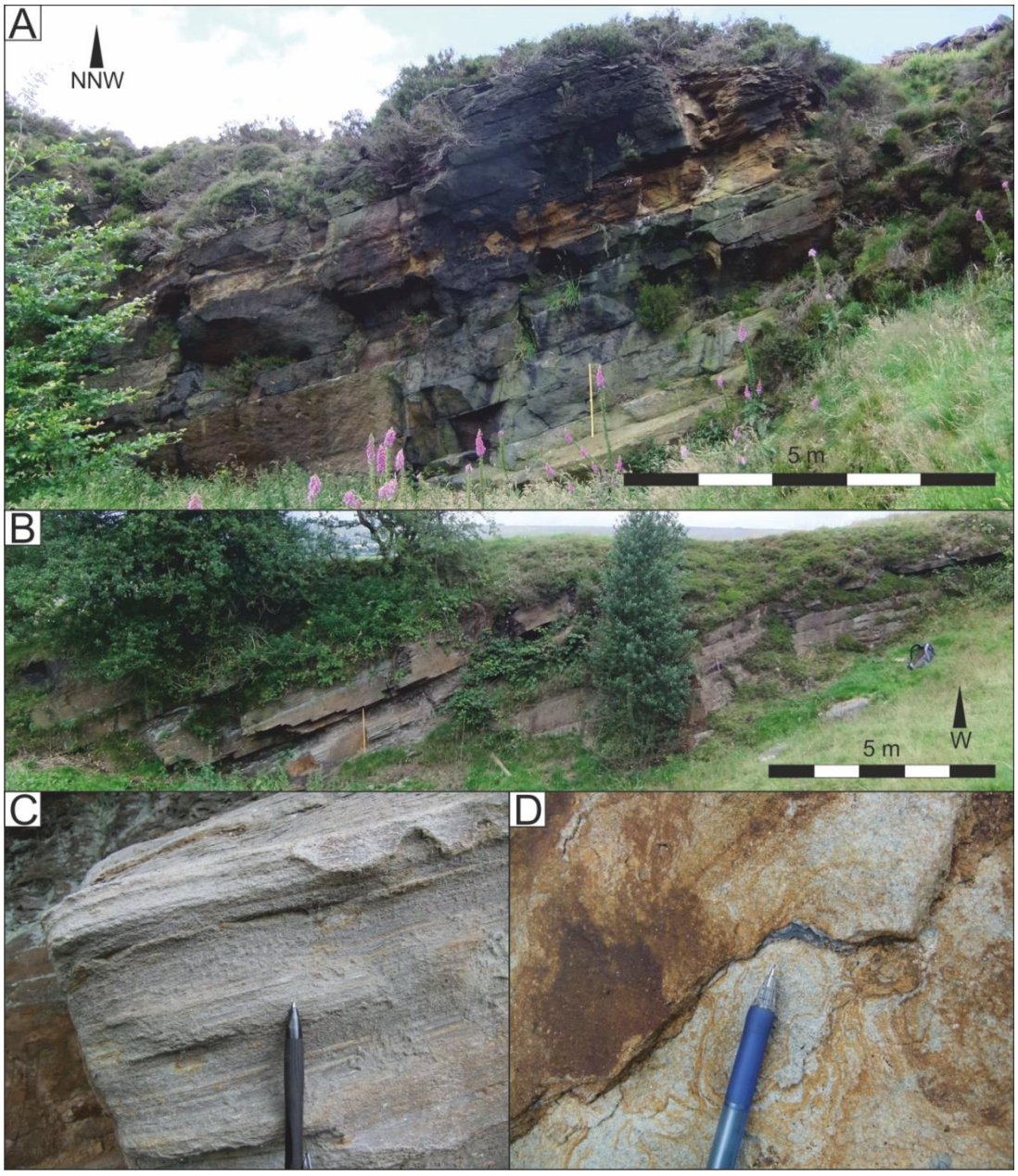

Figure 4.3 (a) Facies 7A: Gilbert-type delta foresets at Noyna Rocks Quarry, tectonic dip is perpendicular to the outcrop. Tectonic dip and depositional angles are listed in Table 4.1. (b) Toeset of siltstone and fine-grained sandstone. (c) Laminated siltstones in toeset with rare bioturbation. (d) Shale and micaceous sandstones in the parting between successive foresets at Faughs Delph Quarry (see Fig.3.13; Table 4.1).

Figure 4.4 (a) Transition from facies 7B at the base of the outcrop to facies 7C above the yellow scale bar. Potter Gap (high) (Table 4.1; see Figs. 3.9; 3.10 for locations). (b) Base of facies 7B foresets. Coarser grained and thicker beds indicating larger grain flows alternated with finer, thin beds. Rolling Gate Crag (Table 4.1, see Fig.3.9 for location) (c, d) Facies 7B foresets cut out by sediment-gravity-flow deposit. Foreset beds contain small pebbles and are internally massive. The recessive intervals are finer-grained bed tops. Location is near Rolling Gate Crag (Table 4.1).

Relative to the 7A-type, 7B-type foresets beds are less concave, substantially coarser grained and thinner, while pebbles occur at higher levels within the bed. In 7A-type foresets, the boundaries between individual beds are formed by shale or silt veneers, whereas in 7B-type foresets these intervals contain cm-scale intervals of medium- to coarse-grained sandstone.

4.4.1.3 Facies 7 Type C (7C): Laminated Gilbert-type delta foresets

These large-scale foresets have a minimal set height of 5 m and typically form in coarse-grained to granular sandstone, with occasional pebbles up to 4 cm in diameter occurring throughout the bed (Fig. 4.5). Individual foreset beds are straight or slightly concave up. Their thickness ranges from several decimetres up to ~2 metres with dips between 11° and 29° (Fig. 4.4a; 4.5b; 4.6a). Internally, these foreset beds are laminated at a cm-scale with slight variations in grain size that define foreset-bed-parallel laminations (Fig. 4.5e, f). Backsets of 0.5 m thickness are observed in a scour-fill near the base of one outcrop within Facies 7C (Fig. 4.5b, c).

Figure 4.5 (next page) (a) Lord's Seat, Barden Fell. Type 7B and 7C foresets are recorded on the left side of the image, and overlain by parallel-laminated sandstones (Facies 9) on the right side of the image. Facies 9 gradually transitions into a massive deposit towards the top (Facies 6). Note that the Facies 9 laminations on the right side of image approximate tectonic dip and were previously interpreted as large-scale foresets (Baines, 1977). (b) Base of succession exposes facies 7B, followed on by facies 7C at ~1 m above the ground surface. Note the erosion surface ~2 m above the yellow scale bar. (c) Opposite view of B, note steep >50° combined depositional/tectonic dip towards the right and the backsets dipping at a shallower angle within the scour that is also observed in B (see Table 4.1 for tectonic and depositional dips). (d) Laminar deposits in the topset succession, tentatively interpreted as upper-flow-regime structures. (e) Map of Barden Fell, indicating outcrop positions on Barden Fell and tectonic dip measurements of the Simonseat Anticline. More comprehensive maps are presented by Hudson (1937) and Baines (1977). (f) Facies 7C erosionally overlain by facies 6 at Potters Gap, Barden Moor (see Fig.3.10c: outcrop 1). (g) Facies 7C at Potters Gap (see Fig.3.10a: outcrop 2).

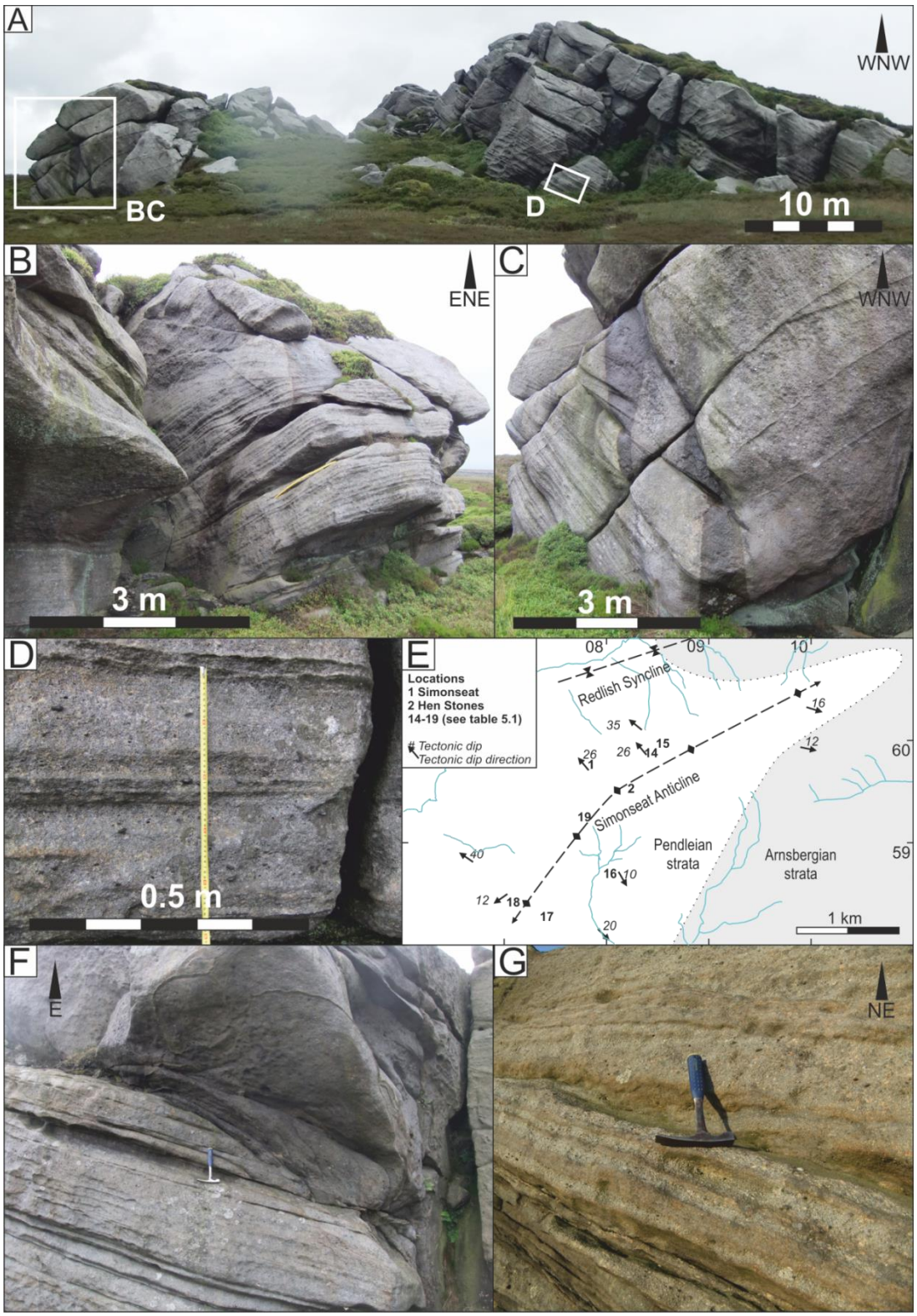

4.4.1.4 Facies 7 Type D (7D): Gilbert-type delta foresets with 'intrasets'

These foresets form in coarse-grained to granular sandstones with occasional <3 cm pebbles. Individual foreset laminae appear straight, and individual foreset beds range from several decimetres up to 2 m in thickness, measured perpendicular

to the foreset angle (Fig. 4.6). Internally, foreset beds typically show bed-parallel laminations at ~5 - 10 cm-scale, with deposition dips of 9° to 23° (Fig. 4.6a). Between these bed-parallel laminations, low to high angle cross laminations occur, dipping obliquely or directly down the foreset (Fig. 4.6b, c, d). These structures were previously termed ‘intrasets’ in the Lower Kinderscout Grit (Collinson, 1968). Frequently the topsets, foresets and toesets of these ’intrasets’ are preserved (Fig. 4.6d). The foreset angle of these intrasets ranges from 19° - 35° depositional dip. Intrasets occasionally show a sigmoidal or sheared shape (Fig. 4.6d). The thickness of individual intrasets can range up to 30 cm but typically ranges from 5 - 10 cm. Transitional forms between Facies 7C and 7D also exist, in which low angle to near-parallel laminations downlap on the foreset surface (Fig. 4.6e, f).

4.4.2 Facies associations

4.4.2.1 Facies association 3: Gilbert-type deltas with fine-grained toesets

Facies 7A is observed in both the Bearing and Warley Wise Grit. In the Warley Wise Grit it occurs at Hardacre Quarry, Farnhill Moor (Fig. 3.15b; Table 4.1), Noyna Rocks Quarry, Foulridge (Fig. 4.3a-c; Table 4.1), and Faugh Delph Quarry, Newchurch in Pendle (Fig. 3.13; Table 4.1). In all these occurrences, the succession is overlain by cross-bedded sandstones (Facies 8). The overlying sandstones are typically coarser-grained than the foreset deposits, suggesting that these deposits are not deposited coevally, but represent later channel deposits that erosionally overlie the foresets (Chapter 3). At Noyna Rocks Quarry, the toeset contains fine-grained sandstones and bioturbated siltstones (Fig. 4.3c). At Faughs Delph Quarry, fine-grained intervals between successive foreset beds can be observed (Fig. 4.3d).

In the Bearing Grit, 7A foresets occur at Whelpstone Crag, Bowland High and at Pen-y-ghent, Askrigg Block (Fig. 3.2; 3.7; Table 4.1). At both locations, these foresets are overlain by cross-bedded strata. At Pen-y-ghent, they are underlain by deposits from a lower cross-bedded channel storey (Fig. 3.7). At Whelpstone Crag the underlying interval is not exposed.

Figure 4.6 (a) Alternation of facies 7B, 7C and 7D at Unnamed Crag 2 (see Table 4.1 for tectonic and depositional dips). Facies 7D occurs in the shallowly dipping lower half of the outcrop, and facies 7C occurs in the steeper upper half. The structureless intervals are referred to as Facies 7B. (b) Close up of intrasets in outcrop depicted in (a). (c) Facies 7D, with very low angle foresets and strongly-developed intrasets. Unnamed Crag 4 (low) (Table 4.1). (d) Close up of intrasets in Unnamed Crag 4, indicating sheared and sigmoidal intrasets. (e, f) Opposite sides of Unnamed Crag 4 (high) showing a transitional form between facies 7C and 7D. Note apparent shallow dipping backsets in (e), which are steeply dipping foresets in (f).

4.4.2.2 Facies association 4: Gilbert-type delta with structureless sandstones in toeset

Facies 7B, 7C and 7D occur in the Bearing Grit and are frequently observed in close association with each other, with cross-bedded sandstones (Facies 8), structureless and crudely-laminated sandstones (Facies 6; Fig. 3.15 c-e) and parallel-laminated sandstones (Facies 9: e.g. Fig. 3.10). Frequently, the base of the succession is formed by structureless or crudely-laminated sandstones ranging up to several metres in thickness. These deposits are interpreted as sediment-gravity-flow deposits that occasionally cut out 7B, 7C, 7D type deposits (Fig. 4.4c, e; 4.5f; 4.6c). Type 7B deposits are frequently observed towards the base of individual outcrops (Fig. 4.4a; 4.5b). Overlying foreset beds more frequently belong to facies type 7C, interbedded with type 7B or 7D deposits (e.g. Fig. 4.4a; 4.5b, c; 4.6a).

At Simon's Seat, the base of the outcrop exposes cross-bedded sandstones (facies 8) dipping at ~26° tectonic dip towards the northwest (Fig. 4.7a; 4.5e). This succession is overlain by an interval of crudely cross-bedded sandstones that transition into a sediment-gravity-flow deposit (Fig. 4.5e; 4.7c, e).

At Lord's Seat, type 7B large-scale foresets are exposed at the base of the outcrop (Fig. 4.5e; Table 4.1). When correcting for tectonic dip obtained at Simon's Seat, these dip at ~20° and are overlain by a thick succession of type 7C foresets dipping at ~25° (Fig. 4.5a, b, c; Table 4.1). Within these foresets, backsets occur in a ~0.5 metre deep scour (Fig. 4.5b, c). This succession is overlain by sub-horizontal, dm-scale, planar-laminated, coarse- to very coarse-grained sandstones, containing abundant pebbles that are separated by thin intervals of medium-coarse-grained sandstones (Fig. 4.5d). This succession becomes structureless towards the top of the outcrop and transitions into a metre-scale sediment-gravity-flow deposit.

At Unnamed Crag 5 (Fig. 4.5e; 4.8; Table 4.1), the top of Type 7C foresets is exposed, dipping at approximately ~17-19° followed on by Type 7D foresets dipping at ~16 -18° (Fig. 4.8c, g). These deposits are overlain by the sediment-gravity-flow deposits that truncate the top of the foresets (Fig. 4.8a, c). Subsequently, these beds are deposited on the delta front with a similar depositional dip (up to 13°) as the foresets (Fig. 4.8a). A thin interval overlying the sediment-gravity-flow deposit is unexposed after which progradation continues with Type 7B foresets, dipping at 23 -27° (Fig. 4.8a, e). This succession is overlain by a

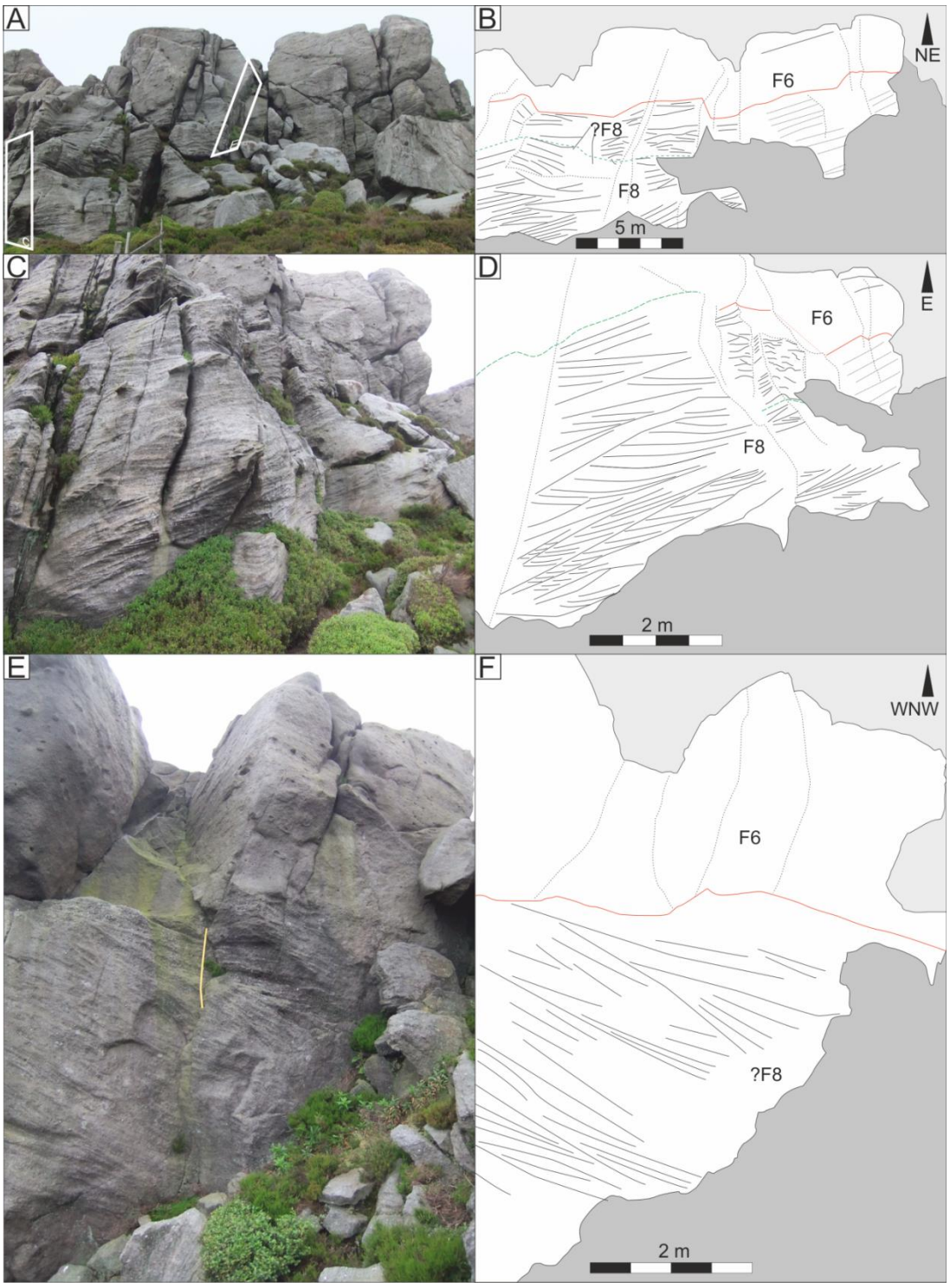

Figure 4.7 (a, b) Overview of Simon's Seat, indicating cross beds (facies 8) at the base of the outcrop, overlain by a crudely cross-bedded interval and sediment-gravity-flow deposits (facies 6), see Fig. 4.5e for location. Green line indicates base of crudely cross-bedded interval, red line indicates base of sediment-gravity-flow deposit (c, d) Close up of cross beds. Note steep tectonic dip of 26°. (e, f) Close-up of crudely-cross-bedded interval and overlying sediment-gravity-flow deposits.

structureless pebbly sediment-gravity-flow deposit (Fig. 4.8e), indicating a repeated alternation between deposition of foresets and sediment-gravity-flow deposits at the delta front.

Similar facies alternations are observed at Potter Gap, at Barden Moor (Fig. 3.10). At a low exposure (Fig. 3.10a, b: outcrop 1), Type 7C foresets, dipping at ~25° are erosionally overlain by several sediment-gravity-flow deposits (Fig. 4.5f) on top of which a thin unexposed interval occurs (Fig. 3.10a). A higher exposure at Potter Gap (Fig. 3.10b: outcrop 2; Fig. 4.4a) records the transition from Type 7B to 7C foresets, corresponding to a substantial increase in foreset angle from 15° at the base of the succession in type 7B to approximately 25° at the top of the succession in Type 7C foresets (Table 4.1). Laterally, this succession is replaced by type 7D deposits, overlain by sediment-gravity-flow deposits (no accurate dip obtained) (Fig. 3.10b: outcrop 3, the same outcrop is shown in Fig. 3.15e).

Unnamed Crag 2 (Table 4.1) is located south of the Obelisk (corresponding to outcrop 4 in Fig. 3.10b). This succession starts within one set of type 7C foresets, erosionally overlain by another set of 7C foresets, both at a relatively shallow dips of ~22°. Successive foresets laminae gradually decrease in angle to ~16° and develop Type 7D foresets with intrasets dipping obliquely down the foreset. Metre-scale intervals of 7D-type foresets are alternated with dm-scale massive intervals of type 7B foresets (Fig. 4.6a, b). Subsequently, the succession steepens to an angle of ~28° and transitions to Type 7C again (Fig. 4.6a). This interval is overlain by cross-bedded sandstones (Fig. 3.10e, f).

Figure 4.8 (next page) (a, b) Overview of Unnamed Crag 5 (Table 4.1; Fig. 4.5e). Foresets occur on the left, and the right side of the image. The occurrences are separated by a major sediment-gravity-flow deposit. (c, d) Close up showing facies 7C, followed by 7D, of which the tops are truncated by a sediment-gravity-flow deposit. Towards the right, the sediment-gravity-flows follow the foreset surface and deposits under relatively steep dips in the delta front (see also a, b). (e, f) Close up of the right side of the figure (a , b): facies 7B, overlain by another, more pebbly and structureless sediment-gravity-flow deposit. (g, h) Close up of the erosion surface in (c, d). Note that the sediment-gravity-flow deposits continue down-foreset in the right hand side of the picture.

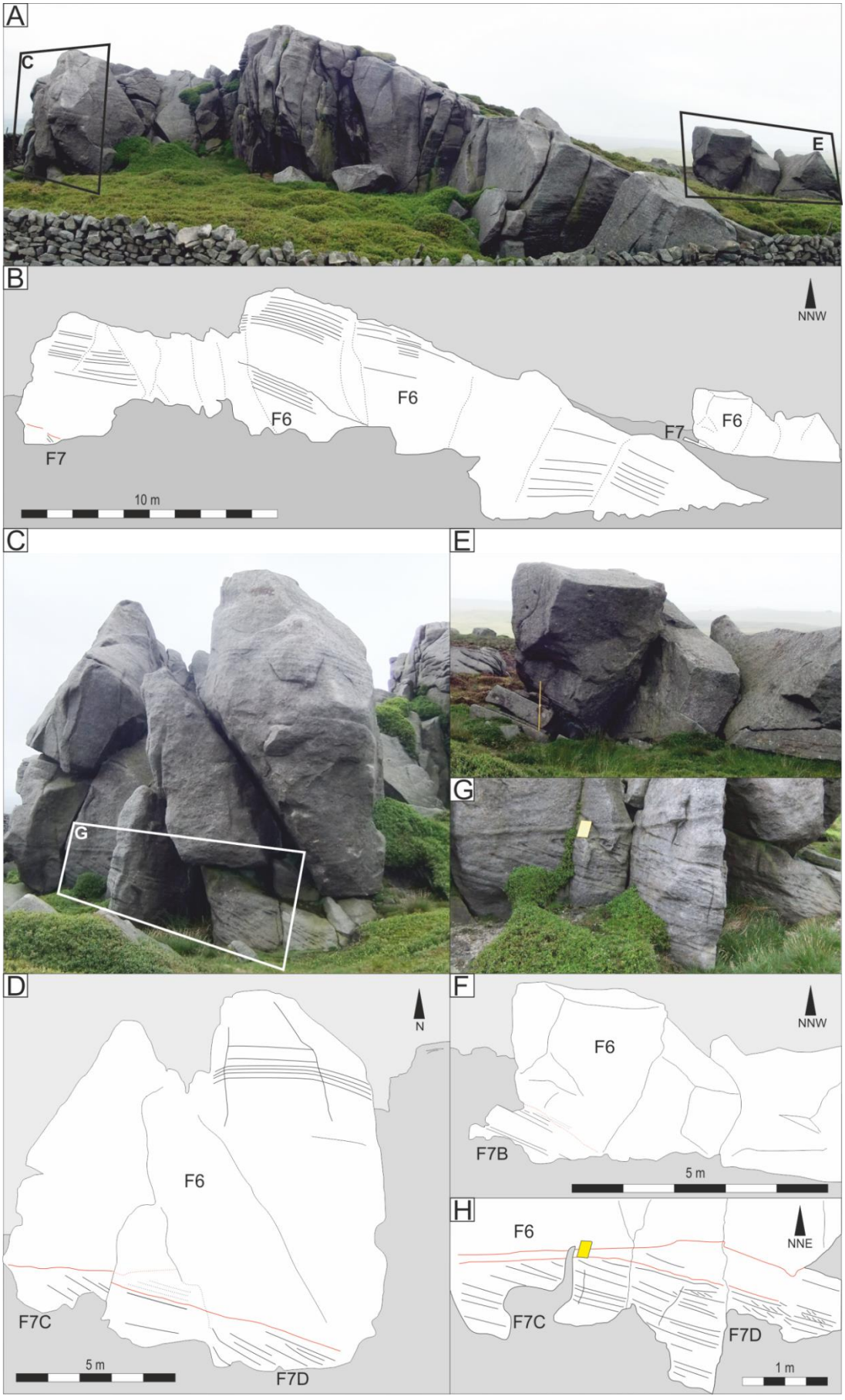
A
C
E
B
NNW
F6
F6
F6
F7
F7
F7
10 m
C
E
G
G
D
N
F6
F7C
5 m
F7D
F
NNW
F6
F7B
5 m
H
F6
NNE
F7C
F7D
1 m

At Unnamed Crag 4 (low), Type 7B foresets, dipping at ~15 -20° occur at the base of the succession. They are overlain by Type 7D foresets with strongly developed intrasets (Fig. 4.6c; Table 4.1). On the northern side of the exposure, this succession is overlain by Type 7C foresets. Traced southward the entire foreset is cut out by a ~7 m thick sediment-gravity-flow deposit with sub-horizontal laminations that become more prominent upwards.

At the SW flank of Barden Moor, several large-scale outcrops occur in which structureless and faintly structured sandstones are observed (Fig. 4.9). This succession is overlain by an unexposed, presumably fine-grained interval, on top of which Gilbert-type deltas occur (e.g. Unnamed Crag 4 (high), and High Bark (Table 4.1). In the lower succession, both faintly-laminated and structureless sediment-gravity-flow deposits are observed. At Rylstone Cross, these deposits are accessible and show an amalgamation of numerous, metre-scale, fining-upward deposits. Some beds show shale clast imbrication indicating E to SE flow directions, which is similar to that of the Gilbert-type deltas (Fig. 4.9e). Towards the top of the outcrop at Rylstone Cross, the longitudinal profile of a large scour fill is recognised in two parallel-orientated outcrops (Fig. 4.9a, c, e). Downdip of the scour, the bed is faintly laminated and contains abundant, aligned pebbles (Fig. 4.9a, g). The backwall of the scour dips steeply upstream and is internally onlapped by shallower dipping laminations that transition updip into a very pebbly, structureless, dewatered interval (Fig. 4.9e). Backsets form the main scour fill and dip at ~15 - 23° to the northwest. The overlying succession shows faint laminations and gradually fines upward to coarse-grained sandstone (Fig. 4.9c, d).

Figure 4.9 (next page) (a, b) Delta-toe sediment-gravity-flow deposits at Rylstone Cross (see Fig.3.9 for location). (c, d) Parallel outcrop to exposure in (a, b). Note the occurrence of intrasets on the left side of the image and the transition into wavy bedforms towards the right downdip of the backsets, interpreted as upper-flow-regime deposits. (e, f) Close up of scour pool margin in (a, b). Note the steep contact, which is characterised by a strong grain-size change and different angle laminations. Inside the scour, laminations fade into a dewatered zone. (g) Organisation of pebbles near the base of the bed in small trains downdip of the scour, similar to e.g. S1 structures (Lowe, 1982).

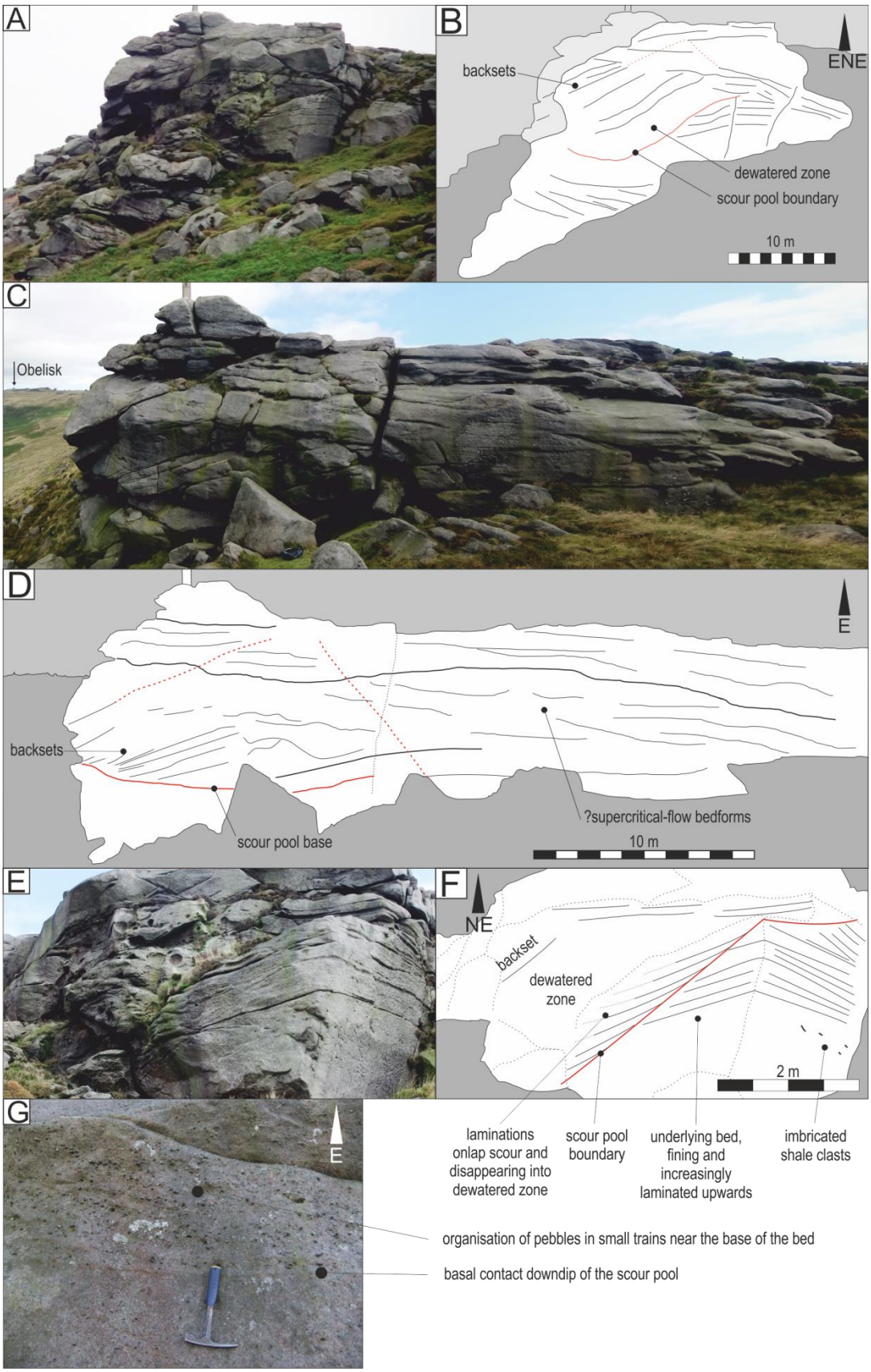
A
B
backsets
ENE
dewatered zone
scour pool boundary
10 m
C
Obelisk
D
E
backsets
scour pool base
?supercritical-flow bedforms
10 m
E
F
NE
backset
dewatered zone
2 m
G
E
laminations onlap scour and disappearing into dewatered zone
scour pool boundary
underlying bed, fining and increasingly laminated upwards
imbricated shale clasts
organisation of pebbles in small trains near the base of the bed
basal contact downdip of the scour pool

#	Name	Grid Ref	Tect. Dip	Facies above	Facies below	Facies	Depositional dip	Facies order
1	Pen-y-ghent (south)	[38364 47304]	~0	F8	F8 (p)	7A	17 18 17 18 16 20 14 15	7A>8
2	Rolling Gate Crag (north)Barden Moor	[40013 46029]	130/8 E	F8	F6	7B	19 18 19 19 20	7B>7C>8
						7C	20 22 22 23 20 21	
3	Rolling Gate Crag (South), Barden Moor	[40000 46009]	130/8 E	-	-	7B	14 11 14	7B>7D,B
						7D	9 9 12 13 / *25 24 30 21 35 33 24 23*	
4	Unnamed Crag 1, (south of The Crags)	[39956 45908]	120/11 E	F8	-	7C	20 21	-
5	Obelisk, Barden Moor	[39930 45884]	165/7 E	F8	F6 & toeset of 7B	7B	26 26	7B>6
						7C	25 23 23	7B>7C
6	Unnamed Crag 2 (south of Obelisk)	[39925 45869]	165/7 E	F8	-	7B	21 25	7C>7D,B,C
						7C	22 23 26 26 25 26 28 29 29	
						7D	10 14 17 17 16 18 / *24 21 23 32 28 28*	
7	Unnamed Crag 3 (south of Obelisk)	[39919 45863]	165/7 E (?)	-	-	7C	23 24 23	7D>7C
						7D	20 16 17 17 / *21*	
8	Potter Gap (low), Barden Moor	[39909 45851]	165/7 E (?)	F6	Unexposed: below F6	7C	27 26 24	7C>6
9	Potter Gap (high), Barden Moor	[39911 45846]	165/7 E (?)	F6		7B	15 15 18 22 22 22	7B>7C
						7C	24 23 25 25 25 24	
10	Unnamed Crag 4 (low) (south of Potter Gap)	[39861 45780]	100/12 E	F6	Unexposed, below F6	7B	15 15 20 19 18 19 19 18 18 18	7B>7C>7D>6 (north)
						7C	21 18 18 (north) 11 (south)	
						7D	17 19 23 21 / *32 32 31 32 30 33 32 (north)* 20 20 20 18 / *34 34 33 (south)*	7C>7D>6 (south)
11	Unnamed Crag 4 (high)	[39897 45807]	100/12 E	F8	Unexposed, below F6	7B	19 20	7B>7C>7D
						7C	17 17 20 20 18 20	
						7D	12 15 / *25 26 25 34*	7B>7D
12	High Bark, Barden Moor	[39826 45728]	90/20 E	F9	Unexposed, below F6	7C	17 18 12	-
13	Quarry at High Crag, Eastby	[40305 45517]	10/14 N	F8	Sub-horizontal structureless tabular beds with rippled bed tops	7B	12 10	-

#	Name	Grid Ref	Tect. Dip	Facies above	Facies below	Facies	Depositional dip	Facies order
14	Lord's Seat, Barden Fell	[40841 45988]	320/26 N (based on Simon-seat)	F9>F6	-	7B	19 21 18	7B>7C >6
						7C	25 25 23 27 23 26 26 28 (backsets 5 7 4)	
						7C/6	2 4 4 4 5 2	
15	Unnamed Crag 5, (west of Lord's Seat)	[40848 45996]	320/26 N (based on Simon-seat)	F6	-	7B	23 26 27	7C>7D> 7C/6 (west) 7B>6 (east)
						7C	17 19 19	
						7D	16 18 / *28 29*	
						6	11 9 13	
16	Long Crag, Barden Fell	[40827 45886]	150/10 E	-	Unexposed, below F6	7B	21 18 16 24 20	7B>7D,B >7C
						7C	25 26 26 20 23 26 25 21 23 22 16 23	
						7D	9 15 11 9 / *22 21 19 22*	
17	Carncliff Crag, Barden Fell	[40723 45838]		-	-	7C	26	
18	Earl Seat, Barden Fell	[40702 45849]	~0	F8	Unexposed, below F6	7C	18	
19	Trunckle Crag, Barden Fell	[40777 45931]	?	-	-	7C	-	
21	Whelpstone Crag (east), Holden Moor	[37640 45947]	95/7 E	F8	-	7A	17 17 13 12 12 17 7	
22	Hardacre Quarry, Farnhill Moor	[40088 44682]	100/7 E	F8	Unexposed, laterally interbedded siltstones and fine-grained sandstones	7A	18 17 23 17 19 21 18 19 15 9 10	
23	Noyna Rocks Quarry, Foulridge	[38965 44264]	180/15 S	F8	Siltstones	7A	18 16 18 20 21 18 22 16 15 15 19	
24	Faughs Delph Quarry, Newchurch in Pendle	[38199 43922]	145/40 S	F8	-	7A	21 16 15 21 16 8 11 12 10 12 13 15 17	

Table 4.1 Exposures at which detailed measurements on foreset dip and facies succession are obtained for Markov Chain analysis. Depositional dip measurements in italic font refer to dip of intrasets. Facies transitions indicated by '>' are clear transitions, intervals denoted by a comma show multiple alternations between different facies types.

4.4.3 Statistical analysis of facies transitions

A Markov chain analysis was attempted to test whether statistically significant relationships are present between different Gilbert delta sub-types. However, the dataset (54 vertical transitions between 6 facies) is too limited (Fig. 4.10); a minimum of ~180 transitions is recommended for a statistically valid analysis between 6 facies (Swan and Sandilands, 1995). Although not validated by statistical analysis, fieldwork observations suggest several common transitions between different facies based on the facies transitions in outcrops listed in Table 3.1 and in additional minor outcrops on Barden Moor and Barden Fell:

- Type 7A foresets are overlain by cross-bedded sandstones and transition into a fine-grained toeset (e.g. Fig. 3.13; 3.15b). These 7A foresets occur at separate locations from 7B, 7C and 7D type foresets and no sediment-gravity-flow deposits are associated with facies 7A.
- Type 7B, 7C, 7D foresets occur together and are closely associated with sediment-gravity-flow deposits: sediment-gravity-flow deposits can truncate the foreset top, overlie the foreset, and occur downsteam of the foreset in the toeset succession (e.g. Fig. 3.10; 4.4c, d; 4.6c; 4.8). Cross-bedded sandstones can overlie these foresets as well (e.g. Fig. 3.10).
- Successive 7B Type foreset beds, separated by finer-grained caps are only observed near the base of outcrops (Fig. 4.4c, d). At higher positions within individual outcrops, type 7C or 7D foresets are more common. The latter are coarse grained throughout, which might make them less prone to weathering and favours their exposure in natural outcrops (Fig. 4.4a).
- Structureless intervals, assigned to facies 7B occur interbedded with facies 7C and 7D (Fig. 4.6a).
- Type 7C foresets generally occur at higher angle than Type 7D foresets when both are exposed in the same outcrop (Fig. 4.6a).
- Sediment-gravity-flow deposits record events that have flowed down the foreset, in which case the outcrops record the actual shoreline position at time of deposition. Foresets underlying these sediment-gravity-flow deposits generally consist of Type 7C or 7D deposits. (e.g. Fig. 4.6c; 4.8g)

- Sediment-gravity-flow deposits are commonly overlain by further sediment-gravity-flow deposits or an unexposed interval after which foreset deposition resumes (e.g. Fig. 3.10; 4.8).

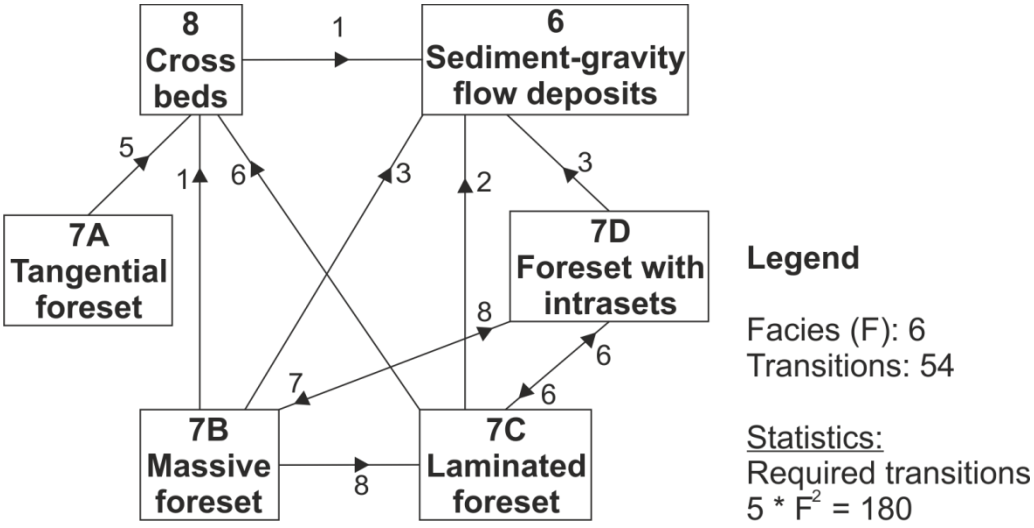

Figure 4.10 Directly exposed transitions between different facies for which a Markov chain analysis was attempted. A strong relation between facies 7B, 7C, 7D foresets and facies 6 sediment-gravity-flow deposits is apparent.

4.4.4: Statistical analysis of depositional dip

Detailed measurements of foreset dip for facies 7A, 7B, 7C and 7D, indicate significant differences (Table 4.1; Fig. 4.11a). Relatively shallow dips occur in Facies 7A (mean: 16, std: 3.7) and Facies 7D (mean: 15.6, std: 3.7). Intermediate dips occur in facies 7B (mean: 18.9, std: 3.7). Steep dips occur in facies 7C (mean: 22.5, std: 3.7) and in the intrasets of facies 7D (mean: 27.6, std: 4.9) (Fig. 4.11a).

The form of the distribution of the range of foreset dips is assessed using a one-sample Kolmogorov-Smirnov test (K-S test) (Fig. 4.11b; Chapman McGrew Jr. and Monroe, 1993) to test whether foreset types are centred on a specific dip-range. The K-S test serves as a goodness-of-fit test and compares the Cumulative Distribution Function (CDF) of the dataset with a standard normal CDF with the same mean and standard deviation as the sample set (Fig. 4.11b). The null hypothesis (h_0) assumes a standard normal distribution, while the alternative hypothesis (h_1) rejects this assumption at a 0.05 significance interval. The null

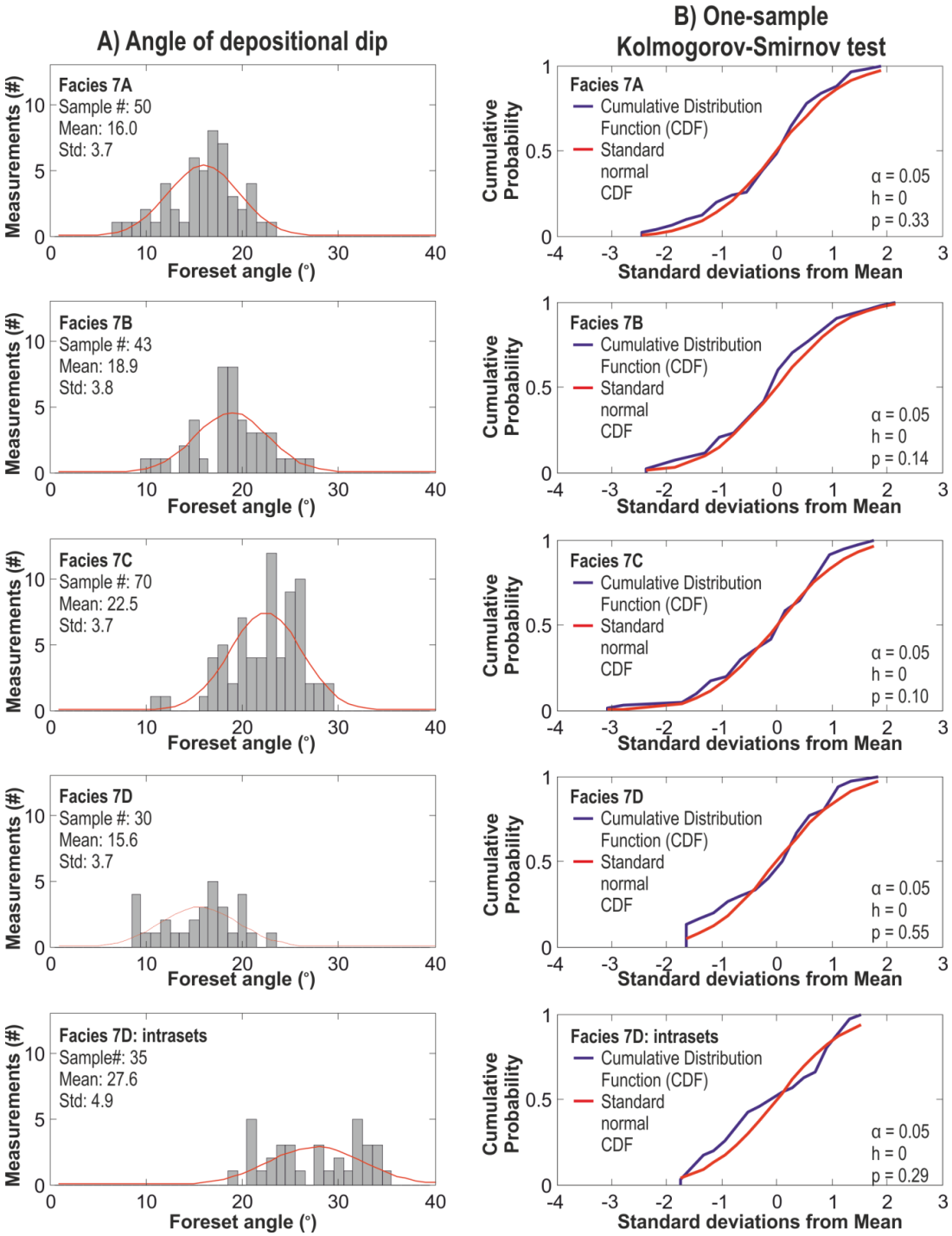

Figure 4.11 (a) Statistical analysis of depositional dip in facies 7A-D, and intrasets within 7D, (see table 4.1). (b) One-sample K-S tests, 'a' indicates confidence interval, 'h' indicates whether H_0 or H_1 is accepted, and 'p' indicates probability (see text for further discussion).

hypothesis could not be rejected at this significance interval for any of the facies, although the small probability value in facies 7B and 7C cast doubt on the validity of the null hypothesis. For example, with a 0.14 significance interval the null-hypothesis would be rejected for facies 7B (Fig. 4.11b).

A visual comparison of the CDF of facies 7A, 7B and 7C suggest a relatively good agreement with the standard normal CDF, implying that these facies probably correspond to a specific range in depositional dip. The CDF of facies 7D and facies 7D: intrasets however strongly differs from a standard normal CDF, which suggests that the distribution is not associated with a specific dip angle (Fig. 4.11b). It can occur on a wide range of relatively shallow dips for facies 7D and a wide range of relatively steep angles for the intrasets in facies 7D (Fig. 4.11a). The reason that the null hypothesis is not rejected is probably related to the small sample size providing, unreliable test results (Table 4.1; Fig. 4.11a).

4.5 Discussion

4.5.1 Facies interpretation: delta front flow processes

4.5.1.1 Facies 7, Type A (7A): Concave up Gilbert-type delta foresets

Facies 7A is interpreted as a Gilbert-delta foreset in which sediments appear to have been deposited predominantly from suspension settling resulting in a gradual transition from sand-grade foreset to silt-grade bottomset (Fig. 4.3; 4.12a). Gilbert-type deltas generally form when sandy to gravelly, fluvio-deltaic channels drain into a relatively deep body of standing water (e.g. Bates, 1953; Leeder, 1999). Homopycnal conditions result in a rapid deceleration of an inertia-dominated jet at the channel mouth, resulting in deposition (e.g. Leeder, 1999). In this case, a significant part of the sediment appears to have been deposited from suspension settling, which corresponds with the relatively fine-grained nature of these deposits and results in foresets at lower-than-repose angles. Towards the top of some individual foresets, faint foreset-parallel laminations are observed. These indicate a minor contribution of bed load transport on the steepest parts of these foresets, probably resulting from grain flows (Fig. 4.12a).

The occurrence of (bioturbated) fine-grained sediments in the toeset, and between individual foresets indicates relatively low rates of deposition when compared to the other large-scale foreset facies (Fig. 4.3c, d).

4.5.1.2 Facies 7, Type B (7B): Structureless Gilbert-type delta foresets

Facies 7B consists of coarse- to very coarse-grained, structureless, poorly sorted foresets (Fig. 4.4, 4.12b). This facies probably result from grain-flow avalanches on the Gilbert-type foreset. This suggests that the delta is characterised by bedload sediment transport that is primarily deposited at the top of foresets, leading to oversteepening and collapse of the foreset, triggering grain-flow avalanches. This depositional model is consistent with the coarse-grained to pebbly nature of these sandstones that in fluvio-deltaic channels is probably transported as bedload, the relatively thin foreset-bed thickness indicating that only minor volumes are associated with individual collapses, and the occurrence of successive facies 7B-type foresets indicating repetitive oversteepening and collapse (Nemec, 1990). The medium- to coarse-grained sandstones separating individual 7B foreset beds might reflect the tops of grain flow-avalanches but could also reflect a minor contribution of suspension settling between successive foreset collapses (Fig. 12b).

Figure 4.12 (next page) Process interpretation (a) Facies 7A: Suspension-settling dominated delta foresets, which most likely occurs during homopycnal conditions. (b) Facies 7B: Grain-flow dominated delta foresets, which indicate a larger bed load component than facies 7A, but do not require higher flow velocities. (c) Facies 7C, indicating traction on the foreset reducing the angle of repose. Traction is related to weak hyperpycnal currents exerting a slight shear stress on the foreset. (d) Facies 7D, foresets containing intrasets suggesting a hyperpycnal current of variable strength. The relatively low angle foresets suggest higher shear stresses than in facies 7C. (e) Facies 6 sediment-gravity-flow deposition, which probably indicate higher flow regimes, and stronger hyperpycnal currents than facies 7D. Strength of hyperpycnal currents in (c – e) is visualised by their thickness.

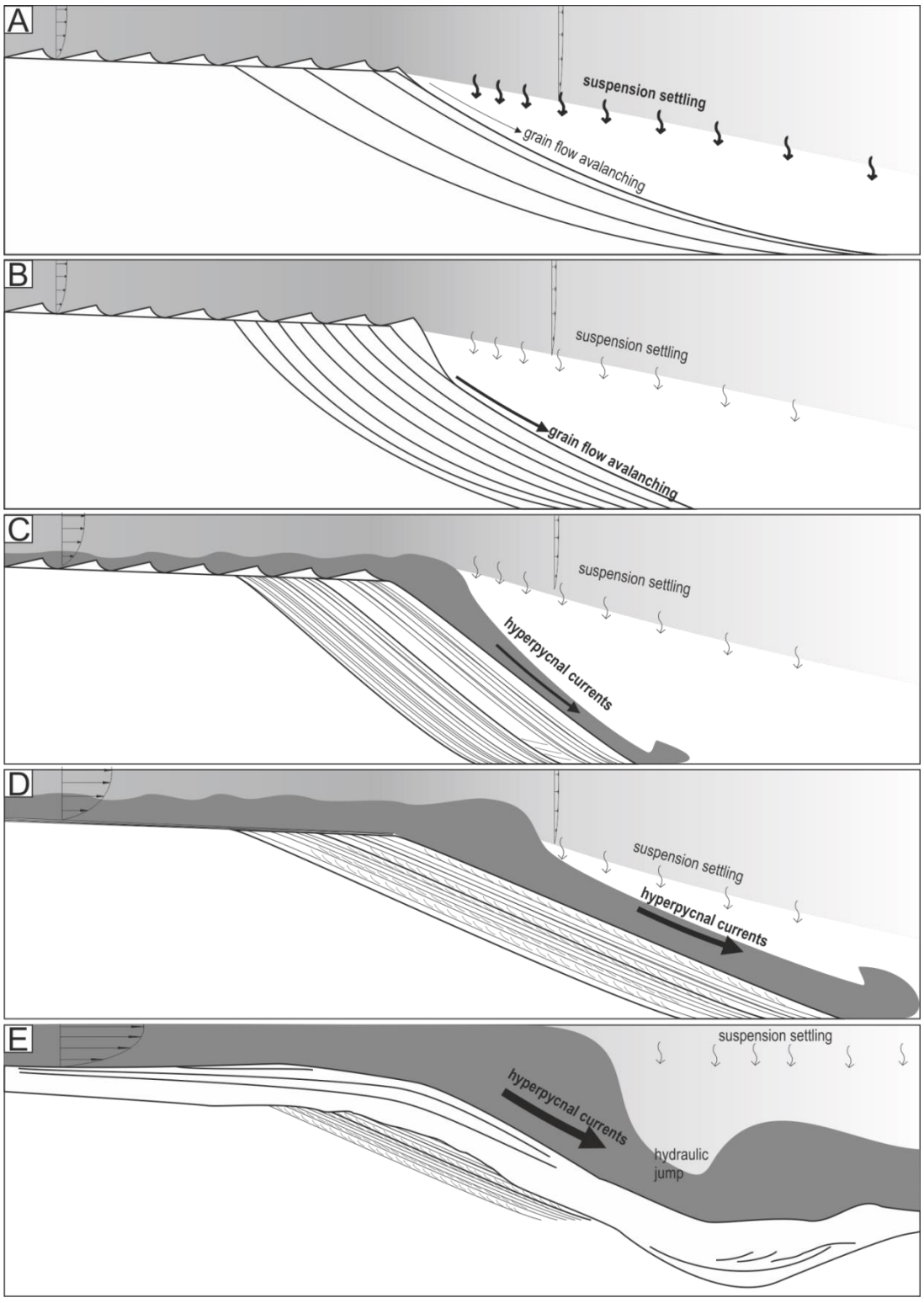

4.5.1.3 Facies 7, Type C (7C): Laminated Gilbert-type delta foresets

Facies 7C consists of internally-laminated foresets, deposited at steep angles (Fig. 4.5; 4.12c). The thickness of laminated foreset beds makes deposition from discrete flow events, such as proposed for Facies 7B, unlikely. Because of the

different range in depositional dip in Facies 7B and 7C, and the close association of these deposits with Facies 7D, the presence of a weak traction current exerting a shear stress on the foreset surface is considered likely (Fig. 4.12c; Table 4.2). In this case, shear stress would provide a continuous impetus for a thin layer of sediment transport on the foreset. Similar to sediment transport on a sub-horizontal surface, coarsest sand grains are probably least affected by the exerted shear stress and will be least mobile, resulting in their deposition near the base of the laminae, providing a sorting mechanism that could result in the observed laminations. Such a gradual process over a longer period can explain both the internal laminations as well as the metre-scale thickness of the individual foreset beds.

Backsets are observed near the base of Type 7C foresets at Lord's Seat (Fig. 4.5b, c). Backsets form when a supercritical flow decelerates and becomes subcritical via a hydraulic jump, which typically occurs at a reduction in the slope, or another disturbance of the flow that reduces its velocity. The hydraulic jump causes rapid sedimentation directly downstream of the position of the hydraulic jump, shifting its position upstream, which is recorded by the formation of backsets (Massari, 1996; Nemec, 1990, Postma and Roep, 1985). The formation of backsets (Fig. 4.5c; 4.12c) thus suggests that supercritical density currents override these foresets and decelerate near their base.

4.5.1.4 Facies 7, Type D (7D): Gilbert-type delta foresets with 'intrasets'

In facies 7D, thick foreset beds occur at relatively low angle in comparison with facies 7B and 7C (Fig. 4.12). These beds are internally laminated, and contain small cross sets termed 'intrasets' between successive laminations (Collinson, 1968). Frequently a toeset, foreset and topset are preserved, suggesting that the full small-scale bedform is preserved (Fig. 4.6). Full preservation implies that these structures do not resemble a truncated, more steeply dipping foreset (e.g. Facies 7C) but are small superimposed structures on the major foreset surfaces that build up (obliquely) downward.

Collinson (1968) proposes that a jet exiting the channel could result in a separation vortex such as occurs during the formation of dunes (Collinson, 1970). If the separation vortex reaches to the base of the foreset this would result in the formation of updip-directed cross bedding similar to countercurrent ripples

(Collinson, 1970). If the vortex is only present near the top of the foreset, downward-oriented intrasets are thought to form. During periods of high flow the separation vortex would disappear due to plunging of the river outflow (hyperpycnal), reducing the foreset angle (Collinson, 1968).

The interpretation of updip-oriented foresets as countercurrent ripples on dunes is considered unlikely because it requires an extremely strong separation vortex to transport coarse-grained to granular sand onto a foreset slope of such height. Formation of backsets, as described above, is a more likely process for these structures. The occurrence of downdip-oriented intrasets is enigmatic, and apart from Collinson (1968) no interpretations for such structures within Gilbert-type deltas are known. However this interpretation is considered unlikely: the re-attachment of the flow to the foreset below a small separation vortex impinging high on the foreset slope would require excess density, while inference of a separation vortex itself suggests a high velocity jet exiting the channel mouth under homo- or hypopycnal conditions.

It is here considered that the intrasets form in response to a variable shear stress exerted by hyperpycnal current (Fig. 4.13) that is stronger than that responsible for facies 7C because of the lower foreset angle in facies 7D (Fig. 4.11, Table 4.2). Subtle variations in the strength of the hyperpycnal outflow are common (Best et al., 2005; Alexander and Mulder, 2002; Mulder et al., 2003; Lamb and Mohrig, 2009; Lamb et al., 2010) and the resultant variability of the shear stress might provide the possibility for small-scale sets to develop (Fig. 4.13). Periods of increased shear strength will reduce the angle of repose of the major foreset surfaces, creating space for a downdip thickening intraset (Fig. 4.13c, 1). A further increase might result in ‘washed-out’ intraset structures (Fig. 4.13c, 2), or structureless intervals (Fig. 4.13c, 3). Subsequent periods of lower shear stress would result in a steeper angle of repose for the major foreset surfaces, resulting in a downdip thinning intraset (Fig. 4.13c, 4). Oblique downward migration of these intrasets could be related to a position relative to the plunge point of a hyperpycnal flow. A lateral position would record a spreading of the plunging current on the foreset surface and experience a current acting obliquely on the foreset.

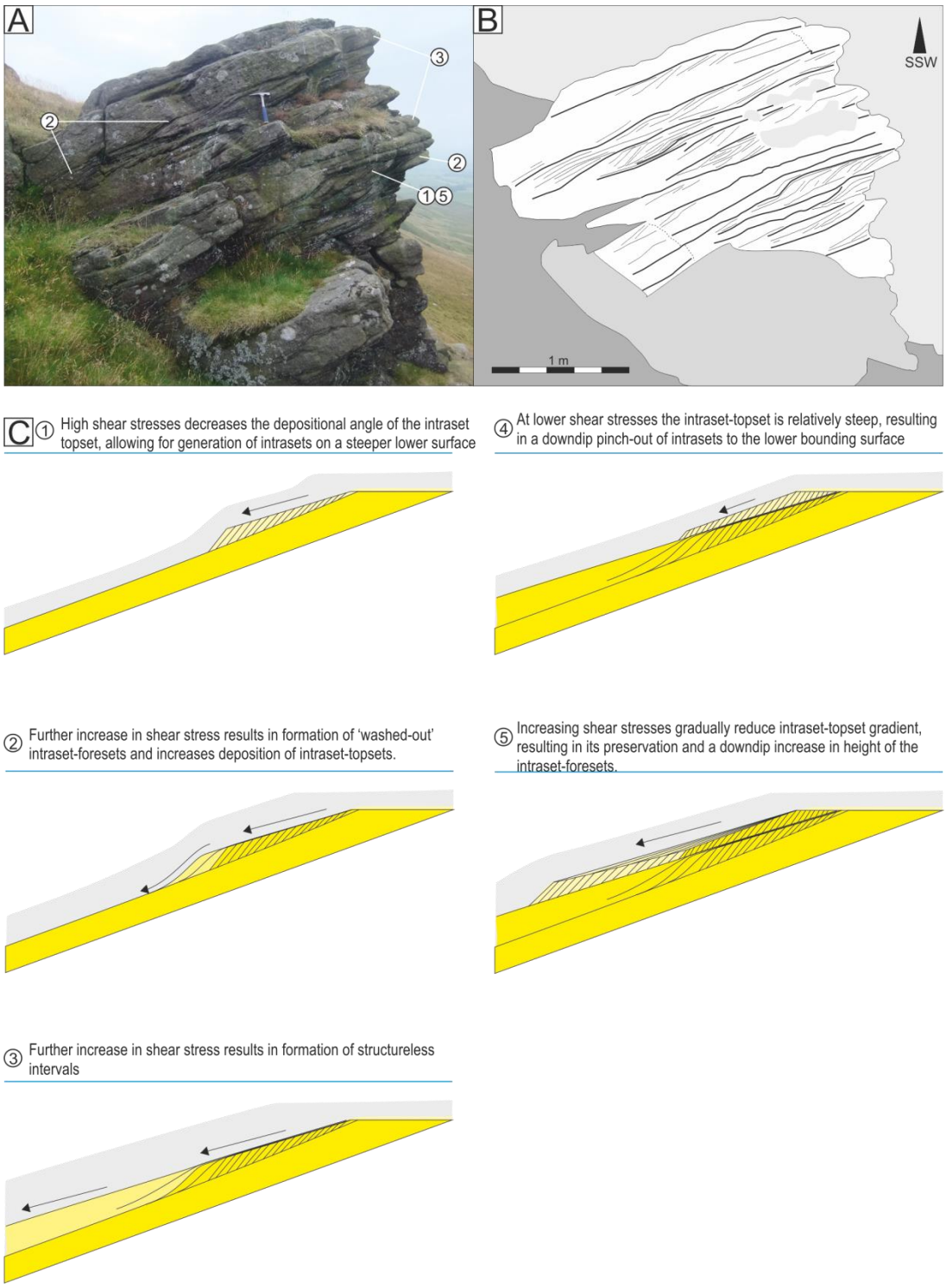

Figure 4.13 (a, b) Well-developed intrasets in facies 7D at south side of Rolling Gate Crag (Table 4.1). Numbers in (a) refer to described stages in (c) of this figure. (c) Inference of intraset formation as a function of variable strength of the hyperpycnal flow, resulting in a variable angle of repose for the major surfaces.

Overall, Facies 7D suggests rapid and continuous progradation of the foresets beds without breaks in coarse- to very coarse-grained sedimentation for several metres. This is further supported by the occurrence of sigmoidal or sheared intrasets (Fig. 4.6d). Sigmoidal intrasets indicate high rates of bed aggradation in which the topset is preserved, and are associated with near-upper stage plain bed conditions and suspension-laden currents (Røe, 1987). Shearing of the intrasets might be related to the combination of a high angle of deposition and the shear stress of the overriding current, as well as high rates of deposition, causing deposition of poorly compacted and dewatered sets (Fig. 4.6d).

4.5.1.5 Facies 6: Structureless and crudely-laminated sandstones

In Chapter 3, these structureless or faintly-laminated, erosionally-based, metre-scale beds are interpreted as sediment-gravity-flow deposits. This is based on the fining upward trend within beds, containing pebbles up to 5 cm in diameter near the base and only rare granules near the top. This structure implies rapid but waning flow conditions that can also explain the typical occurrence of laminations towards the top of the bed. Rare observations of backsets in the delta toe suggest these deposits form from flows that are supercritical.

4.5.2 Facies associations: delta front flow processes

4.5.2.1 Facies association 3: Gilbert-type deltas with fine-grained toesets

The inferred dominant process of suspension settling for facies 7A suggests relatively low energy settings in comparison with the other foreset styles and is in good agreement with the observed bioturbated siltstone toeset, and thin interbedded fines between foreset beds (Fig. 4.3; 4.12a).

4.5.2.2 Facies association 4: Gilbert-type delta with structureless sandstones in toeset

This facies association only occurs in the Bearing Grit and contains structureless and crudely-laminated sandstones (sediment-gravity-flow deposits, facies 6), facies 7B, 7C, 7D foresets, cross-bedded sandstones (facies 8), and

horizontal laminated sandstones (facies 9) that form from an array of flow processes at different flow strengths.

Facies 7B is interpreted as a Gilbert-type delta formed by sedimentation from an inertia-dominated jet under homopycnal conditions. This is similar to Facies 7A and probably records similar flow strengths (Fig. 4.12a, b). The difference between these two facies is thought to relate to grain-size range: the coarser grain size in Facies 7B results in a dominance of bed-load transport over suspended load. This triggers grain-flow events related to oversteepening and collapse at the top of the delta foreset (e.g. Nemec, 1990) instead of the continuous suspension-settling process such as inferred for facies 7A. The coarser grain size and higher rate of bed load transport in these Bearing Grit facies with respect to the Warley Wise Grit is probably related to the differences in efficiency of the fluvial system as a function of basin configuration (see Chapters 2 and 3).

Additionally, the Bearing Grit records higher energy flow regimes, as indicated by the traction currents in facies 7C, 7D and facies 6 sediment-gravity-flow deposits. The laminations in Facies 7C and 7D are most likely related to a shear stress exerted on the foreset thus implying a foreset-overriding current that is likely related to a hyperpycnal river outflow (Fig. 4.12c, d). Typically, rivers that produce hyperpycnal currents on the delta front do so during high flow stage conditions such as during spring melt, after storms or during monsoonal rains. Suspended sediment concentrations tend to increase during flood stages and might temporarily raise the density of fluvial outflow such that hyperpycnal currents can occur on the delta front (Mulder et al., 2003; Morehead et al., 2003; Milliman and Kao, 2005; Dadson et al., 2005). The alternation between facies 7B, and facies 7C and 7D suggests variable (excess) density of fluvial outflow (e.g. Fig. 4.4a; 4.6a; 4.8), and therefore facies 7C and 7D are thought to resemble high flow stage deposits.

Additionally, metre-scale sediment-gravity-flow deposits (Facies 6) are common in this facies association (Fig. 3.15; 3.10; 4.4c, d; 4.6c; 4.8; 4.9). In general, sediment-gravity-flow deposits are a common feature of Gilbert-type deltas, and typically develop as slope failures within sufficiently high foresets (e.g. Postma, 1990). In this facies association, sediment-gravity-flow deposits are typically several metres thick and occasionally reach similar thicknesses as the height of the adjacent foreset. They are normally graded overall, show laminations in the upper part of the

bed and occasionally feature backsets, which has led to a high-density turbidity current interpretation (see Chapter 3). These deposits might be related to a slope-failure mechanism. Such failures would imply a very rapid transition from the initial slope failure to a turbulent current because of the 5 - 16 m foreset height, and have been suggested in slightly higher foresets (e.g. Falk and Dorsey, 1998). This mechanism is not preferred because intermediate stages in the evolution of the slope failure, such as slides or slumps are not observed. Additionally, the slope failure mechanism would imply that these deposits can only be recorded in the lower part of the foreset, while they are also observed near the top of foresets. Finally, the thickness of these gravity flow deposits of up to ~8 m is difficult to reconcile with collapse of a foresets of similar height and transition into a turbulent current.

It is more probable that these sediment-gravity-flow deposits are derived directly from the fluvial system, and result from higher flow stages than Facies 7C and 7D. The inference of a river-derived origin for these sediment-gravity-flow deposits is supported by the occurrence of such deposits within the fluvio-deltaic topset succession at Simon's Seat (Fig. 4.7), Lord's Seat (Fig. 4.5a-d), and Unnamed Crag 5, on Barden Fell (Fig. 4.8). These outcrops suggest that the sediment-gravity-flow deposits are present within the Bearing Grit fluvial system, and probably record higher sediment concentrations and thus flow velocities than facies 7C and 7D (Fig. 4.12e). However, coarse-grained sand was still deposited at >10° angles (e.g. Fig. 4.8a), which implies that the excess density was insufficient to maintain sediment transport of coarse-grained sand in an unconfined and shallow gradient delta toe setting, resulting in rapid deposition (Fig. 4.12e). A thick succession of sediment-gravity-flow deposits in the toeset of the Gilbert-type deltas is exposed at the Rylstone Cross at Barden Moor (Fig. 4.9), where the overlying Gilbert-type deltas are exposed ~15 metres stratigraphically higher at High Bark (Fig. 3.9) . Within this sediment-gravity-flow dominated toeset, most beds show a lenticular nature and contain crude laminations. At the top of this succession, a scour fill containing 4 m high backsets suggest that these flows may have transitioned from a supercritical to a subcritical state, with the implication that the deceleration occurred in the delta toe (Fig. 4.9, 4.12e). Other occurrences of this toeset facies are exposed at Flasby Fell on the western side of Whelpstone Crag and at Bowland Knotts (Fig. 3.15c, d).

4.5.3 Hyperpycnal flow strength

The Carboniferous Central Pennine Basin was an intra-cratonic basin, and is thought to have had reduced salinities or fresh water conditions related to poor connections to the open oceans during low and intermediate sea-level stands (e.g. Collinson, 1988). This setting increases the likelihood of hyperpycnal currents because the reduction in salinity reduces the excess density of the basinal water (Felix et al., 2006). Therefore, low suspended sediment concentrations in the fluvial water can become sufficient to surpass the density of the basinal water. Still, hyperpycnal flows have rarely been inferred to account for deltaic (Collinson 1968) and slope deposits in the basin (O'Beirne, 1996; Jerrett and Hampson, 2007; Waters et al., 2008). The above inference of hyperpycnal currents forming type 7C and 7D delta foresets provides a unique opportunity to estimate their strength via measurements of the depositional angle, and thus provide a quantification of whether hyperpycnal flows might play an important role in sediment transport into the basin.

Figure 4.14 (next page) (a) Forces acting on grains on a horizontal surface. Only water flow can exert a bed-parallel force on the grain, resulting in sediment motion if shear stress is larger than the critical Shields stress. (b) Forces acting on grains on a sloping surface. Gravity (Fg) can be expressed as vectors bed-parallel and bed-normal to the sloping surface. The bed-parallel vector reduces the amount of shear stress required to surpass the critical Shield stress, facilitating sediment motion. (c) At angle of repose, the bed-parallel vector of gravity is equal to the critical Shields stress, implying that the slope cannot become steeper. (d) Relation between foreset angle and shear stress required to surpass the critical shield stress based on equation 1 for Facies 7C and 7D. Black dots denote experimental data from Kostic et al. (2002), coloured dots indicate field measurements (see Fig. 4.11) (e) Definition sketch of a hyperpycnal current, see text for discussion of parameters, (f) Estimates of the density and flow depth 'H' of a hyperpycnal current, relative to the foreset angle. Coloured markers are estimates for foreset types 7C and 7D using the scaling approach of Kostic et al. (2002), lines are constructed using equation 11.

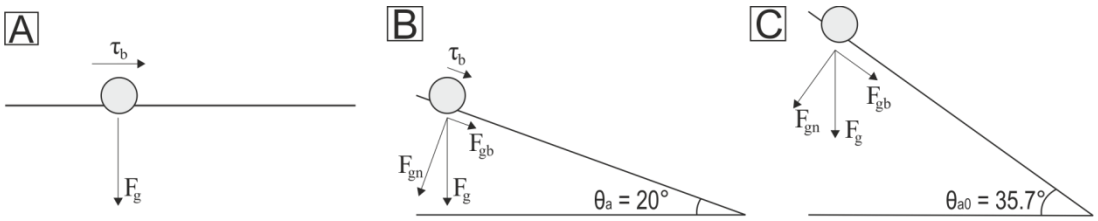
A
τ_b
F_g
B
τ_b
F_{gb}
F_{gn}
F_g
$\theta_a = 20°$
C
F_{gb}
F_{gn}
F_g
$\theta_{a0} = 35.7°$

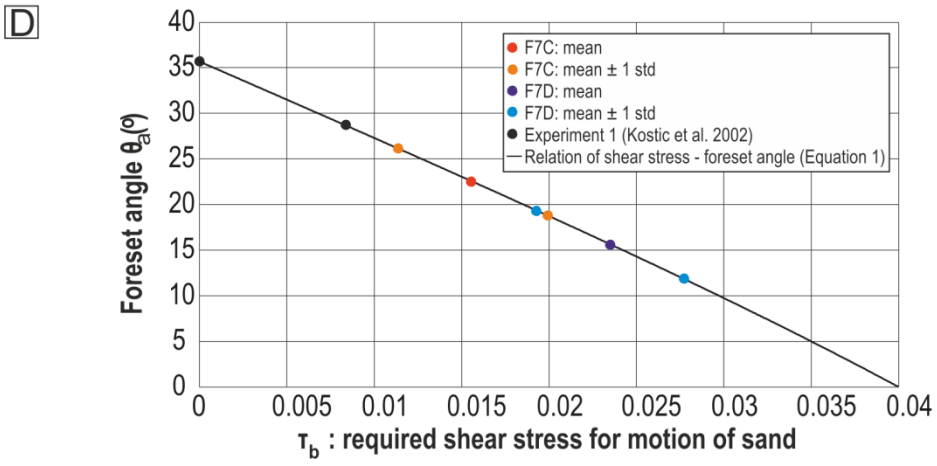
D
Foreset angle θ_a(°)
τ_b : required shear stress for motion of sand
F7C: mean
F7C: mean ± 1 std
F7D: mean
F7D: mean ± 1 std
Experiment 1 (Kostic et al. 2002)
Relation of shear stress - foreset angle (Equation 1)
0
5
10
15
20
25
30
35
40
0
0.005
0.01
0.015
0.02
0.025
0.03
0.035
0.04

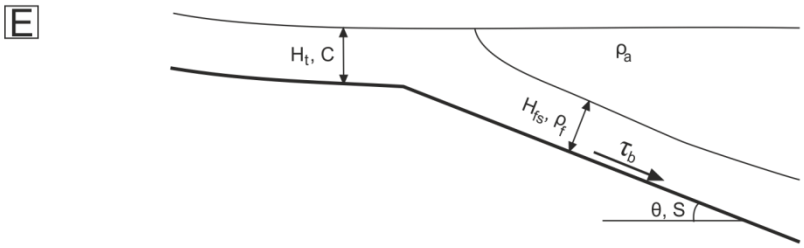
E
H_t, C
ρ_a
H_{fs}, ρ_f
τ_b
θ, S

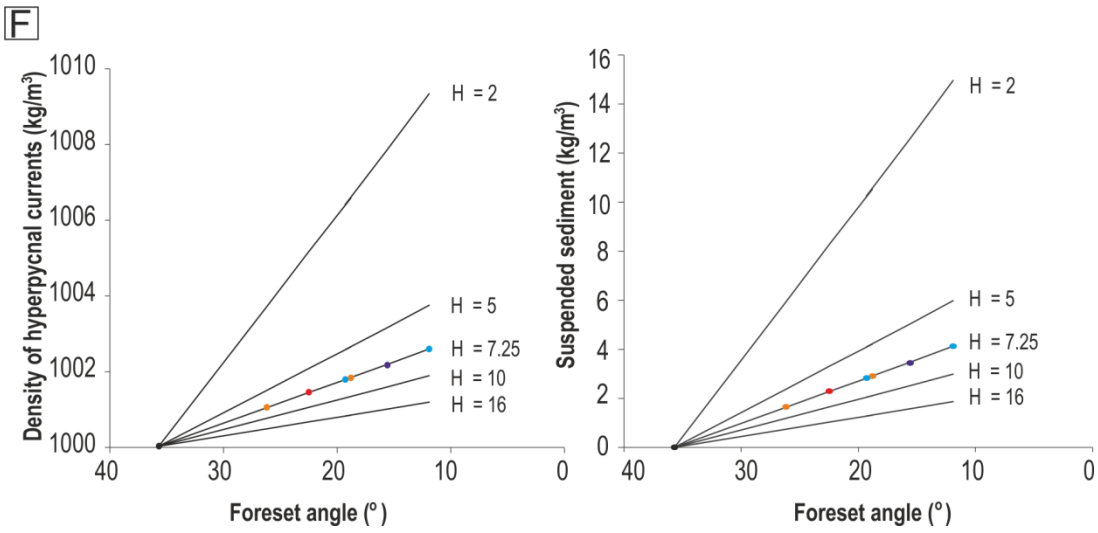
F
Density of hyperpycnal currents (kg/m³)
Foreset angle (°)
H = 2
H = 5
H = 7.25
H = 10
H = 16
1000
1002
1004
1006
1008
1010
40
30
20
10
0
Suspended sediment (kg/m³)
Foreset angle (°)
0
2
4
6
8
10
12
14
16

Transport of sand-grade sediment implies that individual grains experience a critical Shields stress of at least ~0.04. On a horizontal bed, such as in rivers, sediment motion results solely from the shear stress exerted by the flow of water across the bed (Fig. 4.14a). Such a shear stress is not required for angle of repose foresets because the bed-parallel vector of gravity (F_{gb}) is sufficiently large to result in sediment transport (Fig. 4.14c). At lower-than-repose angles, the bed-parallel vector of gravity is insufficient for sediment motion (Fig. 4.14b). However, when an additional shear stress acts on such foreset, for example due to a hyperpycnal current, their combined force can surpass the critical Shields stress, resulting in sediment motion (Fig. 4.14b). Weak shear stresses reduce the foreset angle slightly while stronger shear stresses can lower the foreset angle substantially, implying that the strength of the overriding current can be derived from the observed foreset angles (Kostic et al., 2002).

The well-developed laminations in foreset types 7C and 7D suggest a traction current on these foresets. The strength of the shear stress exerted by this traction current can be estimated via the difference between the angle of repose and the angle of deposition (Fig. 4.11a; 4.14d; Kostic et al., 2002). Using an estimate for the critical Shields stress (~0.004) and angle of repose (35.7°), Equation 1, below, (Equation 10 of Kostic et al., 2002) is used to quantify the relation between foreset angle and shear stress exerted by an overriding current (Fig. 4.14d). The 35.7° angle of repose is observed in the experiments of Kostic et al. (2002). It corresponds closely to the maximum depositional angle of 35° observed in the type 7D intrasets, indicating that such angles do also occur in the Bearing Grit.

$$tan\ \theta_a = tan\ \theta_{a0}\left(1 - \frac{1}{\cos\theta_a}\frac{\tau_b}{\tau_{c0}^*}\right) \qquad 1$$

In this equation θ_a denotes the foreset angle, where θ_{a0} indicates the foreset angle without additional Shields stress. Parameter τ_b indicates the shear stress required for the onset of sand motion in the presence of an overriding turbidity current, and τ_{c0}^* indicates the critical Shields stress on a (sub-)horizontal bed. For Facies 7C, a mean reduction of the foreset angle of 12.5° is estimated with respect to the maximum observed angle of 35°, corresponding to a required bed shear stress of ~0.0157 (Fig. 4.14d; Table 4.2: column T_b). For Facies 7D the mean foreset reduction is 19.4°, indicating a bed shear stress of ~0.0236 acted on this foreset (Fig. 4.14d; Table 4.2: column T_b).

#		θ_a	T_b	$(C)_p$: field Mass concentration (kg/m³)	Density (kg/m³)	Excess density (kg/m³)
Max.		35.7	0.0000	0	1000.0	0
F7C	M+1 Std	26.2	0.0113	1.645	1001.0	1.02
	M	22.5	0.0157	2.286	1001.4	1.42
	M-1 Std	18.8	0.0199	2.898	1001.8	1.80
F7D	M+1 Std	19.3	0.0194	2.825	1001.8	1.76
	M	15.6	0.0236	3.436	1002.1	2.14
	M-1 Std	11.9	0.0277	4.033	1002.5	2.51

Parameters	Exp.1 (m)	Field (p)	
Flow depth (H_t) (in m)	0.0155	7.25*	*Based on an estimated 0.4 m dune height, an estimated dune preservation of 0.33 (Leclair, 2002) and a dune height/water depth relation 0.167 (Leeder, 1999)
Bed load grain size (D) (in mm)	0.422*	1.5**	* medium-grained sand, ** coarse- to very coarse-grained sand
Grain size suspended load (in mm)	0.0218*	0.0517**	* fine silt, **coarse silt (established by scaling medium-grained sand to coarse-/very coarse-grained sand)
Mass Concentration $(C)_m$ (in kg/m³)	55.6	-	Concentration of suspended sediment before plunge in experiment 1 (Kostic et al., 2002)
Specific density (-)	1.036	-	Specific density of water with suspended sediment with a concentration of 55.6 g/L in comparison to ambient water in experiment 1 (Kostic et al., 2002)

Table 4.2 Estimates for critical Shields stress, suspended sediment concentrations and excess density of fluvial outflow. Note that suspended sediment concentrations do not assume additional factors that might influence the density difference between fluvial and basinal water. See text for discussion.

4.5.4 Froude scaling

In laboratory experiments Kostic et al. (2002) measured the reduction of foreset angle in response of hyperpycnal flows while recording the sediment concentration and excess density before plunging. Subsequently, Froude-scaling has been used to apply these results to field scenarios (Kostic et al., 2002). The

following equation is used to scale the effect of bed shear stress on foreset angle between experimental and field data (Kostic et al., 2002).

$$\frac{(\tau_b)_p}{(\tau_b)_m} = \left(\lambda_{H_t}\right)^{5/6}(\lambda_C)(\lambda_D)^{-1} \quad 2$$

In this equation, τ_b indicates the bed shear stress that is required for the onset of sand motion in the presence of an overriding turbidity current for respectively the model (m) and upscaled prototype (p). Lambda (λ) indicates the ratio between the model and prototype for the following parameters: flow depth on the topset (H_t), sediment concentration (C), and grain size (D). When substituting these ratios with the original parameters for experimental and prototype (field) data, Equation 2 can be rewritten to estimate sediment concentrations.

$$\frac{(\tau_b)_p}{(\tau_b)_m} = \left(\frac{(H_t)_p}{(H_t)_m}\right)^{5/6}\left(\frac{(C)_p}{(C)_m}\right)\left(\frac{(D)_p}{(D)_m}\right)^{-1} \quad 3$$

$$(C)_p = \frac{(C)_m}{\left(\frac{(\tau_b)_m}{(\tau_b)_p}\right)\left(\frac{(H_t)_p}{(H_t)_m}\right)^{5/6}\left(\frac{(D)_m}{(D)_p}\right)} \quad 4$$

$$(C)_p = (C)_m\left(\frac{(\tau_b)_p}{(\tau_b)_m}\right)\left(\frac{(H_t)_m}{(H_t)_p}\right)^{5/6}\left(\frac{(D)_p}{(D)_m}\right) \quad 5$$

Using Equation 5, suspended sediment concentrations are estimated for the shear stresses in facies 7C and 7D derived via Equation 1 (Fig. 4.14; Table 4.2). The model case (Eq. 5: m-values) is resembled by the original measurements by Kostic et al. (2002) (($T_b)_m$ = 0.0084; $(C)_m$ = 55.6; $(H_t)_m$= 0.0155; $(D)_m$ = 0.422). For the prototype case (Eq. 5: p-values) bed shear stresses derived for Facies 7C and 7D are used (Fig. 4.14; Table 4.2: column T_b) in combination with flow depth $(H)_p$ and grain-size estimates $(D)_p$ of 7C and 7D foreset types (Table 4.2).

The above scaling method suggests that the shear stress exerted on the 7C and 7D foresets corresponds to suspended sediment concentrations of 1.6 – 4.0 kg/m^3, which equates to fluvial outflow densities of 1001.0 – 1002.5 kg/m^3 when assuming that the ambient water has a density of 1000 kg/m^3 (Table 4.2). Such suspended sediment concentrations and associated densities can be obtained in nearly all modern rivers, particularly during flood events (Mulder and Syvitski, 1995). This indicates that the inference of a hyperpycnal flow as a cause for the foreset angle reduction in facies 7C and 7D is realistic.

The above estimates provide a useful insight in the strength of hyperpycnal currents that is required to reduce the foreset angle. However, the upscaling of the experimental results relies heavily on the flow depth estimate on the topset (Equation 5). This is difficult to establish in most ancient deposits. Dune heights, such as used here, are an imprecise method of establishing flow depth that depends on the fraction of a dune that is preserved (e.g. Leclair, 2002) and the relation between the dune height and water depth, which are both highly variable (e.g. Leeder, 1999).

A different method to estimate suspended sediment concentrations uses a relation in which bed shear stress is expressed as a function of the density and height of a gravity current on a specific gradient.

$$\tau_b = \rho_f * g' * H_{fs} * S \quad (6)$$

$$g' = \frac{\rho_f - \rho_a}{\rho_f} \quad (7)$$

Here, τ_b represents the bed shear stress, g' represents the reduced density that consists of the density of a gravity current (ρ_f) and the density of the ambient water (ρ_a) (Fig. 4.14e). The height of this current on the foreset is given by H_{fs}, and the gradient of deposition by S (Fig. 4.14e). Inserting Equation 7 into Equation 6 allows for simplification.

$$\tau_b = \rho_f * \frac{\rho_f - \rho_a}{\rho_f} * H_{fs} * S \quad (8)$$

$$\tau_b = (\rho_f - \rho_a) * H_{fs} * S \quad (9)$$

$$\tau_b = \Delta\rho * H_{fs} * S \quad (10)$$

$$[\Delta\rho * H_{fs}] = \frac{\tau_b}{S} \quad (11)$$

Equation 11 states that the foreset gradient (S) and bed shear stress (τ_b) are dependent on a multiplication of excess density ($\Delta\rho$) with flow depth (H_{fs}): high excess densities imply a shallow flow depth and vice versa.

Because both the bed shear stress and foreset angle are known parameters, Equation 11 allows for additional insight into the relation between flow depth and excess density in foreset types 7C and 7D. Foreset angle is plotted against density for the shear-stress estimates using several flow depths (Fig. 4.14f). Suspended sediment concentration are based on the assumption that the excess density of the

turbidity current is caused entirely by suspended sediment and a density of 1000 kg/m^3 for basinal water.

Figure 4.14f highlights that the Froude-scaling approach in Kostic et al. (2002) assumes that the 7.25 m flow depth estimated for the fluvial system (H_t) is similar to the flow depth of the hyperpycnal current (H_{fs}; Fig. 4.14e, f). This assumption probably indicates a slight underestimate of the hyperpycnal flow depth H_{fs}) because hyperpycnal currents are probably thicker than the flow depth in the fluvial channel because of dilution at the plunge point and at the contact between the hyperpycnal current and the ambient water (Lamb and Mohrig, 2009). Note that the maximum measured foreset height of 16 m sets an upper limit to the thickness of the hyperpycnal currents. Additionally, these plots highlight the low suspended sediment concentration and densities of these currents. A 7.25 m or thicker hyperpycnal flow on the foreset (H_{fs}) corresponds to river outflow density of ~1002.5 kg/m^3 and suspended sediment concentrations of 4 kg/m^3 or less for the 7D type foresets (Table 4.2; Fig. 4.14f). If shallower fluvio-deltaic channels are assumed, hyperpycnal flows could be thinner and thus denser as well (Fig. 4.14f). However, even a thin hyperpycnal flow of 2 m is relatively weak with densities of up to 1.009 kg/m^3 corresponding to a suspended sediment concentration of ~15 kg/m^3. For reference, high density turbidity currents have a minimum sediment volume concentration of ~9% near the base of the flow (Lowe, 1982), corresponding to ~238 kg/m^3 suspended sediment concentration.

The densities and suspended sediment concentrations calculated for facies 7C and 7D (e.g. Fig. 4.5; 4.6) should be considered as order of magnitude estimations rather than accurate values (Table 4.2). Both the critical Shields stress on a sub-horizontal bed, and the angle of repose without shear stress related to an overriding current are end-member assumptions that might slightly affect the outcome but could be improved by detailed grain-size analyses. More importantly, the flow-depth estimate (Table 4.2; Fig. 4.14f) is crude and strongly affects outcomes, although densities and suspended sediment concentrations of the hyperpycnal currents remain relatively low even if hyperpycnal currents are substantially thinner than expected (Fig. 4.14f). Additionally, the estimates assume that density differences are entirely dependent on suspended sediment concentration (Kostic et al., 2002). In the Craven Basin, dissolved load and cooler temperatures of the fluvial outflow as well as salinity of the basinal water could affect the excess

density (e.g. Felix et al., 2006). Furthermore, a mean density of the river water underestimates the potential for plunging flows as it assumes that the entire flow depth has the same density. Channelized flows are typically stratified with the suspended sediment concentration decreasing logarithmically with height above the bed (Rouse, 1937; Felix et al., 2006). In such a case, near-bed suspended-sediment concentration might be high and result in a plunging flow, whereas low densities at the top of the fluvial water column results in a homo- or hypopycnal outflow (Felix et al., 2006).

These estimates are here interpreted as confirming the Millstone Grit river system as a coarse-grained sand-dominated fluvial system with limited suspended sediment (e.g. Mulder and Syvitski, 1995). This corresponds well with the occurrence of Gilbert-type deltas because these require relatively deep basins with respect to fluvio-deltaic channel depth (Bates, 1953; Leeder, 1999). Large volumes of mud- or silt-grade suspended sediment would result in a shallowing of the basin near the channel mouth, impeding the formation of Gilbert-type deltas and facilitating the formation of a mouth-bar deltas type. Additionally, the shear stress estimates indicate that the observed reductions of the coarse-grained foreset angle require only weak hyperpycnal currents. Because these deposits maintain >10 degree depositional dip, it is considered unlikely that these currents are capable of significant transport of sand-grade sediment into the marine domain at substantially lower gradients.

4.5.5 Previous depositional models

The progradational delta front model (Collinson, 1968; Sims, 1988) is here inferred for the Gilbert-type deltas in the Warley Wise Grit and the incised valley fill model is here inferred for the Gilbert-type deltas in the Bearing Grit (Hampson, 1997, Jones and Chisholm, 1997). The alternate channel bar model is here rejected (Fig. 4.1; McCabe, 1975, 1977; Baines, 1977; Jones, 1980; Jones and McCabe, 1980). This model envisions a Mississippi-size fluvial system with deep deltaic distributary channels of ~1 - 2 km wide and up to ~30 m deep, containing alternate bank-attached bars. During low flow stage, the river would flow along the thalweg, while during high flow stage the alternate bars would become mobile and migrate downstream. These bars are thought to form large-scale foresets on the slipface;

preservation of large alternate bars would occur when the channel is abandoned (McCabe, 1977).

In the alternate bar model, large-scale foresets of up to 40 m height in the Millstone Grit Group are considered analogous to 30 m high alternate bars such as occur in deep distributary channels of the Mississippi river (without slipfaces/coarse-grained foresets), suggesting that the Millstone Grit Group was deposited by a Mississippi-size river (McCabe, 1977). However, comparison of the sediment volume estimates in Chapter 3, with the current sediment flux in the Mississippi (Hovius, 1998) indicates that the Millstone Grit drainage system is at least an order magnitude smaller. The total sediment volume during the Pendle and Bearing Grit deposition times is estimated to have been c. 1000 km^3 over a sea-level cycle of ~100 kyr (26.5 Mt/yr; Fig. 3.17; 3.18), whereas the current suspended sediment load at the mouth of the Mississippi is 400 Mt/yr (Hovius, 1998). This suggests that the Millstone Grit Group is deposited by a significantly smaller river system in which, therefore, such deep and wide distributary channels are unlikely to have occurred.

At Barden Moor, large-scale foresets occur in up to 500 m wide outcrops along two stratigraphic levels that extend for at least 3 km perpendicular to flow (Fig. 3.9). In the alternate bar model, these discrete levels would represent two vertically stacked km-scale channels. Alternatively, these discrete levels are interpreted as two pulses of coastline progradation in which the individual <500 m wide outcrops represent the Gilbert-type delta fronts fed by deltaic channels of corresponding scale, alternated with intervals of fine-grained deposition between distributary channels and Gilbert-type deltas. Such depositional scales are considered more appropriate for the sediment volumes and system scale estimated for the Bearing and Warley Wise Grit (Fig. 3.17; 3.18).

Besides the discrepancy between sediment loads and river size, Mississippi and Millstone Grit river types strongly differ as well. The Mississippi is a mud-rich system implying it has high bank stability, thus promoting the occurrence of deep distributary channels (Gouw and Berendsen, 2007). Coarse-grained fluvial systems such as the Millstone Grit sediments generally form shallow, braided channels belts and numerous periods of deposition within the Millstone Grit Group conform to this model (e.g. Bristow, 1993a; Martinsen, 1993; Martinsen et al., 1995; Waters et al.,

2008). Large-scale foresets, for which the alternate bar model was proposed, only occur in the Bearing Grit (Baines, 1977), the Lower Kinderscout Grit (McCabe, 1975; 1977), and the Roaches-Ashover Grit (Jones, 1980). Unlike most other Millstone Grit Group sandstones, these three systems are associated with the infill of deep basins, making these successions more prone to valley incision than shallow water deltas (Chapter 2; Chapter 3). This leads to an alternative interpretation for the formation of large-scale foresets as Gilbert-type delta fronts in incised valley fill successions (e.g. Fig. 3.19e; Hampson, 1997; Jones and Chisholm, 1997). A fourth occurrence of Gilbert-type deltas in the Warley Wise Grit (Sims, 1988; Chapter 3) can straightforwardly be explained as a Gilbert-type delta front in a progradational succession (Fig. 3.19g).

Modern braided systems probably form a better analogue than the Mississippi river due to the similarity in grain size and associated fluvial style. This raises the question, however, of whether large-scale foresets may also develop as part of intrachannel bedsets in such rivers. For example, large-scale, 8 m high foresets have been described for a mid-channel bar in the Jamuna River, Bangladesh (Ashworth et al., 2000; Best et al., 2003). However, these foresets form a bar margin slipface that only occurs on the tail of the bar. This implies that even if the channel is abandoned and thus the bar tail is preserved, such foresets are limited to a very small part of the deposited bar, while the majority of the bar is formed by a stacked succession of dunes (e.g. Reesink and Bridge, 2011; Reesink et al., 2014). This is unlike the outcrop character of the large-scale foresets in the Millstone Grit where the large-scale foreset forms the entire bar. Additionally, these 8 m high foresets occur in one of the world's largest rivers with an annual sediment load of >500 Mt and a depth of 40 m, suggesting that this river might feature significantly larger structures than most braided rivers (Best et al., 2003). Even large rivers such as the glacial-stage Rhine (Siegenthaler and Huggenberger, 1993), and the present-day Brahmaputra do not reach preserved dune heights of over 6 m (Bristow, 1993b) while dunes in the Carboniferous Rough Rock do not reach over 4 m (Bristow, 1993a).

4.5.6 Hypothesis of climate forcing

It has been suggested above that facies 7A in the Gilbert-type delta with fine-grained toesets facies association represents a low energy fluvial flow regime, whereas the alternation between facies 7B, 7C, 7D foresets and sediment-gravity-flow deposits in the Gilbert-type delta facies association with structureless represents the depositional products of increasingly energetic fluvial flow regimes (Fig. 4.12). It is here further suggested that the differences between flow regimes in the Bearing and Warley Wise Grit can be related to the periodic occurrence of high magnitude river floods and might correspond to different climatic conditions during sea-level rise (Bearing Grit) and fall (Warley Wise Grit).

Radiometric dating suggests that marine band occurrences during the Namurian are within the 100 – 400 kyr eccentricity range, with a dominant 100 kyr cyclicity during the Pendleian and early Arnsbergian (Waters and Condon, 2012). The 100 kyr periodicity suggests that Southern Hemisphere ice sheet growth and decay during the Pendleian may have been similar to the last 900 kyr of the Pleistocene (e.g. Rygel et al., 2008). The 100 kyr sea-level cycle during the Pleistocene results from rapid ablation of ice sheets during peak summer insolation at high latitude, broadly aligning with strong eccentricity-modulation of precession and with strong obliquity (Fig. 4.15a; Oerlemans, 1991; Ruddiman, 2006).

Meanwhile, the equatorial position of the Craven Basin and Millstone Grit drainage system suggests that there is a potential for the development of monsoonal climate from the Asbian onwards (Fig. 3.3; Vanstone, 1996; Wright and Vanstone 2001; Falcon Lang, 1999a, 1999b). This is similar to inference of monsoonal climate along the western margin of low-latitude regions of Pangaea from the Asbian onwards (e.g. Poulsen et al., 2007; Tabor and Poulsen, 2008; Allen et al., 2011).

Monsoonal climate variations occur in equatorial regions during periods of strong seasonality. Rapid warming of the continents relative to the oceans during summer results in strong moisture-laden landward winds, resulting in heavy rains and high fluvial discharge, particularly in mountainous areas. During winter monsoon, weather patterns reverse, resulting in a drier climate. This alternation can

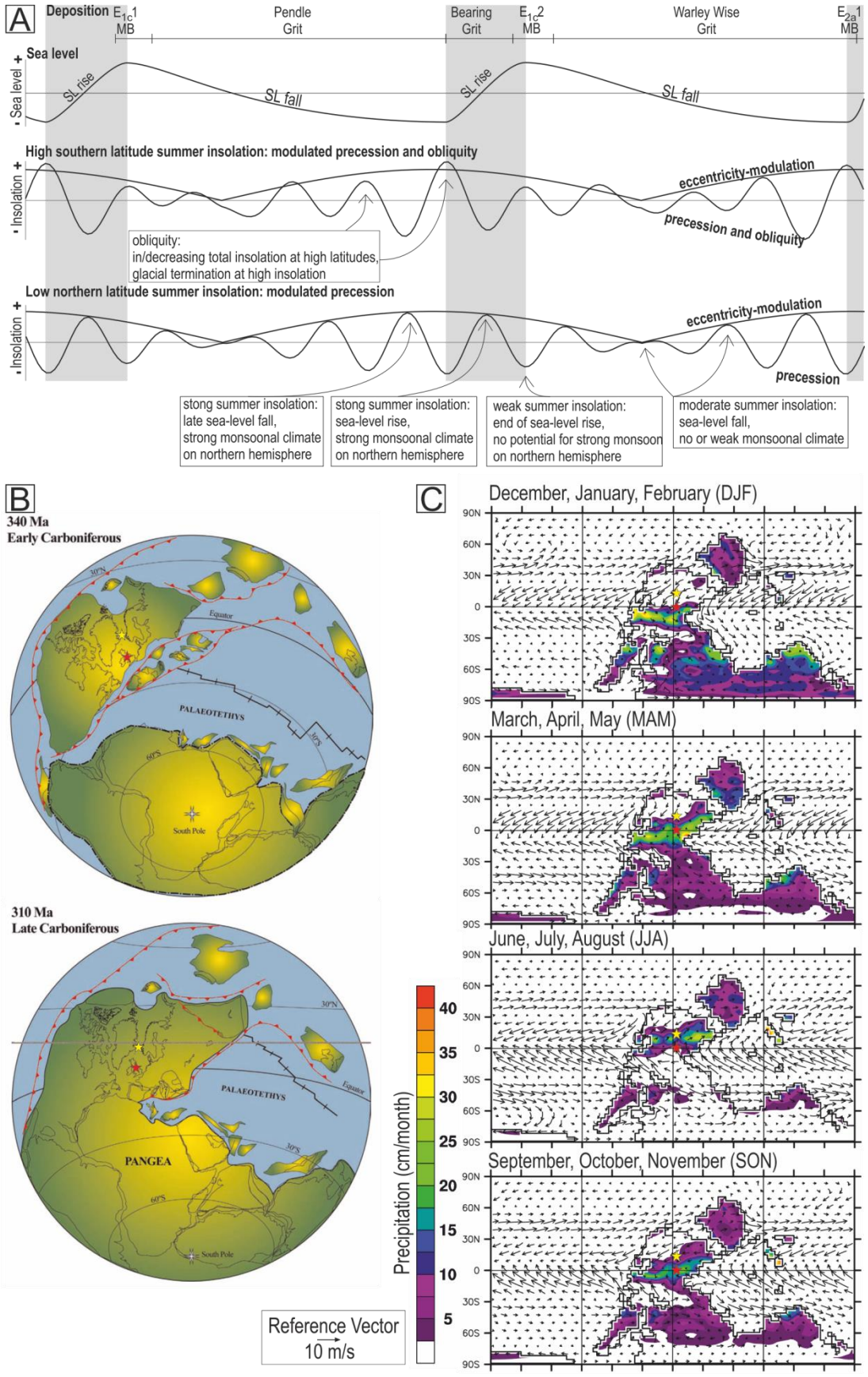
A
Deposition
E1c1 MB
Pendle Grit
Bearing Grit
E1c2 MB
Warley Wise Grit
E2a1 MB
Sea level
+
- Sea level
SL rise
SL fall
SL rise
SL fall
High southern latitude summer insolation: modulated precession and obliquity
+
- Insolation
eccentricity-modulation
precession and obliquity
obliquity:
in/decreasing total insolation at high latitudes,
glacial termination at high insolation
Low northern latitude summer insolation: modulated precession
+
- Insolation
eccentricity-modulation
precession
stong summer insolation:
late sea-level fall,
strong monsoonal climate
on northern hemisphere
stong summer insolation:
sea-level rise,
strong monsoonal climate
on northern hemisphere
weak summer insolation:
end of sea-level rise,
no potential for strong monsoon
on northern hemisphere
moderate summer insolation:
sea-level fall,
no or weak monsoonal climate
B
340 Ma
Early Carboniferous
30°N
Equator
PALAEOTETHYS
30°S
60°S
South Pole
310 Ma
Late Carboniferous
30°N
Equator
PALAEOTETHYS
PANGEA
30°S
60°S
South Pole
Reference Vector
10 m/s
C
December, January, February (DJF)
March, April, May (MAM)
June, July, August (JJA)
September, October, November (SON)
90N
60N
30N
0
30S
60S
90S
Precipitation (cm/month)
40
35
30
25
20
15
10
5

Figure 4.15 (previous page) (a) Conceptual, simplified model of the relation between deposition of the stratigraphic units, sea-level variations, high latitude southern hemisphere insolation and low latitude northern hemisphere summer insolation (see text for discussion). (b) Palaeogeographical reconstructions indicating approximate positions of Greenland, providing an estimate of the updip extent of the Millstone Grit fluvial system (yellow star) and the Craven Basin position (red star) (from: Cocks and Torsvik, 2006). (c) 65 kyr snapshots of spatial patterns of monthly precipitation and wind directions based on a GCM model for late Paleozoic (Sakmarian, ~290 Myr) palaeogeography (from: Horton et al., 2012). GCM results indicate arid conditions in the entire drainage basin during winter (map DJF), wet conditions limited to the lower drainage basin during spring (map MAM), and wet conditions throughout the drainage basin in summer and autumn (maps JJA and SON).

result in variable sediment transport, which is recorded in the stratigraphic record (Postma et al., 1993; Weltje and de Boer, 1993; Goodbred and Kuehl, 2000; Bookhagen et al., 2005; Clift et al., 2008). The strength of monsoonal climate is closely related to precession, which had a ~19 kyr period during the Carboniferous (Berger, 1989). Precession determines whether a hemisphere is in perihelion (closest to the sun) or aphelion (furthest away) or intermediate position during summer and thus controls the strength of seasonality (Ruddiman, 2001). Because the difference between perihelion and aphelion is dependent on the ellipse-shape of earth's orbit, precession is strongly modulated by eccentricity with the strongest influence of precession and strongest monsoonal conditions during maximum eccentricity.

The influence of eccentricity on deglaciations at high latitude, and on monsoonal strength due to modulation of precession implies a coincidence of both events: monsoonal conditions are strongest during deglaciations (Fig. 4.15a; e.g. Rossignol-Strick, 1983).

The Millstone Grit drainage system derived sediment from Caledonian uplands located to the north of the equatorial Craven Basin in present day Greenland (Morton and Whitham, 2002), which was located between ~10 and 20° latitude (Fig. 4.15b; Cocks and Torsvik, 2006; Blakey, 2008). This implies that the drainage system had a length of ~1000 - 2000 km and was located in the (seasonal) tropics and is likely to have received variable (monsoonal) precipitation throughout the year. Global Circulation Model (GCM) studies of late Paleozoic (Sakmarian, ~290

Myr) palaeogeography (Horton et al., 2012) indicate that continental, low latitude Northern Hemisphere climate during strong eccentricity is characterised by large variations in mean annual precipitation at precession time scales: the wettest configurations are associated with summer in perihelion and the driest configurations are associated with summer in aphelion. At weak eccentricity values this half-precession time-scale variation in precipitation is nearly absent. This indicates that during glacial periods (low eccentricity), monsoonal conditions are nearly absent, while they are large during the deglaciation (high eccentricity).

Map images of long term (65 kyr) monthly precipitation averages of the GCM indicate that the Millstone Grit drainage area was characterised by a highly seasonal precipitation regime throughout a year (Fig. 4.15c; Horton et al., 2012). Such long term average includes both periods of high and low eccentricity and thus averages the wet and dry seasons at half-precession period. However, it does provide insight into the spatial discharge patterns throughout a year. During winter, the entire drainage area of the Millstone Grit river system is arid (Fig. 4.15c, map DJF). During spring, mainly the lower reaches of the river system are characterised by a high precipitation regime (Fig. 4.15c, map MAM), whereas during summer the upper part of the drainage basin experiences high precipitation (Fig. 4.15c, map JJA). During autumn, the zone of high precipitation is again located in the lower part of the Millstone Grit drainage system (Fig. 4.15c, map SON).

Combining the temporal precipitation trends at eccentricity time-scale with spatial trends in mean annual precipitation, it is considered likely that high amplitude river floods occur in the Millstone Grit drainage basin when summer occurs in perihelion at periods of high eccentricity. Such seasonal river floods are a common discharge pattern for modern monsoonal climates (e.g. Kale, 2002), and are increasingly recognised by distinct sedimentological patterns in fluvial settings (e.g. Alexander and Fielding, 2006; Fielding et al., 2009; Allen et al., 2011, 2013).

Carboniferous deglaciations are related to the Southern Hemisphere (SH) warming and thus coincide with SH summer in perihelion (i.e. highest SH summer insolation, Fig. 4.15a; Horton et al., 2010). The subsequent Northern Hemisphere (NH) summer in perihelion (i.e. highest NH summer insolation) occurs half a precession cycle later (~10 kyr). This implies that strong monsoonal conditions in

the Millstone Grit drainage system should occur when sea-level rise has already progressed significantly (Fig. 4.15a).

The Bearing Grit is interpreted as an incised-valley fill and its deposition thus broadly coincides with sea-level rise (Fig. 4.15a; Chapter 3). More precisely, the in-valley occurrence of Gilbert-type deltas (Chapter 3) suggests that sea-level must have risen several tens of metres to generate sufficient accommodation space within the incised valley (Fig. 3.19e). These deposits are interpreted as river-flood-dominated systems based on traction currents in facies 7C and 7D (Fig. 4.5; 4.6), and river-derived sediment-gravity-flow deposits (e.g. Fig. 4.7; 4.8), which fits with the hypothesis of strong monsoonal conditions during deglaciation.

At Pen-y-ghent on the Askrigg Block (Fig. 3.2; 3.5), a facies 7A Gilbert-type delta is recorded at the top of Bearing Grit incised valley fill (Fig. 3.7). This outcrop suggests that the coastline has transgressed substantially, and thus indicates continued sea-level rise. These deposits are substantially finer-grained (medium-coarse-grained sandstone) and do not show indications of river floods. The change from sediment-gravity-flow-dominated facies association at lower levels in the Bearing Grit to the Gilbert-type delta with fine-grained toesets association near the top of the Bearing Grit is thought to represent a reduction of monsoonal activity that might occur towards the end of sea-level rise (Fig. 4.15a).

Only the Gilbert-type delta association with fine-grained toesets occurs in the Warley Wise Grit. Facies 7A does not include sedimentological structures that suggest the presence of hyperpycnal currents, and is not associated with river-derived sediment-gravity-flow deposits either. Therefore, no evidence is observed to suggest the activity of flood events during deposition of the Warley Wise Grit. This succession is interpreted as a forced regressive shallow water succession, thus coinciding with the construction of a large southern hemisphere ice sheet. Such periods corresponds to relatively low eccentricity forcing and thus in a weak modulation of precession (Fig. 4.15a). This implies small differences between summer in perihelion and aphelion, resulting in only limited seasonality during which monsoonal conditions might either be weak or entirely absent. This fits well with the observations in the Warley Wise Grit.

In Chapter 3, a higher sediment transport efficiency was inferred for the Pendle and Bearing Grit, relative to the Warley Wise Grit. This might provide an

alternative explanation for the occurrence of hyperpycnal and sediment-gravity-flows deposits in the Bearing Grit. The larger sediment volume in the Pendle/Bearing Grit fluvial system suggests that rivers carried larger sediment loads and might thus reach hyperpycnal conditions more frequently. It is considered likely that an increase in fluvial efficiency would also increase the relative ease with which the Bearing Grit system can trigger hyperpycnal currents and sediment gravity flows. However, the frequent alternations between low and very high fluvial flow regimes suggest the frequent occurrence of major flood events in the Bearing Grit (e.g. Fig. 3.10; 4.8), which is not explained solely by fluvial efficiency and fits with a monsoonal climate hypothesis. Additionally, peak monsoonal conditions might result in a heightened sediment flux for a period of a few thousand years, which could explain the significant pulse of progradation associated with the deposition of the in-valley Gilbert-type deltas.

So far, field studies in the equatorial Pennsylvanian succession at the western margin of Pangaea have broadly indicated a strongly seasonal or monsoonal climate during several periods, including the Pendleian (E1 zone of Allen et al., 2011; 2013) in which flood-dominated deposits are recognised (e.g. Gibling et al., 2010). In the Carboniferous successions in the UK, cyclical climate variation has also been suggested for the older Visean successions (Falcon Lang, 1999a, 1999b; Wright and Vanstone, 2001) and for younger Westphalian succession (Broadhurst et al., 1980). The variation in deltaic style between the Bearing Grit incised valley fill and Warley Wise Grit regressive succession provides a further suggestion of monsoonal conditions at the eastern margin of Pangaea during the Pendleian, and provide a differentiation between climatic conditions during sea-level rise and sea-level fall that has been predicted based on climate modelling of the Carboniferous (e.g. Peyser and Poulsen, 2008; Horton et al., 2012) but whose expression in outcrop has not, to date, been recognised.

4.6 Conclusions

Detailed facies descriptions of a coarse-grained fluvio-deltaic system in the Carboniferous Craven Basin, England, distinguish four different Gilbert-type foreset styles: (1) homopycnal suspension dominated foresets, (2) homopycnal grain flow dominated foresets, (3) hyperpycnal internally-laminated foresets, (4) hyperpycnal laminated foresets with superimposed bedforms or 'intrasets' migrating down-foreset. The formation of foresets with superimposed 'intrasets' are related to variations in shear stress and thus in the excess density of the river outflow. Estimates based on the reduction of the mean foreset angle in the hyperpycnal foreset types suggest relatively weak excess density for the fluvial outflow. Facies associations indicate that homopycnal suspension-dominated foresets occur in separate settings; the others occur together and are frequently associated with sediment-gravity-flow deposits. Sediment-gravity-flow deposits are observed in the fluvial domain, on foresets and in the toeset of the Gilbert-type deltas, and have been interpreted as derived from within the fluvial system rather than delta front failures. The alternation between these different foreset types and sediment-gravity-flows is interpreted to record different, incrementally higher fluvial flood stages. The occurrence of the sediment-gravity-flow-dominated Gilbert-type delta facies association is limited to an incised valley fill, whereas the suspension-dominated type occurs both at the top of the incised valley fill and within an overlying regressive succession. Based on the equatorial position of the Craven Basin and the location of its drainage basin in the seasonal tropics, the sediment-gravity-flow-dominated Gilbert-type delta association within the incised valley is tentatively linked to monsoonal river flood activity.

Chapter 5 Overview of the Controls on Facies and Sedimentary Architecture in the Carboniferous Central Pennine Basin

5.1 Abstract

The relative importance of external controls on the stratigraphic character of a sedimentary system depends strongly on the temporal and spatial scales at which it is evaluated. Methodologies presented in earlier chapters are applied to the Millstone Grit Group of the Carboniferous Central Pennine Basin in entirety. On a large scale, the Millstone Grit Group can be defined as a glacio-eustatically-influenced shelf margin that is predominantly controlled by long-term sea-level variation, major avulsions and long-term variations in subsidence rates. On short timescales, the interplay of bathymetry and sea-level fluctuations forms the most important control on stratigraphic development, which corresponds well with the hypotheses developed through analogue modelling and field study of the Pendleton Formation. Water depth in the receiving basin partially controls the depth of valley incision during sea-level fall, probably through more efficient incision on of the shelf margin. The deepest incised valleys are associated with the infill of the deepest depocentres within the Central Pennine Basin, and correspond to large turbidite fans. Shallower incised valleys occur on lower shelf clinoforms, and correspond to relatively small turbidite systems, qualitatively supporting the inference of variations in the efficiency of sediment transport. Broad erosional sheet sandstones result from rapid extension of the coastline during sea-level fall when the Central Pennine Basin is fully infilled, and occur as feeder systems to perched lowstand deltas; in both cases the fluvial system cannot incise into a shelf margin. The position of incised valleys is likely controlled by lateral variations in bathymetry and previous phases of deposition. Fluvial systems abandon former sites of rapid progradation and focus in areas where the shelf margin is located further upstream, promoting valley incision in these locations during subsequent sea-level falls. Lateral variations in the basin-margin morphology might form an important predictor of incised valley positions in settings similar to the Namurian Central Pennine Basin.

5.2 Introduction

Incised valleys are a common feature of the Millstone Grit Group of the Carboniferous Central Pennine Basin. Their character ranges from deep incised valleys containing Gilbert-type deltas near the valley mouth and fronted by major turbidite systems (e.g. Chapter 3; Hampson, 1997; Jones and Chisholm, 1997; Hampson et al., 1999), to more regular incised valleys filled by braided channel deposits (e.g. Martinsen, 1993; Church and Gawthorpe, 1994; Wignall and Maynard, 1996; Waters et al., 2008; Hampson et al., 1999), to very wide and shallow valleys or sheets filled by braided channelized sandstones (e.g. Maynard, 1992; Hampson, 1996; Hampson et al., 1999). In general terms, these incised valleys are related to sea-level fall but the variation between different valley types has not yet been explained consistently in terms of variable depositional circumstances.

From the Pendleian up to the Alportian, the Millstone Grit Group in the Central Pennine Basin is developed coevally with the Yoredale carbonate and siliciclastic cycles on the shelf located north of the Central Pennine Basin. Although a general northern provenance of the Millstone Grit fluvial system has been established for a long time (e.g. Sorby, 1859; Gilligan, 1919; Morton and Whitham, 2002), the relationship between the Pendleian - Alportian Millstone Grit fluvial system and the Yoredale system was not elucidated. Recently, Pendleian and Arnsbergian incised valley fills of the Millstone Grit Group have been recognised within the Yoredale succession (Chapter 3; Waters et al., 2014), providing a clear indication of the relationship between the Yoredale and Millstone Grit facies associations. The Yoredale facies are thought to form a highstand shelf - delta system, while the Millstone Grit forms a downdip lowstand shelf to shelf edge delta system that is fed while the Yoredale depositional area is bypassed and presumably emergent (Fig. 5.1). Simultaneously, small northward-draining fluvio-deltaic systems of the Morridge Formation (cf. Waters et al., 2009) shed sediments from the Wales-Brabant High into the southern parts of the Central Pennine Basin (e.g. Morton et al., 2014).

Within the Millstone Grit succession of the Central Pennine Basin ~50 goniatite marine bands occur, representing high amplitude maximum flooding surfaces. However, substantially fewer incised valleys are recognised, indicating that

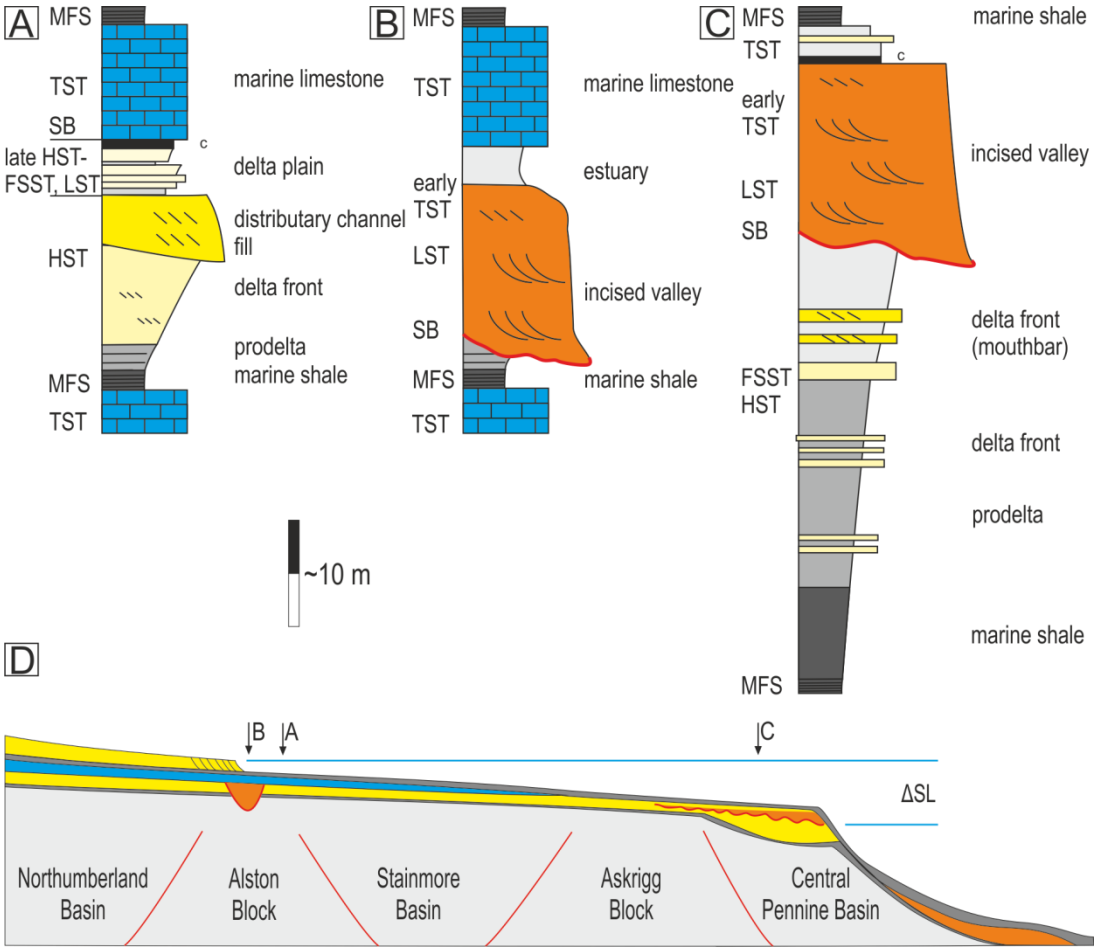

Figure 5.1 (a, b) Yoredale cycle with deltaic deposition during sea-level highstand and incision by Millstone Grit incised valley systems during falling stage (modified from Tucker et al., 2009). (c) Idealised Millstone Grit cycle in a shallow water setting. (d) Idealised relationship between Yoredale and Millstone Grit lithofacies assocations in a longitudinal section. Clastic depostion in the Yoredale succession predominantly reflects fine-grained highstand deposits. These systems are largely bypassed during deposition of the coarse-grained Millstone Grit sediments in the Central Pennine Basin during relatively low sea level. During transgression and highstand, formation of Yoredale Limestones indicates a switch-off of sediment supply that in the Central Pennine Basin is reflected by highly condensed marine bands.

they do not occur during each sea-level cycle or have not yet been recognized as such (e.g. Chapter 3; Waters and Condon, 2012). Typically, several sea-level cycles describe an increasingly sand-rich succession with incised valleys occurring in the higher cycles of such succession (e.g. Waters and Condon, 2012). This idea is encapsulated in the mesothem model (Ramsbottom, 1977a) and the major cyclothem

model (Martinsen et al., 1995). The mesothem model noticed increasingly sand-rich deposits during successive sea-level cycles on the Askrigg Block and Craven Basin, and linked this to the occurrence of major faunal renewals (i.e. new goniatite species) at the top of these sand-rich intervals. This indicated that major regressive events were followed by major transgressive events (Ramsbottom, 1977a). Flaws of this model have been debated in detail by Holdsworth and Collinson (1988), but in short indicate that the correlation of faunal renewal and major regressive events is not consistent. More recently, these major faunal renewals have been related to long-duration non-glacial periods (Waters and Condon, 2012). The major cyclothem model defines major cycles as bounded by the occurrence of long duration shale intervals, separating longer duration sequences in the Craven Basin for the Pendleian – Chokierian interval (Martinsen, 1990, 1993; Martinsen et al., 1995).

This chapter aims to elucidate the relative importance of additional controls besides sea level on the character of incised valleys based on the ideas developed in this thesis and available literature. The successive sub-basins of the Central Pennine Basin provide several deep depocentres separated by shallower segments, providing a repetition of similar basinal conditions that can be used to test the consistency of a basin depth control on the behaviour of the fluvio-deltaic system. Additionally, a comparison of the activity and sedimentary character is made between the Millstone Grit Group in the Central Pennine Basin, the Yoredale succession on the shelf, and the Morridge Formation in the southern part of the Central Pennine Basin.

5.3 Methods

The evolution of the approximate lowstand coastline in mapped on approximate mesothem-scale based on published literature and 1:50,000 geological maps of the British Geological Survey. This is combined with thickness estimates of the sedimentary succession, and the occurrence and character of incised valleys. This provides a framework in which the large-scale changes in character of the Millstone Grit Group can be discussed, as well as the hypotheses developed from analogue modelling (Chapter 2) and observations in the Pendleton Formation in the Craven Basin (Chapters 3 and 4).

Additionally, the character of the deposition in the Central Pennine Basin is compared to time-equivalent deposition on the Yoredale Shelf. The depositional character in this succession should reflect changes in the Central Pennine Basin, since they likely reflect different parts of a single depositional system.

5.4 Results

5.4.1 E_{1a} - E_{1c} zone (Pendleian; Fig. 5.2a)

This interval presents the lower part of major cycle MC1 (Martinsen et al., 1995) or mesothem N1 (Table 5.1; Ramsbottom, 1977a). This subdivision of mesothem N1 or major cycle MC1 results from the significantly further progradation of the coastline in the Bowland sub-basin during the E_{1c} period relative to subsequent sea-level cycles during the E_{2a} interval (cf. Fig. 5.2a and 5.2b).

In the Central Pennine Basin, the initial stage of infill by the Millstone Grit Group is associated with the Pendle Grit turbidite system during the $E_{1c}1$ cycle. The Pendle Grit system extended the lowstand coastline into a rapidly deepening basin that reached depths of ~300 m after the feeder of the Pendle Grit Member prograded ~10 - 15 km (Chapter 3; Fig. 5.2a). Subsequent valley incision resulted in a <500 m thick sand-dominated turbidite succession in the Bowland sub-basin, indicating substantial deepening southward (Chapter 3). The infill of the incised valley is referred to as the Bearing Grit and reaches a thickness of ~30 m and a width of 12 km on the northern side of the Askrigg Block, widening to >40 km downdip and obtaining thicknesses of ~85 m (e.g. Fig. 3.5; 3.8; 5.2a). Near the incised valley mouth, the Bearing Grit contains stacked Gilbert-type deltas, indicative of deposition during sea-level rise. Updip, the Bearing Grit incised valley probably extends in the Rogerley Channel on the Alston Block (Dunham 1990). Waters et al. (2014) suggest that the infill of the Rogerley Channel consists of two stacked incised valley fills, the lower of which incises into the Crag Limestone and could represent a feeder to the Pendle and Bearing Grits.

During the subsequent $E_{1c}2$ cycle, the Warley Wise Grit was deposited on the Askrigg Block and in the Craven Basin where it formed a relatively shallow-

Regional Sub-stage	Index	Ammonoid zone	Sub-Index	Diagnostic Ammonoid	Meso-them	Major Cycle	
Yeadonian	G_{1b}	Ca. cumbriense	$G_{1b}1$	Ca. cumbriense	N11		Fig. 5.4c
				Anthracoceras			Fig. 5.4b
	G_{1a}	Ca. cancellatum	$G_{1a}1$	Ca. cancellatum			
Marsdenian	R_{2c}	B. superbilinguis	$R_{2c}2$	V. sigma	N10		Fig. 5.4a
			$R_{2c}1$	B. superbilinguis			
	R_{2b}	B. bilinguis	$R_{2b}5$	B. metabilinguis	N9		Fig. 5.3d
			$R_{2b}4$	B. eometabilinguis			Fig. 5.3c
			$R_{2b}3$	B. bilinguis			
			$R_{2b}2$	B. bilinguis			
			$R_{2b}1$	B. bilinguis			
	R_{2a}	B. gracilis	$R_{2a}1$	B. gracilis			
Kinderscoutian	R_{1c}	R. reticulatum	$R_{1c}5$	-	N8		Fig. 5.3b
			$R_{1c}4$	R. coreticulatum			
			$R_{1c}3$	R. reticulatum			Fig. 5.3a
			$R_{1c}2$	R. reticulatum			
			$R_{1c}1$	R. reticulatum			
	R_{1b}	R.eoreticulatum	$R_{1b}3$	R. stubblefieldi	N7		Fig. 5.2d
			$R_{1b}2$	R. nodosum			
			$R_{1b}1$	R. eoreticulatum			
	R_{1a}	H. magistrorum	$R_{1a}5$	R. dubium	N6		
			$R_{1a}4$	R. todmordense			
			$R_{1a}3$	R. subreticulatum			
			$R_{1a}2$	R. circumplicatile			
			$R_{1a}1$	H. magistrorum			
Alportian	H_{2c}	V. eostriolatus	$H_{2c}2$	Hm. prereticulatus			
			$H_{2c}1$	V. eostriolatus			
	H_{2b}	Ho. undulatum	$H_{2b}1$	Ho. undulatum	N5		
	H_{2a}	Hd. proteum	$H_{2a}1$	Hd. proteum			
Chokierian	H_{1b}	H. beyrichianum	$H_{1b}2$	I. sp nov.	N4	MC3	Fig. 5.2c
			$H_{1b}1$ a - b	H. beyrichianum			
	H_{1a}	I. subglobosum	$H_{1a}3$	I. subglobosum			
			$H_{1a}2$	I. subglobosum			
			$H_{1a}1$	I. subglobosum			

Arnsbergian	E_{2c}	N. stellarum	$E_{2c}4$	N. nuculum	N3	MC2	Fig. 5.2c
			$E_{2c}3$	N. nuculum			
			$E_{2c}2$	N. nuculum			
			$E_{2c}1$	N. stellarum			
	E_{2b}	Ct. edalensis	$E_{2b}3$	Ct. nititoides	N2		
			$E_{2b}2$ a - c	Ct. nitidus			
			$E_{2b}1$ a - c	Ct. edalensis			
	E_{2a}	C. cowlingense	$E_{2a}3$	E. yatesae	N1	MC1	Fig. 5.2b
			$E_{2a}2\beta$	Anthracoceras			
			$E_{2a}2\alpha$	C. gressinghamense			
			$E_{2a}2$	E. ferrimontanum			
			$E_{2a}1$ a - c	C.cowlingense			
Pendleian	E_{1c}	C. malhamense	$E_{1c}2$	-			Fig. 5.2a
			$E_{1c}1$	C. malhamense			
	E_{1b}	C. brandoni	$E_{1b}2$ a - b	T. pseudobilinguis			
			$E_{1b}1$	C. brandoni			
	E_{1a}	C. leion	$E_{1a}1$ a - c	C.leion			

Table 5.1 Ammonoid zone stratigraphy and mesothem zones of Waters and Condon (2012). Inclusion of an Anthracoceras marine band based on Hampson et al. (1996). Major cycles based on Martinsen et al. (1995). Abbreviations for ammonoids B: Bilinguites, Ca: Cancelloceras, C: Cravenoceras, Ct: Cravenoceratoides, E: Eumorphoceras, H: Hodsonites, Hd: Hudsonoceras, Hm: Homoceratoides, Ho: Homoceras, I: Isohomoceras, N: Nuculoceras, R: Reticuloceras, V: Verneulites

---

Figure 5.2 (next page) Coastline reconstructions for (a) Late Pendleian, incised valley margins (red dashed line) based on Chapter 3, (b) Early Arnsbergian, red lines indicate area of minor valley incision, (c) Middle Arnsbergian to Chokierian interval, red lines indicate area of broad incision (d) Alportian to Middle Kinderscoutian, red lines indicate position of major channel belt complex of Steele (1988). Shaded area indicates the Millstone Grit Group outcrop belt. Grey lines indicate (inactive) tectonic lineaments that defined the structural template during the early Carboniferous. Numbers indicate 1) Lake District High, 2) Askrigg Block, 3) Lancaster Fells sub-basin, 4) Bowland sub-basin, 5) Harrogate sub-basin, 6) Cleveland High, 7) Rossendale sub-basin, 8) Huddersfield sub-basin, 9) Gainsborough Trough, 10) Holme High, 11) Derbyshire Basin, 12) Edale Gulf, 13) Goyt Trough, 14) Widmerpool Gulf, 15) East Midlands Shelf

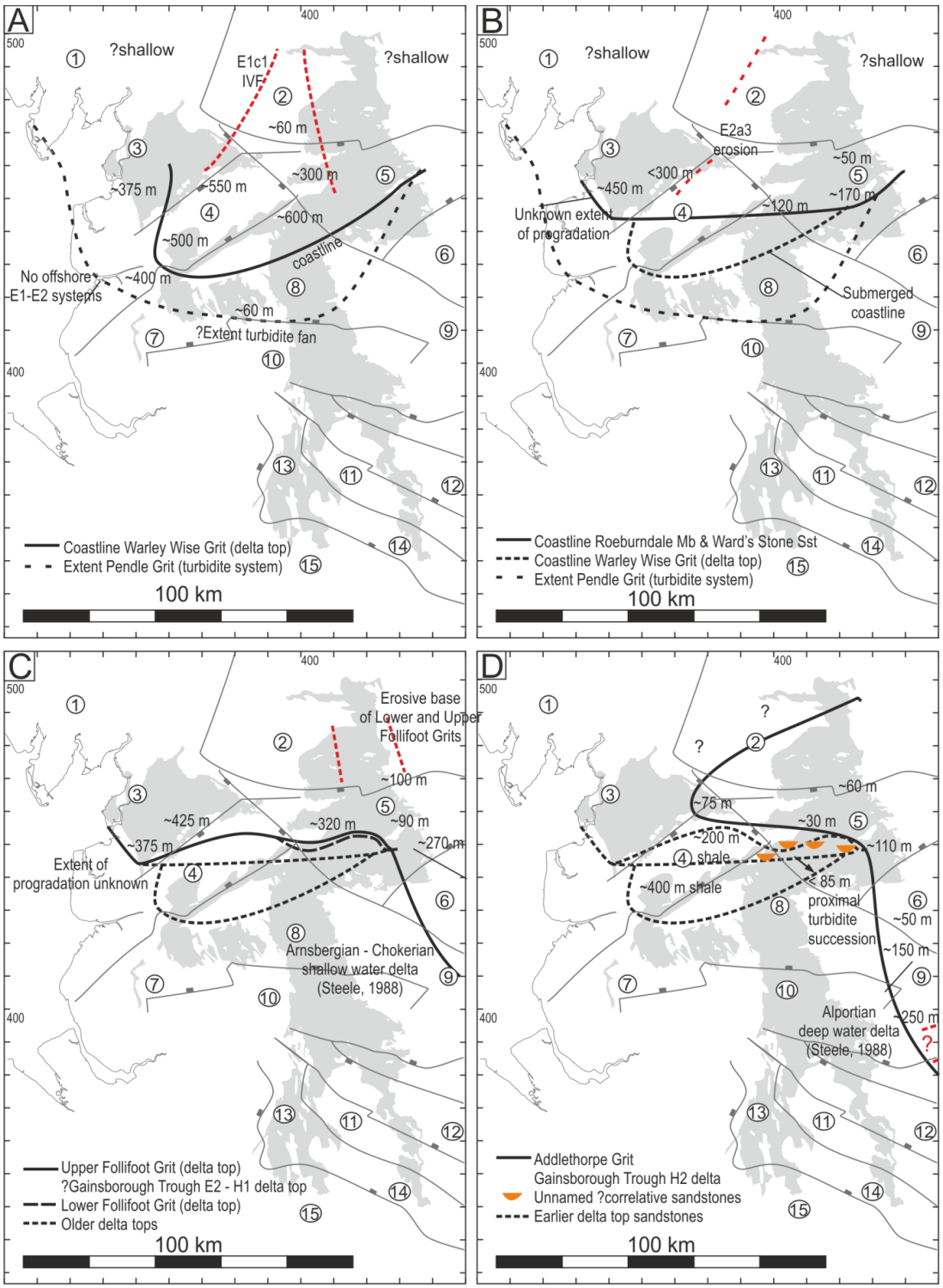

water deltaic system. The lowstand coastline prograded ~30 km into the Bowland sub-basin while in the Harrogate- and Lancaster Fells sub-basins the coastline shifted approximately ~7 km (Chapter 3; Fig. 5.2a).

In the Yoredale facies, this level coincides with the interval between the Great Limestone and the Corbridge Limestone (Brand, 2011). Besides the Rogerley

Channel infill (e.g. Elliot, 1976; Waters et al., 2014), the Rothley Grits represent an E_{1c} incised valley fill in the Northumberland Trough (Young and Lawrence, 1998; Waters et al., 2014). Additionally, an incised valley fill succession is recognised in the Northumberland Trough at Howick (e.g. Farmer and Jones, 1969; Lemon, 2006). In the south of the Central Pennine Basin, the turbiditic Minn Sandstones are deposited during the E_{1b} to E_{2a} interval (Morton et al., 2014).

5.4.2 E_{2a} zone (Early Arnsbergian, Fig. 5.2b)

This interval coincides with the upper part of mesothem N1 or major cycle MC1 (Table. 5.1; Ramsbottom, 1977a; Martinsen, 1993; Martinsen et al., 1995). During the early Arnsbergian (E_{2a}), deposition of the Millstone Grit Group was mainly restricted to the Askrigg Block and Craven Basin (e.g. Martinsen, 1993). Prodelta and distal delta slope deposits might have reached the northern side of the Gainsborough Trough (Steele, 1988).

In the Craven Basin, deposition of sand was focused in the western Lancaster Fells sub-basin and eastern part of the Harrogate sub-basin. In the Bowland sub-basin, sediment supply was limited and the coastline stepped back substantially (e.g. Martinsen, 1993). In the Lancaster Fells sub-basin, the Roeburndale Member is deposited on top of the previously deposited fluvio-deltaic Warley Wise Grit over multiple sea-level cycles ($E_{2a}1$ – $E_{2a}3$; Table 5.1; Brandon et al., 1998; Waters et al., 2009). It consists mainly of delta-slope siltstones and interbedded turbiditic sandstones, but also contains subordinate pro-delta mudstones and impersistent delta-top sandstones. The delta-top sandstones contain palaeosols, indicating emergence during successive sea-level lowstands. They occur in proximal locations at several intermediate levels, and are separated by tens to hundreds of metres of slope sediments, indicating high subsidence rates and resulting in an overall aggradational stacking pattern during this period (Brandon et al., 1998).

On the Askrigg Block, the Roeburndale succession is represented by the Upper Howgate Edge and Tan Hill Grits (Martinsen, 1993). The Upper Howgate Edge represents a minor incised valley fill on the western part of the Askrigg block and is characterised by relatively isolated erosionally-based channels. The overlying Tan Hill Grit represents a widespread, erosionally-based sheet sandstone (Martinsen, 1990).

Basinward, the Roeburndale Member consists entirely of slope facies and reaches thicknesses of 450 m (Aitkenhead et al., 1992). In the outcrop area of the Lancaster Fells sub-basin, the Roeburndale Member is entirely overlain by the fluvial Ward's Stone Sandstone ($E_{2a}3$). The latter unit probably represents an incised valley fill (Brandon et al., 1998; Waters and Condon, 2012) that extends beyond the outcrop belt. The potential downdip equivalent of the Ward's Stone Sandstone is unknown.

Laterally, the Roeburndale Member is not defined but in the Bradford area, a 90 – 240 m thick succession of similar lithology is reported below the Marchup Grit (Waters, 2000). The Marchup Grit ($E_{2a}2$) forms a major fluvio-deltaic sandstone deposited in the Harrogate sub-basin (Cooper and Burgess, 1993; Waters, 2000) and correlates to the Sapling Clough deltaic sandstone, an intermediate level within the Roeburndale Member (Brandon et al., 1995). In the Harrogate sub-basin, no sandstones are present at the stratigraphic level of the Ward's Stone Sandstone (e.g. Martinsen, 1990, 1993; Cooper and Burgess, 1993; Waters, 2000).

Brandon et al. (1995) correlate the Ward's Stone Sandstone of the Lancaster Fells sub-basin with the erosionally-based Red Scar Grit and Pickersett Edge Grit on the Askrigg Block, implying the occurrence of a major incised valley draining towards the Lancaster Fells sub-basin. However, currently ongoing mapping on the Pateley Bridge Geological Sheet 61 in the western Harrogate sub-basin suggest that the Red Scar Grit of the Askrigg Block might be correlated to the Red Scar/Marchup Grit of the Harrogate sub-basin (Waters, personal communication) as is also suggested in Cooper and Burgess (1993). Updip, the Red Scar Grit of the Askrigg Block potentially corresponds to the upper part of the Rogerley Channel (Waters et al., 2014).

Within the Yoredale facies, the E_{2a} interval coincides with the Corbridge and Thornbrough Limestones (e.g. Brand, 2011; Waters et al., 2014). In the Northumberland Trough, the Thornbrough Limestone is incised by the E_{2a} Shaftoe Grits incised valley fill succession (Young and Lawrence, 1998; Waters et al., 2014).

In the south of the Central Pennine Basin deposition of the turbiditic Minn Sandstones up to the $E_{2a}2$ subzone (Morton et al., 2014).

5.4.3 E_{2b} – E_{2c} zone (Middle to Late Arnsbergian, Fig. 5.2c)

This interval coincides with the N2 and N3 mesothems (Table 5.1; Ramsbottom, 1977a) and major cycle MC2 (Martinsen et al., 1995). The lower part of the E_{2b} zone (N2 mesothem) is shale-dominated and the upper part is only associated with the deltaic Nesfield Sandstone that is deposited in the Harrogate sub-basin (Martinsen, 1990; 1993; Cooper and Burgess, 1993; Waters, 2000). During this period, limited sediment supply reaches the Central Pennine Basin. Upstream, this period is correlated with the occurrence of the Newton and Styford Limestones in the Northumberland Trough (Brand, 2011; Waters et al., 2014). At the southern margin of the Central Pennine Basin the Hurdlow Sandstones present a minor influx of turbiditic sandstones that are time-equivalent to the Nesfield Sandstone (Morton et al., 2014).

In the Harrogate sub-basin, the E_{2c} zone (N3 mesothem) is capped by the deltaic Lower Follifoot Grit/Middleton Grit and corresponds to an erosionally-based fluvial sandstone on the Askrigg Block (e.g. Martinsen, 1993; Waters and Condon, 2012). Laterally, the Silver Hills deltaic sandstones are deposited in the Lancaster Fells sub-basin (Arthurton et al., 1988; Brandon et al., 1998). In the Lancaster Fells sub-basin and the eastern part of the Harrogate sub-basin the maximum extent of the lowstand coastline falls outside of the outcrop extent and cannot be determined. In the western part of the Harrogate sub-basin, the sandstone steps back with respect to the Marchup Grit coastline that was formed during the Early Arnsbergian.

The E_{2c} – H_2 period is not associated with Yoredale Limestones (Waters et al., 2014) and appears absent or corresponds to a condensed section (Dunham and Wilson, 1985; Dunham, 1990).

5.4.4 H_{1a} – H_{1b} zones (Chokierian, Fig. 5.2c)

This interval coincides with the N4 mesothem and major cycle MC3 (Table 5.1; Ramsbottom, 1977a; Martinsen et al., 1995). It is capped by the Brocka Bank/Upper Follifoot Grit deltaic sandstones (Martinsen, 1993; Cooper and Burgess, 1993; Martinsen et al., 1995; Waters, 2000; Waters and Condon, 2012). On the southern Askrigg Block, the Upper Follifoot Grit overlies marine mudstones and is associated with the development of pedogenically modified lateral interfluves (Martinsen, 1993), suggesting that this sandstone represents a minor incised valley

(Waters and Condon, 2012). In the western part of the Harrogate sub-basin, the coastline retrogrades slightly or aggrades vertically with respect to the previous Lower Follifoot Grit coastline, while the coastlines in the Lancaster Fells and eastern Harrogate sub-basins cannot be determined due to the outcrop extent. In the Gainsborough Trough, a major shallow water delta system arrives from a north-easterly direction during the Arnsbergian-Chokierian period (Fig. 5.2c; Steele, 1988), although chronostratigraphic constraints are too limited for detailed correlations to the Craven Basin.

5.4.5 H_{2a} – R_{1b} (Alportian – Middle Kinderscoutian, Fig. 5.2d)

This interval coincides with the N5 – N7 mesothems (Table 5.1; Ramsbottom, 1977a) and has not been defined according to the major cyclothem model (Martinsen et al., 1995). The N5 mesothem (Alportian, H_{2a} – H_{2b}) is not associated with sandstone deposition but is solely defined on the occurrence of the *Hudsonoceras* and *Homoceras* goniatites (Table 5.1). In the Gainsborough Trough however, the Alportian period probably corresponds to the deposition of a large turbidite-fronted delta system (Steele, 1988), fed by an E-W trending, >10 km wide channel belt complex that probably represents an incised valley (Fig. 5.2d). This coincides with the occurrence of the fluvio-deltaic to turbiditic Cheddleton Sandstones on the southern margin of the Central Pennine Basin (Morton et al., 2014).

The overlying N6 mesothem (H_{2c} – R_{1a}) is characterised by some sandstones at intermediate levels in the Lancaster Fells and Garstang areas although their precise position with respect to individual marine bands is ill-constrained (e.g. Brandon et al., 1998). In the Yoredale area, this period broadly coincides with deposition of the Dipton Foot Shell bed (R_{1a} – R_{1c}) (e.g. Brand, 2011; Waters et al., 2014). In the southern Central Pennine Basin, the Kinderscoutian (R_{1a} –R_{1c} zone) is represented by the fluvio-deltaic to turbiditic Kniveden Sandstones (Morton et al., 2014).

During the N7 mesothem (R_{1b}), the succession becomes increasingly sand-rich, which is represented by the Libishaw Sandstone on the Askrigg Block, and the Addlethorpe Grit in the Harrogate sub-basin (Cooper and Burgess, 1993). Potentially, this succession correlates to the Knott Copy Grit in the Lancaster Fells

sub-basin close to the Askrigg Block margin, which would imply a basin wide sandstone occurrence of this deltaic system (Fig. 5.2d; Arthurton et al., 1988; Brandon et al., 1998). Additionally, in this approximate stratigraphic interval an unnamed <85 m thick proximal turbidite channel succession is formed in the western part of the Harrogate sub-basin, near the transition to the Central Lancashire High and Bowland sub-basin (Waters, 2000). Formerly this unnamed interval was referred to as the Addlethorpe Grit (Stephens et al., 1953).

5.4.6 R_{1c} zone (Late Kinderscoutian, Fig. 5.3a, b)

The late Kinderscoutian coincides with Mesothem N8 and forms a period of large sediment input in the Central Pennine Basin (Table 5.1; Ramsbottom, 1977a). During 5 sea-level cycles, 4 major sandstones successions are deposited in the Central Pennine Basin, resulting in a ~70 km southward shift of the coastline over a period of ~ 1 Myr (Fig. 5.3a, b; Waters and Condon, 2012).

The fluvial Addingham Edge Grit occurs in the western part of the Harrogate sub-basin and the proximal part of the Bowland sub-basin (Fig. 5.3a; Waters, 2000). This stratigraphic level is associated with substantial progradation of the coastline into the Rossendale sub-basin. It is correlated to the turbiditic Parsonage Sandstone that crops out in the Rossendale and Huddersfield areas and to the areas west of the Central Pennine Basin (Fig. 5.3a; e.g. Earp et al., 1961; Waters, 2000). In the central part of the East Irish Sea Basin (offshore), turbiditic sandstones equivalent to the Parsonage Sandstone occur, overlain by argillaceous deposits equivalent to later Kinderscoutian deposits (Waters et al., 2011).

This succession is followed by the Long Ridge Sandstone ($R_{1c}3$) and the Doubler Stones Sandstone ($R_{1c}4$) in the western Harrogate sub-basin (Fig. 5.3b; Waters, 2000), which southward form the Lower Kinderscout Grit, and are correlated to the turbiditic Todmorden Grit in the Rossendale sub-basin (Fig. 5.3a). Hampson (1995, 1997) interpreted two major incised valleys within the Lower Kinderscout Grit succession (LKG sandstone 6; LKG sandstone 8) and these might correspond to the above sandstones. LKG sandstones 1 -5, and LKG sandstone 7 occur below these incised valley fills and represent clinoforms fronted by a turbidite system that indicate substantial progradation prior to valley incision (Hampson, 1995, 1997). They are here considered similar to the Surgill Sandstones of the

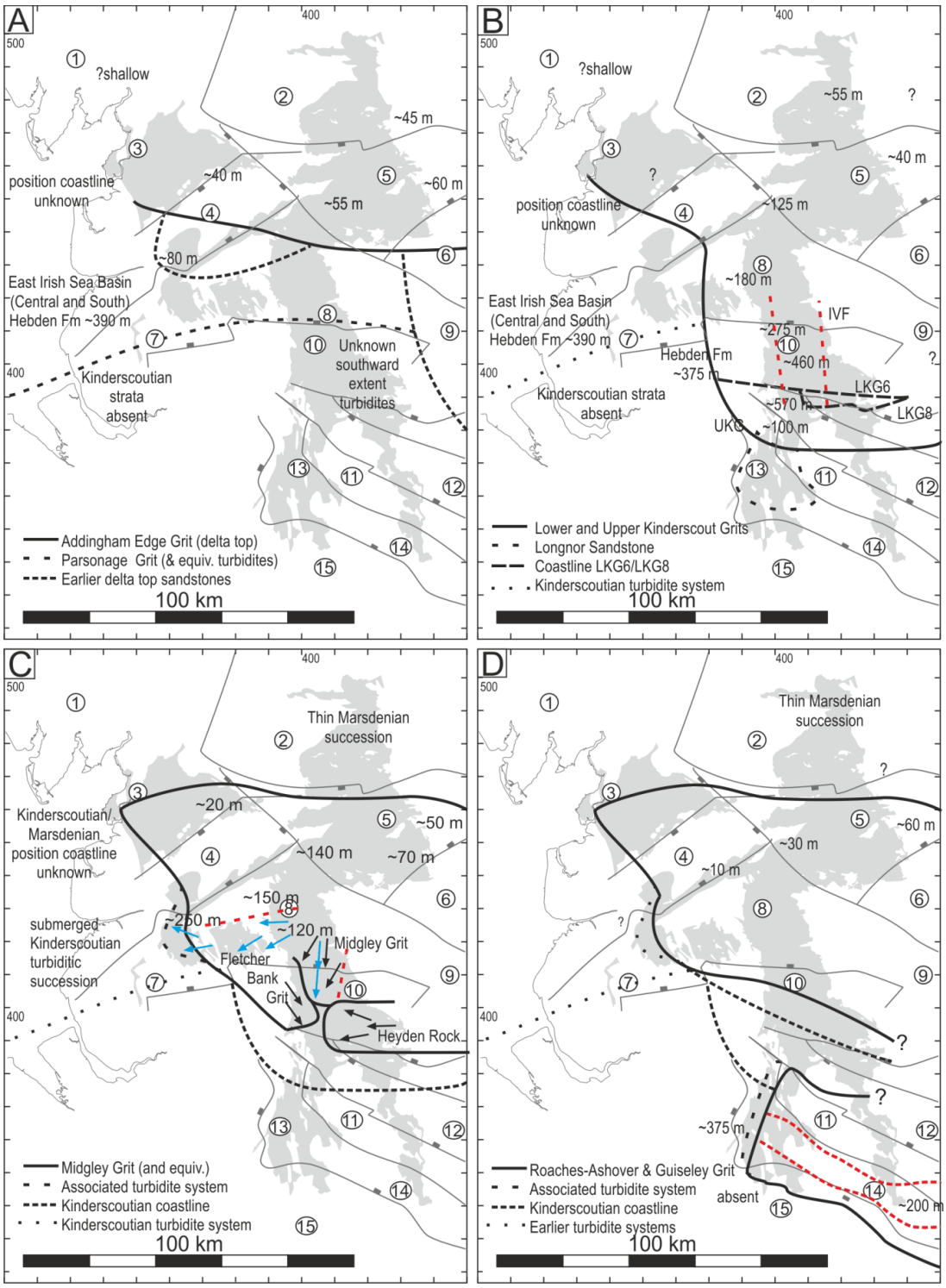

Figure 5.3 Approximate coastline reconstructions for (a) Upper Kinderscoutian, (b) Upper Kinderscoutian, red lines indicate approximate area of valley incision in the Lower and Upper Kinderscout Grits, (c) Early Marsdenian, blue arrows indicate flow directions, and red lines indicate approximate valley position based on Church (1994), black arrows indicate flow directions based on Waters et al. (2012), (d) Middle Marsdenian, incised valley position based on Jones and Chisholm (1997) . See text for discussion on stratigraphic intervals.

Pendle Grit system (Chapter 3). LKG 6 forms a prominent incised valley that fed a lowstand turbidite fan (i.e. the Mam Tor and Shale Grit turbidite systems; Hampson, 1997). The infill of this valley is associated with the occurrence of stacked Gilbert-type deltas and reaches into the Edale Gulf. The LKG8 incised valley extends further downdip into the Edale Gulf. Both incised valleys rapidly increase in thickness downdip. In LKG6 and LKG8, the incised valley fills reach thicknesses of up to ~150 m and ~55 m, respectively (Hampson, 1997).

In the western Harrogate sub-basin, the succeeding sea-level cycle is characterised by the High Moor Sandstone, which is equivalent to the Upper Kinderscout Grit (Waters, 2000). The Upper Kinderscout Grit forms another incised valley fill in the Huddersfield – Edale area (e.g. Hampson, 1997), and onlaps the Derbyshire High. It is correlated to the turbiditic Longnor Sandstone in the Goyt Trough and western margin of the Widmerpool Gulf (Fig. 5.3b; e.g. Collinson, 1988).

On the Askrigg Block, in the Lancaster Fells sub-basin, and the eastern Harrogate sub-basin, marine band control is too limited to allow a correlation of individual sandstones. However, fluvio-deltaic sandstones are deposited throughout these areas during the Late Kinderscoutian (Fig. 5.3b; e.g. Cooper and Burgess, 1993; Brandon et al., 1998).

In the Northumberland to Stainmore Trough, the Dipton Foot Shell bed is generally overlain by intermittently developed Millstone Grit type sandstones, indicating that the Millstone Grit has replaced the Yoredales as the dominant lithofacies (Waters et al., 2014). The Millstone Grit sandstones of Kinderscoutian are coarse-grained fluvial sandstones with sharp bases but are generally not marked by major erosional surfaces. They form a succession of several 10s of metres and are typically referred to as the First Grit (e.g. Waters et al., 2014).

5.4.7 R_{2a} – R_{2b}3 interval (early Marsdenian, Fig. 5.3c)

This interval forms the lower part of Mesothem N9 (Table 5.1; Ramsbottom, 1977a). During this period, sediment supply from the Millstone Grit fluvial system shifted from a predominantly northern source to a more easterly route (e.g. Jones and Chisholm, 1997; Waters et al., 2008).

At the base of the N9 mesothem ($R_{2a}1$) the Alum Crag Grit turbidite system is deposited in the southern part of the Bowland sub-basin (Brettle et al., 2002). Deposition of this turbidite system occurs on top of the Kinderscoutian Todmorden Grit turbidite system and downdip of the late Kinderscoutian coastline.

During the successive $R_{2b}1$ cycle, the Readycon Dean Flags and erosionally-based East Carlton Grit form a single fluvio-deltaic succession (Brettle et al., 2002) that probably corresponds to the turbiditic Howells Head Flags (Wignall and Maynard, 1996).

A subsequent major sandstone interval occurs during the $R_{2b}3$ sea-level cycle. During this period, three major sandstones bodies with distinct flow directions, the Midgley Grit, Fletcher Bank Grit and Heyden Rock Grits are deposited (Fig. 5.3c; Waters et al., 2012), resulting in the creation of a marked erosional surface that has been interpreted as an incised valley system (e.g. Wignall and Maynard, 1996; Brettle et al., 2002). Outcrops in the Bowland – and Huddersfield sub-basin indicate a west to southern flow directions (Fig. 5.3c; Church, 1994), resulting in the formation of a ~100 m correlative turbidite fan deposit that is deposited on top of the Alum Crag Grit turbidite succession (Fig. 5.3c). This is based on a section in the Blackburn Sewer Tunnel (Collinson et al., 1977).

On the Holme High a different succession is deposited (Fig. 5.3c; Waters et al., 2012). Here, the Fletcher Bank Grit forms a coarse-grained sandstone, deposited by a south-eastward flowingfluvio-deltaic system that occurs in the Bowland and Huddersfield sub-basins and pinches out on the western part of the Holme High (Fig. 5.3c; e.g. Earp et al., 1961; Waters et al., 2012). The Midgley Grit was formed by a southward flowing fluvio-deltaic system (Waters et al., 2012) and records a downstream fining to fine-grained turbiditic strata that occur at the base of the succession in distal locations. The Heyden Rock forms a coarse-grained to pebbly sandstone formed by a westward flowing fluvio-deltaic system (Waters et al., 2012).

The Marsdenian succession in the central and southern part of the Irish Sea Basin is ~360 m thick and might (in part) correspond to this period (Waters et al., 2011), indicating substantial westward progradation during the Marsdenian period in general.

5.4.8 $R_{2b}4 – R_{2b}5$ interval (Middle Marsdenian, Fig. 5.3d)

This interval forms the upper part of the N9 mesothem (Table 5.1; Ramsbottom, 1977a). The $R_{2b}4$ cycle is not characterised by sandstone deposition in the Central Pennine Basin. During the $R_{2b}5$ sea-level cycle, the Roaches -Ashover Grit in the Widmerpool Gulf (Fig. 5.3d; e.g. Jones and Chisholm, 1997) and the Guiseley Grit in the northern part of the Central Pennine Basin form time-equivalent sand bodies separated by a small area along the outcrop belt lacking sandstones (Fig. 5.3d; e.g. Waters and Davies, 2006; Waters et al., 2008). The Roaches-Ashover Grit forms a major SE-NW trending incised valley fill succession characterised by stacked Gilbert-type deltas in the Widmerpool Gulf, and fronted by a sand-rich turbidite fan up to 375 m thick (e.g. Jones and Chisholm, 1997). The time-equivalent deltaic Guiseley Grit (e.g. Waters, 2000) forms a shallow water succession deposited on the former Kinderscoutian and Marsdenian shelf areas (Fig. 5.3d). During the $R_{2b}5$ cycle, the southerly-sourced Brockholes Sandstone represents a shallow water deposit that interdigitate with the Roaches Grit (Morton et al., 2014).

5.4.9 R_{2c} interval (Late Marsdenian, Fig. 5.4a)

This interval coincides with the N10 mesothem (Table 5.1; Ramsbottom, 1977a). No sand bodies are known for the initial $R_{2c}1$ cycle. During the subsequent $R_{2c}2$ cycle, the Brooksbottom Grit and Huddersfield White Rock form major deltaic sandstones that are deposited in large parts of the Central Pennine Basin (Fig. 5.4a; Waters et al., 2008). This is incised by the Chatsworth Grit, a major incised valley fill that drains towards the southeast of the Central Pennine Basin (Fig. 5.4a; Waters et al., 2008). This valley reaches dimensions of ~30 m depth and ~20 km width in proximal locations and ~55 m depth and ~33 km width downstream (Waters et al., 2008). The downdip equivalent of the Chatsworth incised valley fill is located outside of the outcrop area and is therefore unknown (Fig. 5.4a).

5.4.10 $G_{1a} – G_{1b}$ interval (Yeadonian, Fig. 5.4b,c)

This interval coincides with the N11 mesothem (Table 5.1; Ramsbottom, 1977a). The lower part of the succession consists of the Lower and Upper Haslingden Flags in the west of the Central Pennine Basin while all other areas are typically represented by a thick mudstone-dominated succession. The Haslingden Flags form

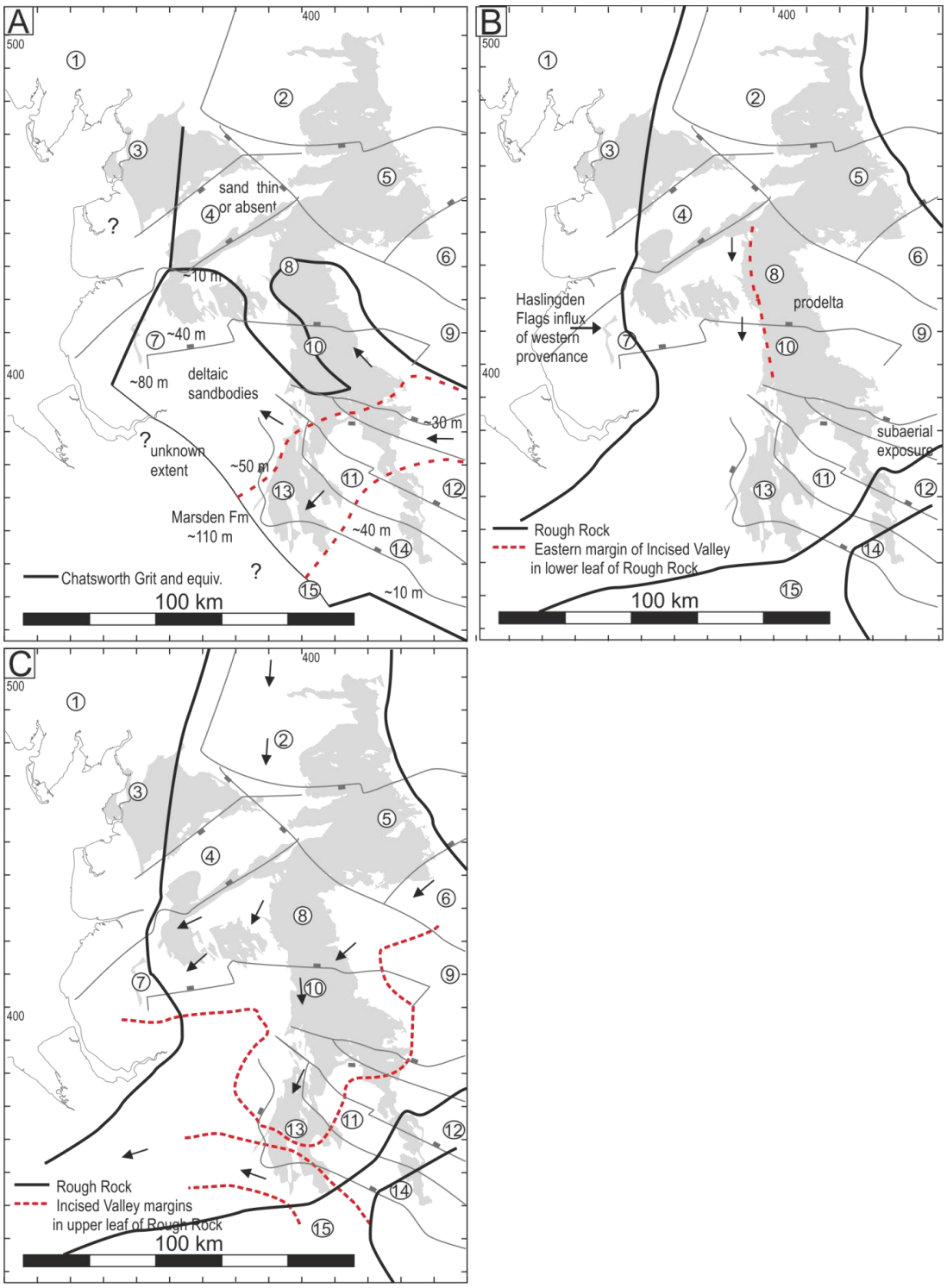

Figure 5.4 Approximate coastline reconstructions for (a) Upper Marsdenian, valley position based on Waters et al. (2008), (b) Yeadonian, valley margin for lower leaf Rough Rock based on Hampson et al. (1996). Depositional outline based on Hallsworth and Chisholm (2008). (c) Yeadonian, valley margins for upper leaf Rough Rock based on Hampson et al. (1996). See text for discussion

relatively fine-grained, elongate deltaic sandstones deposited during relatively high sea-level conditions (e.g. Collinson and Banks, 1975; Maynard, 1992; Hampson et al., 1996), and have a distinct westerly provenance (e.g. McLean and Chisholm, 1996). The Upper Haslingden Flags are followed by a coarse-grained, lower interval of the Rough Rock Grit in the western part of the Central Pennine Basin (Fig. 5.4b; Bristow, 1988, 1993a; Hampson et al., 1996) and has been interpreted as a shallow and wide N-S trending incised valley (Hampson et al., 1996). During the subsequent cycle, the upper part of the Rough Rock forms another broad and shallow incised valley system, supplied mainly from a northerly river system. An additional, smaller incised valley system is present on the tectonically-influenced East Midland Shelf that is supplied by an easterly river system of northern provenance (Fig. 5.4c; Hampson et al., 1996; Church and Gawthorpe, 1994; Hallsworth and Chisholm, 2008). Potentially, this easterly branch also contains some sediment from a southern provenance (Morton et al., 2014). Notably, the wide and shallow incised valley fills from the northerly fluvial system thin down dip, whereas downstream thickening is a more common pattern for incised valley fills (cf. Hampson et al., 1996).

Northward, in the Northumberland Trough and on the Alston Block, this system is typically referred to as the Second Grit and forms a similar succession as the First Grit (Waters et al., 2014).

5.5 Discussion

The relevance of individual external controls on the stratigraphic character of a sedimentary system strongly depends on the duration and strength of forcing mechanisms, as well as the scale at which a system is analysed. First, the large-scale patterns in the Namurian succession are discussed, before focussing on the relative importance of external controls on incised valley formation.

5.5.1 Shelf margin construction

During the Early Carboniferous the area located north of the Craven Fault System behaved differently from the Central Pennine Basin to the south. In the Midland Valley, Northumberland Trough, and Stainmore Trough (Fig. 3.1), sedimentation rates were sufficiently high to maintain shallow water conditions

during the syn-rift phase of the Carboniferous extensional province in southern Scotland and Northern England. Meanwhile, carbonate ramps in the Central Pennine Basin gradually drowned at various stages during the Early Carboniferous, after which slow hemipelagic sedimentation resulted in a progressive deepening of the basin up to the Late Pendleian (Fig. 5.5; e.g. Evans and Kirby, 1999; Waters and Davies, 2006; Waters et al., 2009). The difference between the Central Pennine Basin and the northward located areas has been related to the occurrence of granite intrusions in the Alston and Askrigg Blocks that might have increased their buoyancy and integrity (Fig. 5.5; e.g. Bott, 1961; Leeder et al., 1989) but might also be related to the general northern provenance of clastic sediment, implying that these northern areas regularly received clastic sediment while the Central Pennine Basin was starved of clastic sediment (cf. Fraser and Gawthorpe, 2003).

From the Asbian up to the Late Pendleian, the Midland Valley to the Craven Fault System can be defined as a shelf, rather than separate basins as relatively thin, continuous limestone and clastic intervals (i.e. Yoredale cycles) are deposited throughout this area. Shelves form an integral part of shelf margin systems and can be defined morphologically as shallow marine platforms adjacent to deeper basin of hundreds or thousands of metres depth, separated by a slope of substantially steeper gradient than the shelf (Porebski and Steel, 2003; Helland-Hansen et al., 2012). A recent classification subdivides between structural shelves, in which the shelf-edge is a structural feature; sedimentary shelves, resulting from differential sediment supply that triggers a progradation of the break of slope close to the coastline; and combined sedimentary – structural shelves in which a shelf is constructed as a structural shelf and propagated as a sedimentary shelf (Helland-Hansen et al., 2012).

Following the above classification, the Carboniferous succession in northern England can be described as a combined sedimentary – structural shelf. During the Asbian – early Pendleian, the shelf edge was maintained at the Craven Fault System (Fig. 5.5). Deposition of the Yoredale Group did not propagate the shelf edge but did infill minor shelf topography resulting from differential subsidence.

Figure 5.5 (next page) Schematic cross section of the Central Pennine Basin and northward located shelf indicating the discussed stratigraphic intervals.

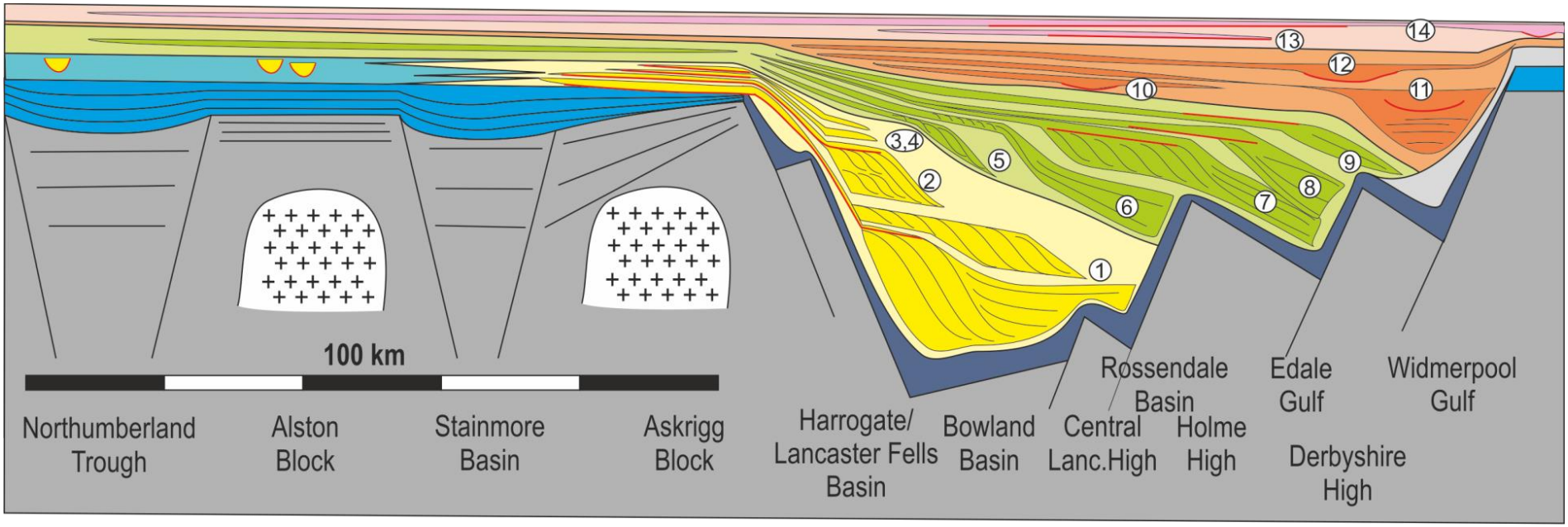

Asbian - Brigantian Yoredale facies
Asbian - Pendleian Bowland Shale Fm
Pendleian - Alportian Yoredale facies
Pendleian - Alportian Millstone Grit Gp (Pendleton - Samlesbury Fm)
Kinderscoutian Millstone Grit (Hebden Fm)
Marsdenian Millstone Grit Gp (Marden Fm)
Yeadonian Millstone Grit Gp (Rossendale Fm)
Southerly derived systems (undifferentiated)

1) E1c interval - Pendle Grit Mb and Warley Wise Grit
2) E2a interval - Roeburndale Mb and Ward's Stone Sst
3) E2b - E2c interval - Lower Follifoot Grit
4) H1a - H1b interval - Upper Follifoot Grit
5) H2a - R1b interval - Addlethorpe Grit
6) R1c interval - Addingham Edge Grit
7) R1c interval - Lower Kinderscout Grit 6
8) R1c interval - Lower Kinderscout Grit 8
9) R1c interval - Upper Kinderscout Grit
10) R2a - R2b3 interval - Midgley Grit
11) R2b4 - R2b5 interval - Roaches-Ashover Grit
12) R2c interval - Chatsworth Grit
13) G1a - G1b interval - Lower leaf Rough Rock
14) G1a - G1b interval - Upper leaf Rough Rock

North of the Craven Fault System, the shelf extended at least to the northern margin of the Northumberland Trough, suggesting a minimum shelf width of ~160 km, parallel to SSW flow directions. Notably, the Southern Uplands that form the northern boundary of the Northumberland Trough transitioned eastward into a shelfal area (e.g. Fig. 3.1; Waters et al., 2009), implying that offshore Scotland the shelf might have extended further northward. Crude estimates place the highstand coastline (i.e. above which no marine influences are observed) near the northern margin of the Midland Valley (Cope et al., 1992), suggesting a maximum shelf width of >250 km orthogonal to the Craven Fault System parallel to SSW flow directions.

Such wide shelves are difficult for fluvial systems to traverse unless sea level falls below shelf edge (Muto and Steel, 2002b). If sea level remains above or at the shelf break, the rapidly increasing length of the fluvial system would make it less efficient at transporting sediment (Chapter 3), while increasing volumes of sediment are required to maintain progradation of the coastline (e.g. Muto et al., 2007).

During the Asbian –Brigantian period, sea-level variations were limited: 10 – 50 metres (Wright and Vanstone, 2001) or less than 30 m (Rygel et al., 2008; Davies, 2008). Incisional channels in the Yoredale succession of this stratigraphic interval are rare (Burgess and Mitchell, 1975), which suggests that sea level probably did not frequently or significantly fall below shelf edge, and might explain the rare entry of siliciclastic sediment on the northern margin of the Central Pennine Basin.

The Pendleian coincides with the first major phase of Gondwanan glaciation on the Southern Hemisphere (e.g. Davies, 2008; Waters and Condon, 2012). At this stage, sea-level fluctuations reach higher amplitudes and estimates range from 60 - 100 metres (Rygel et al., 2008), or 65 ± 15 m (Crowley and Baum, 1991). Such sea-level variations are capable of lowering sea level significantly below shelf edge, resulting in incised valleys. In these valleys, the fluvial system is confined and maintains a steep fluvial gradient, facilitating sediment transport across a wide shelf into the Central Pennine Basin. This does not exclude the inference of tectonic changes in the source area (Morton and Whitham, 2002), or changes in sediment yield due to increased precipitation in the source area (Cliff et al., 1991) as a cause

for the origin of the Millstone Grit Group, but enhances the likelihood of sediment transport to reach the Central Pennine Basin.

On the multi-million year timescale of shelf construction and propagation into the Central Pennine Basin, regional tectonics and long term evolution in the magnitude of sea-level variations are considered as dominant forcing mechanisms.

5.5.2 Large-scale shelf margin propagation

During the Namurian, the shelf edge propagated southward, fed by the sediment supply of the Millstone Grit fluvial system during periods of low sea level. This system infilled successive sub-basins diachronously, resulting in a ~115 km southward shift of the lowstand coastline over a ~13 Myr duration of the Namurian (Fig. 5.5; Ramsbottom, 1966), which is similar to the rates seen in many small shelf margin systems (e.g. Carvajal et al., 2009).

In cross section, the succession in the Central Pennine Basin can be subdivided into two major phases: the Pendleian – Alportian and the Kinderscoutian - Yeadonian. During the Pendleian, a major influx of sediment supply entered at the northern margin of the basin, after which during the Arnsbergian to Alportian period, deposits of successive sea-level cycles stack in an aggradational or retrogradational pattern (Fig. 5.5). Notably, the poorly-constrained data of the Gainsborough Trough indicates that the coastline did prograde during the Arnsbergian – Alportian period eastward of the outcrop belt in the Central Pennine Basin, indicating marked lateral differences.

A second major phase of sediment input occurs from the Late Kinderscoutian up to the Yeadonian. During this period, deposits in successive cycles form a predominantly progradational pattern (Fig. 5.5). The Late Kinderscoutian phase forms a period of high sediment input during which the coastline is rapidly shifted southward (Fig. 5.5). On the shelf area where initially the Yoredale cycles were formed, this phase of progradation is reflected by the widespread deposition of Millstone Grit Group sediments of several 10’s of metres, referred to as the First Grit (Waters et al., 2014), representing the topset of a shelf clinoform.

The Marsdenian succession follows continuously on the Kinderscoutian succession in the Central Pennine Basin but is characterised by a shift in the inflow direction of the fluvial system (Fig. 5.5). The Pendleian to early Marsdenian deposits were derived from a north to north-easterly river system and resulted mainly in a southward shift of the coastline. During deposition of the Late Marsdenian succession sediment supply is shifted to a dominant easterly fluvial system, resulting in a westward progradation of the coastline (Fig. 5.3c, d; 5.4a). Notably, the easterly river system has a similar provenance to the northerly system, suggesting that this shift represents a major upstream avulsion and not an entirely different fluvial system (e.g. Chisholm and Hallsworth, 2005: Waters et al., 2008). Additionally, increasingly active fluvial systems start to supply sediment from southern source areas as well (Chisholm and Hallsworth, 2005: Waters et al., 2008). During the Marsdenian, the remaining basinal areas, such as the Widmerpool Gulf and areas west of the main Millstone Grit outcrop belt were infilled (Fig. 5.5). On the onshore section of the Yoredale Shelf, the Marsdenian succession is largely absent (Dunham and Wilson, 1985; Dunham, 1990) implying that the fluvial system was located further eastward.

The Yeadonian succession follows continuously on the Marsdenian succession. The main river system reverts to a northern route while an additional fluvial system of northern provenance enters through the Widmerpool Gulf (Fig. 5.4b, c; Hallsworth and Chisholm, 2008). Notably, the Lower and Upper Haslingden Flags indicate a distinct, western or southern source (McLean and Chisholm, 1996) implying that basinal areas in these directions were infilled and spilling into the Central Pennine Basin. At this period the entire Central Pennine Basin is characterised by shallow water conditions, implying that no shelf clinoform is present anymore (Fig. 5.5). On the Yoredale shelf area, the Yeadonian interval broadly coincides with the deposition of a sandstone-dominated interval that is commonly referred to as the Second Grit (Waters et al., 2014).

During the Namurian, three major glaciation periods, C1 during the Pendleian – Middle Arnsbergian; C2 during the Chokierian – Alportian; and C3 during the Late Kinderscoutian – Westphalian period occurred (Waters and Condon, 2012; cf. Fielding et al., 2008). The Late Arnsbergian and Early to Middle Kinderscoutian represent periods of minor sea-level fluctuations and sea-level highstand. The Pendleian – Middle Arnsbergian is associated with the infill of the

Craven Basin, followed by deposition in the Gainsborough Trough during the Chokierian and Alportian. From the Late Kinderscoutian onwards, the remainder of the Central Pennine Basin is infilled. During the intermediate periods, only minor amounts of clastic sediment are supplied. On the Yoredale shelf area this is indicated by the Middle Arnsbergian (E_{2b}) Styford and Newton Limestones, and Early to Middle Kinderscoutian ($R_{1a} – R_{1b}$) Dipton Foot Shell Bed (Waters et al., 2014). In the Central Pennine Basin, these periods are characterised by the deposition of thick shale successions. Periods of high sediment input of northern provenance are mirrored by the smaller systems along the southern margin of the Central Pennine Basin. This suggests a basin wide control on sediment input, which is most easily explained by eustatic sea-level variations.

Large-scale avulsions in the position of the Millstone Grit fluvial system between a northerly and easterly route forms an additional major control on the infill of the Central Pennine Basin. Tectonic reorganisations in the fluvial domain upstream of the shelf area are unknown and cannot be ruled out as a controlling mechanism. However, during the Namurian the shelf itself was dominated by gradual thermal subsidence during the upper part of the Namurian (e.g. Johnson, 1984) and tectonic activity is limited to local strike-slip faulting near the boundary between the Southern Uplands and the Northumberland Trough in the Canonbie area (Chadwick et al., 1995; Waters et al., 2014). This makes a tectonic cause for these avulsions unlikely, since modelling of lateral tectonic tilting suggest that significant tectonic movements are required, particularly in highly mobile braided systems (Sheets et al., 2002; Hickson et al., 2005; Kim et al., 2010). It is here suggested that these large-scale shifts in the position of the fluvial system do not necessarily reflect an external control but might simply result from aggradation of the fluvial systems. Deposition of the First and Second Grit successions will have resulted in several tens of metres of regional aggradation in the position of the channel belt complexes. Presumably, the rates of deposition outside these braid belts is less substantial, which would lead to super elevation of the channel belt and subsequent shifts in their position. Recent modelling of channel stacking patterns (e.g. Straub et al., 2009; Wang et al., 2011; Straub and Wang, 2013) might provide further insight into the large-scale organisation of such channel belts.

Finally, subsidence rates appear to have reduced during the Namurian. In the Bowland and Lancaster Fells sub-basins, subsidence rates during the Pendleian –

Arnsbergian phase appear substantially higher than during later periods (cf. Kirby et al., 2000). This is also apparent from the large thickness of the Roeburndale Member, which is deposited on top of the former Warley Wise Grit delta top (Brandon et al., 1998). Such high rates might have prevented progradation of the coastline due to the creation of substantial accommodation space on the topset, resulting in an aggradational to retrogradational stacking pattern. Subsequent lower subsidence rates are well-illustrated by the relatively thin succession between the Late Arnsbergian Lower Follifoot Grit and the Chokierian Upper Follifoot Grit, which are separated by a 12 – 45 m thick succession (Cooper and Burgess, 1993; Waters, 2000) while probably representing a period of ~4 Myr (Waters and Condon, 2012).

5.5.3 Effect of variations in basin depth on valley incision

In Chapter 2, the curvature and gradient on the fluvial profile are related to basin depth and sea-level variations, and considered responsible for changes in the efficiency of sediment transport of both coarser-grained sediment, and larger volumes. Additionally, the efficiency and likelihood of incised valley formation is coupled to basin depth. Chapter 3 documents valley incision in the shelf margin of the Bowland sub-basin after progradation of the shelf clinoform into water depths of >300 m, resulting in the formation of a ~550 metre thick lowstand turbidite fan deposit (the Pendle Grit), and an incised valley that reaches depths of ~85 m and contains Gilbert-type deltas near its mouth.

The style of incised valley infill in the Bearing Grit is similar to the Lower Kinderscout Grit (LKG 6 and LKG 8; Hampson, 1997) and the Roaches-Ashover Grit (Jones and Chisholm, 1997). These systems are classified as ‘Valley fill sandstones with giant foresets’ (Hampson et al., 1999) and contain Gilbert-type deltas near the valley mouth where the incised valleys reach depths of (~55 - 80 m). These incised valleys correlate downstream with large turbidite fans indicating that the shelf had a substantial height (Fig. 5.6a). For the incised valleys in the Lower Kinderscout Grit and Roaches-Ashover Grit these turbidite successions reach thicknesses of ~570 m and ~360 m. respectively (Waters et al., 2009).

Hampson et al. (1999) also define ‘Valley fill sandstones’. These systems form thinner valley fill successions (30 – 40 m) that are frequently wider (<30 km)

than the ‘valley fill sandstones with giant foresets’ (Hampson et al., 1999). This group is thought to include valley fills such as the Ward’s Stone Sandstone, Upper Kinderscout Grit, Midgley Grit, and Chatsworth Grit. For the Upper Kinderscout and Midgley Grits, the valley incised in a shelf edge of 100 -250 m height and supplied sand directly to the slope, resulting in minor turbidite deposits (Fig. 5.6b). For other systems, the downdip systems are not exposed but it is considered likely that these systems incised into a shelf margin.

During the Yeadonian, ‘sheet-like sandstone’ incised valley types are deposited, characterised by a very wide belt of channelized sandstones that extends across the Central Pennine Basin (Maynard, 1992; Bristow, 1993a; Hampson et al., 1996; Hampson et al., 1999). At this time, no areas of deep water conditions remain in the Central Pennine Basin, thus fluvial incision cannot be related to incision of a shelf margin (Fig. 5.6c). Read (1991; 1992) suggests that the Lower Follifoot Grit might represent a similar situation to the Rough Rock. In the Lower and Upper Follifoot Grit, and probably the Tan Hill Grit, broad zones of erosion occur in the fluvial system on the Askrigg Block, corresponding to perched lowstand deltas formed on a submerged shelf (Fig. 5.6d).

The subdivision of different incised valley types as defined by Hampson et al. (1999) can be applied to the hypothesis of a basin depth control on the development of incised valleys. The deepest incised valleys are infilled by ‘valley fill sandstones with giant foresets’ and might coincide with the highest amplitude sea-level falls. However, because this valley type occurs solely during the initial infill of the various sub-basins of the Central Pennine Basin, and coincides with incision in the highest shelf margins, a basin depth (or shelf height) control on the incision depth is considered more likely (Fig. 5.6a). The ‘valley fill sandstones’ category (Hampson et al., 1999) is associated with incision into a shallower shelf edge in cases where the down dip system is observed (the Upper Kinderscout Grit; the Midgley Grit). In such circumstances, higher progradation rates of the shelf clinoform are likely, resulting in a less efficient process of valley incision (Fig. 5.6b).

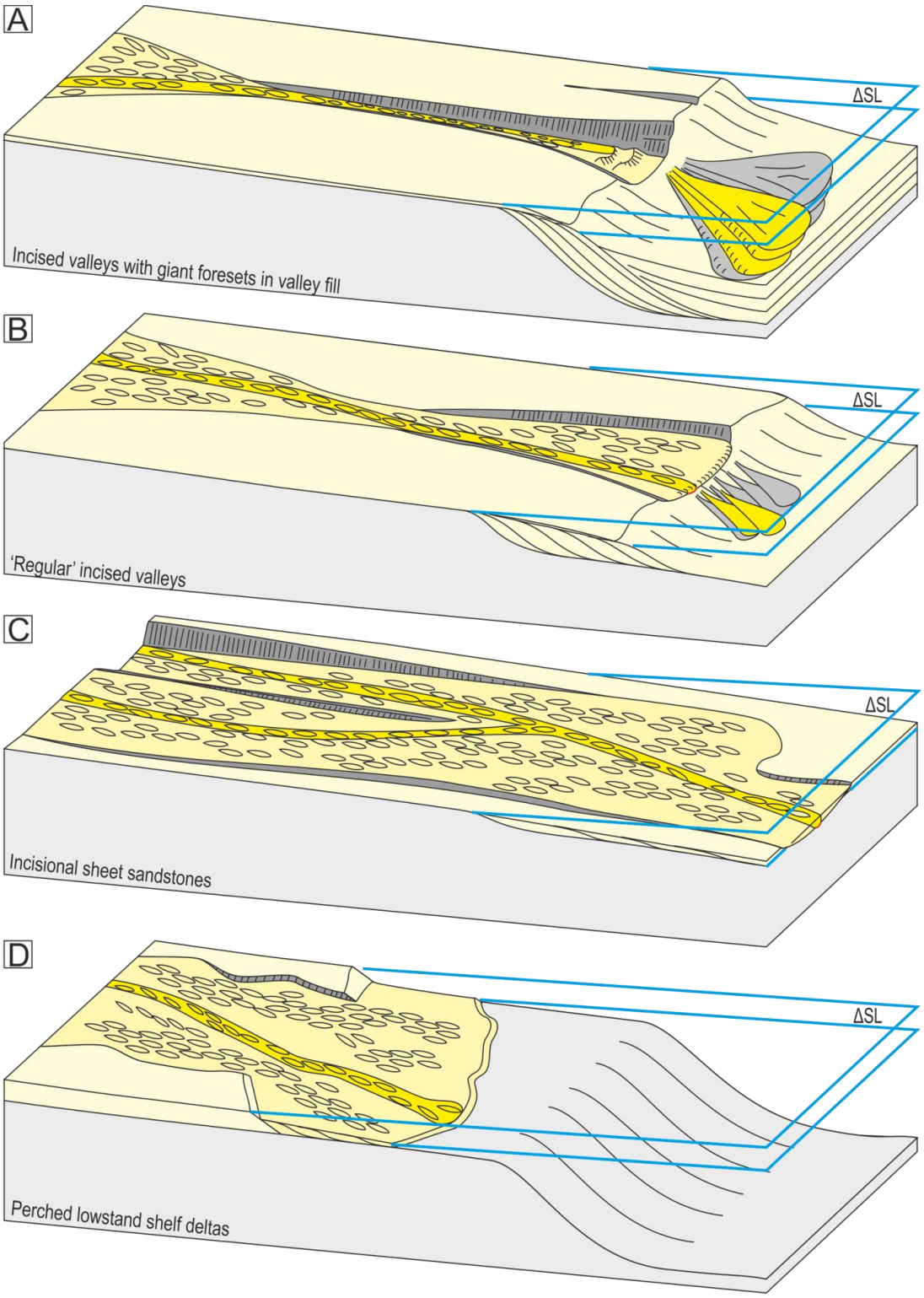
A
ΔSL
Incised valleys with giant foresets in valley fill
B
ΔSL
'Regular' incised valleys
C
ΔSL
Incisional sheet sandstones
D
ΔSL
Perched lowstand shelf deltas

Figure 5.6 (previous page) Effect of basin depth or clinoform height on incised valley character. In each model, the same magnitude sea-level fall is drawn. (a) Deep incised valleys occur at the margins of deep basins. Shelf clinoform progradation is slow, resulting in efficient valley incision. Sediment delivery onto the slope can cause the formation of large lowstand fans. During sea-level rise, these valleys are characterised by the occurrence of Gilbert-type deltas in the specific case of the Central Pennine Basin, (b) Incised valleys in shallower basin. Higher rates of shelf clinoform progradation results in less efficient valley incision and smaller turbidite systems. (c) Erosionally-based sheet sandstones. Sea-level fall does not trigger shelf incision but forces a rapid progradation of the fluvial system, causing a broad, shallow erosional surface. Potentially, upstream variations in sediment or water discharge are more easily recognised in such incised valleys and are drawn upper left corner. (d) If sea-level fall does not reach below shelf edge, perched lowstand deltas are formed that correspond to wide zones of limited erosion similar to the sheet sandstones depicted in (c).

During the formation of the incised valleys of the Rough Rock, shallow water conditions occurred throughout in the Central Pennine Basin, implying that sheet-like sandstones do not reflect incision of a shelf margin. Holbrook and Bhattacharya (2012) suggest that such wide, low relief erosional surfaces can form through numerous avulsions of the individual channels when, during a sea-level fall, the fluvial profile is extended along a (shelf) profile of similar gradient (Holbrook, 1996). Such process results in a wide, smooth, shallow incised surface similar to those described for the Rough Rock incised valleys. Potentially, incision might be further enhanced by discharge variations such as inferred for the Bearing Grit incised valley fill (Chapter 4). Such variations can alter the gradient of the fluvial profile (Fig. 5.6c; e.g. Holbrook et al., 2006; Bijkerk et al., 2013) and would affect the updip parts of incised valleys most strongly, suggesting that the incised valley should become deeper in upstream directions while the sequence boundary becomes more irregular (Holbrook and Bhattacharya, 2012). For both the lower and upper Rough Rock incised valleys a downstream thinning of the valley fill is reported (cf. Hampson et al., 1996), but further investigation is required before such a hypothesis can be validated.

During formation of the incised valley of the Lower Follifoot Grit, sea level did not fall below the shelf edge based on the occurrence of correlative deltaic sediments deposited on the shelf that formed during deposition of the earlier Marchup or Warley Wise Grit. This suggests that these incised valleys fed perched lowstand delta on a shallow water shelf (Fig. 5.6d). Similar to the sheet-like sandstones described above, incision related to sea-level fall is probably limited in such cases, resulting in wide but shallow valleys.

5.5.4 Effect of basin depth on sediment volumes

In the previous section, incised valley types are related to differences in shelf height. Whether these different valley types also have an effect on the sediment volumes has not been tested quantitatively. Depositional systems are generally too poorly constrained in the outcrop belts of the Central Pennine Basin to calculate sediment volumes such as performed for the Pendle, Bearing and Warley Wise Grit (Chapter 3). Additionally, sediment supply to the Millstone Grit Group appears to have varied substantially at several timescales (see discussion above). Sediment supply variations due to long term changes in sea-level variations, (e.g. Waters and Condon, 2012), pulses of tectonic rejuvenation (e.g. Holdsworth and Collinson, 1988), and/or large-scale avulsions of the fluvial system (e.g. Martinsen et al., 1995) make quantitative testing of the hypothesis of sediment volume dependence on basin depth impossible.

Further testing of this hypothesis should be executed in a better constrained field area. In Chapter 2, the experiments and the literature case study on the Maastrichtian Fox Hill - Lewis shelf margin of Southern Wyoming both suggest increases in sediment bypass to the shelf in the order of 10 – 30 per cent. Therefore, the fourfold increase in sediment volume estimated in Chapter 3 suggests that additional processes also play a role in this system.

5.5.5 Effect of lateral variations in basin depth on incised valley position

Lateral variations in the height of the shelf margin are inferred as a control on the position of the fluvial system, and consequently on the position of incised valleys (Fig. 5.7; Chapter 2, 3). During the Pendleian $E_{1c}1$ cycle, the Bowland sub-

basin represented the deepest depocentre along the Pendle Grit coastline. In this area a large turbidite lowstand fan was deposited, fed by a major incised valley (e.g. Fig. 5.7a, b, c). Deposition of this turbidite fan substantially reduced the water depth for subsequent successions, allowing rapid progradation during successive sea-level cycles. The Warley Wise Grit is thickest and most sand-rich in the same depositional area as the Bearing Grit incised valley fill, which is probably related to underfilling of the incised valley during the subsequent transgression (Fig. 5.7d; Chapter 3). This steered deposition towards the Bowland sub-basin, resulting in substantially further progradation of the coastline in the Bowland sub-basin than in the Lancaster Fells and Harrogate sub-basins (e.g. Figs. 5.2a; 5.7d; Chapter 3). During the subsequent Arnsbergian period, deposition focusses either in the Lancaster Fells or Harrogate sub-basin (cf. Fig. 5.2a, b, c), which might be related to northward position of the coastline in these areas relative to the Bowland sub-basin (Fig.5.2b, c). Unconfined fluvial systems seeking the shortest or steepest path preferentially drain towards these areas (Fig. 5.7e), increasing the likelihood of valley incision in these areas during subsequent sea-level falls (Fig. 5.7f).

During the Marsdenian $R_{2c}5$ sea-level cycle a similar situation occurred. During this cycle westward deltaic advance by the Guiseley Grit occurred over a widespread area on a lowstand shelf that was formed during the Kinderscoutian. Southward, the Roaches- Ashover Grit developed south of the Kinderscoutian coastline in the deep water Widmerpool Gulf (e.g. Fig. 5.7a, b, c). Subsequently, incision occurred at the southern limit of the depositional system, resulting in the infill of the Widmerpool Gulf by a large turbidite fan. In this case, the Widmerpool Gulf represented the most updip area of deep water conditions, which would facilitate incision in this area (e.g. Fig. 5.7a, b, c), rather than the more northern area in which the Guiseley Grit was deposited.

5.5.6 Effect of basin structure on incised valleys width

In the Roaches - Ashover Grit and the Lower Kinderscout Grit (LKG8) a downdip valley narrowing is mentioned from ~12 to ~5 km and >20 km to <5 km respectively (Hampson, 1995; Hampson et al., 1999; Jones and Chisholm, 1997). This suggests that the deepest, distal parts of the ‘Valley fill sandstones with giant

foresets' have a funnel-like geometry, whereas coastal incised valleys typically widen downstream (e.g. Blum et al., 2013).

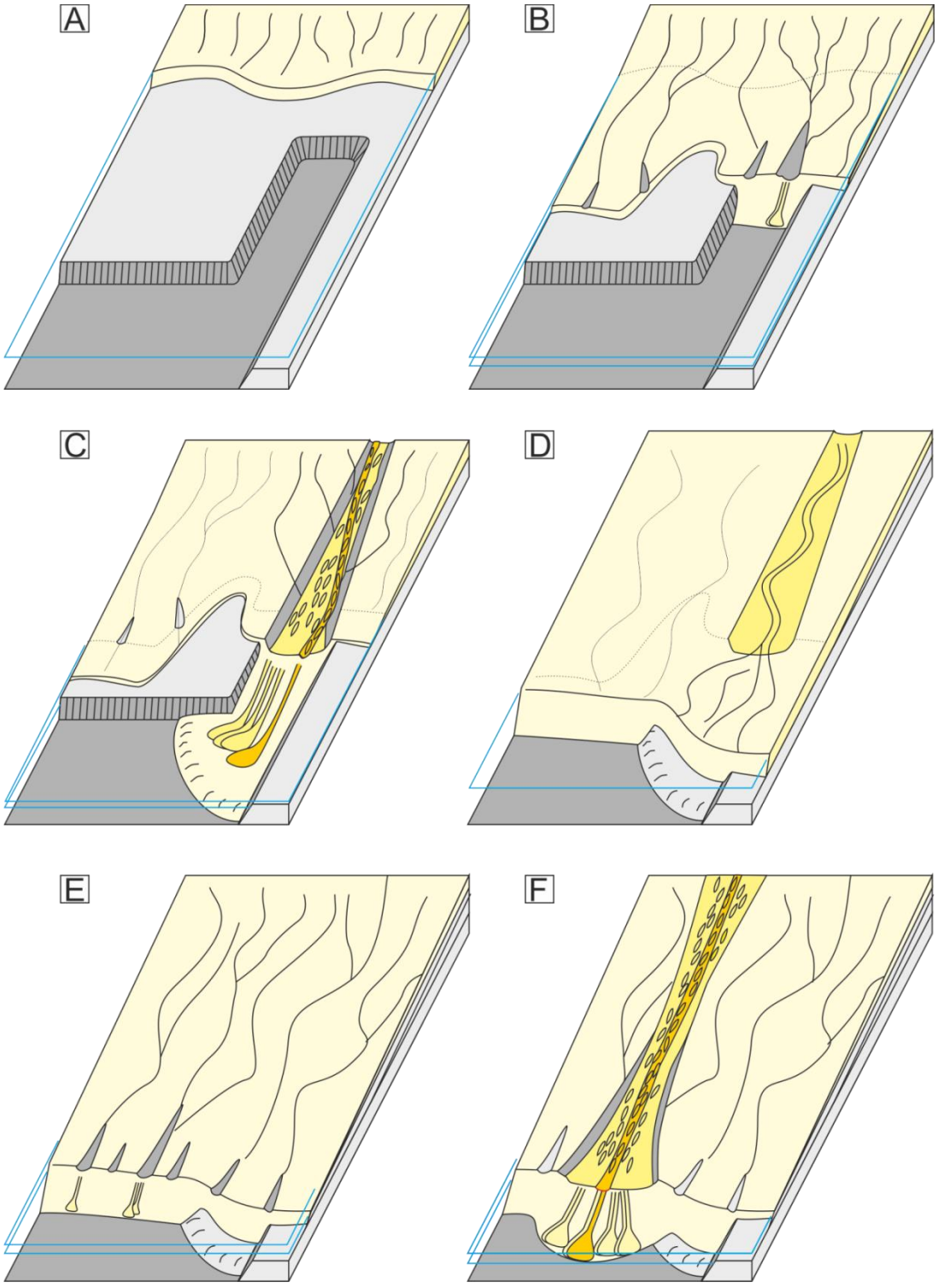

Figure 5.7 (previous page) Conceptual model of lateral variations in basin depth. (a) In basins of limited or no variation, the position of the fluvial system will be unaffected. (b) Progradation into zone of lateral differences in basin depth. During sea-level fall, upstream knick-point migration will be faster and more efficient in zones of slow coastline progradation associated with the deeper segments (Fig. 5.6) and result in the capture of additional streams by the incipient incised valley (cf. van Heijst and Postma, 2001). In the case of the Guiseley Grit and Roaches-Ashover Grit such process might have formed an area of non-deposition next to the incised valley, assuming that both areas were fed by the same river system. (c) Valley incision focussed in the deep segment, forming a major turbidite fan. Potentially, incised valleys are further confined by bounding faults that define basin margins. (d) Subsequent fluvial systems can remain confined within the former incised valley if underfilled. Such process probably occurred during deposition of the Pendleian Warley Wise Grit (Chapter 3), (e) Otherwise fluvial systems are likely to seek the steepest longitudinal profile, focussing fluvial systems in areas where the coastline is close by. During sea-level fall, the presence of fluvial systems will favour incision in these locations, particularly when these areas are deeper as well, resulting in more efficient incision (Fig. 5.6). (f) Valley incision results in localised progradation of the coastline, influencing subsequent periods of deposition.

On the northern margin of the Askrigg Block, the width of the Bearing Grit valley is ~12.5 km, but it widens rapidly downdip to ~ 40 km in the Craven Basin (Chapter 3), indicating an opposite trend to the examples in the Lower Kinderscout Grit and Roaches Ashover Grit (Hampson et al., 1999). Valley narrowing typically forms an initial stage of incised valley formation that occurs during periods of accelerating sea-level fall (e.g. Strong and Paola, 2008). This is generally followed by a phase in which valleys widen due to lateral migration of channels that further excavate valley margins during periods or reduced sea-level fall or still stand (e.g. Strong and Paola, 2008; Martin et al., 2011; Blum et al., 2013). If related to sea-level variations, the downdip narrowing in the Lower Kinderscout and the Roaches-Ashover Grits would suggest a very rapid transition from sea-level fall to sea-level rise. Because such narrowing is not observed in the otherwise similar Bearing Grit, an alternative explanation based on a different orientation of major structural lineaments is preferred. In the Craven Basin, the Bearing Grit drains perpendicular to the Craven Fault system and lateral variations in basin depth are gradual.

Contrastingly, the Lower Kinderscout Grit and the Roaches-Ashover fluvial system drains into the narrow, structurally-defined Edale and Widmerpool Gulf, where these structural lineaments might have contributed to the confinement of the incised valley (e.g. Holbrook and Bhattacharya, 2012).

5.5.7 Effect of discharge

In Chapter 4, distinct facies patterns in Gilbert-type delta foresets, 'intrasets', and sediment gravity flow deposits in the delta front of the Bearing Grit incised valley fill are interpreted as hyperpycnal flood deposits of variable strengths, suggesting that the river system during infill of the incised valley is flood-prone. The absence of such facies in the forced regressive Warley Wise Grit is thought to indicate the absence of such flood-prone conditions (Chapter 4). This difference has been related tentatively to variable monsoonal conditions at precession timescales.

Flood-prone Gilbert-type foresets similar to those in the Bearing Grit incised valley fill are also recognised for the Lower Kinderscout Grit (McCabe, 1975, 1977) and the Roaches-Ashover Grit (Jones, 1980; Jones and McCabe, 1980), suggesting similar flow conditions in these valleys. In incised valley fills without Gilbert-type deltas, flood deposits are more difficult to recognise due to the absence of the Gilbert-type deltas that form the clearest indicator of flow conditions. Flood events might be recognised by structureless sandstones, which in braided rivers have been linked to hyperconcentrated sediment concentrations (Martin and Turner, 1998), or by longitudinal changes in the incisional style (Fig. 5.6c; see discussion section 5.5.3; Holbrook et al., 2006). Structureless sandstones have been observed in both the Rough Rock (Hampson et al., 1996) and the Chatsworth Grit (Waters et al., 2008) but detailed sedimentological analysis would be required to determine whether these structureless sandstones are indeed related to such river floods.

Climate variability inferred from incised valley character should be corroborated by additional indications from other parts of the depositional system. Long term evolution of coal occurrences and palaeosol character of the Asbian to Pendleian Yoredale succession in the Northumberland Trough suggests that after a semi-arid climate period from the Late Asbian to Early Brigantian, climate reverted to a humid, seasonal climate from the Mid-Brigantian to the Pendleian (Lemon, 2006). Additionally, high frequency paralic 'coal-measure facies' in the Pendleian

strata in the Midland Valley of Scotland provide further indications for a strongly seasonal climate (e.g. Read, 1989). Between the Black Metals Limestone and Index Limestone, 25 laterally persistent coal seams occur in a ~200 m thick succession, characterised by 4 regressive successions (Read, 1994; 1995). The Pendleian succession of the Midland Valley of Scotland contains three additional limestones (Read, 1989; Ramsbottom, 1977b; Dean et al., 2011), which combined with the 1 Myr duration of the Pendleian (Waters and Condon, 2012) suggests that this succession is characterised by Milankovitch-order forcing mechanisms. Accurate radiometric dating is not available but it is here considered most likely that the Black Hosie and Index Limestones represent peak flooding surfaces at long-period eccentricity (400 kyr). This implies that the 4 regressive successions represent sea-level cycles at a short-period eccentricity (~100 kyr), while coal seam formation occurred at precession time-scales. Coal formation at this time-scale would reflect wet-dry cycles consistent with a seasonal monsoonal climate (cf. Van den Belt, 2012).

5.6 Conclusions

The fill of the Carboniferous Central Pennine Basin by the Namurian Millstone Grit Group forms a south- and westward prograding shelf margin that extends up dip into the mixed limestone and siliciclastic succession on the northward located shelf. The large-scale stratigraphic pattern appears predominantly controlled by long-term sea-level variation, major avulsions and long-term variations in subsidence rates. Long-term variations between glacial and non-glacial periods control sediment delivery to the Central Pennine Basin, with sand delivery associated with low sea level during the glacial periods. Large-scale avulsions between a northerly and easterly fluvial pathway control the areas and direction of progradation while decreasing subsidence rates during the Namurian increasingly promoted progradation.

On a shorter and smaller scale, conceptual models of external controls on the stratigraphic character of the Millstone Grit Group in the Central Pennine Basin are tested. These models are developed from analogue modelling and field examination focussing on incised valley position and character. Four valley types are recognised

from literature: deeply incised valleys with Gilbert-type deltas, regular incised valleys, broad erosional sheet sandstones, and incised valleys corresponding to perched lowstand deltas.

Differences in valley types are mainly related to the depth of incision, and correspond closely with the depth of the adjoining basin. The deepest incised valleys are associated with the infill of the deepest depocentres within the Central Pennine Basin, whereas shallower incised valleys correspond to smaller shelf clinoforms. Broad erosional sheet sandstones probably resulted from rapid extension of the coastline during sea-level fall when the Central Pennine Basin is mostly infilled and a shelf margin was absent. Broad erosional sheet sandstones, suggesting that the shelf was not incised, were also formed when perched lowstand deltas formed on still submerged shelves. The analogue modelling inference that deeper basins and associated deeper valley also results in more efficient sediment transport could not be quantified. Gilbert-type deltas facies associated with large discharge variations during sea-level rise are consistently present in the fills of deep incised valleys, suggesting a discharge/climate influence. Some indications of climate or discharge variations occur outside these valley types and further work is required to establish the importance of climate influences on the sedimentary character.

The position of incised valleys is likely controlled by previous phases of deposition and lateral variations in basin depth. Slowly prograding systems, associated with deep water shelf margins are more prone to incision, which in combination with marked lateral variations in shelf margin height controls the position of incised valleys and associated turbidite fan systems. These areas are consequently characterised by rapid progradation of the coastline. Subsequently, fluvial systems abandon these locations and focus in areas where the coastline is located furthest upstream, promoting valley incision in these locations. Lateral variations in the basin-margin morphology is likely an important predictor of incised valley positions in settings similar to the Namurian Central Pennine Basin.

List of References

ADDISON, R., 1997, Geology of the Silsden and Cononley district 1:10.000 sheets (SE04NW and SD94NE), British Geological Survey Technical Report WA/97/22.

AITKENHEAD, N., BRIDGE, D.M., RILEY, N.J., and KIMBELL, S.F., 1992, Geology of the country around Garstang: Memoir of the British Geological Survey, Sheet 67 (England and Wales).

AITKENHEAD, N., and RILEY, N.J., 1996, Kinderscoutian and Marsdenian successions in the Bradup and Hag Farm boreholes, near Ilkley, west Yorkshire: Proceedings of the Yorkshire Geological Society, v. 51, p. 115-125.

ALEXANDER, J., and FIELDING, C.R., 2006, Coarse-Grained Floodplain Deposits in the Seasonal Tropics: Towards a Better Facies Model: Journal of Sedimentary Research, v. 76, p. 539-556.

ALEXANDER, J., and MULDER, T., 2002, Experimental quasi-steady density currents: Marine Geology, v. 186, p. 195-210.

ALLEN, J.P., FIELDING, C.R., GIBLING, M.R., and RYGEL, M.C., 2011, Fluvial response to paleo-equatorial climate fluctuations during the late Paleozoic ice age: Geological Society of America Bulletin, v. 123, p. 1524-1538.

ALLEN, J.P., FIELDING, C.R., RYGEL, M.C., and GIBLING, M.R., 2013, Deconvolving Signals of Tectonic and Climatic Controls From Continental Basins: An Example From the Late Paleozoic Cumberland Basin, Atlantic Canada: Journal of Sedimentary Research, v. 83, p. 847-872.

ALLMENDINGER, R.W., CARDOZO, N.C., and FISHER, D., 2012, Structural Geology Algorithms: Vectors & Tensors: Cambridge, England, Cambridge University Press, 302 p.

ARTHURTON, R.S., 1984, The Ribblesdale fold belt, NW England - a Dinantian-early Namurian dextral shear zone, *in* Hutton, D.W.H., and Sanderson, D.J., eds., Variscan Tectonics of the North Atlantic Region, Geological Society, London, Special Publications, v. 14, p. 131-138.

ARTHURTON, R.S., JOHNSON, E.W., and MUNDY, D.J.C., 1988, Geology of the country around Settle: Memoir of the British Geological Survey, Sheet 60 (England and Wales).

ASHWORTH, P.J., BEST, J.L., RODEN, J.E., BRISTOW, C.S., and KLAASSEN, G.J., 2000, Morphological evolution and dynamics of a large, sand braid-bar, Jamuna River, Bangladesh: Sedimentology, v. 47, p. 533-555.

BAGNOLD, R.A., 1962, Auto-Suspension of Transported Sediment; Turbidity Currents: Proceedings of the Royal Society of London. Series A. Mathematical and Physical Sciences, v. 265, p. 315-319.

BAINES, J.G., 1977, The Stratigraphy and Sedimentology of the Skipton Moor Grits (Namurian E1c) and their Lateral Equivalents [unpublished PhD thesis]: University of Keele, Keele 226 p.

BATES, C.C., 1953, Rational Theory of Delta Formation: AAPG Bulletin, v. 37, p. 2119-2162.

BERGER, A., 1989, The Spectral Characteristics of Pre-Quaternary Climatic Records, an Example of the Relationship between the Astronomical Theory and Geo-Sciences, *in* Berger, A., Schneider, S., and Duplessy, J.C., eds., Climate and Geo-Sciences: NATO ASI Series, Springer Netherlands, p. 47-76.

BEST, J.L., ASHWORTH, P.J., BRISTOW, C.S., and RODEN, J., 2003, Three-dimensional sedimentary architecture of a large, mid-channel sand braid bar, Jamuna River, Bangladesh: Journal of Sedimentary Research, v. 73, p. 516-530.

BEST, J.L., KOSTASCHUK, R.A., PEAKALL, J., VILLARD, P.V., and FRANKLIN, M., 2005, Whole flow field dynamics and velocity pulsing within natural sediment-laden underflows: Geology, v. 33, p. 765-768.

BIJKERK, J.F., POSTMA, G., TEN VEEN, J., MIKES, D., VAN STRIEN, W., and DE VRIES, J., 2013, The role of climate variation in delta architecture: lessons from analogue modelling: Basin Research, v. 25, p. 1-18.

BISAT, W.S., 1923, The Carboniferous Goniatites of the North of England and Their Zones: Proceedings of the Yorkshire Geological Society, v. 20, p. 40-124.

BLACK, W.W., 1950, The Carboniferous Geology of the Grassington Area, Yorkshire: Proceedings of the Yorkshire Geological Society, v. 28, p. 29-42.

BLACK, W.W., 1958, The Structure of the Burnsall-Cracoe District and Its Bearing on the Origin of the Cracoe Knoll-Reefs: Proceedings of the Yorkshire Geological Society, v. 31, p. 391-414.

BLAKEY, R.C., 2008, Gondwana paleogeography from assembly to breakup - A 500 m.y. odyssey, *in* Fielding, C.R., Frank, T.D., and Isbell, J.L., eds., Resolving the Late Paleozoic Ice Age in Time and Space, Geological Society of America Special Papers, v. 441, p. 1-28.

BLUM, M., and HATTIER-WOMACK, J., 2009, Climate change, sea-level change, and fluvial sediment supply to deepwater depositional systems, *in* Kneller, B., Martinsen, O.J., and McCaffrey, W.D., eds., External Controls on Deep Water Depositional Systems: Climate, Sea-Level and Sediment Flux, SEPM Special Publication, v. 92, p. 15-39.

BLUM, M., MARTIN, J., MILLIKEN, K., and GARVIN, M., 2013, Paleovalley systems: Insights from Quaternary analogs and experiments: Earth-Science Reviews, v. 116, p. 128-169.

BLUM, M.D., and TORNQVIST, T.E., 2000, Fluvial responses to climate and sea-level change: a review and look forward: Sedimentology, v. 47, p. 2-48.

BOGGS JR, S., 2006, Principles of Sedimentology and Stratigraphy (4th ed.): Upper Saddle River, Pearson Prentice Hall - Pearson Education, Inc., 662 p.

BOOKHAGEN, B., THIEDE, R.C., and STRECKER, M.R., 2005, Late Quaternary intensified monsoon phases control landscape evolution in the northwest Himalaya: Geology, v. 33, p. 149-152.

BOTT, M.H.P., 1961, Geological Interpretation of Magnetic Anomalies over the Askrigg Block: Quarterly Journal of the Geological Society, v. 117, p. 481-493.

BOURGET, J., ZARAGOSI, S., RODRIGUEZ, M., FOURNIER, M., GARLAN, T., and CHAMOT-ROOKE, N., 2013, Late Quaternary megaturbidites of the Indus Fan: Origin and stratigraphic significance: Marine Geology, v. 336, p. 10-23.

BRAND, P.J., 2011, The Serpukhovian and Bashkirian (Carboniferous, Namurian and basal Westphalian) faunas of northern England: Proceedings of the Yorkshire Geological Society, v. 58, p. 143-165.

BRANDON, A., AITKENHEAD, N., CROFTS, R.G., ELLISON, R.A., EVANS, D.J., and RILEY, N.J., 1998, Geology of the country around Lancaster: Memoir of the British Geological Survey, Sheet 59 (England and Wales).

BRANDON, A., RILEY, N.J., WILSON, A.A., and ELLISON, R.A., 1995, Three new early Namurian (E1c-E2a) marine bands in central and northern England, UK, and their bearing on correlations with the Askrigg Block: Proceedings of the Yorkshire Geological Society, v. 50, p. 333-355.

BRETTLE, M.J., MCILROY, D., ELLIOTT, T., DAVIES, S.J., and WATERS, C.N., 2002, Identifying cryptic tidal influences within deltaic successions: an example from the Marsdenian (Namurian) interval of the Pennine Basin, UK: Journal of the Geological Society, v. 159, p. 379-391.

BRIDGE, D.M., 1988, Geology of the area aroung Hurst Green and Wilpshire, British Geological Survey Technical Report WA/88/43.

BRISTOW, C.S., 1988, Controls on sedimentology in the Rough Rock Group, *in* Besly, B.M., and Kelling, G., eds., Sedimentation in a Synorogenic Basin Complex: The Upper Carboniferous of Northwest Europe, Blackie, Glasgow, p. 114-131.

BRISTOW, C.S., 1993a, Sedimentology of the Rough Rock: a Carboniferous braided river sheet sandstone in northern England, *in* Best, J.L., and Bristow, C.S., eds., Braided Rivers, Geological Society, London, Special Publications, v. 75, p. 291-304.

BRISTOW, C.S., 1993b, Sedimentary structures exposed in bar tops in the Brahmaputra River, Bangladesh, *in* Best, J.L., and Bristow, C.S., eds., Braided Rivers, Geological Society, London, Special Publications, v.75, p. 277-289.

BROADHURST, F.M., SIMPSON, I.M., and HARDY, P.G., 1980, Seasonal Sedimentation in the Upper Carboniferous of England: The Journal of Geology, v. 88, p. 639-651.

BURGESS, I.C., and MITCHELL, M., 1975, Visean Lower Yoredale Limestones on the Alston and Askrigg Blocks, and the Base of the D2 Zone in Northern England: Proceedings of the Yorkshire Geological Society, v. 40, p. 613-630.

CARDOZO, N., and ALLMENDINGER, R.W., 2013, Spherical projections with OSXStereonet: Computers & Geosciences, v. 51, p. 193-205.

CARTIGNY, M.J.B., EGGENHUISEN, J.T., HANSEN, E.W.M., and POSTMA, G., 2013, Concentration-Dependent Flow Stratification In Experimental High-Density

Turbidity Currents and Their Relevance To Turbidite Facies Models: Journal of Sedimentary Research, v. 83, p. 1046-1064.

CARVAJAL, C., 2007, Sediment volume partitioning, topset processes and clinoform architecture - understanding the role of sediment supply, sea level, and delta types in shelf margin building and deepwater sand bypass: the Lance-Fox Hills-Lewis system in S. Wyoming [unpublished PhD thesis]: The University of Texas at Austin, 171 p.

CARVAJAL, C., and STEEL, R., 2009, Shelf-Edge Architecture and Bypass of Sand to Deep Water: Influence of Shelf-Edge Processes, Sea Level, and Sediment Supply: Journal of Sedimentary Research, v. 79, p. 652-672.

CARVAJAL, C., STEEL, R., and PETTER, A., 2009, Sediment supply: The main driver of shelf-margin growth: Earth-Science Reviews, v. 96, p. 221-248.

CARVAJAL, C.R., and STEEL, R.J., 2006, Thick turbidite successions from supply-dominated shelves during sea-level highstand: Geology, v. 34, p. 665-668.

CASTELLTORT, S., and VAN DEN DRIESSCHE, J., 2003, How plausible are high-frequency sediment supply-driven cycles in the stratigraphic record?: Sedimentary Geology, v. 157, p. 3-13.

CATUNEANU, O., ABREU, V., BHATTACHARYA, J.P., BLUM, M.D., DALRYMPLE, R.W., ERIKSSON, P.G., FIELDING, C.R., FISHER, W.L., GALLOWAY, W.E., GIBLING, M.R., GILES, K.A., HOLBROOK, J.M., JORDAN, R., KENDALL, C.G.S.C., MACURDA, B., MARTINSEN, O.J., MIALL, A.D., NEAL, J.E., NUMMEDAL, D., POMAR, L., POSAMENTIER, H.W., PRATT, B.R., SARG, J.F., SHANLEY, K.W., STEEL, R.J., STRASSER, A., TUCKER, M.E., and WINKER, C., 2009, Towards the standardization of sequence stratigraphy: Earth-Science Reviews, v. 92, p. 1-33.

CHADWICK, R.A., and EVANS, D.J., 2005, A seismic atlas of southern Britain - images of subsurface structure: Occassional Publication, v. 7: Keyworth, Nottingham, British Geological Survey.

CHADWICK, R.A., HOLLIDAY, D.W., HOLLOWAY, S., and HULBERT, A.G., 1995, The Structure and Evolution of the Northumberland-Solway Basin and Adjacent Areas: Subsurface Memoir of the British Geological Survey: London, HMSO.

CHAPMAN MCGREW JR, J., and MONROE, C.B., 1993, An Introduction to Statistical Problem Solving in Geography: Oxford, England, Wm. C. Brown Publishers, 305 p.

CHISHOLM, J.I., 1981, Growth faulting in the Almscliff Grit (Namurian E1) near Harrogate, Yorkshire: Transactions of the Leeds Geological Association, v. 9, p. 61-70.

CHISHOLM, J.I., and HALLSWORTH, C.R., 2005, Provenance of Upper Carboniferous sandstones in east Derbyshire: role of the Wales-Brabant high: Proceedings of the Yorkshire Geological Society, v. 55, p. 209-233.

CHISHOLM, J.I., and WATERS, C.N., 2012, Syn-sedimentary deformation of the Ashover Grit (Pennsylvanian, Namurian, Marsdenian Substage) deltaic succession around Wirksworth, Derbyshire, UK: Proceedings of the Yorkshire Geological Society, v. 59, p. 25-36.

CHUBB, L.J., and HUDSON, R.G.S., 1925, The Nature of the Junction between the Lower Carboniferous and the Millstone Grit of North-West Yorkshire: Proceedings of the Yorkshire Geological Society, v. 20, p. 257-291.

CHURCH, K.D., 1994, Sequence Stratigraphy of the late Namurian (Marsdenian to Yeadonian) delta systems in northern England [unpublished PhD thesis]: University of Manchester, Manchester, 352 p.

CHURCH, K.D., and GAWTHORPE, R.L., 1994, High resolution sequence stratigraphy of the late Namurian in the Widmerpool Gulf (East Midlands, UK): Marine and Petroleum Geology, v. 11, p. 528-544.

CLIFF, R.A., DREWERY, S.E., and LEEDER, M.R., 1991, Sourcelands for the Carboniferous Pennine river system: constraints from sedimentary evidence and U-Pb geochronology using zircon and monazite, *in* Morton, A.C., Todd, S.P., and Haughton, P.D.W., eds., Developments in Sedimentary Provenance Studies: Geological Society, London, Special Publications, v. 57, p. 137-159.

CLIFT, P.D., GIOSAN, L., BLUSZTAJN, J., CAMPBELL, I.H., ALLEN, C., PRINGLE, M., TABREZ, A.R., DANISH, M., RABBANI, M.M., ALIZAI, A., CARTER, A., and LÜCKGE, A., 2008, Holocene erosion of the Lesser Himalaya triggered by intensified summer monsoon: Geology, v. 36, p. 79-82.

COAL AUTHORITY, 2012, Online available data in map viewer: http://coal.decc.gov.uk/en/coal/cms/publications/data/map/map.aspx

COCKS, L.R.M., and TORSVIK, T.H., 2006, European geography in a global context from the Vendian to the end of the Palaeozoic, *in* Gee, D.G., and Stephenson, R.A., eds., European Lithosphere Dynamics, Geological Society, London, Memoirs, v.32, p. 83-95.

COLLIER, R.E.L., 1991, The Lower Carboniferous Stainmore Basin, N. England: extensional basin tectonics and sedimentation: Journal of the Geological Society, v. 148, p. 379-390.

COLLINSON, J.D., 1968, Deltaic sedimentation units in the Upper Carboniferous of Northern England: Sedimentology, v. 10, p. 233-254.

COLLINSON, J.D., 1970, Bedforms of the Tana River, Norway: Geografiska Annaler. Series A, Physical Geography, v. 52, p. 31-56.

COLLINSON, J.D., 1988, Controls on Namurian sedimentation in the Central Province basins of northern England, *in* Besly, B.M., and Kelling, G., eds., Sedimentation in a Synorogenic Basin Complex: The Upper Carboniferous of Northwest Europe, Blackie, Glasgow, p. 85-101.

COLLINSON, J.D., and BANKS, N.L., 1975, The Haslingden Flags (Namurian G1) of South-East Lancashire: Bar Finger Sands in the Pennine Basin: Proceedings of the Yorkshire Geological Society, v. 40, p. 431-458.

COLLINSON, J.D., JONES, C.M., and WILSON, A.A., 1977, The Marsdenian (Namurian R2) succession west of Blackburn: Implications for the evolution of Pennine Delta Systems: Geological Journal, v. 12, p. 59-76.

COLLINSON, J.D., MOUNTNEY, N.P., and THOMPSON, D.B., 2006, Sedimentary Structures: London, Terra Pubilishing, 292 p.

COOPER, A.H., and BURGESS, I.C., 1993, Geology of the Country around Harrogate: Memoir of the British Geological Survey, Sheet 62 (England and Wales).

COPE, J.C.W., GUION, P.D., SEVASTOPULO, G.D., and SWAN, A.R.H., 1992, Carboniferous, *in* Cope, J.C.W., Ingham, J.K., and Rawson, P.F., eds., Atlas of Palaeogeography and Lithofacies, Geological Society, London, Memoirs, v. 13, p. 67-86.

COVAULT, J.A., ROMANS, B.W., GRAHAM, S.A., FILDANI, A., and HILLEY, G.E., 2011, Terrestrial source to deep-sea sink sediment budgets at high and low sea levels: Insights from tectonically active Southern California: Geology, v. 39, p. 619-622.

COWARD, M.P., 1993, The effect of Late Caledonian and Variscan continental escape tectonics on basement structure, Paleozoic basin kinematics and subsequent Mesozoic basin development in NW Europe, *in* Parker, J.R., ed., Petroleum Geology of Northwest Europe: Proceedings of the 4th Conference, Geological Society, London, Petroleum Geology Conference series, v.4, p. 1095-1108.

CRABAUGH, J.P., and STEEL, R.J., 2004, Basin-floor fans of the Central Tertiary Basin, Spitsbergen: relationship of basin-floor sand-bodies to prograding clinoforms in a structurally active basin, *in* Lomas, S.A., and Joseph, P., eds., Confined Turbidite Systems, Geological Society, London, Special Publications, v.222, p. 187-208.

CROWLEY, T.J., and BAUM, S.K., 1991, Estimating Carboniferous sea-level fluctuations from Gondwanan ice extent: Geology, v. 19, p. 975-977.

DADSON, S., HOVIUS, N., PEGG, S., DADE, W.B., HORNG, M.J., and CHEN, H., 2005, Hyperpycnal river flows from an active mountain belt: Journal of Geophysical Research: Earth Surface, v. 110, p. F04016.

DAKYNS, J.R., 1892, On the Gelogy of the Country between Grassington and Wensleydale: Proceedings of the Yorkshire Geological Society, v. 12, p. 133-144.

DAKYNS, J.R., FOX-STRANGWAYS, C., RUSSELL, R., and DALTON, W.H., 1879, The Geology of The Country Between Bradford and Skipton: Memoir of the Geological Survey of Great Britain, England and Wales, Quarter Sheet 92SE.

DAKYNS, J.R., TIDDEMAN, R.H., GUNN, W., and STRAHAN, A., 1890, The Geology of the Country around Ingleborough, with parts of Wensleydale and Wharfedale: Memoir of the Geological Survey, England and Wales, Quarter Sheet 97SW.

DAVIES, S., HAMPSON, G., FLINT, S., and ELLIOT, T., 1999, Continental-scale sequence stratigraphy of the Namurian, Upper Carboniferous and its applications to reservoir prediction, *in* Fleet, A.J., and Boldy, S.A.R., eds., Petroleum Geology of Northwest Europe: Proceedings of the 5th Conference, Geological Society, London, Petroleum Geology Conference series, v.5, p. 757-770.

DAVIES, S.J., 2008, The record of Carboniferous sea-level change in low-latitude sedimentary successions from Britain and Ireland during the onset of the late Paleozoic ice age, *in* Fielding, C.R., Frank, T.D., and Isbell, J.L., eds., Resolving the Late Paleozoic Ice Age in Time and Space, Geological Society of America Special Papers, v. 441, p. 187-204.

DAVYDOV, V.I., CROWLEY, J.L., SCHMITZ, M.D., and POLETAEV, V.I., 2010, High-precision U-Pb zircon age calibration of the global Carboniferous time scale and Milankovitch band cyclicity in the Donets Basin, eastern Ukraine: Geochemistry Geophysics Geosystems, v. 11, p. Q0AA04.

DEAN, M.T., BROWNE, M.A.E., WATERS, C.N., and POWELL, J.H., 2011, A lithostratigraphical framework for the Carboniferous succesions of northern Great Britain (Onshore), British Geological Survey Research Report, RR/10/07, p. 174.

DEIBERT, J.E., and CAMILLERI, P.A., 2006, Sedimentologic and tectonic origin of an incised-valley-fill sequence along an extensional marginal-lacustrine system in the Basin and Range province, United States: Implications for predictive models of the location of incised valleys: AAPG Bulletin, v. 90, p. 209-235.

DEWEY, J.F., 1982, Plate tectonics and the evolution of the British Isles: Journal of the Geological Society, v. 139, p. 371-412.

DUNHAM, K.C., 1990, Geology of the Northern Pennine Orefield: Volume 1, Tyne to Stainmore (2nd Edition), Economic memoir of the British Geological Survey, sheets 19 and 25, and parts of 13, 24, 26, 31, 32 (England and Wales).

DUNHAM, K.C., and STUBBLEFIELD, C.J., 1944, The stratigraphy, structure and mineralization of the Greenhow mining area, Yorkshire: Quarterly Journal of the Geological Society, v. 100, p. 209-268.

DUNHAM, K.C., and STUBBLEFIELD, C.J., 1945, Discussion on: The Stratigraphy, Structure and Mineralization of the Greenhow Mining Area, Yorkshire: Quarterly Journal of the Geological Society, v. 101, p. 135-137.

DUNHAM, K.C., and WILSON, A.A., 1985, Geology of the Northern Pennine Orefield: Volume 2, Stainmore to Craven, Economic memoir of the British Geological Survey, Sheets 40, 41 and 50, and parts of 31, 32, 51, 60 and 61 (England and Wales).

DUNHAM, S.K., 1974, Granite beneath the Pennines in North Yorkshire: Proceedings of the Yorkshire Geological Society, v. 40, p. 191-194.

EAGAR, R.M.C., BAINES, J.G., COLLINSON, J.D., HARDY, P.G., OKOLO, S.A., and POLLARD, J.E., 1985, Trace Fossil Assemblages and their Occurrence in Silesian (Mid-Carboniferous) Deltaic Sediments of the Central Pennine Basin, England, *in* Curran, H., ed., Biogenic Structures: Their Use in Interpreting Depostional Environments, SEPM Special Publication v. 35, p. 99-149.

EARP, J.R., MAGRAW, D., POOLE, E.G., LAND, D.H., and WHITEMAN, A.J., 1961, Geology of the Country around Clitheroe and Nelson: Memoir of the Geological Survey of Great Britain, Sheet 68 (England and Wales).

EDMONDS, D.A., HOYAL, D.C.J.D., SHEETS, B.A., and SLINGERLAND, R.L., 2009, Predicting delta avulsions: Implications for coastal wetland restoration: Geology, v. 37, p. 759-762.

ELLIOTT, T., 1975, The Sedimentary History of a Delta Lobe from a Yoredale (Carboniferous) Cyclothem: Proceedings of the Yorkshire Geological Society, v. 40, p. 505-536.

ELLIOTT, T., 1976, The morphology, magnitude and regime of a Carboniferous fluvial-distributary channel: Journal of Sedimentary Research, v. 46, p. 70-76.

ETHRIDGE, F.G., WOOD, L.J., and SCHUMM, S.A., 1998, Cyclic variables controlling fluvial sequence development: Problems and perspectives, *in* Shanley, K.W., and McCabe, P.W., eds., Relative Role of Eustasy, Climate, and Tectonism in Continental Rocks, SEPM Special Publication, v. 59, p. 17-29.

EVANS, D.J., and KIRBY, G.A., 1999, The architecture of concealed Dinantian carbonate sequences over the Central Lancashire and Holme highs, northern England: Proceedings of the Yorkshire Geological Society, v. 52, p. 297-312.

FALCON-LANG, H.J., 1999a, The Early Carboniferous (Asbian-Brigantian) Seasonal Tropical Climate of Northern Britain: PALAIOS, v. 14, p. 116-126.

FALCON-LANG, H.J., 1999b, The Early Carboniferous (Courceyan–Arundian) monsoonal climate of the British Isles: evidence from growth rings in fossil woods: Geological Magazine, v. 136, p. 177-187.

FALCON-LANG, H.J., and DIMICHELE, W.A., 2010, What Happened to the Coal Forests during Pennsylvanian Glacial Phases?: PALAIOS, v. 25, p. 611-617.

FARMER, N., and JONES, J.M., 1969, The Carboniferous, Namurian Rocks of the coast section from Howick Bay to Foxton Hall, Northumberland: Transactions of the Natural History Society of Northumberland, Durham and Newcastle Upon Tyne, v. 17, p. 1-27.

FELIX, M., PEAKALL, J., and MCCAFFREY, W.D., 2006, Relative Importance of Processes That Govern the Generation of Particulate Hyperpycnal Flows: Journal of Sedimentary Research, v. 76, p. 382-387.

FIELDING, C.R., ALLEN, J.P., ALEXANDER, J., and GIBLING, M.R., 2009, Facies model for fluvial systems in the seasonal tropics and subtropics: Geology, v. 37, p. 623-626.

FIELDING, C.R., FRANK, T.D., BIRGENHEIER, L.P., RYGEL, M.C., JONES, A.T., and ROBERTS, J., 2008, Stratigraphic imprint of the Late Palaeozoic Ice Age in eastern Australia: a record of alternating glacial and nonglacial climate regime: Journal of the Geological Society, v. 165, p. 129-140.

FRASER, A.J., and GAWTHORPE, R.L., 1990, Tectono-stratigraphic development and hydrocarbon habitat of the Carboniferous in northern England, *in* Hardman, R.F.P., and Brooks, J., eds., Tectonic Events Responsible for Britain's Oil and Gas Reserves, Geological Society, London, Special Publications, v. 55, p. 49-86.

FRASER, A.J., and GAWTHORPE, R.L., 2003, An Atlas of Carboniferous Basin Evolution in Northern England: Geological Society, London, Memoirs, v. 28, 76 p.

FRINGS, R.M., 2008, Downstream fining in large sand-bed rivers: Earth-Science Reviews, v. 87, p. 39-60.

GALLAGHER, J., 2011, Sedimentology, diagenesis and geochemistry of the Great Limestone, Carboniferous, northern England [unpublished PhD thesis]: Durham University 434 p.

GAWTHORPE, R.L., 1987, Tectono-sedimentary evolution of the Bowland Basin, N England, during the Dinantian: Journal of the Geological Society, v. 144, p. 59-71.

GAWTHORPE, R.L., GUTTERIDGE, P., and LEEDER, M.R., 1989, Late Devonian and Dinantian basin evolution in northern England and North Wales, *in*

Gutteridge, P., Arthurton, R.S., and Nolan, S.C., eds., The Role of Tectonics in Devonian and Carboniferous Sedimentation in the British Isles: Occasional Publication of the Yorkshire Geological Society, Yorkshire Geological Society, p. 1-23.

GIBLING, M.R., BASHFORTH, A.R., FALCON-LANG, H.J., ALLEN, J.P., and FIELDING, C.R., 2010, Log Jams and Flood Sediment Buildup Caused Channel Abandonment and Avulsion in the Pennsylvanian of Atlantic Canada: Journal of Sedimentary Research, v. 80, p. 268-287.

GILBERT, G.K., 1883, The topographic features of lake shores: USGS. Annual Report 5-B: Washington, US Government Printing Office, 73 p.

GILBERT, G.K., 1890, Lake Bonneville: USGS Numbered Series: Monograph: Washington, 438 p.

GILLIGAN, A., 1919, The Petrography of the Millstone Grit of Yorkshire: Quarterly Journal of the Geological Society, v. 75, p. 251-294.

GOODBRED, S.L., and KUEHL, S.A., 2000, Enormous Ganges-Brahmaputra sediment discharge during strengthened early Holocene monsoon: Geology, v. 28, p. 1083-1086.

GOUW, M.J.P., and BERENDSEN, H.J.A., 2007, Variability of Channel-Belt Dimensions and the Consequences for Alluvial Architecture: Observations from the Holocene Rhine–Meuse Delta (The Netherlands) and Lower Mississippi Valley (U.S.A.): Journal of Sedimentary Research, v. 77, p. 124-138.

HALLSWORTH, C.R., and CHISHOLM, J.I., 2008, Provenance of late Carboniferous sandstones in the Pennine Basin (UK) from combined heavy mineral, garnet geochemistry and palaeocurrent studies: Sedimentary Geology, v. 203, p. 196-212.

HALLSWORTH, C.R., MORTON, A.C., CLAOUÉ-LONG, J., and FANNING, C.M., 2000, Carboniferous sand provenance in the Pennine Basin, UK: constraints from heavy mineral and detrital zircon age data: Sedimentary Geology, v. 137, p. 147-185.

HAMPSON, G.J., 1995, Incised valley fills and sequence stratigraphy of selected Carboniferous delta systems in the U.K. [unpublished PhD thesis]: University of Liverpool, 438 p.

HAMPSON, G.J., 1997, A sequence stratigraphic model for deposition of the Lower Kinderscout Delta, an Upper Carboniferous turbidite-fronted delta: Proceedings of the Yorkshire Geological Society, v. 51, p. 273-296.

HAMPSON, G.J., DAVIES, S.J., ELLIOT, T., FLINT, S.S., and STOLLHOFEN, H., 1999, Incised valley fill sandstone bodies in Upper Carboniferous fluvio–deltaic strata: recognition and reservoir characterization of Southern North Sea analogues, *in* Fleet, A.J., and Boldy, S.A.R., eds., Petroleum Geology of Northwest Europe: Proceedings of the 5th Conference, Geological Society, London, Petroleum Geology Conference series, v. 5, p. 771-788.

HAMPSON, G.J., ELLIOTT, T., and FLINT, S.S., 1996, Critical application of high resolution sequence stratigraphic concepts to the Rough Rock Group (Upper Carboniferous) of northern England, *in* Howell, J.A., and Aitken, J.F., eds., High Resolution Sequence Stratigraphy: Innovations and Applications, Geological Society, London, Special Publications, v. 104, p. 221-246.

HAMPSON, G.J., JEWELL, T.O., IRFAN, N., GANI, M.R., and BRACKEN, B., 2013, Modest Change In Fluvial Style With Varying Accommodation In Regressive Alluvial-To-Coastal-Plain Wedge: Upper Cretaceous Blackhawk Formation, Wasatch Plateau, Central Utah, U.S.A: Journal of Sedimentary Research, v. 83, p. 145-169.

HASZELDINE, R.S., 1984, Carboniferous North Atlantic palaeogeography; stratigraphic evidence for rifting, not megashear or subduction: Geological Magazine, v. 121, p. 443-463.

HASZELDINE, R.S., 1989, Evidence against crustal stretching, north-south tension and Hercynian collision, forming the British Carboniferous basins, *in* Gutteridge, P., Arthurton, R.S., and Nolan, S.C., eds., The Role of Tectonics in Devonian and Carboniferous Sedimentation in the British Isles.

HAUGHTON, P.D.W., BARKER, S.P., and MCCAFFREY, W.D., 2003, 'Linked' debrites in sand-rich turbidite systems – origin and significance: Sedimentology, v. 50, p. 459-482.

HELLAND-HANSEN, W., and HAMPSON, G.J., 2009, Trajectory analysis: concepts and applications: Basin Research, v. 21, p. 454-483.

HELLAND-HANSEN, W., STEEL, R.J., and SØMME, T.O., 2012, Shelf genesis revisited: Journal of Sedimentary Research, v. 82, p. 133-148.

HICKS, P.F., 1957, The Yoredale Series and Millstone Grit of the south west corner of the Askrigg Block [unpublished PhD thesis]: University of Leeds, 218 p.

HICKSON, T.A., SHEETS, B.A., PAOLA, C., and KELBERER, M., 2005, Experimental test of tectonic controls on three-dimensional alluvial facies architecture: Journal of Sedimentary Research, v. 75, p. 710-722.

HIND, W., 1902, On the Characters of the Carboniferous Rocks of the Pennine System: Proceedings of the Yorkshire Geological Society, v. 14, p. 422-464.

HOLBROOK, J., SCOTT, R.W., and OBOH-IKUENOBE, F.E., 2006, Base-level buffers and buttresses: A model for upstream versus downstream control on fluvial geometry and architecture within sequences: Journal of Sedimentary Research, v. 76, p. 162-174.

HOLBROOK, J.M., 1996, Complex fluvial response to low gradients at maximum regression; a genetic link between smooth sequence-boundary morphology and architecture of overlying sheet sandstone: Journal of Sedimentary Research, v. 66, p. 713-722.

HOLBROOK, J.M., and BHATTACHARYA, J.P., 2012, Reappraisal of the sequence boundary in time and space: Case and considerations for an SU (subaerial unconformity) that is not a sediment bypass surface, a time barrier, or an unconformity: Earth-Science Reviews, v. 113, p. 271-302.

HOLDSWORTH, B.K., and COLLINSON, J.D., 1988, Millstone Grit cyclicity revisited, *in* Besly, B.M., and Kelling, G., eds., Sedimentation in a Synorogenic Basin Complex: The Upper Carboniferous of Northwest Europe, Blackie, Glasgow, p. 132-152.

HORTON, D.E., POULSEN, C.J., MONTAÑEZ, I.P., and DIMICHELE, W.A., 2012, Eccentricity-paced late Paleozoic climate change: Palaeogeography, Palaeoclimatology, Palaeoecology, v. 331–332, p. 150-161.

HORTON, D.E., POULSEN, C.J., and POLLARD, D., 2010, Influence of high-latitude vegetation feedbacks on late Palaeozoic glacial cycles: Nature Geoscience, v. 3, p. 572-577.

HOVIUS, N., 1998, Controls on sediment supply by large rivers, *in* Shanley, K.W., and McCabe, P.W., eds., Relative Role of Eustasy, Climate, and Tectonism in Continental Rocks, SEPM Special Publication, v. 59, p. 3-16.

HUDSON, R.G.S., 1937, The Millstone Grit Succession of the Simonseat Anticline, Yorkshire: Proceedings of the Yorkshire Geological Society, v. 23, p. 319-349.

HUDSON, R.G.S., and MITCHELL, G.H., 1937, The Carboniferous geology of the Skipton Anticline: Geological Survey of Great Britain Summary of Progress for 1935, v. Part 2, p. 1-45.

HUGHES, R.A., 1987, Geology of the White Hill area (SD 65 NE). British Geological Survey Technical Report WA/87/47.

HUNT, D., and TUCKER, M.E., 1992, Stranded parasequences and the forced regressive wedge systems tract – Deposition during base-level fall: Sedimentary Geology, v. 81, p. 1-9.

JERRETT, R.M., and HAMPSON, G.J., 2007, Sequence stratigraphy of the upper Millstone Grit (Yeadonian, Namurian), North Wales: Geological Journal, v. 42, p. 513-530.JERRETT, R.M., HODGSON, D.M., FLINT, S.S., and DAVIES, R.C., 2011, Control of Relative Sea Level and Climate on Coal Character in the Westphalian C (Atokan) Four Corners Formation, Central Appalachian Basin, U.S.A: Journal of Sedimentary Research, v. 81, p. 420-445.

JOHNSON, G.A.L., 1984, Subsidence and sedimentation in the Northumberland Trough: Proceedings of the Yorkshire Geological Society, v. 45, p. 71-83.

JOHNSON, G.A.L., HODGE, B.L., and FAIRBAIRN, R.A., 1962, The Base of the Namurian and of the Millstone Grit in North-Eastern England: Proceedings of the Yorkshire Geological Society, v. 33, p. 341-362.

JONES, C.M., 1980, Deltaic Sedimentation in the Roaches Grit and Associated Sediments (Namurian R2b) in the South-West Pennines: Proceedings of the Yorkshire Geological Society, v. 43, p. 39-67.

JONES, C.M., and CHISHOLM, J.I., 1997, The Roaches and Ashover Grits: Sequence stratigraphic interpretation of a 'turbidite-fronted delta' system: Geological Journal, v. 32, p. 45-68.

JONES, C.M., and MCCABE, P.J., 1980, Erosion surfaces within giant fluvial cross-beds of the Carboniferous in northern England: Journal of Sedimentary Research, v. 50, p. 613-620.

JONES, T.W., 1943, The Geology of the Beamsley Anticline: Proceedings of the Leeds Philosophical and Literary Society, v. 4, p. 146-166.

KANE, I.A., 2010, Development and flow structures of sand injectites: The Hind Sandstone Member injectite complex, Carboniferous, UK: Mar Pet Geol, v. 27, p. 16-16.

KANE, I.A., CATTERALL, V., MCCAFFREY, W.D., and MARTINSEN, O.J., 2010a, Submarine channel response to intrabasinal tectonics: The influence of lateral tilt: AAPG Bulletin, v. 94, p. 189-219.

KANE, I.A., MCCAFFREY, W.D., and PEAKALL, J., 2010b, On the Origin of Paleocurrent Complexity Within Deep Marine Channel Levees: Journal of Sedimentary Research, v. 80, p. 54-66.

KANE, I.A., MCCAFFREY, W.D., and MARTINSEN, O.J., 2009, Allogenic vs. Autogenic Controls on Megaflute Formation: Journal of Sedimentary Research, v. 79, p. 643-651.

KIM, W., SHEETS, B.A., and PAOLA, C., 2010, Steering of experimental channels by lateral basin tilting: Basin Research, v. 22, p. 286-301.

KIRBY, G.A., BAILY, H.E., CHADWICK, R.A., EVANS, D.J., HOLLIDAY, D.W., HOLLOWAY, S., HULBERT, A.G., PHARAOH, T.C., SMITH, N.J.P., and AITKENHEAD, N., 2000, The stucture and evolution of the Craven Basin and adjacent areas: Subsurface Memoir of the British Geological Survey: London, The Stationery Office.

KNIGHTON, A.D., 1999, Downstream variation in stream power: Geomorphology, v. 29, p. 293-306.

KOSTIC, S., and PARKER, G., 2003a, Progradational sand-mud deltas in lakes and reservoirs. Part 1. Theory and numerical modeling: Journal of Hydraulic Research, v. 41, p. 127-140.

KOSTIC, S., and PARKER, G., 2003b, Progradational sand-mud deltas in lakes and reservoirs. Part 2. Experiment and numerical simulation: Journal of Hydraulic Research, v. 41, p. 141-152.

KOSTIC, S., PARKER, G., and MARR, J.G., 2002, Role of turbidity currents in setting the foreset slope of clinoforms prograding into standing fresh water: Journal of Sedimentary Research, v. 72, p. 353-362.

LAMB, M.P., MCELROY, B., KOPRIVA, B., SHAW, J., and MOHRIG, D., 2010, Linking river-flood dynamics to hyperpycnal-plume deposits: Experiments, theory, and geological implications: Geological Society of America Bulletin, v. 122, p. 1389-1400.

LAMB, M.P., and MOHRIG, D., 2009, Do hyperpycnal-flow deposits record river-flood dynamics?: Geology, v. 37, p. 1067-1070.

LECLAIR, S.F., 2002, Preservation of cross-strata due to the migration of subaqueous dunes: an experimental investigation: Sedimentology, v. 49, p. 1157-1180.

LEEDER, M., 1999, Sedimentology and Sedimentary Basins: From Turbulence to Tectonics: Oxford, Blackwell Science, xvi+592 p.

LEEDER, M., FAIRHEAD, D., LEE, A.G., STUART, G., CLEMMEY, H., EL-HADDAHEH, B., and GREEN, C., 1989, Sedimentary and tectonic evolution of the Northumberland Basin, *in* Gutteridge, P., Arthurton, R.S., and Nolan, S.C., eds., The Role of Tectonics in Devonian and Carboniferous Sedimentation in the British Isles: Occasional Publication of the Yorkshire Geological Society, Yorkshire Geological Society, p. 207-223.

LEEDER, M.R., 1982, Upper Palaeozoic basins of the British Isles--Caledonide inheritance versus Hercynian plate margin processes: Journal of the Geological Society, v. 139, p. 479-491.

LEEDER, M.R., and ALEXANDER, J., 1987, The origin and tectonic significance of asymmetrical meander-belts: Sedimentology, v. 34, p. 217-226.

LEEDER, M.R., and MCMAHON, A.H., 1988, Upper Carboniferous (Silesian) basin subsidence in northern Britain, *in* Besly, B.M., and Kelling, G., eds., Sedimentation in a Synorogenic Basin Complex: The Upper Carboniferous of Northwest Europe, Blackie, Glasgow, p. 43-52.

LEEDER, M.R., and STRUDWICK, A.E., 1987, Delta-Marine Interactions: a Discussion of Sedimentary Models for Yoredale-type Cyclicity in The Dinantian of Northern England, *in* Miller, J., Adams, A.E., and Wright, V.P., eds., European Dinantian Environments, John Wiley & Sons Ltd., p. 115-130.

LEMON, K., 2006, The climatic, eustatic and tectonic controls on the Mid Carboniferous (Visean and Namurian) strata of Northumbria, England. [unpublished PhD thesis]: University of Durham, Durham, 351 p.

LISIECKI, L.E., and RAYMO, M.E., 2005, A Pliocene-Pleistocene stack of 57 globally distributed benthic $d^{18}O$ records: Paleoceanography, v. 20, p. PA1003.

LOWE, D.R., 1982, Sediment gravity flows: II. Depositional models with special reference to the deposits of high-density turbidity currents: Journal of Sedimentary Petrology, v. 52, p. 279-297.

MACKIN, J.H., 1948, Concept of the Graded River: Geological Society of America Bulletin, v. 59, p. 463-512.

MARTIN, C.A.L., and TURNER, B.R., 1998, Origins of massive-type sandstones in braided river systems: Earth-Science Reviews, v. 44, p. 15-38.

MARTIN, J., CANTELLI, A., PAOLA, C., BLUM, M., and WOLINSKY, M., 2011, Quantitative Modeling of the Evolution and Geometry of Incised Valleys: Journal of Sedimentary Research, v. 81, p. 64-79.

MARTINSEN, O.J., 1990, Interaction between eustacy, tectonics and sedimentation with particular reference to the Namurian E1c-H2c of the Craven-Askrigg area, northern England [unpublished PhD thesis]: University of Bergen, 271 p.

MARTINSEN, O.J., 1993, Namurian (Late Carboniferous) Depositional Systems of the Craven-Area, Northern England: Implications for Sequence-Stratigraphic Models, *in* Posamentier, H.W., Summerhayes, C.P., Haq, B.U., and Allen, G.P., eds., Sequence Stratigraphy and Facies Associations, Special Publication of the IAS v. 18, Blackwell Publishing Ltd., p. 247-281.

MARTINSEN, O.J., COLLINSON, J.D., and HOLDSWORTH, B.K., 1995, Millstone Grit Cyclicity Revisited, II: Sequence Stratigraphy and Sedimentary Responses to Changes of Relative Sea-Level, *in* Plint, A.G., ed., Sedimentary Facies Analysis, Blackwell Publishing Ltd., p. 305-327.

MARTINSEN, O.J., SØMME, T.O., THURMOND, J.B., HELLAND-HANSEN, W., and LUNT, I., 2010, Source-to-sink systems on passive margins: theory and practice with an example from the Norwegian continental margin, *in* Vining, B.A., and Pickering, S.C., eds., Petroleum Geology: From Mature Basins to New Frontiers – Proceedings of the 7th Petroleum Geology Conference, Geological Society, London, Petroleum Geology Conference series, v. 7, p. 913-920.

MASSARI, F., 1996, Upper-flow-regime stratification types on steep-face, coarse-grained, Gilbert-type progradational wedges (Pleistocene, southern Italy): Journal of Sedimentary Research, v. 66, p. 364-375.

MAYNARD, J.R., 1992, Sequence stratigraphy of the Upper Yeadonian of northern England: Marine and Petroleum Geology, v. 9, p. 197-207.

MAYNARD, J.R., HOFMANN, W., DUNAY, R.E., BENTHAN, P.N., DEAN, K.P., and WATSON, I., 1997, The Carboniferous of Western Europe; the development of a petroleum system: Petroleum Geoscience, v. 3, p. 97-115.

MAYNARD, J.R., and LEEDER, M.R., 1992, On the periodicity and magnitude of Late Carboniferous glacio-eustatic sea-level changes: Journal of the Geological Society, v. 149, p. 303-311.

MCCABE, P.J., 1975, The Sedimentology and Stratigraphy of the Kinderscout Grit Group (Namurian, R1) between Wharfedale and Longdendale [unpublished PhD thesis]: University of Keele, Keele, 172 p.

MCCABE, P.J., 1977, Deep distributary channels and giant bedforms in the Upper Carboniferous of the Central Pennines, northern England: Sedimentology, v. 24, p. 271-290.

MCLEAN, D., and CHISHOLM, J.I., 1996, Reworked palynomorphs as provenance indicators in the Yeadonian of the Pennine Basin: Proceedings of the Yorkshire Geological Society, v. 51, p. 141-151.

MILLIMAN, JOHN D., and KAO, S.J., 2005, Hyperpycnal Discharge of Fluvial Sediment to the Ocean: Impact of Super-Typhoon Herb (1996) on Taiwanese Rivers: The Journal of Geology, v. 113, p. 503-516.

MOREHEAD, M.D., SYVITSKI, J.P., HUTTON, E.W.H., and PECKHAM, S.D., 2003, Modeling the temporal variability in the flux of sediment from ungauged river basins: Global and Planetary Change, v. 39, p. 95-110.

MORTON, A., WATERS, C., FANNING, M., CHISHOLM, I., and BRETTLE, M., 2014, Origin of Carboniferous sandstones fringing the northern margin of the Wales-Brabant Massif: insights from detrital zircon ages: Geological Journal, p. n/a-n/a.

MORTON, A.C., and WHITHAM, A.G., 2002, The Millstone Grit of northern England: a response to tectonic evolution of a northern sourceland: Proceedings of the Yorkshire Geological Society, v. 54, p. 47-56.

MOSELEY, F., 1972, A tectonic history of northwest England: Journal of the Geological Society, v. 128, p. 561-594.

MULDER, T., and ALEXANDER, J., 2001, The physical character of subaqueous sedimentary density flows and their deposits: Sedimentology, v. 48, p. 269-299.

MULDER, T., and SYVITSKI, J.P.M., 1995, Turbidity Currents Generated at River Mouths during Exceptional Discharges to the World Oceans: The Journal of Geology, v. 103, p. 285-299.

MULDER, T., SYVITSKI, J.P.M., MIGEON, S., FAUGÈRES, J.-C., and SAVOYE, B., 2003, Marine hyperpycnal flows: initiation, behavior and related deposits. A review: Marine and Petroleum Geology, v. 20, p. 861-882.

MUNDY, D.J.C., and ARTHURTON, R.S., 1980, FIELD MEETINGS 1978: Proceedings of the Yorkshire Geological Society, v. 43, p. 29-38.

MUTO, T., 2001, Shoreline autoretreat substantiated in flume experiments: Journal of Sedimentary Research, v. 71, p. 246-254.

MUTO, T., and STEEL, R.J., 2002a, Role of autoretreat and AS changes in the understanding of deltaic shoreline trajectory: a semi-quantitative approach: Basin Research, v. 14, p. 303-318.

MUTO, T., and STEEL, R.J., 2002b, In Defense of Shelf-Edge Delta Development during Falling and Lowstand of Relative Sea Level: Journal of Geology, v. 110, p. 421-436.

MUTO, T., STEEL, R.J., and SWENSON, J.B., 2007, Autostratigraphy: A framework norm for genetic stratigraphy: Journal of Sedimentary Research, v. 77, p. 2-12.

MUTO, T., and SWENSON, J.B., 2005, Large-scale fluvial grade as a nonequilibrium state in linked depositional systems: Theory and experiment: Journal of Geophysical Research: Earth Surface, v. 110, p. F03002.

NEMEC, W., 1990, Aspects of Sediment Movement on Steep Delta Slopes, *in* Colella, A., and Prior, D.B., eds., Coarse-Grained Deltas, Blackwell Publishing Ltd., p. 29-73.

O'BEIRNE, A.M., 1996, Controls on Silesian sedimentation in the Pennine Basin, UK and Appalachian Basin, Eastern Kentucky [unpublished PhD thesis]: Oxford Brookes University.

OERLEMANS, J., 1991, The role of ice sheets in the Pleistocene climate: Norsk Geologisk Tidsskrift, v. 71, p. 155-161.

PAOLA, C., HELLER, P.L., and ANGEVINE, C.L., 1992a, The large-scale dynamics of grain-size variation in alluvial basins, 1: Theory: Basin Research, v. 4, p. 73-90.

PAOLA, C., PARKER, G., SEAL, R., SINHA, S.K., SOUTHARD, J.B., and WILCOCK, P.R., 1992b, Downstream Fining by Selective Deposition in a Laboratory Flume: Science, v. 258, p. 1757-1760.

PAOLA, C., STRAUB, K., MOHRIG, D., and REINHARDT, L., 2009, The "unreasonable effectiveness" of stratigraphic and geomorphic experiments: Earth-Science Reviews, v. 97, p. 1-43.

PEAKALL, J., ASHWORTH, P., and BEST, J., 1996, Physical modelling in fluvial geomorphology: principles, applications and unresolved issues, *in* Rhoads, B.L., and Thorn, C.E., eds., The Scientific Nature of Geomorphology: Chichester, John Wiley and Sons, p. 221-253.

PETTER, A.L., and MUTO, T., 2008, Sustained alluvial aggradation and autogenic detachment of the alluvial river from the shoreline in response to steady fall of relative sea level: Journal of Sedimentary Research, v. 78, p. 98-111.

PEYSER, C.E., and POULSEN, C.J., 2008, Controls on Permo-Carboniferous precipitation over tropical Pangaea: A GCM sensitivity study: Palaeogeography, Palaeoclimatology, Palaeoecology, v. 268, p. 181-192.

PHILIPS, J., 1836, Illustrations of the geology of Yorkshire, Part II. The Mountain Limestone District: London, John Murray, 253 p.

PLINK-BJÖRKLUND, P., and STEEL, R., 2002, Sea-level fall below the shelf edge, without basin-floor fans: Geology, v. 30, p. 115-118.

PLINK-BJÖRKLUND, P., and STEEL, R., 2005, Deltas on Falling-Stage and Lowstand Shelf Margins, The Eocene Central Basin of Spitsbergen: Importance of Sediment Supply, *in* Giosan, L., and Bhattacharya, J., eds., River Deltas-Concepts, Models, and Examples, SEPM Special Publication, v. 83, p. 179-206.

PLINK-BJÖRKLUND, P., and STEEL, R., 2007, Type II Shelf Margin, Hogsnyta, Norway: Attached Slope Turbidite System, *in* Nilsen, T.H., Shew, R.D., Steffens, G.S., and Studlick, J.R.J., eds., Atlas of Deep-Water Outcrops: American Association of Petroleum Geologists, Studies in Geology 56, p. 282-286.

PLINK-BJÖRKLUND, P., and STEEL, R.J., 2004, Initiation of turbidity currents: outcrop evidence for Eocene hyperpycnal flow turbidites: Sedimentary Geology, v. 165, p. 29-52.

PLINT, A.G., 1988, Sharp-Based Shoreface Sequences And 'Offshore Bars' In The Cardium Formation Of Alberta: Their Relationship To Relative Changes In Sea Level *in* Wilgus, C.K., Hastings, B.S., Kendall, C.G.S.C., Posamentier, H.W., Ross, H.W., and Van Wagoner, J.C., eds., Sea Level Changes - An Integrated Approach, SEPM Special Publication, v. 42, p. 357-370.

PLINT, A.G., and WADSWORTH, J.A., 2006, Delta-Plain Paleodrainage Patterns Reflect Small-Scale Fault Movement and Subtle Forebulge Uplift: Upper Cretaceous Dunvegan Formation, Western Canada Foreland Basin, *in* Dalrymple, R.W., Leckie, D.A., and Tillman, R.W., eds., Incised Valleys in Time and Space, SEPM Spec. Publ. 85, p. 219-237.

POREBSKI, S.J., and STEEL, R.J., 2003, Shelf-margin deltas: their stratigraphic significance and relation to deepwater sands: Earth-Science Reviews, v. 62, p. 283-326.

POSAMENTIER, H.W., and ALLEN, G.P., 1999, Fundamental Concepts of Sequence Stratigraphy, Siliciclastic Sequence Stratigraphy—Concepts and Applications, SEPM Concepts in Sedimentology and Paleontology 7, p. 9-51.

POSAMENTIER, H.W., ALLEN, G.P., JAMES, D.P., and TESSON, M., 1992, Forced Regressions in a Sequence Stratigraphic Framework - Concepts, Examples, and Exploration Significance: AAPG Bulletin, v. 76, p. 1687-1709.

POSAMENTIER, H.W., JERVEY, M.T., and VAIL, P.R., 1988, Eustatic controls on clastic deposition I - conceptual framework, *in* Wilgus, C.K., Hastings, B.S., Kendall, C.G.S.C., Posamentier, H.W., Ross, H.W., and Van Wagoner, J.C., eds., Sea Level Changes - An Integrated Approach, SEPM Special Publication, v. 42, p. 110-124.

POSAMENTIER, H.W., and VAIL, P.R., 1988, Eustatic controls on clastic deposition II - sequence and system tract models, *in* Wilgus, C.K., Hastings, B.S., Kendall, C.G.S.C., Posamentier, H.W., Ross, H.W., and Van Wagoner, J.C., eds., Sea Level Changes - An Integrated Approach, SEPM Special Publication, v. 42, p. 125-154.

POSTMA, G., 1990, An analysis of the variation in delta architecture: Terra Nova, v. 2, p. 124-130.

POSTMA, G., HILGEN, F.J., and ZACHARIASSE, W.J., 1993, Precession-punctuated growth of a Late Miocene submarine-fan lobe on Gavdos (Greece): Terra Nova, v. 5, p. 438-444.

POSTMA, G., KLEINHANS, M.G., MEIJER, P.T., and EGGENHUISEN, J.T., 2008, Sediment transport in analogue flume models compared with real-world sedimentary systems: a new look at scaling evolution of sedimentary systems in a flume: Sedimentology, v. 55, p. 1541-1557.

POSTMA, G., and ROEP, T.B., 1985, Resedimented Conglomerates in the Bottomsets of Gilbert-Type Gravel Deltas: Journal of Sedimentary Petrology, v. 55, p. 874-885.

POULSEN, C.J., POLLARD, D., MONTAÑEZ, I.P., and ROWLEY, D., 2007, Late Paleozoic tropical climate response to Gondwanan deglaciation: Geology, v. 35, p. 771-774.

PRÉLAT, A., HODGSON, D.M., and FLINT, S.S., 2009, Evolution, architecture and hierarchy of distributary deep-water deposits: a high-resolution outcrop investigation from the Permian Karoo Basin, South Africa: Sedimentology, v. 56, p. 2132-2154.

PRINCE, G.D., and BURGESS, P.M., 2013, Numerical Modeling of Falling-Stage Topset Aggradation: Implications for Distinguishing Between Forced and Unforced Regressions In the Geological Record: Journal of Sedimentary Research, v. 83, p. 767-781.

RAMSBOTTOM, W.H.C., 1966, A pictoral diagram of the Namurian Rocks of the Pennines: Transactions of the Leeds Geological Association, v. 7, p. 181-184.

RAMSBOTTOM, W.H.C., 1974, Dinantian and Namurian, *in* Rayner, D.H., and Hemingway, J.E., eds., The Geology and Mineral Resources of Yorkshire: Occasional Publication of the Yorkshire Geological Society: Leeds, Yorkshire Geological Society, p. 45-87.

RAMSBOTTOM, W.H.C., 1977a, Major cycles of transgression and regression (mesotherms) in the Namurian: Proceedings of the Yorkshire Geological Society, v. 41, p. 261-291.

RAMSBOTTOM, W.H.C., 1977b, Correlation of the Scottish Upper Limestone Group (Namurian) with that of the North of England: Scottish Journal of Geology, v. 13, p. 327-330.

RAMSBOTTOM, W.H.C., 1979, Rates of transgression and regression in the Carboniferous of NW Europe: Journal of the Geological Society, v. 136, p. 147-153.

RAMSBOTTOM, W.H.C., CALVER, M.A., EAGAR, R.M.C., HODSON, F., HOLLIDAY, D.W., STUBBLEFIELD, C.J., and WILSON, R.B., 1978, A Correlation of Silesian Rocks in the British Isles: Special Report of the Geological Society, v. 10.

RAMSBOTTOM, W.H.C., RHYS, G.H., and SMITH, E.G., 1962, Boreholes in the Carboniferous of the Ashover District, Derbyshire: Bulletin of the Geological Survey of Great Britain, v. 12, p. 75-168.

READ, W.A., 1989, The influence of basin subsidence and depositional environment on regional patterns of coal thickness within the Namurian fluvio-deltaic sedimentary fill of the Kincardine Basin, Scotland, *in* Whateley, M.K.G., and Pickering, K.T., eds., Deltas: Sites and Traps for Fossil Fuels, Geological Society, London, Special Publications, v. 41, p. 333-344.

READ, W.A., 1991, The Millstone Grit (Namurian) of the southern pennines viewed in the light of eustatically controlled sequence stratigraphy: Geological Journal, v. 26, p. 157-165.

READ, W.A., 1992, Reply to: 'The Millstone Grit (Namurian) of the southern Pennines viewed in the light of eustatically controlled sequence stratigraphy' by W.A. Read: Geological Journal, v. 27, p. 175-180.

READ, W.A., 1994, The frequencies of Scottish Pendleian allocycles: Scottish Journal of Geology, v. 30, p. 91-93.

READ, W.A., 1995, Sequence stratigraphy and lithofacies geometry in an early Namurian coal-bearing succession in central Scotland, *in* Whateley, M.K.G., and Spears, D.A., eds., European Coal Geology, Geological Society, London, Special Publications, v. 82, p. 285-297.

READING, H.G., 1996, Sedimentary Environments: Processes, Facies and Stratigraphy: Oxford, Blackwell Publishing, 688 p.

REESINK, A.J.H., ASHWORTH, P.J., SAMBROOK SMITH, G.H., BEST, J.L., PARSONS, D.R., AMSLER, M.L., HARDY, R.J., LANE, S.N., NICHOLAS, A.P., ORFEO, O., SANDBACH, S.D., SIMPSON, C.J., and SZUPIANY, R.N., 2014, Scales and causes of heterogeneity in bars in a large multi-channel river: Río Paraná, Argentina: Sedimentology, v. 61, p. 1055-1085.

REESINK, A.J.H., and BRIDGE, J.S., 2011, Evidence of Bedform Superimposition and Flow Unsteadiness In Unit-Bar Deposits, South Saskatchewan River, Canada: Journal of Sedimentary Research, v. 81, p. 814-840.

REID, C.T., 1996, The Alportian and Kinderscoutian (Namurian) of North Yorkshire: the Sedimentary Response to Eustatic Variation [unpublished PhD thesis]: University of Keele, Keele, 233 p.

RICE, S.P., and CHURCH, M., 2001, Longitudinal profiles in simple alluvial systems: Water Resources Research, v. 37, p. 417-426.

RIGBY, J.K., and MUNDY, D.J.C., 2000, Lower Carboniferous sponges from the Craven Reef Belt of North Yorkshire: Proceedings of the Yorkshire Geological Society, v. 53, p. 119-128.

RILEY, N.J., 1996, Bivalves from the Croft House Bh., Bradford Sheet 69: Implications for the late Pendleian/early Arnsbergian stratigraphy: BGS Report WH96/140R, p. 1-4.

RILEY, N.J., and MCNESTRY, A., 1988, Biostratigraphy and Correlation of Boulsworth and Holme Chapel Boreholes., British Geological Survey Technical Report, Stratigraphy Series WH/88/375 (PD/88/338): Keyworth, Notthinghamshire, Britisch Geological Survey.

RITCHIE, B.D., GAWTHORPE, R.L., and HARDY, S., 2004, Three-dimensional numerical modeling of deltaic depositional sequences 2: Influence of local controls: Journal of Sedimentary Research, v. 74, p. 221-238.

RITTENOUR, T.M., BLUM, M.D., and GOBLE, R.J., 2007, Fluvial evolution of the lower Mississippi River valley during the last 100 k.y. glacial cycle: Response to glaciation and sea-level change: Geological Society of America Bulletin, v. 119, p. 586-608.

ROSE, W.C.C., and DUNHAM, K.C., 1977, Geology and hematite deposits of South Cumbria, Sheet 58, Part 48: Economic Memoir of the British Geological Survey.

ROSS, C.A., and ROSS, J.R.P., 1985, Late Paleozoic depositional sequences are synchronous and worldwide: Geology, v. 13, p. 194-197.

ROSSIGNOL-STRICK, M., 1983, African monsoons, an immediate climate response to orbital insolation: Nature, v. 304, p. 46-49.

ROWELL, A.J., and SCANLON, J.E., 1957a, The Relation between the Yoredale Series and the Millstone Grit on the Askrigg Block: Proceedings of the Yorkshire Geological Society, v. 31, p. 79-90.

ROWELL, A.J., and SCANLON, J.E., 1957b, The Namurian of the North-West Quarter of the Askrigg Block: Proceedings of the Yorkshire Geological Society, v. 31, p. 1-38.

RUDDIMAN, W.F., 2001, Earth's Climate: Past and Future: New York, W.H. Freeman and Company, 465 p.

RUDDIMAN, W.F., 2006, Orbital changes and climate: Quaternary Science Reviews, v. 25, p. 3092-3112.

RYGEL, M.C., FIELDING, C.R., FRANK, T.D., and BIRGENHEIER, L.P., 2008, The magnitude of late Paleozoic glacioeustatic fluctuations: a synthesis: Journal of Sedimentary Research, v. 78, p. 500-511.

SCHLAGER, W., 1993, Accommodation and supply -a dual control on stratigraphic sequences: Sedimentary Geology, v. 86, p. 111-136.

SCHUMM, S.A., and LICHTY, R.W., 1965, Time, space, and causality in geomorphology: American Journal of Science, v. 263, p. 110-119.

SHANLEY, K.W., and MCCABE, P.J., 1994, Perspectives on the Sequence Stratigraphy of Continental Strata: AAPG Bulletin, v. 78, p. 544-568.

SHEETS, B.A., HICKSON, T.A., and PAOLA, C., 2002, Assembling the stratigraphic record: depositional patterns and time-scales in an experimental alluvial basin: Basin Research, v. 14, p. 287-301.

SIEGENTHALER, C., and HUGGENBERGER, P., 1993, Pleistocene Rhine gravel: deposits of a braided river system with dominant pool preservation, *in* Best, J.L., and Bristow, C.S., eds., Braided Rivers, Geological Society, London, Special Publications, v. 75, p. 147-162.

SIMPSON, G., and CASTELLTORT, S., 2012, Model shows that rivers transmit high-frequency climate cycles to the sedimentary record: Geology, v. 40, p. 1131-1134.

SIMS, A.P., 1988, The evolution of a sand-rich basin-fill sequence in the Pendleian (Namurian, E1c) of North-West England [unpublished PhD thesis]: University of Leeds, Leeds, 255 p.

SINHA, S.K., and PARKER, G., 1996, Causes of Concavity in Longitudinal Profiles of Rivers: Water Resources Research, v. 32, p. 1417-1428.

SØMME, T.O., HELLAND-HANSEN, W., and GRANJEON, D., 2009, Impact of eustatic amplitude variations on shelf morphology, sediment dispersal, and sequence stratigraphic interpretation: Icehouse versus greenhouse systems: Geology, v. 37, p. 587-590.

SOPER, N.J., WEBB, B.C., and WOODCOCK, N.H., 1987, Late Caledonian (Acadian) transpression in north-west England: timing, geometry and geotectonic significance: Proceedings of the Yorkshire Geological Society, v. 46, p. 175-192.

SORBY, H.C., 1859, The Structure and Origin of the Millstone-grit of South Yorkshire: Proceedings of the Yorkshire Geological Society, v. 3, p. 669-675.

STEEL, R., PLINK-BJÖRKLUND, P., and MELLERE, D., 2007, Storvola, Type I Shelf Margin, Norway, *in* Nilsen, T.H., Shew, R.D., Steffens, G.S., and Studlick, J.R.J., eds., Atlas of Deep-Water Outcrops: American Association of Petroleum Geologists, Studies in Geology 56, p. 274-281.

STEELE, R.P., 1988, The Namurian sedimentary history of the Gainsborough Trough, *in* Besly, B.M., and Kelling, G., eds., Sedimentation in a Synorogenic Basin Complex: The Upper Carboniferous of Northwest Europe, Blackie, Glasgow, p. 102-113.

STEPHENS, J.V., EDWARDS, W., STUBBLEFIELD, C.J., and MITCHELL, G.H., 1941, The Faunal Divisions of the Millstone Grit Series of Rombalds Moor and Neighbourhood: Proceedings of the Yorkshire Geological Society, v. 24, p. 344-372.

STEPHENS, J.V., MITCHELL, G.H., and EDWARDS, W., 1953, Geology of the Country between Bradford and Skipton: Memoirs of the Geological Survey of Great Britain, England and Wales.

STRAUB, K.M., PAOLA, C., MOHRIG, D., WOLINSKY, M.A., and GEORGE, T., 2009, Compensational Stacking of Channelized Sedimentary Deposits: Journal of Sedimentary Research, v. 79, p. 673-688.

STRAUB, K.M., and WANG, Y., 2013, Influence of water and sediment supply on the long-term evolution of alluvial fans and deltas: Statistical characterization of basin-filling sedimentation patterns: Journal of Geophysical Research: Earth Surface, v. 118, p. 1602-1616.

STRONG, N., and PAOLA, C., 2008, Valleys that never were: time surfaces versus stratigraphic surfaces: Journal of Sedimentary Research, v. 78, p. 579-593.

SWAN, A.R.H., and SANDILANDS, M., 1995, Introduction to Geological Data Analysis: Oxford, England, Blackwell Science Ltd., 446 p.

SWENSON, J.B., and MUTO, T., 2007, Response of coastal plain rivers to falling relative sea-level: allogenic controls on the aggradational phase: Sedimentology, v. 54, p. 207-221.

TABOR, N.J., and POULSEN, C.J., 2008, Palaeoclimate across the Late Pennsylvanian–Early Permian tropical palaeolatitudes: A review of climate indicators, their distribution, and relation to palaeophysiographic climate factors: Palaeogeography, Palaeoclimatology, Palaeoecology, v. 268, p. 293-310.

TONKS, L.H., 1925, The Millstone Grit and Yoredale Rocks of Nidderdale: Proceedings of the Yorkshire Geological Society, v. 20, p. 226-256.

TUCKER, M.E., GALLAGHER, J., and LENG, M.J., 2009, Are beds in shelf carbonates millennial-scale cycles? An example from the mid-Carboniferous of northern England: Sedimentary Geology, v. 214, p. 19-34.

VAN DEN BELT, F.J.G., 2012, Sedimentary cycles in coal and evaporite basins and the reconstructino of Palaeozoic climate [unpublished PhD thesis]: Utrecht University, 100 p.

VAN HEIJST, M.W.I.M., and POSTMA, G., 2001, Fluvial response to sea-level changes: a quantitative analogue, experimental approach: Basin Research, v. 13, p. 269-292.

VAN HEIJST, M.W.I.M., POSTMA, G., MEIJER, X.D., SNOW, J.N., and ANDERSON, J.B., 2001, Quantitative analogue flume-model study of rivershelf systems: principles and verification exemplified by the Late Quaternary Colorado riverdelta evolution: Basin Research, v. 13, p. 243-268.

VAN WAGONER, J.C., POSAMENTIER, H.W., MITCHUM, R.M., VAIL, P.R., SARG, J.F., LOUTIT, T.S., and HARDENBOL, J., 1988, An overview of the fundamentals of sequence stratigraphy and key definitions, *in* Wilgus, C.K., Hastings, B.S., Kendall, C.G.S.C., Posamentier, H.W., Ross, H.W., and Van Wagoner, J.C., eds., Sea Level Changes - An Integrated Approach, SEPM Special Publication, v. 42, p. 37-45.

VANSTONE, S., 1996, The influence of climatic change on exposure surface development: a case study from the Late Dinantian of England and Wales, *in* Strogen, P., Somerville, I.D., and Jones, G.L., eds., Recent Advances in Lower Carboniferous Geology, Geological Society, London, Special Publications, v. 107, p. 281-301.

VOLLER, V.R., and PAOLA, C., 2010, Can anomalous diffusion describe depositional fluvial profiles?: Journal of Geophysical Research: Earth Surface, v. 115, p. F00A13.

VOLLMER, S., and KLEINHANS, M.G., 2007, Predicting incipient motion, including the effect of turbulent pressure fluctuations in the bed: Water Resources Research, v. 43, p. W05410.

WALKER, C.T., 1955, Current-Bedding Directions in Sandstones of Lower Ret1culoceras Age in the Millstone Grit of Wharfedale, Yorkshire: Proceedings of the Yorkshire Geological Society, v. 30, p. 115-132.

WALLINGA, J., TÖRNQVIST, T.E., BUSSCHERS, F.S., and WEERTS, H.J.T., 2004, Allogenic forcing of the late Quaternary Rhine–Meuse fluvial record: the interplay of sea-level change, climate change and crustal movements: Basin Research, v. 16, p. 535-547.

WANG, Y., STRAUB, K.M., and HAJEK, E.A., 2011, Scale-dependent compensational stacking: An estimate of autogenic time scales in channelized sedimentary deposits: Geology, v. 39, p. 811-814.

WATERS, C.N., 2000, Geology of the Bradford district: Sheet description of the British Geological Survey, 1:50.000 Series Sheet 69 Bradford (England and Wales). BGS, 41 p.

WATERS, C.N., CHISHOLM, J.I., BENFIELD, A.C., and O'BEIRNE, A.M., 2008, Regional evolution of a fluviodeltaic cyclic succession in the Marsdenian (late Namurian Stage, Pennsylvanian) of the Central Pennine Basin, UK: Proceedings of the Yorkshire Geological Society, v. 57, p. 1-28.

WATERS, C.N., CHISHOLM, J.I., HOUGH, E., and EVANS, D.J., 2012, Geology of the Glossop district - a brief explanation of the geological map. *Sheet explanation of the British Geological Survey* 1:50.000 Sheet 86 Glossop (England and Wales).

WATERS, C.N., and CONDON, D.J., 2012, Nature and timing of Late Mississippian to Mid-Pennsylvanian glacio-eustatic sea-level changes of the Pennine Basin, UK: Journal of the Geological Society, v. 169, p. 37-51.

WATERS, C.N., and DAVIES, J.R., 2006, Carboniferous: extensional basins, advancing deltas and coal swamps, *in* Brenchley, P.J., and Rawson, P.F., eds., The Geology of England and Wales (Second edition): London, The Geological Society London, p. 173-223.

WATERS, C.N., MILLWARD, D., and THOMAS, C.W., 2014, The Millstone Grit Group (Pennsylvanian) of the Northumberland–Solway Basin and Alston Block of northern England: Proceedings of the Yorkshire Geological Society, v. 60, p. 29-51.

WATERS, C.N., SOMERVILLE, I.D., JONES, N.S., CLEAL, C.J., COLLINSON, J.D., WATERS, R.A., BESLY, B.M., DEAN, M.T., STEPHENSON, M.H., DAVIES, J.R., FRESHNEY, E.C., JACKSON, D.I., MITCHELL, W.I., POWELL, J.H., BARCLAY, W.J., BROWNE, M.A.E., LEVERIDGE, B.E., LONG, S.L., and MCLEAN, D., 2011, A revised correlation of Carboniferous Rocks in the British Isles: Geological Society of London Special Report, v. 26: Bath, UK, Geological Society of London, 186 p.

WATERS, C.N., WATERS, R.A., BARCLAY, W.J., and DAVIES, J.R., 2009, A lithostratigraphical framework for the Carboniferous successions of southern Great Britain (Onshore), British Geological Survey Research Report, RR/09/01.

WELLS, M.R., ALLISON, P.A., PIGGOTT, M.D., PAIN, C.C., HAMPSON, G.J., and DE OLIVEIRA, C.R.E., 2005, Large sea, small tides: the Late Carboniferous seaway of NW Europe: Journal of the Geological Society, v. 162, p. 417-420.

WELTJE, G., and DE BOER, P.L., 1993, Astronomically induced paleoclimatic oscillations reflected in Pliocene turbidite deposits on Corfu (Greece): Implications for the interpretation of higher order cyclicity in ancient turbidite systems: Geology, v. 21, p. 307-310.

WIGNALL, P.B., and MAYNARD, J.R., 1996, High-resolution sequence stratigraphy in the early Marsdenian (Namurian, Carboniferous) of the central Pennines and adjacent areas: Proceedings of the Yorkshire Geological Society, v. 51, p. 127-140.

WILSON, A.A., 1957, The geology of the country between Masham and Great Whernside [unpublished PhD thesis]: University of Durham, Durham, 516 p.

WILSON, A.A., 1960, The Carboniferous Rocks of Coverdale and Adjacent Valleys in the Yorkshire Pennines: Proceedings of the Yorkshire Geological Society, v. 32, p. 285-316.

WILSON, A.A., and THOMPSON, A.T., 1959, Marine Bands of Arnsbergian Age (Namurian) in the South-Eastern Portion of the Askrigg Block, Yorkshire: Proceedings of the Yorkshire Geological Society, v. 32, p. 45-67.

WRIGHT, S., and PARKER, G., 2005a, Modeling downstream fining in sand-bed rivers. I: formulation: Journal of Hydraulic Research, v. 43, p. 613-620.

WRIGHT, S., and PARKER, G., 2005b, Modeling downstream fining in sand-bed rivers. II: application: Journal of Hydraulic Research, v. 43, p. 621-631.

WRIGHT, V.P., and VANSTONE, S.D., 2001, Onset of Late Palaeozoic glacio-eustasy and the evolving climates of low latitude areas: a synthesis of current understanding: Journal of the Geological Society, v. 158, p. 579-582.

WROBLEWSKI, A.F.-J., 2006, Relative Influences of Tectonism, Climate, and Sea Level on Valley Incision and Sedimentary Fill: New Insights from Upper Cretaceous and Paleocene Examples, *in* Dalrymple, R.W., Leckie, D.A., and Tillman, R.W., eds., Incised Valleys in Time and Space, SEPM Spec. Publ. 85, p. 309-326.

YOUNG, B., and LAWRENCE, D.J.D., 1998, The Morpeth Group of 1:50 000 scale sheet 14 (Morpeth): lithostratigraphy and local details, British Geological Survey Technical Report, WA/98/10.

Appendix 1: Borehole details

	Boreholes	Grid reference	BGS Ref. #	TD(m)	Spud	Strata (base)	Strata (top)	Type	Ref
1	Aldfield 1	[424050 468100]	SE 26 NW/6	130.76	1945	Carboniferous Lst (?)	Lower Follifoot Grit (Arnsbergian)	Hydrocarbon	1
2	Ashfold Side Beck 1	[411600 466150]	SE 16 NW/3	292.91	1967	Hargate End Lst (Asbian)	Red Scar Grit (Arnsbergian)	Claro Water Board	1,3
3	Boulsworth 1	[392680 434790]	SD 93 SW/14	1920.2	1963	Stockdale Farm Fm (Tournaisian/Chadian)	Todmorden Grit/Parsonage Sst (Kinderscoutian)	Hydrocarbon	1
4	Blacko	[384950 441830]	SD 84 SW/2	170.08	1955	Pendle Grit Member (Pendleian)	Warley Wise Grit (Pendleian)	Craven Water Board	1,3
5	Bewerley Mines No. 1B	[410700 466230]	SE 16 NW/6	-	-	-	-	Ore	3
6	Croft House, Cononley	[398710 447010]	SD 94 NE/7	53.34	1936	Warley Wise Grit (Pendleian)	Bradley Flags (Pendleian)	Water	1,4
7	IGS Croft House	[419820 488830]	SE 18 NE/5	168.62	1974	Crow Limestone (Pendleian)	Scar House Beds (Arnsbergian)	Research - (IGS/BGS)	1
8	Ellenthorpe 1	[442270 467050]	SE 46 NW/7	1096.7	1945	Massive Limestone (C_2 S_1)	(Triassic)	Hydrocarbon	1
9	Grimwith Reservoir 15	[405760 464240]	SE 06 SE/15	60.66	?	Grassington Grit (Pendleian)	Grassington Grit (Pendleian)	Yorkshire Water Authority	1
10	Grimwith Reservoir LP18	[406120 463840]	SE 06 SE/32	79.2	1975	Gayle Cyclothem (Brigantian)	Grassington Grit (Pendleian)	Yorkshire Water Authority	1
11	Heywood 1	[383851 408976]	SD 80 NW/141	1619	1984	Chadburn Lst (Arundian)	Rough Rock (Yeadonian)	Hydrocarbon	2
12	Holme Chapel	[386080 428780]	SD 82 NE/69	1982.4	1974	Stockdale Farm Fm (Tournaisian/Chadian)	Rough Rock (Yeadonian)	Hydrocarbon	1,2
13	Low Bradley 1	[401950 447860]	SE 04 NW/363	613.56	1991	Bowland Shale Fm (Pendleian)	Bradley Flags (Pendleian)	Hydrocarbon	1,2
14	Moor Park Farm	[425750 453190]	SE 25 SE/9	60.96	1974	Warley Wise Grit (Pendleian)	Bearing/Pendle Grit Member (Pendleian)	Water	1
15	Roddlesworth 1	[365490 421120]	SD 62 SE/274	2508.5	1985	Limestone (Courceyan?/Chadian)	Fletcher Bank Grit (Marsdenian)	Hydrocarbon	2
16	IGS Roosecote	[323040 468660]	SD 26 NW/19	800.88	1970	St. Bees Sst (Triassic)	Limestones (Dinantian)	Research - (IGS/BGS)	1
17	Sawley 1	[424510 465020]	SE 26 NW/15	394.72	1945	Limestone (Lower Carboniferous)	Follifoot Grit Gp (Chokierian/Alportian)	Hydrocarbon	1
18	Tholthorpe	[446820 466890]	SE 46 NE/7	929.64	1965	Carboniferous (?)	Sherwood Sst Gp (Permian)	Hydrocarbon	1
19	Whitmoor 1	[358740 463150]	SD 56 SE/1	1559.1	1966	Hetton Beck Lst Mb (Chadian)	Ward's Stone Sst (Arnsbergian)	Hydrocarbon	1
20	Weeton 1	[429800 446380]	SE 24 NE/29	1979.3	1984	Gavell's Clough Sst (Arnsbergian)	?Haw Back Lst (Chadian)	Hydrocarbon	1,2
21	British Geological Survey (http://mapapps.bgs.ac.uk/geologyofbritain/home.html,					Basement (Lower Palaeozoic			

http://www.bgs.ac.uk/data/boreholescans/home.html),

[2] Data provided by CGG Data Management Limited (UK), [3] Brandon et al. (1995), [4] Riley (1996)